



UNIVERSITY OF
BIRMINGHAM

**Analysis of Emerging Environmental Contaminations
Using Advanced Instrumental Tools: Application to
Human and Environmental Exposure**

by

Khanh Hoang Nguyen

M.Sc, B.Sc (Hons)

A thesis submitted to the University of Birmingham

for the degree of

DOCTOR OF PHILOSOPHY (Ph.D)

Division of Environmental Health and Risk Management

College of Life and Environmental Science

The University of Birmingham

Edgbaston, B15 2TT

United Kingdom

July 2018

UNIVERSITY OF
BIRMINGHAM

University of Birmingham Research Archive

e-theses repository

This unpublished thesis/dissertation is copyright of the author and/or third parties. The intellectual property rights of the author or third parties in respect of this work are as defined by The Copyright Designs and Patents Act 1988 or as modified by any successor legislation.

Any use made of information contained in this thesis/dissertation must be in accordance with that legislation and must be properly acknowledged. Further distribution or reproduction in any format is prohibited without the permission of the copyright holder.

Acknowledgements

Firstly, I would like to express my sincere gratitude to my supervisor and ELUTE project coordinator Prof. Stuart Harrad for his constant help, support and academic supervision throughout my Ph.D project. I would also like to thank my co-supervisor Dr. Mohamed Abdallah for his invaluable suggestions, comments and guidance. Mohamed and Stuart have been always patient and full of encouragement and helped me develop many skills in and out of the lab. I truly could not ask for better supervisors.

The Marie Curie-EID program, the ELUTE and INTERWASTE project have provided funding for my research as well as many travel opportunities for collaboration, training courses and attending conferences. I would like to thank Thermo Fisher Scientific Bremen for hosting my secondment and giving me access to Q-Exact instrument. My sincere thanks also go to Kyle D'Silva and Thomas Moehring who supervised me during my secondment in Thermo Fisher.

I also would like to thank Dr. Eric Reiner and Dr. Gregg Tomy for hosting me during my ELUTE and INTERWASTE secondment.

A big-big thanks to my ELUTE fellows Leon and Ari. You have been always there for me and motivated me through my difficult times. It has been a fantastic 3 years working and sharing a house with you. I will cherish our friendship and memories forever.

Thanks to my colleagues and friends in Public Health building William Stubbings, Jiangmeng Kuang, Daniel Drage, Gopal Pawar, Tuan Vu, Yessica Ortiz Carrizales, Fang Tao, Layla Al-Omran, Jennifer Ebele Anekwe, Ana Miralles-Marco, Salim Ali Sakaroun.

A great thanks to the lab manager Maria Thompson and research group secretaries Kate Nauta and Sally Gladwin.

Last but not least, this PhD journey could not be finished with the endless love and support from my family members and friends.

Abstract

High throughput analytical methods based on UPLC-APCI-HRMS and/or UPLC-ESI-HRMS were developed for the multi-residue analysis of pharmaceuticals, personal care products (PPCPs), brominated flame retardants (BFRs) and their degradation/transformation products. The PPCPs method was successfully applied to analysis of freshwater samples from Egypt. Target PPCPs were ubiquitous in the Egyptian aquatic environment and displayed relatively high concentrations in an effluent sample from a hospital wastewater treatment plant. The BFRs method was applied to screen for legacy BFRs, novel BFRs and their potential degradation/transformation products in simulated landfill leachate samples. *In vitro* bioassays were developed to study for the first time the metabolism of the novel BFRs TBECH by human liver microsomes and EH-TBB and FM550 by human skin S9 fractions. TBECH was metabolised by hepatic CYP450-mediated enzymes to produce a complex mixture of hydroxylated, debrominated and α -oxidation metabolites. EH-TBB and TPhP (in the FM550 mixture) underwent biotransformation by carboxylesterases in human skin S9 fractions. Kinetic modelling of the studied hepatic and dermal human biotransformation reactions revealed that exposure to multiple chemicals significantly influences the metabolic rates of target compounds. *In vitro* – *in vivo* extrapolations were also modelled to investigate the xenobiotic clearance capacities of human liver and skin.

Table of Contents

List of Figures	VIII
List of Tables	X
Abbreviations	XII
List of Publications	XV
Chapter 1 Introduction	1
1.1. Orbitrap mass spectrometry	2
1.2. Novel Brominated Flame Retardants	6
1.2.1. Production, usage and physicochemical properties	6
1.2.2. Toxicity and health effects	11
1.2.3. Occurrence in major environmental compartments of concern	11
1.2.3.1. Indoor dust exposure	12
1.2.3.2. Indoor air exposure	20
1.2.3.3. Dietary Exposure	21
1.2.4. Human body burdens of NBFRs	24
1.2.5. NBFRs metabolism	26
1.2.6. Current knowledge gaps	28
1.3. Pharmaceutical and Personal Care Products	29
1.3.1. Introduction	29
1.3.2. Physicochemical properties	29
1.3.3. Toxicity and health effects	30
1.3.4. Occurrence in major environment compartments of concern	32
1.3.4.1. Wastewater and surface water	32
1.3.4.2. Sediment and sewage sludge	34
1.3.5. PPCPs in biota	35
1.3.6. Current knowledge gaps	36
1.4. Aims of this thesis	37
Chapter 2 Analytical Method	39
2.1. Orbitrap MS tuning	40
2.2. Data Analysis	42
2.2.1. Targeted Analysis	42
2.2.2. Untargeted analysis	44

2.2.3. Biotransformation kinetic model.....	48
2.3. Analysis of blanks, LODs and LOQs	49
2.4. Statistical Analysis.....	49
Chapter 3 Method development for simultaneous analysis of multiple pharmaceuticals and personal care products in water by UPLC-HRMS.....	51
3.1. Synopsis	52
3.2. Materials and methods	52
3.2.1. Chemicals and standards	52
3.2.2. Sample preparation and extraction.....	55
3.3. Instrument Analysis	56
3.4. Method Validation and quantification	57
3.5. Quality assurance/quality control (QA/QC)	57
3.6. Results and discussions.....	58
3.6.1 Chromatographic separation and mass spectrometry.....	58
3.6.2. Quantification and validation	63
3.6.2.1. Method linearity	63
3.6.2.2. Accuracy and precision	64
3.6.2.3 Detection and quantification limits.....	70
3.6.3. Application to surface water samples.....	72
3.7. Conclusions.....	78
Chapter 4 Simultaneous targeted and untargeted screening of BFRs and transformation products by UPLC-HRMS: application to samples of waste leachate and samples generated by <i>in vitro</i> challenge of mouse liver microsomes with EH-TBB, BEH-TEBP and BTBPE.....	79
4.1. Synopsis	80
4.2. Experiments	80
4.2.1. Chemicals	80
4.2.2. Leachate sample preparation and extraction	81
4.2.3. <i>In vitro</i> incubation experiments.....	83
4.2.4. Extraction of <i>in vitro</i> samples	83
4.3. Method development	83
4.3.1. Analysis of pure BFR standards.....	83

4.3.2. LC(-)APCI/(-ESI)-HRMS analysis for targeted and untargeted analysis of BFRs.....	94
4.4. BFRs screening in leachate samples	98
4.4.1. Targeted screening of BFRs	98
4.4.2. Untargeted screening of brominated contaminants	103
4.5. Screening of biotransformation products of EH-TBB, BEH-TEBP and BTBPE following <i>in vitro</i> incubation with mouse liver microsomes (MLM)	108
4.5.1. Characterisation of parent compounds	108
4.5.2. Metabolite identification	111
4.6. Conclusion	114
Chapter 5 <i>In vitro</i> metabolism of 1,2-Dibromo-4-(1,2-dibromethyl)cyclohexane by Human Liver Microsomes	116
5.1. Synopsis	117
5.2. Introduction.....	117
5.3. Experiments	119
5.3.1. Chemicals and Standards	119
5.3.2. <i>In Vitro</i> Incubation Experiments	120
5.3.3. Sample extraction.....	120
5.3.4. Instrumental analysis.....	121
5.3.4.1. UPLC-Orbitrap MS analysis	121
5.3.4.2. GC x GC TOF-MS analysis	121
5.3.5. QA/QC	122
5.4. Metabolic profile of TBECH	126
5.5. Kinetics of TBECH metabolism by HLM	132
5.6. Conclusions.....	136
Chapter 6 EH-TBB and Firemaster 550 metabolism by Human Skin S9 Fractions.....	138
6.1. Synopsis	139
6.2. Introduction.....	139
6.3. Experiments	141
6.3.1. Chemicals and Standards	141
6.3.2. <i>In vitro</i> Incubation Experiments.....	141

6.3.3. Sample extraction.....	142
6.3.4. Instrumental analysis.....	142
6.4. QA/QC.....	144
6.5. Results.....	144
6.5.1. Metabolic profiles of EH-TBB and FM550.....	144
6.5.2. Metabolic kinetics of EH-TBB and FM 550 metabolism by HS-S9.....	148
6.5.3. <i>In vitro</i> – <i>in vivo</i> extrapolation for clearance of EH-TBB.....	151
6.5.4. Implications for human exposure.....	152
6.6. Limitations of this study	153
6.7. Conclusions.....	153
Chapter 7 Summary and Conclusions	155
7.1. Summary.....	156
7.2. Research gap and future perspectives.....	159
References	161

List of Figures

Chapter 1 Introduction

Figure 1.1: Schematic components of the Q Exactive Orbitrap mass spectrometer series (Michalski et al., 2011b). 4

Figure 1.2: Chemical structures of selected legacy and novel BFRs. 10

Chapter 2 Analytical Method

Figure 2.1: Acceptable mass accuracy calibration in negative (A) and positive (B) ESI mode. 41

Figure 2.2: Compound Discoverer workflow for untargeted screening of emerging contaminants and their metabolites 44

Chapter 3 Method development for simultaneous analysis of multiple pharmaceuticals and personal care products in water by UPLC-HRMS

Figure 3.1: Names and chemical structures of PPCPs in this study 55

Figure 3.2: Extracted Ion Chromatogram of our target PPCPs and Internal Standards in calibration standard level 3 62

Figure 3.3: Concentrations of PPCPs (ng/L) in effluent samples from waste water treatment plants in Assiut city, Egypt 76

Figure 3.4: Concentrations (ng/mL) of PPCPs in surface water samples collected from Assiut city, Egypt 77

Chapter 4 Simultaneous targeted and untargeted screening of BFRs and transformation products by UPLC-HRMS: application to samples of waste leachate and samples generated by *in vitro* challenge of mouse liver microsomes with EH-TBB, BEH-TEBP and BTBPE

Figure 4.1: (-)APCI-HRMS Mass spectra of the identification ion cluster for each BFR standard studied in this chapter 88

Figure 4.2: Peak area heat map of detected BFRs in leachate samples 99

Figure 4.3: Independent samples Kruskal-Wallis test results for BFRs detected in leachate samples 102

Figure 4.4: Overlay chromatogram of Unknown Compound A in leachate samples and its isotopic pattern 105

Figure 4.5: Overlay chromatogram of Unknown Compound B in leachate samples and its isotopic pattern 105

Figure 4.6: Overlay chromatogram of Unknown Compound D in leachate samples and its isotopic pattern 106

Figure 4.7: Chemical structures of tentatively identified TBBPA-related contaminants in leachate testing samples. 107

Figure 4.8: (-)APCI-LC-HRMS extracted ion chromatograms of BEH-TEBP (A), EH-TBB (B) and BTBPE (C) in *in vitro* MLM samples exposed to 10 μ M of individual NBFRs for 60 min 108

Figure 4.9: BEH-TEBP and EH-TriBB as impurities in EH-TBB dosing solution analyzed by (-)APCI-LC-HRMS 110

Figure 4.10: BEH-TriBP as impurity in BEH-TEBP dosing solution analyzed by (-)APCI-LC-HRMS 110

Figure 4.11: Overlay chromatogram of M1 (M3) and its chromatogram in MLM samples exposed to 10 μ M of EH-TBB <i>in vitro</i>	113
Figure 4.12: Overlay chromatogram of M2 and its spectrum in MLM samples exposed to 10 μ M of EH-TBB <i>in vitro</i>	114
Chapter 5 In vitro metabolism of 1,2-Dibromo-4-(1,2-dibromethyl)cyclohexane by Human Liver Microsomes	
Figure 5.1: Principal component analysis score plot of negative control blanks and human liver microsomes samples exposed to 10 μ M TBECH mixture for 60 minutes	123
Figure 5.2: Isotopic pattern of metabolites 1-5 recorded by LC-Orbitrap MS in comparison with isotope simulation	124
Figure 5.3: Selected UPLC-ESI-Orbitrap/MS chromatograms of monohydroxy (M1, peaks 1, 2 and 3) and dihydroxy (M2, peaks 4, 5 and 6) metabolites formed by HLM exposure to 10 μ M of technical TBECH (a and c) and β -TBECH (b and d) for 60 minutes	127
Figure 5.4: GC x GC - TOFMS total ion current chromatogram of HLM sample exposed to 10 μ M TBECH mixture for 60 minutes. The hypothesized metabolite C ₈ H ₁₁ Br ₃ could not be identified.	130
Figure 5.5: Selected UPLC-Orbitrap/MS chromatograms of metabolites M3 (peaks 7 and 8), M4 (peaks 9, 10, 11, 12, 13 and 14) and M5 (peaks 15 and 16) formed by HLM following exposure to 10 μ M technical TBECH (a, c and e) and β -TBECH (b, d and f) for 60 minutes	131
Figure 5.6: Proposed metabolic pathways of TBECH by Human Liver Microsomes	132
Figure 5.7: Kinetic analysis of TBECH mixture (A) and β -TBECH (B) metabolite formation rate by human liver microsomes using the Michaelis-Menten model.	135
Chapter 6 EH-TBB and Firemaster 550 metabolism by Human Skin S9 Fractions	
Figure 6.1: TBBA and MTBBA in a Human S9 Skin fraction (HS-S9) sample exposed to 10 μ M of EH-TBB	145
Figure 6.2: (-)ESI-MS/MS spectrum of ion 249.03204 by UPLC-Orbitrap HRMS	146
Figure 6.3: Proposed metabolic pathways of EH-TBB and TPhP by human skin S9 fraction	148
Figure 6.4: Kinetic analysis of TBBA formation of EH-TBB (A) and FM550 mixture (B) by human skin S9 fraction using the Michaelis-Menten model.	149
Figure 6.5: Kinetic analysis of DPhP formation from FM550 mixture by human skin S9 fractions	151

List of Tables

Chapter 1 Introduction

Table 1.1: Physicochemical properties of some legacy and novel BFRs reported by U.S EPA (commercial PBDEs) or estimated by EPI Suite TM v4.11	8
Table 1.2: Summary median concentrations of some common novel brominated flame retardants in indoor dust (ng g ⁻¹)	16
Table 1.3: Physicochemical properties of some common PPCPs	29

Chapter 2 Analytical Method

Table 2.1: Tuning ions for mass accuracy in positive and negative ESI mode on UPLC-Orbitrap MS instrument	40
Table 2.2: Descriptive analysis “nodes” of Compound Discoverer 2.0 Software used in untargeted screening of chemicals and metabolites.	46

Chapter 3 Method development for simultaneous analysis of multiple pharmaceuticals and personal care products in water by UPLC-HRMS

Table 3.1: List of 29 target PPCPs in this study	52
Table 3.2: PPCPs identified by LC-Orbitrap HRMS	59
Table 3.3: Linearity coefficient and calibration equation for PPCPs analysis by UPLC-HRMS in this study	63
Table 3.4: Method accuracy expressed as % recovery at 3 spiked concentration levels of PPCPs in Milli-Q water	65
Table 3.5: Intra- and inter-day precision expressed as RSD% for targeted PPCPs	66
Table 3.6: Precision for complex matrices expressed as RSD% for triplicate analysis of target PPCPs	68
Table 3.7: IDLs, IQLs and MQLs for the developed PPCP analysis method by UPLC-HRMS	70
Table 3.8: PPCPs concentrations in Egyptian effluent and surface water samples.	73

Chapter 4 Simultaneous targeted and untargeted screening of BFRs and transformation products by UPLC-HRMS: application to samples of waste leachate and samples generated by *in vitro* challenge of mouse liver microsomes with EH-TBB, BEH-TEBP and BTBPE

Table 4.1: Different sample categories in stimulated leachate test	82
Table 4.2: BFR standards used in this chapter and their accurate ion masses analyzed by LC-(-)APCI-HRMS.	85
Table 4.3: LC gradient for the analysis of BFRs standard mixture	94
Table 4.4: Optimized (-)APCI Orbitrap MS parameters for targeted and untargeted analysis of BFRs	95
Table 4.5: Retention time of BFR standards analyzed by (-)APCI-LC-HRMS on Accucore RP-MS column	95
Table 4.6: Optimized (-)ESI Orbitrap MS parameters for metabolite identification of EH-TBB, BEH-TEBP and BTBPE by MLM <i>in vitro</i>	96
Table 4.7: Compound Discoverer parameters of main working nodes for screening of BFRs and brominated contaminants	97

Table 4.8: Nonparametric Kruskal-Wallis Test result for distribution of each detected BFR across all sample categories	100
Table 4.9: P value for pairwise comparison of contaminant levels in each sample category via Dunn post hoc after significant Kruskal-Wallis Test.	101
Table 4.10: Some potential brominated contaminants list found by Compound Discoverer	104
Chapter 5 <i>In vitro</i> metabolism of 1,2-Dibromo-4-(1,2-dibromomethyl)cyclohexane by Human Liver Microsomes	
Table 5.1: Potential metabolites of technical TBECHE mixture produced via incubation with human liver microsomes	128
Table 5.2: Kinetic parameters derived from non-linear regression (Michaelis-Menten model) of the formation of metabolites resulting from incubation of the TBECHE mixture and β -TBECHE with human liver microsomes	133
Chapter 6 EH-TBB and Firemaster 550 metabolism by Human Skin S9 Fractions	
Table 6.1: Optimized Orbitrap parameters for the analysis of EH-TBB, FM550 and their potential metabolites by UPLC-Orbitrap MS (LC flow rate 400 μ L/min)	143
Table 6.2: Monitoring ions for parent compounds and internal standards in different ionisation modes of the UPLC-HRAM Orbitrap/MS	143
Table 6.3: SIM-MS ² parameters for ion 249.03204 by (-)ESI-UPLC-Orbitrap HRMS	146
Table 6.4: Exposure levels of human skin S9 fraction to EH-TBB and FM550 mixture	149
Table 6.5: Kinetic parameters derived from non-linear regression (Michaelis-Menten model) of the formation of TBBA resulting from incubation of HS-S9 with pure EH-TBB and FM550 mixture in this study and comparison with EH-TBB incubation with HLM (Roberts et al. 2012)	150
Table 6.6: Estimated <i>in vitro</i> and <i>in vivo</i> clearance of EH-TBB by human skin (this study) and human liver (Roberts et al., 2012)	151

Abbreviations

2,4,6-TBP	2,4,6-Tribromophenol
AGC	Automated gain control
AIF	All ion fragmentation
ANOVA	Analysis of variance
APCI	Atmospheric chemical ionisation
APPI	Atmospheric Pressure Photoionization
AR	Androgen receptor
BB-101	Polybrominated biphenyl 101
BEH-TEBP	Bis(2-ethylhexyl) tetrabromophthalate
BFRs	Brominated flame retardants
BTBPE	1,2-Bis(2,4,6-tribromophenoxy) ethane
Bw	Body weight
CES1	Carboxylesterase 1
CID	Collision induced dissociation
CL_h	<i>In vivo</i> hepatic clearance
CL_{int}	<i>In vitro</i> hepatic clearance
Cr	Creatinine
CRTs	Cathode ray tube monitor
CYP450	Cytochrome P450
DBBPA	Dibromobisphenol A
DBDPE	Decabromodiphenyl ethane
DBE-DBCH, TBECH	4-(1-2-dibromoethyl)-1,2-dibromocyclohexane
DCM	Dichloromethane
DDC-CO	Dechlorane plus
Deca-BDE	Decabrominated diphenyl ether
DIA	Data Independent Analysis
DMSO	Dimethyl sulfoxide
DPhP	Diphenyl Phosphate
EC	Emerging contaminant
EH-TBB	2-Ethylhexyl-2,3,4,5-tetrabromobenzoate
ESI	Electrospray ionisation
FM550	FireMaster 550
FRs	Flame retardants
FS	Full scan
FWHM	Full width half maximum
GC	Gas chromatography
HBB	Hexabromobenzene
HBB	Hexabromobenzene
HBCDDs	Hexabromocyclododecanes
HCD	Higher Energy Collisional Dissociation
HCDBCO	Hexachlorocyclopentadienyl-Dibromocyclooctane
HDPE	High-density polyethylene

HESI	Heated electrospray ionisation
HLM	Human liver microsomes
HRMS	High resolution mass spectrometry
HS-S9	Human skin S9 Fractions
IDL	Instrumental detection limit
IQL	Instrumental quantification limit
IS	Internal standard
IT	Ion injection time
K_m	Michaelis constant
K_{ow}	n-octanol/water partition coefficient
LCDs	Liquid-crystal displays
LMH	Leghorn male hepatoma
LOD	Limit of detection
LOQ	Limit of quantification
L_w	Lipid weight
M.W	Molecular weight
m/z	Mass to charge ratio
MDL	Method detection limit
MeO-TBBPA	Methoxylated Tetrabromobisphenol A
MLM	Mouse liver microsomes
MQL	Method quantification limit
MRM	Multiple Reaction Monitoring
MS	Mass spectrometry
NBFRs	Novel brominated flame retardants
ND	Non-detected
NSAIDs	Nonsteroidal Anti-inflammatory Drugs
OBTMPI	Octabromotrimethylphenyl indane
Octa-BDE	Octabrominated diphenyl ether
OWCs	Organic wastewater contaminants
PBB-Acr	Pentabromobenzyl acrylate
PBBz	Pentabromobenzene
PBDE	Polybrominated diphenyl ether
PBEB	Pentabromoethylbenzene
PBEB	Pentabromoethylbenzene
PCA	Principal component analysis
Penta-BDE	Pentabrominated diphenyl ether
pKa	Acid dissociation constant
PPCPs	Pharmaceutical and personal care products
PRM	Parallel reaction monitoring
PTFE	Polytetrafluoroethylene
QA/QC	Quality assurance/quality control
Q_h	Hepatic blood flow
Q_{skin}	Skin blood flow
QuEChERS	Quick easy cheap efficient rugged safe

RLM	Rat liver microsomes
RRF	Relative response factor
RSD	Relative standard deviation
S:N	Signal to noise
SIM	Single ion monitoring
SPE	Solid phase extraction
SRM	Single reaction monitoring
STPs	Sewage treatment plants
T₃	Triiodothyronine
TBA	Thiobarbituric acid
TBBA	2,3,4,5-tetrabromobenzoic acid
TBBPA	Tetrabromobisphenol A
TBBPA-BDBPE	TetrabromobisphenolA bis(2,3-dibromopropyl ether
TBCT	Tetrabromo-o-chlorotoluene
TBMB	2,3,4,5-tetrabromomethylbenzoate
TBMEHP	Mono (2-ethylhexyl) tetrabromophthalate
TBPA	Tetrabromophthalic acid
TBP-AE	2,4,6-Tribromophenyl allyl ether
TBP-AE	Allyl-2,4,6-tribromophenyl ether
TBP-BAE	2-bromoallyl-2,4,6-tribromophenyl ether
TBP-DBPE	2,4,6-Tribromophenyl 2,3-dibromopropyl ether
TBP-DBPE	2-3-dibromopropyl-2,4,6-tribromophenyl ether
TCEP	Tris (2-chloroethyl) phosphate
TDBP-TAZTO	Tris(2,3-dibromopropyl) isocyanurate
TDS	Total Diet Study
TIC	Total ion current
TPhP	Triphenyl Phosphate
TriBBPA	Tribromobisphenol A
UNEP	United nations Environment Programme
UPLC	Ultra performance liquid chromatography
USEPA	United States environmental protection agency
V_{max}	Maximum metabolic rate
WEEE	Waste Electrical and Electronic Equipment
WWTPs	Waste water treatment plants

List of Publications

1. **Nguyen, K.-H.**, Abou-Elwafa Abdallah, M., Moehring, T., Harrad, S., 2017. *Biotransformation of the Flame Retardant 1,2-Dibromo-4-(1,2-dibromoethyl)cyclohexane (TBECH) in Vitro by Human Liver Microsomes*. Environ. Sci. Technol. 51, 10511–10518.
2. Abou-Elwafa Abdallah, M., **Nguyen, K.-H.**, Harrad, S., *A rapid method for analysis of 30 Pharmaceutical and Personal Care Products in water by LC-Orbitrap HRMS* (Submitted to Journal of Chromatography A)

Conference Presentations

OP = oral presentation; **PP** = Poster presentation and **CA** = contributing author

1. **Nguyen, K.H.**, Ganci, A.P., Abdallah, M., Moehring, T., Harrad, S., *Application of Orbitrap HRAM Mass Spectrometry to untargeted identification of NBFRs and their metabolites*, Dioxin 2016, Florence, Italy (**PP**)
2. **Nguyen, K.H.**, Ganci, A.P., Abdallah, M., Moehring, T., Harrad, S., *Explore the potential of state of the art Mass Spectrometry and dedicated software in identification of NBFRs and their metabolite/degradation products*, ISES 2016, Utrecht, The Netherlands (**OP**)
3. **Nguyen, K.-H.**, Peters, L.I., Ganci, A.P., Abdallah, M., Harrad, S., *Identification of Novel Brominated Flame Retardants in Leachate samples using a High Resolution High Accuracy Mass Spectrometer*, BFR2017, York, UK (**PP**)
4. **Nguyen, K.-H.**, Abdallah, M., Anekwe, J., Harrad, S. *Application of LC-Orbitrap HRMS with positive/negative ion-switching for analysis of Pharmaceutical and Personal Care Products (PPCPs)*, Dioxin 2017, Vancouver, Canada (**PP**)
5. **Nguyen, K.-H.**, Peters, L.I., Ganci, A.P., Abdallah, M., Harrad, S., *Biotransformation of flame retardant 1,2-Dibromo-4-(1,2-dibromomethyl)cyclohexane (TBECH) in vitro by Human Liver Microsomes*, Dioxin 2017, Vancouver, Canada (**OP – Otto Hutzinger student presentation award**)
6. Ganci, A.P., Abdallah, M., Peters, L.I., **Nguyen, K. H.**, Moehring, T., Vane, C., Harrad, S., *Legacy PBDEs and NBFRs in sediment samples of the river Thames using liquid chromatography coupled to a high resolution accurate mass Orbitrap mass spectrometer*, BFR2017, York, UK (**CA**)
7. Ganci, A.P., Abdallah, M., Peters, L.I., **Nguyen, K. H.**, Moehring, T., Harrad, S., *Investigating the in vitro metabolism of NBFRs by trout liver microsomes using a high resolution accurate mass benchtop Q-Exactive Orbitrap mass spectrometer*, BFR2017, York, UK (**CA**)

Chapter 1

Introduction

In recent years, more and more chemicals of emerging concern have been discovered in the environment with the aid of advances in analytical science and instrumentation. These chemicals pose potential risks to the environment and human health. However their fate, toxicity and exposure pathways are not yet fully understood. An emerging contaminant (EC) therefore was defined by the USEPA as *“a chemical or material characterized by a perceived, potential, or real threat to human health or the environment or by a lack of published health standards. A contaminant also may be “emerging” because of the discovery of a new source or a new pathway to humans”* (USEPA, 2010). By this definition, ECs cover both truly new compounds that were not detected previously and chemicals which have been around but just recently have been brought to the attention of the scientific community. The list of ECs comprises at least hundreds of organic and inorganic pollutants belonging to numerous chemical categories. Some prime examples of ECs are novel brominated flame retardants (NBFRs) and pharmaceutical and personal care products (PPCPs). One of the important challenge of studying ECs in general and NBFRs and PPCPs in particular is how to simultaneously analyse a broad suit of chemicals in a sample. With the recent advances in mass spectrometry (MS) e.g. Orbitrap MS technology, this challenge can be addressed. In this chapter, the Orbitrap MS technology will be introduced and potential applications of UPLC-Orbitrap MS in environmental science will be discussed. Additionally, background information about NBFRs and PPCPs will also be introduced with focus on their main human exposure pathways and associated human and wildlife health risks.

1.1. Orbitrap mass spectrometry

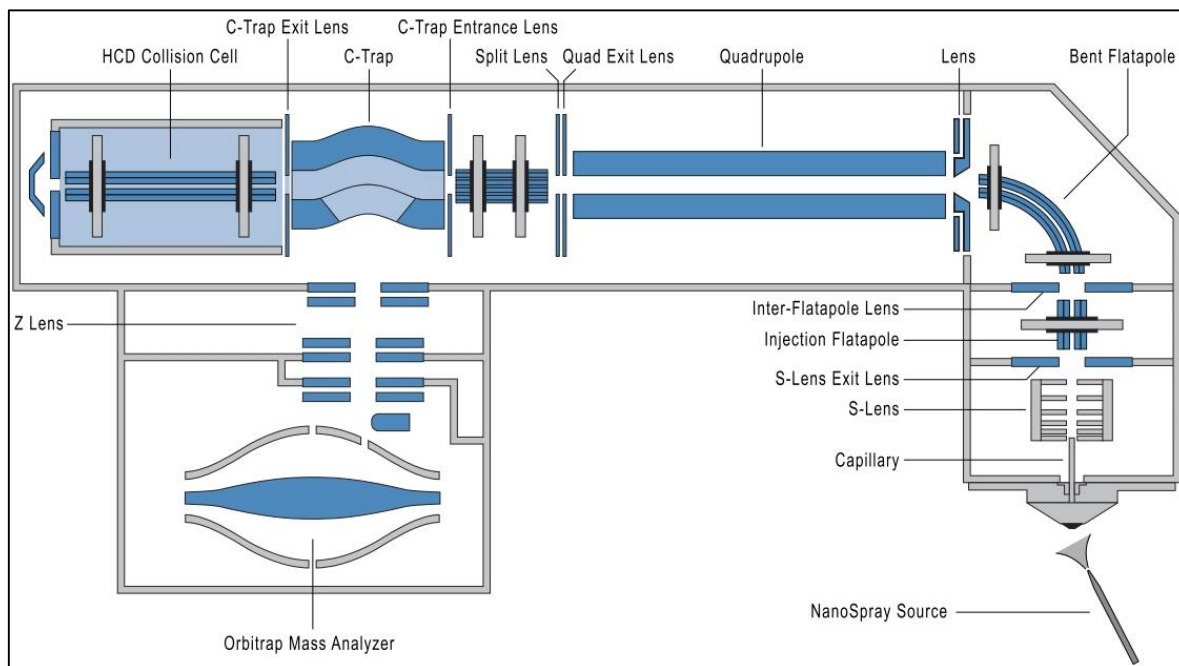
Mass spectrometry is a powerful analytical technique that ionises chemicals into ions (positive or negative, singly or multiply charged) then sorts and separates them by a mass analyzer based on their mass to charge ratio (m/z). Such information together with other parameters such as ion intensities and retention time (if the MS is coupled to a chromatography instrument such as liquid chromatography or gas chromatography) allow identification and quantification of chemicals within a sample. For samples generated from complex matrices (e.g. environmental or food), it is extremely important for a MS instrument to have high selectivity in order to differentiate between a chemical of interest and interferences. The selectivity of an instrument is reflected by its mass resolution,

which is defined as the ability to distinguish between two ions with very small differences in their m/z (ΔM) and calculated as the ratio of ion mass over ΔM (IUPAC, 1997). An MS platform that is capable of delivering mass resolution power more than 10,000 is considered a high resolution mass spectrometer (HRMS).

There are various types of HRMS, each with their own limitations and advantages. Some common types of mass spectrometry systems for environmental analysis are sector field, time of flight, Fourier transform ion cyclotron resonance, and Orbitrap. A sector field MS instrument often consisted of both magnetic sector and electric sector that provide high reproducibility, sensitivity and resolution. However, they are bulky, expensive and has limited application in untargeted screening analysis. The Fourier transform ion cyclotron resonance (FT-ICR) MS can provide extremely high resolution power up to over 1,000,000 (Ghaste et al., 2016) but it is very expensive and performs at relatively slow scan rate. FT-ICR-MS is also a complex system that takes up a large laboratory space. The time of flight (TOF) instruments have high scan rates, dynamic range and resolution power (up to 60,000) but limited precursor selectivity in MS/MS experiments (Eichhorn et al., 2012; Ghaste et al., 2016).

Orbitrap technology is the most recent advance in mass spectrometry that has been invented by Alexander Makarov in 2000 (Makarov, 2000). Schematic representation of an Orbitrap mass spectrometer (Q Exactive series) is shown in Figure 1.1. Samples are introduced into the Ion Max Atmospheric Pressure Ionization housing via a nanospray needle. The instrument is capable of ionizing samples by three different ionization technique: Electro Spray Ionization (ESI), Atmospheric Pressure Chemical Ionization (APCI) and Atmospheric Pressure Photoionization (APPI), each technique can be used in positive (+), negative (-) or alternative switching positive/negative (+)/(-) polarity. The ion beams enter the mass spectrometer via a S-Lens system and then it is transmitted to the quadrupole through a series of flatapole to remove neutral particles. The quadrupole can act as a precursor selection unit, which filters out unwanted ions based on a preselected mass range. After exiting the quarupole, the ion beam is accumulated in the C-Trap. After a package of ions (which can contain multiple ions beams) is trapped in the C-Trap (defined by AGC Target number), MS/MS fragmentation can be done in the Higher Energy Collisional Dissociation (HCD) cell if needed, then the ion package is introduced into the Orbitrap mass analyzer through the Z Lens.

Figure 1.1: Schematic components of the Q Exactive Orbitrap mass spectrometer series (Michalski et al., 2011b).



The Orbitrap mass analyzer consists of an outer barrel-like electrode and a coaxial inner spindle-like electrode (Figure 1.1) (Qizhi et al., 2005). Once an ion package entered the Orbitrap, they start to oscillate back and forth around the inner electrode. This orbital movement creates an image current which can be converted into a mass spectrum by Fourier transformation (Qizhi et al., 2005, Annette Michalski et al., 2011) at up to 150,000 FWHM in early models and 1,000,000 FWHM in some modern ones.

Some typical scan functions can be carried out by an Orbitrap MS instrument are: Full Scan (FS), All Ion Fragmentation (AIF), Single Ion Monitoring (SIM), Parallel Reaction Monitoring (PRM) and Data Independent Analysis (DIA). Additionally, different scan functions can be used in one method, either each function in a different time range; or alternating analysis throughout a time period. In order to choose a proper MS data acquisition mode for a particular analysis, it is necessary to understand the mechanism of each mode.

Full Scan mode provides mass spectrum of ions without any preselection in the quadrupole or further fragmentation. A data dependent MS/MS acquisition can be performed if needed after a full scan cycle. This mode is Full MS-ddMS² or TopN acquisition where a full scan is obtained and then N highest intensity m/z (Top N) are

fragmented in subsequent N number of PRM scans, each scan feature one among N previously mentioned m/z in the order from highest to lowest intensity.

All Ion Fragmentation allows fragmentation of all the ions produced by the ionization source. This can be done by 2 types of induction: in source collision induced dissociation (in source CID) and HCD. The in source CID technique utilizes the nebulizer, drying or sheath gas to collide with the ions formed in the atmospheric pressure region (before entering the entrance cone) (Parcher et al., 2017). Whereas the HCD cell fragments ion packages (introduced via the C-trap) with prefilled nitrogen gas (Figure 1.1), in-source CID and HCD can be applied together for a pseudo MS³ experiment.

Single Ion Monitoring mode is similar to Selected Ion Monitoring mode in single quad and triple quad instruments where a narrow population of precursors ion (can be as narrow as ± 0.2 m/z) was preselected by the quadrupole and analyzed in the Orbitrap.

Parallel Reaction Monitoring is somewhat comparable to Single Reaction Monitoring (SRM) or Multiple Reaction Monitoring (MRM) in triple quad instruments, however, the HCD cell serves as Q2 and the Orbitrap serves as Q3. Basically, a precursor ion is selected by the quadrupole, fragmented by the HCD cell, and all the fragmentation ions are analyzed by the Orbitrap.

In Data Independent Analysis, samples are often infused into the MS via syringe pump. A mass range of ions of interested (e.g. 400 to 1000 m/z) is then divided into smaller, equal mass segments (e.g. 400 to 410 m/z, 410 to 420 m/z, ..., 990 to 1000 m/z) and MS/MS experiments are done on these segments, continuously.

Depending on the purposes of a particular experiment, different Orbitrap MS parameters including ionization mode, polarity and scan mode can be chosen accordingly.

Commercially available in 2005, UPLC-Orbitrap HRMS is a state of the art platform, which consist of ultra performance liquid chromatography coupled to Orbitrap MS. It has soon become very popular in biosciences applications such as proteomics or metabolomics thanks to its fast separation, high resolution, accurate ion masses (up to less than 1 ppm mass deviation) features (Dunn et al., 2008; Lu et al., 2008; A Michalski et al., 2011; Yates et al., 2009). With these features, it is thought that UPLC-Orbitrap HRMS is also suitable to study other classes of chemicals in addition to protein and

metabolites such as pharmaceuticals or environmental contaminants. However, the potential of Orbitrap technology has not been fully explored and its capabilities are not fully exploited in the field of environmental analysis. Recently, a HPLC-Orbitrap MS method has been developed to analyze 27 brominated flame retardants (BFRs) in fish using Atmospheric Pressure Photoionization (APPI) (Zacs and Bartkevics, 2015). The method was reported to be rapid, sensitive (method limit of detections 0.001 – 0.25 ng g⁻¹ sample) and selective where almost no background noise was observed at quantifying m/z of detected BFRs in fish samples. Comparable results of BFRs in fish were achieved in comparison with a gas chromatography (GC)-HRMS method, which is often referred to as the gold standard platform to analyze this class of chemical. Additionally, in contrast to GC, chromatographic separation of the method was done using liquid chromatography that can avoid degradation of some thermal labile BFRs (Zacs and Bartkevics, 2015). This demonstrated the great potential of Orbitrap technology in environmental science studies.

Therefore, in this thesis we aim to investigate the UPLC-Orbitrap-HRMS as an advanced platform for analysis of environmental contaminants, particularly brominated flame retardants and pharmaceutical and personal care products.

1.2. Novel Brominated Flame Retardants

1.2.1. Production, usage and physicochemical properties

Brominated flame retardants (BFRs) have been used extensively as additive/reactive flame retardants (FRs) to improve the fire resistance of combustible consumer products such as electronic equipment, flexible foam, plastics, textiles, wood and a wide range of other materials. Among the various classes of BFRs, polybrominated diphenyl ethers (PBDEs) have attracted the most attention with respect to environmental contamination. In May 2009, the Penta-BDE and Octa-BDE commercial mixtures were listed under the United Nations Environment Programme (UNEP) Stockholm Convention on persistent organic pollutants (POPs) due to their toxicity, persistence, bioaccumulation and long-range atmospheric transport. Manufacture and new use of Deca-BDE has also been restricted severely in Europe and the United States of America, and it is currently under active consideration for listing under the Stockholm Convention. Such restrictions on PBDEs without concomitant relaxation of fire retardancy regulations has paved the way

for increased use of novel or emerging brominated flame retardants (NBFRs/EBFRs), as alternatives for PBDEs. For example, 1,2-bis(2,4,6-tribromophenoxy) ethane (BTBPE) and decabromodiphenyl ethane (DBDPE) have been suggested as replacements for Octa-BDE and Deca-BDE commercial mixtures, respectively (Brown et al., 2014).

To date, the exact production volume of NBFRs is still unknown but it was estimated to be around 100,000 metric tons per year (Harju et al., 2008). This number however covered only 21 NBFRs. Among those, 4 additive FRs namely DBDPE, BTBPE, bis(2-ethylhexyl) tetrabromophthalate (BEH-TEBP) and 2-ethylhexyl-2,3,4,5-tetrabromobenzoate (EH-TBB) are produced in higher volume than others and consequently have attracted more attention from environmental scientists. They were all classified as high production volume chemical in the US (produced or imported more than 500 tons per year) (USEPA, 2006; WHO, 1997). DBDPE is marketed under the trade names Saytex 8010 (Albermarle Corp.), FR-1410 (Dead Sea Bromine Co.) and Firemaster 2100R (Chemtura Corp.) and used in high-impact polystyrene (HIPS), engineering and thermoset plastic (e.g. ABS, polyamides, polycarbonates, etc.), wires and cables. BTBPE, EH-TBB and BEH-TEBP were produced by Chemtura Chemical Corporation and used in different flame retardant formulations: Firemaster 680 (BTBPE), Firemaster 550 (EH-TBB:BEH-TEBP in 4:1 ratio), Firemaster BZ-54 (EH-TBB:BEH-TEBP in 2.5:1 ratio) and DP-45 (BEH-TEBP) (Davis and Stapleton, 2009; Stapleton et al., 2008).

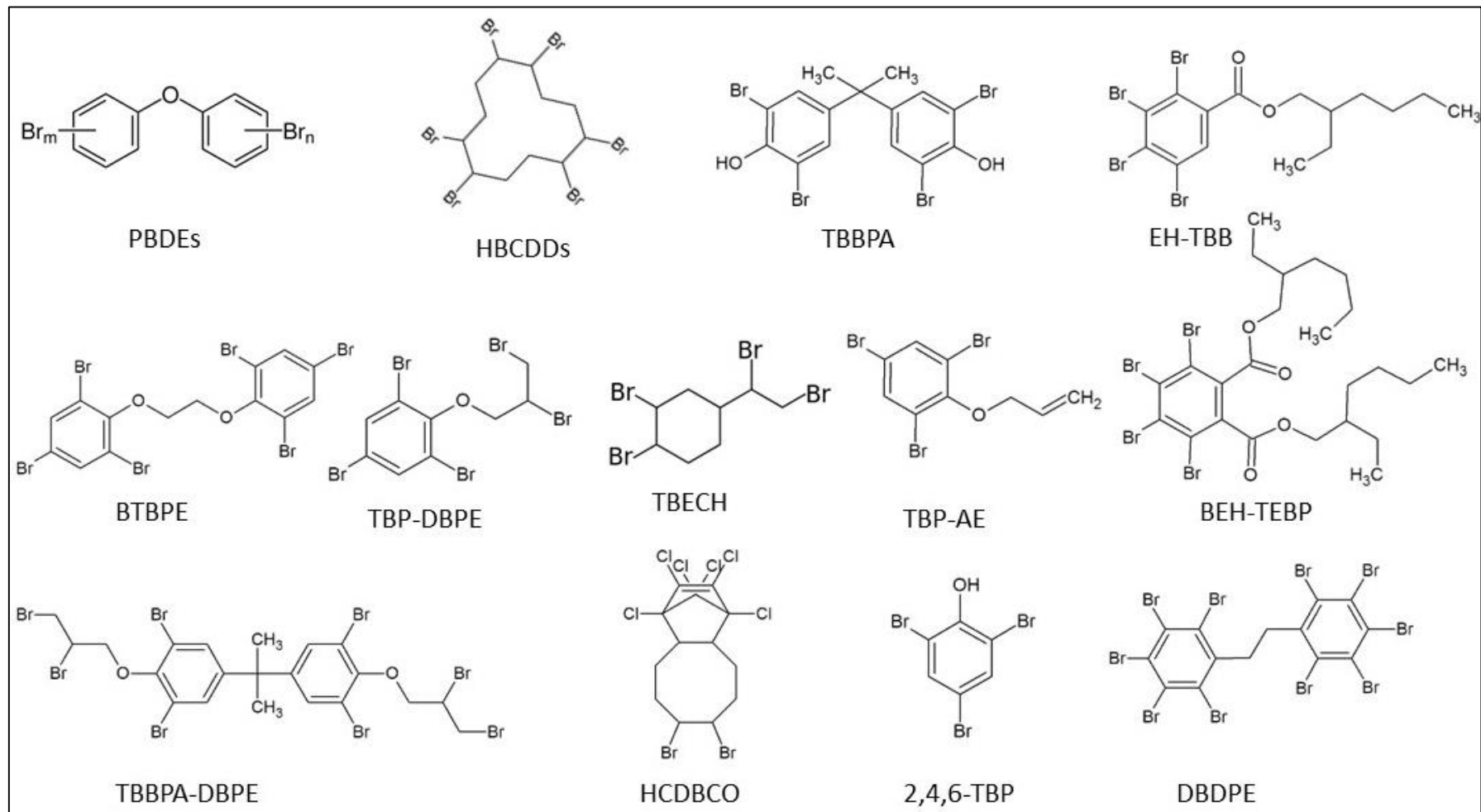
It is clear that the physicochemical properties of NBFRs are similar to that of legacy BFRs such as PBDEs, TBBPA or HBCDDs (Table 1.1). They often have high K_{ow} (octanol-water partition coefficient) and low water solubility values, meaning these compounds tend to accumulate in lipid-rich (e.g. adipose tissues) rather than in aqueous media. Due to these properties, NBFRs have the potential to bioaccumulate inside living organisms and biomagnify from lower to higher trophic levels in a food chain. Their vapour pressures are usually quite low, in the range of semi volatile organic compounds. NBFRs' chemical structures also resemble closely those of legacy BFRs with many bromine moieties usually directly attached to an aromatic ring (Figure 1.2). It is thought that they are endocrine disrupting chemical (EDC) candidates (Kovarich et al., 2011; Mankidy et al., 2014; Saunders et al., 2015b, 2013).

Table 1.1: Physicochemical properties of some legacy and novel BFRs reported by U.S EPA (commercial PBDEs) or estimated by EPI Suite™ v4.11

Abbreviation	Other abbreviation	CAS number	Compound	Chemical formula	Log K _{ow}	Vapor pressure at 25 °C (mm Hg)	Water solubility at 25 °C (µg/L)
BEH-TEBP	TBPH	26040-51-7	Bis(2-ethylhexyl) tetrabromophthalate	C ₂₄ H ₃₄ Br ₄ O ₄	11.95	1.71E-11	1.91E-3
BTBPE		37853-59-1	1,2-Bis(2,4,6-tribromophenoxy) ethane	C ₁₄ H ₈ Br ₆ O ₂	9.15	2.38E-10	0.22
Commercial Deca-BDE				C ₁₂ Br ₁₀ O	6.27	3.2E-8	< 1
Commercial Octa-BDE				C ₁₂ H ₂ Br ₈ O	6.29	9.0E-10 - 1.7E-9	< 1
Commercial Penta-BDE				C ₁₂ H ₅ Br ₅ O	6.64 – 6.97	2.2E-7 - 5.5E-7	13.3
DBDPE		84852-53-9	Decabromodiphenyl ethane	C ₁₄ H ₄ Br ₁₀	13.64	1.9E-13	0.97E-3

DBE-DBCH	TBECH	3322-93-8	4-(1-2-Dibromoethyl)-1,2-dibromocyclohexane	C ₈ H ₁₂ Br ₄	5.24	1.05E-4	915
EH-TBB	TBB	183658-27-7	2-Ethylhexyl-2,3,4,5-tetrabromobenzoate	C ₁₅ H ₁₈ Br ₄ O ₂	8.75	3.43E-8	3.41
HBB		87-82-1	Hexabromobenzene	C ₆ Br ₆	7.33	1.68E-8	226
HBCDDs	HBCD	3194-55-6	Hexabromocyclododecanes	C ₁₂ H ₁₈ Br ₆	7.74	1.68E-8	3.07
HCDBCO	DBHCTD	51936-55-1	Hexachlorocyclopentadienyl-dibromocyclooctane	C ₁₃ H ₁₂ Br ₂ Cl ₆	7.91	1.07E-7	0.14
PBEB		85-22-3	Pentabromoethylbenzene	C ₈ H ₅ Br ₅	7.48	4.65E-6	104.7
TBBPA		79-94-7	Tetrabromobisphenol A	C ₁₅ H ₁₂ Br ₄ O ₂	5.90	6.24E-6	1
2,4,6-TBP		118-79-6	2,4,6-Tribromophenol	C ₆ H ₃ Br ₃ O	4.18	3.03E-4	>1000
TBP-AE	ATE	3278-89-5	2,4,6-Tribromophenyl allyl ether	C ₉ H ₇ Br ₃ O	5.59	1.10E-5	>1000
TBP-DBPE	DPTE	35109-60-5	2,4,6-Tribromophenyl 2,3-dibromopropyl ether	C ₉ H ₇ Br ₅ O	6.34	6.22E-7	79.8

Figure 1.2: Chemical structures of selected legacy and novel BFRs.



1.2.2. Toxicity and health effects

Currently, the toxicological effects of NBFRs are still not very well-studied and available data is scarce. DBDPE administered rats showed significantly increased thyroid hormone Triiodothyronine (T₃), Thiobarbituric acid (TBA) and decreased Creatinine (Cr) levels in comparison with control group (F. Wang et al., 2010a). Furthermore, DBDPE metabolites tended to accumulate in liver and kidney more than in adipose tissue. This indicated DBDPE and its metabolites have potential to influence the endocrine system and cause oxidative stress (F. Wang et al., 2010a). Similarly, it was also reported that DBDPE could inhibit antioxidant enzymes and therefore trigger oxidative stress in fish liver (Feng et al., 2013). By using human liver subcellular fractions, Smythe et al., 2017 found DBDPE able to inhibit deiodinases and sulfotransferases in human liver. This was also the first time a non-hydroxylated contaminant was reported to express such effects.

Mice exposed to tris(2,3-dibromopropyl) isocyanurate (TDBP-TAZTO) for 28 days showed severe toxic effects on mice lung, and altered lung and liver ultrastructure, especially mitochondria e.g. enhanced hepatocyte apoptosis and mitochondria degeneration in liver and mitochondria swelling in lung (J. Li et al., 2015). Using chicken LMH cells in conjunction with *in silico* modelling, Asnake et al., 2015 reported three NBFRs namely TBP-AE, TBP-BAE and TBP-DBPE inhibited androgen receptor (AR) activation, possibly by docking to the ligand binding pockets of chicken AR. The endocrine toxicities of other NBFRs in animal models have also been reported. For example, in fish, an EH-TBB and BEH-TEBP mixture and HCDBCO altered gene expression and decrease fecundity (Saunders et al., 2015a, 2015b), β -DBE-DBCH disrupted thyroid axis (Park et al., 2011), and BTBPE affected transcriptional responses (Giraud et al., 2017).

In short, NBFRs do not usually express acute toxicity (Hardy et al., 2012; F. Wang et al., 2010a) but instead mainly chronic effects on the endocrine system of target organism by different mechanisms.

1.2.3. Occurrence in major environmental compartments of concern

Non-occupational human exposure to so-called “legacy” BFRs such as PBDEs, HBCDDs and TBBPA occurs mainly through ingestion of indoor dust and diet with lesser contributions from indoor air inhalation and dermal absorption (although substantial uncertainty exists about the magnitude of the latter) (Abdallah and Harrad, 2014, 2011; Lorber, 2008). Currently, very limited data are available for NBFRs in terms of human exposure; however considering the fact they share quite similar physicochemical properties with conventional BFRs, it is plausible to hypothesise that human exposure to NBFRs will occur via pathways similar to those for “legacy” BFRs (Table 1.1).

1.2.3.1. Indoor dust exposure

For PBDEs, house dust has been highlighted as accounting for 82 % of the estimated intake of PBDEs in the U.S population (Lorber, 2008). Unsurprisingly therefore, an increasing volume of data are emerging about the presence of NBFRs especially BEH-TEBP, EH-TBB, DBDPE, and BTBPE in indoor dust.

As NBFRs is a general term covering a wide range of organobromine compounds with different physicochemical properties, most studies only focus on a limited number of chemicals in this group. The most common compounds analyzed and which frequently exhibit the highest concentrations in indoor media are: EH-TBB, BEH-TEBP, DBDPE, BTBPE, and HBB. More studies on other NBFRs are needed.

Concentrations of these 5 common NBFRs in indoor dust are usually in the low ng g^{-1} range. Among different non-occupational indoor microenvironment categories, houses have received the most attention, followed by offices and cars. Available data indicates that concentrations of DBDPE and BTBPE in office dust surpass those in house dust, while those of other NBFRs are comparable between different microenvironments.

Harrad et al. (2008) reported median concentrations in UK house, office and car dust of 24, 99 and 100 ng g^{-1} for DBDPE and 5.3 ng g^{-1} , <MDL, and <MDL for BTBPE in the respective microenvironments. A recent study on house dust from Birmingham, UK found pentabromoethylbenzene (PBEB), EH-TBB, BEH-TEBP, BTBPE and DBDPE at median concentrations of 0.3, 4.1, 1.2, 36, 74 ng g^{-1} in kitchen dust and 0.4, 12, 75, 4.5, and 120 ng g^{-1} in living room/bedroom dust, respectively (Kuang et al., 2016). DBDPE concentrations in UK living room/bedroom dust sampled during 2006-07 (median, 24 ng

g^{-1}) were significantly exceeded by those in dust sampled in 2015 (median, 120 ng g^{-1}) (Kuang et al., 2016). Similar concentrations of EH-TBB, BTBPE and DBDPE to those reported by Kuang et al., 2016 in house dust collected in 2015 were found in a separate study conducted in Birmingham on house dust sampled in 2013 and 2014 by Al-Omran and Harrad, 2015. They also discovered that BEH-TEBP concentrations significantly increase with decreasing dust particle size, however this was not the case for other NFRs in the study. House and office dust collected in Birmingham in 2015 were frequently detected with a broad suite of NFRs including α - and β -4-(1-2-dibromoethyl)-1,2-dibromocyclohexane (DBE-DBCH), pentabromobenzene (PBBz), tetrabromo-*o*-chlorotoluene (TBCT), pentabromotoluene (PBT), 1,2,4,5-tetrabromo-3,6-dimethylbenzene (TBX), 2-3-dibromopropyl-2,4,6-tribromophenyl ether (TBP-DBPE), hexabromobenzene (HBB), syn- and anti-dechlorane plus (DDC-CO), tetrabromobisphenolA bis(2,3-dibromopropyl ether (TBBPA-BDBPE), PBEB, EH-TBB, BTBPE, and BEH-TEBP (Tao et al., 2016). The median concentration of NFRs in house and office dust samples mostly fell between <0.01 to 62 ng g^{-1} with some exceptions: TBBPA-BDBPE in house dust (1000 ng g^{-1}) and BTBPE, BEH-TEBP, DBDPE and TBBPA-DBPE in office dust (160 , 160 , 440 and 2300 ng g^{-1}) (Tao et al., 2016). By comparison with results from a previous study in the same area (Harrad et al., 2008), the authors suggested that restrictions on legacy FRs have increased demand for NFRs in the UK (reflected by the significant higher concentrations of BTBPE and DBDPE in office dust and DBDPE in house dust over the time course 2007 to 2015) (Tao et al., 2016).

Inspection of the global database reveals clear geographical differences in the relative abundance of different NFRs. Specifically, in North America, EH-TBB and BEH-TEBP predominate, but in Asia, especially China, BTBPE and DBDPE are the most abundant. In an urban area of Guangzhou, South China; Wang et al. (2010) reported BTBPE, DBDPE, PBT, PBEB and HBB to be present in house dust at median concentrations (range) of 6.47 (nd-211), 2733 (100-47000), 1.52 (0.22-12), 0.15 (nd-2.05) and 18.1 (1.95-483) ng g^{-1} respectively. Significantly increased levels of BTBPE (by a factor between 1 and 8) and DBDPE (by between 40-400 times) between 2010 and 2015 were observed in dust from 3 sites in Longtang, China (Zheng et al., 2015).

In North America, Stapleton et al. (2008) reported geometric mean concentrations of 39.4, 17.7, 91.1, and 65.8 ng g⁻¹ for DBDPE, BTBPE, EH-TBB and BEH-TEBP, respectively in home vacuum bags collected in Boston, US in 2006 (n=19). Another study compared NBFR concentrations in dust collected from the living areas of sixteen homes in northern California, US in 2006 with those in detected in dust collected in the same homes in 2011. Concentrations of BTBPE stayed relatively static over time while EH-TBB, BEH-TEBP and DBDPE exhibited an increasing trend over the 5 years period (Dodson et al., 2012). A wide range of current use BFRs were detected in house dust sampled during 2007-2008 in Vancouver, Canada, specifically: allyl-2,4,6-tribromophenyl ether (TBP-AE), pentabromobenzyl acrylate (PBB-Acr), octabromotrimethylphenyl indane (OBTMPI), 2-bromoallyl-2,4,6-tribromophenyl ether (TBP-BAE), EH-TBB, BEH-TEBP, BTBPE, HBB, PBB, PBT, TBP-DBPE, PBEB, TBCT, BB-101 and TBX; with EH-TBB and BEH-TEBP present at much higher levels than others (Shoeib et al., 2012). Similar patterns were also observed elsewhere in Canada (Abbasi et al., 2016; Fan et al., 2016; Venier et al., 2016).

A consistent finding across all studies to date is that the EH-TBB:BEH-TEBP ratio in dust differs markedly (in both directions) from the 4:1 value present in commercial Firemaster 550 (Ali et al., 2011; Stapleton et al., 2008). The implication of these observations is that there exist sources additional to FM-550 (e.g. use of BEH-TEBP as a plasticizer) and/or that there are substantial differences in the environmental behavior (e.g. volatility, degradation rate) of the two compounds.

Another noteworthy observation is that dust in e-waste recycling facilities and adjacent houses often contains much higher concentration of NBFRs than residential dust from locations not impacted by e-waste recycling. Urban and suburban house dust collected in 2008 in Vietnam showed BTBPE and DBDPE to be present at maximum concentrations of 100 and 150 ng g⁻¹, respectively, while those in two Vietnamese e-waste recycling sites were 6 to 10 times higher: 620 ng g⁻¹ for BTBPE and 1,600 ng g⁻¹ for DBDPE (Tue et al., 2013).

Besides e-waste impacted areas, dust samples from some other less common microenvironments were also found to contain very high NBFRs levels. Allen et al. (2013) reported a suite of NBFRs in dust from carpets and air vents on airplanes (n=40,

sampled in 2010) at much higher concentrations than reported elsewhere for house, car or office dust. Median concentrations of BTBPE, HBB, EH-TBB and BEH-TEBP were 330, 100, 350 and 640 ng g⁻¹ for carpet dust and 1300, 45, 740 and 1200 ng g⁻¹ for air vent dust, respectively. Recently, La Guardia and Hale (2015) detected extremely high levels of EH-TBB and BEH-TEBP in dust from houses of 4 gymnasium coaches (averages of 2580 and 1850 ng g⁻¹ respectively) with even higher concentrations (averages of 40800 and 24300 ng g⁻¹ respectively) found in dust from their corresponding work places.

Table 1.2: Summary median concentrations of some common novel brominated flame retardants in indoor dust (ng g⁻¹)

Location	Sampling time	Sample type	N	EH-TBB	BEH-TBEP	DBDPE	BTBPE	TBBPA-DBPE	α -DBE-DBCH	β -DBE-DBCH	Reference
Sweden	2012	Office, store, school, apartment	27	9.1	140	12	17		1.2		Newton et al., 2015
UK	2006 2007	House	30			24	5.3				Stuart et al., 2008
		Office	18			99	<dl				
		Car	20			100	<dl				
UK	2007 2008	Classroom	36	9	96	98	9	107			Ali et al., 2011
Belgium	2008	House	39	1	13	153	2	78			
		Office	6	7	64	721	19	306			
Romania	2010	House	47	5	20	170	5				Diru et al., 2012
	2008	House	25			140.8	<2.0				

Czech Republic		Car	30			98.8	<2.1				Kalachova et al., 2012
Norway	2012	House	48	16.1	132	512	8.73	1.93	1.72		Cequier et al., 2014
		Classroom	6	2.67	99.9	179	13.4	0.269	3.31		
Germany	NA	House	20	<3.0	343	146	<10				Fromme et al., 2014
Boston, US	2002 2003	House	38	409 ^b	377 ^b		22 ^b				Johnson et al., 2013
California, US	2010 2011	House	59	337	186	82.8	22.3		0.91	0.75	Brown et al., 2014
		Fire station	27	2687	2076	161	28.4		<0.64	ND	
Vancouver Canada	2007 2008	House	116	120	99		30				Shoeib et al., 2012
India	2006	Commercial buildings	NA			67	220				Devanathan et al., 2011
		EWRS	NA			120	65000				
		Residential buildings	NA			15	48				

New Zealand	2008	House	50	4 ^a	17 ^a	26 ^a	3 ^a				Ali et al., 2012a
Pakistan	NA	House	15	0.4	5.8	90	15				Ali et al., 2013
		Car	15	0.5	6.5	65	10.5				
Kuwait	NA	House	15	6.6	54	220	6.8				Ali et al., 2013
		Car	15	13	85	202	4				
Egypt	2013	House	17	0.81	0.12		0.24			0.18	Hassan and Shoeib, 2015
		Office	5	7.14	0.09		1.26			0.04	
		Car	9	5.81	0.6		2.36			0.42	
Thailand	2007 2008	E-waste storage facilities	25			890					Muenhor et al., 2010
Vietnam	2008	House	13			40 – 46 ^c	7.1 - 3.1 ^c				Tue et al., 2013
		House and workshop in 2 EWRS	20			220 – 230 ^c	17 – 56 ^c				

Japan	2009	House				220					Mizouchi et al., 2015
	2010	School				50					
South China	2008	House in	27			63.1	20				Wang et al., 2010
	2009	EWRS									
	2007	House in urban area	19			2733	6.47				
China	2010	House and public places	81	130	120	1100	120				Qi et al., 2014

^a: arithmetic mean ^b: geometric mean ^c: median range

*: $\alpha+\beta$ DBE-DBCH; EWRS: E-waste recycling sites; n: sample number

1.2.3.2. Indoor air exposure

The first report about BTBPE and DBDPE in household air was published by Karlsson et al., 2007. In 5 samples from Örebro, Stockholm and Norrköping in Sweden, the authors found DBDPE in one from Örebro at 22.9 pg m^{-3} while BTBPE was not detected in any samples. Recently, indoor air from twelve offices, stores, and apartments in Stockholm was assessed (Newton et al., 2015). Geometric mean concentrations of NFRs in these samples were: DBE-DBCH ($\alpha+\beta$) 43 pg m^{-3} , PBT 10 pg m^{-3} , HBB 7.2 pg m^{-3} , BEH-TEBP 42 pg m^{-3} , and DBDPE 79 pg m^{-3} . In Norway, Cequier et al., 2014 monitored a broad range of NFRs in air samples from 48 households, with mean (maximum) concentrations of: DBE-DBCH 222 pg m^{-3} (4120), TBP-AE 6.69 pg m^{-3} (69.3), TBX 64.5 pg m^{-3} (2830), PBB 9.30 pg m^{-3} (50.8), PBT 14.3 pg m^{-3} (213), PBEB 1.29 pg m^{-3} (30.6), TBP-DBPE 5.49 pg m^{-3} (132), DBDPE 38.2 pg m^{-3} (963), and HBB 12.4 pg m^{-3} (297).

Saito et al. (2007) observed 2,4,6-tribromophenol (TBP) and HBB in air inside Tokyo homes ($n=18$) at concentrations in the range $\text{nd}-6800 \text{ pg m}^{-3}$ and $\text{nd}-710 \text{ pg m}^{-3}$, respectively. Concentrations in office buildings in the same area ($n=14$) also contained TBP ($\text{nd}-2800 \text{ pg m}^{-3}$) and HBB ($\text{nd}-950 \text{ pg m}^{-3}$) (Saito et al., 2007). In comparison, atmospheric concentrations of TBP in 2 houses in Hokkaido, Japan fell between 220 and 690 pg m^{-3} which was an order of magnitude higher than adjacent outdoor air (Takigami et al., 2009). Residential indoor air in Guangzhou, China was detected with DBDPE at median concentration 74.9 pg m^{-3} (Ding et al., 2016). In the eastern United States, elevated concentrations were detected of EH-TBB and BEH-TEBP in air sampled within a gymnasium. When air was sampled within 30 cm of a foam pit in this gymnasium, concentrations as high as 26100 pg m^{-3} of EH-TBB and 16900 pg m^{-3} of BEH-TEBP were recorded; however when samples were collected further from the pit, concentrations reduced to 5010 pg m^{-3} and 2660 pg m^{-3} , respectively (Carignan et al., 2013).

One of the main pathways for occupational exposure to NFRs is through indoor air and dust inhalation and ingestion in working environments. As expected, air samples inside e-waste recycling facilities exhibited high concentrations of NFRs. The inhalable dust fraction in air samples taken from an electronic recycling facility in Örebro, Sweden contained DBDPE (range, $<20-790 \text{ pg m}^{-3}$) and BTBPE (range, $130-11850 \text{ pg m}^{-3}$) (Julander et al., 2005). Moreover, even higher concentrations were reported in air from

other e-waste recycling plants in Sweden, namely 10 to 1200 pg m⁻³ for DBDPE and 600 to 67000 pg m⁻³ for BTBPE (Pettersson-Julander et al., 2004; Sjödin et al., 2001). Dismantling halls displayed the highest concentrations in these plants. Elsewhere in Scandinavia, Rosenberg et al., 2011 observed elevated concentrations of DBDPE (4500-1,700,000 pg m⁻³), BTBPE (nd-57,000 pg m⁻³) and HBB (nd-560,000 pg m⁻³) in two Finnish waste electrical and electronic equipment recycling sites.

The available data suggest that the sources of non-dietary human exposure to NBFRs are predominantly indoor but that one should also consider outdoor media if the studying area is impacted by industrial and/or e-waste recycling activities. With very limited data, however, it is hard to conclude how much these activities contribute to the total NBFR exposure via air inhalation of residents living in contaminated area. More research on indoor and outdoor air in the vicinity of industrial zones and e-waste recycling sites is recommended.

1.2.3.3. Dietary Exposure

Dietary exposure is unarguably a major human exposure pathway for legacy BFRs such as PBDEs and HBCDDs (Abdallah and Harrad, 2014, 2011; Lorber, 2008). Given the similarity between the physicochemical properties of these legacy BFRs and NBFRs, it is reasonable to hypothesize that the diet will also be a substantial pathway of human exposure to the latter. There are several approaches to dietary exposure assessment. The most commonly employed is the Total Diet Study (TDS) or market basket approach in which a sample list is generated from a total diet survey that covers categories of food and drink commonly consumed by the study population. Samples are ideally prepared as consumed for analysis rather than analyzed raw. Subsequent determination of concentrations of target contaminants (e.g. NBFRs) in these samples, combined with information on the rate at which such foodstuffs are consumed, permits estimation of total dietary exposure to the study population. An alternative is analysis of NBFRs in a smaller number of human foodstuffs such as a selection of fish and shell-fish. The limited data to date, suggest relatively low levels of NBFRs in the food supply. Unlike the situation in dust samples, PBEB appears in seafood samples at higher or comparable levels to other NBFRs like EH-TBB or BEH-TEBP.

Lake trout samples from Lake Ontario, Canada during the period 1979 to 2004 showed high BTBPE and PBEB concentrations up to $2.6 \pm 0.3 \text{ ng g}^{-1} \text{ l.w}$ for BTBPE (mean, 1993 samples) and $320 \pm 156 \text{ ng g}^{-1} \text{ l.w}$ (mean, 1988 samples) for PBEB (Ismail et al., 2009). Another Canadian seafood study reported NBFs in American eels to fall in the ranges ($\text{ng g}^{-1} \text{ l.w}$): PBT (nd-19.1), PBEB (nd-2.7), TBP-DBPE (nd-75.9) and EH-TBB (nd-5.2) (Sühring et al., 2014). Further south, some common NBFs in wildlife from San Francisco Bay (white croaker, shiner surfperch, cormorant egg and harbor seal) were analyzed for but not detected, with the exception of frequently detection of PBEB in harbor seal blubber (maximum $0.5 \text{ ng g}^{-1} \text{ l.w}$) (Klosterhaus et al., 2012).

In TDS studies, targeted NBFs were only occasionally detected at low concentrations, mainly in fish and sometimes in meat. This suggests that at this moment, NBFs affect the food chain primarily via aquatic environments. Fernandes et al., 2009 used a TDS approach consisting of more than 100 samples of vegetables, meats, fish, dairy products and processed foods to assess the presence of NBFs in UK foods. HBB and DBDPE were not detected in any samples but BTBPE was occasionally detected at low levels, mainly in foods of animal origin such as: mackerel ($0.03 \text{ ng g}^{-1} \text{ w.w}$), ox kidney ($0.05 \text{ ng g}^{-1} \text{ w.w}$), chicken liver ($0.04 \text{ ng g}^{-1} \text{ w.w}$), lemon sole ($0.04 \text{ ng g}^{-1} \text{ w.w}$), and pork ($0.06 \text{ ng g}^{-1} \text{ w.w}$) (Fernandes et al., 2009). Similar findings were reported in other European countries (Sahlström et al., 2015; Tlustos et al., 2010; Xu et al., 2015). Recently, Tao et al., 2017 monitored 16 NBFs in meat, liver, seafood, eggs and dairy products purchased in UK supermarket and found β -BDE-DBCH to be the predominant chemical accounting for $64.5 \pm 23.4 \%$ of total NBFs. Among detected NBFs, β -BDE-DBCH showed the highest detection frequency at 100% following by α -DBE-DBE (97%), EH-TBB (77%), BEH-TEBP (63%) and BTBPE (60%); their average concentrations ranged from <0.04 to $85 \text{ ng g}^{-1} \text{ lw}$ (Tao et al., 2017). In Irish foods, HBB, DBDPE and BTBPE were not detected in any of 100 composite samples studied (Tlustos et al., 2010). Meat, seafood, and processed seafood purchased from Belgian supermarkets showed no detectable levels of HCDBCO, BTBPE EH-TBB, and BEH-TEBP except BTBPE and BEH-TEBP in smoked salmon (0.035 and $0.084 \text{ ng g}^{-1} \text{ w.w}$, respectively) (Xu et al., 2015). Aggregated Swedish diet samples from five categories (fish, meat, dairy products, vegetable oils and egg) exhibited NBF concentrations that only exceeded the limit of quantification (LOQ)

levels in fish samples with the exception of BTBPE in eggs which was detected at an average concentration of $3.9 \text{ pg g}^{-1} \text{ w.w.}$ (Sahlström et al., 2015).

Monitoring programs also suggest one pathway via industrial activities have the potential to pollute aquatic environments may include waste water treatment plants. Molluscs along the northern coast of Spain showed non-detectable levels of EH-TBB, BEH-TEBP, BTBPE and DBDPE with the exception of EH-TBB in wild mussel ($0.06 \pm 0.01 \text{ ng g}^{-1} \text{ w.w.}$) and BTBPE in raft cultured mussels and clams (0.16 ± 0.06 and $0.1 \pm 0.02 \text{ ng g}^{-1} \text{ w.w.}$, respectively) (Villaverde-de-Sáa et al., 2013). Isobe et al. (2012) also reported low concentrations of BTBPE and DBDPE in mussels from coastal waters of China, Japan, Hong Kong, Cambodia, Vietnam, Malaysia, Indonesia, and India. However, by comparison, concentrations of EH-TBB, BEH-TEBP, and BTBPE observed in molluscs from the Yadkin River, United States, downstream from a textile manufacturing waste water treatment plant outfall were among the highest reported worldwide: nd to 2,220, nd to 1,370 and nd to $303 \text{ ng g}^{-1} \text{ l.w.}$, respectively (La Guardia et al., 2012). The highest concentrations were all found at the outfall, with concentrations declining markedly in samples taken along the river at 16.8, 25.2 and 44.6 km distant from the outfall. Highly elevated concentrations of BB-153 in shellfish along the French coast were found at a site heavily impacted by chemical, petroleum and steel industries, up to $81.8 \text{ pg g}^{-1} \text{ w.w.}$ (Munsch et al., 2015). In Eastern China, composite foodstuffs including fish, shrimp, chicken, duck, pork, livers and eggs were detected with considerable levels of PBEB, HBB, EH-TBB, BEH-TEBP, BTBPE, and DBDPE (Labunska et al., 2015). Their mean concentration ranges were: <0.17 to 6.81, <0.15 to 6.49, <0.20 to 62.2, <0.25 to 16.3, <0.35 to 15.0 and <0.45 to 45.3 $\text{ng g}^{-1} \text{ l.w.}$, respectively. In general, dietary samples from e-waste impacted areas often exhibited higher concentrations of NBFRs than their corresponding control samples (Labunska et al., 2015).

Interestingly, BTBPE and DBDPE were also reported in commercial honey from Brazil, Morocco, Portugal and Spain at low concentrations (range, $<\text{LOD}$ to $4.22 \text{ pg g}^{-1} \text{ fresh weight}$) (Mohr et al., 2014). Moreover, Liu et al. (2014) detected PBB, HBB and DBDPE in baby foods (formula, cereal and puree) from the U.S and Chinese markets within the ranges 1.35 to 128.4, 0.75 to 11.4 and 3.34 to 48.8 $\text{pg g}^{-1} \text{ fresh weight}$, respectively.

Besides direct exposure via food consumption, one should also pay attention to indirect human exposure to NBFRs which could happen through contact between foodstuffs (Polder et al., 2016) and kitchen dust, NBFR-containing kitchenware, kitchen utensils, food packaging materials and food storage containers. Kuang et al. (2016) found PBEB, EH-TBB, BEH-TEBP, BTBPE and DBDPE in UK kitchen dust at notable maximum concentrations: 25, 290, 420, 10 and 450 ng g⁻¹, respectively. Evidence of DBDPE contamination was found in electric frying pans and thermo cups purchased in Europe (Puype et al., 2015; Samsonek and Puype, 2013). Some UK black plastic kitchen utensils were measured with considerable amount of BTBPE, BEH-TEBP, DBDPE and EH-TBB, even up to 1000 µg g⁻¹ of BTBPE in one utensil (Kuang et al., 2018). The authors also estimated that 20% of NBFRs can be transfer from cooking utensils to hot cooking oil using a simulated cooking experiment (Kuang et al., 2018). Moreover, frequent detection of BATE, PBT, PBB, PBEB, HBB, TBP-DBPE, BTBPE and DBDPE with up to 560 ng g⁻¹ l.w (TBP-DBPE) was observed in fat samples from kitchen hoods (n=15) which suggests kitchens may play an important role in NBFR exposure (Bendig et al., 2013).

1.2.4. Human body burdens of NBFRs

One of the very first studies about NBFRs in biological samples reported HBB in Japanese human adipose tissue samples at concentrations ranging between 0.35 and 0.65 ng g⁻¹ w.w (Yamaguchi et al., 1988a). The authors moreover suggested that PBB and 1,2,4,5-tetrabromobenzene (TeBB) found in the tissues may be HBB metabolites as these were found in earlier rat metabolism studies (Yamaguchi et al., 1988b, 1986). HBB was also detected in Danish, Finnish and New Zealand breast milk (Mannetje et al., 2013; Shen et al., 2008) and in Norwegian and Northern Chinese serum samples (Cequier et al., 2015, 2013; Zhu et al., 2009).

Of all NBFRs, 2,4,6-tribromophenol (2,4,6-TBP) appears the most commonly detected in human blood. Thomsen et al. (2001) found 2,4,6-TBP at concentrations 10-100 times higher than those of seven indicator PBDEs and TBBPA in plasma of three occupational groups in Norway. Human blood samples in U.S also contained 2,4,6-TBP at a median concentration of 3.0 ng g⁻¹ l.w (median) which was hypothesised to arise from human exposure to 2,4,6-TBP and/or metabolites of BDE-100 and BDE-154 (Qiu et al., 2009). A large scale study in Nunanvik Inuit adults in Canada revealed the presence of 2,4,6-

TBP (geometric mean, 58 ng L⁻¹ w.w) in blood plasma was significantly related to seafood consumption (Dallaire et al., 2009). Elsewhere, Kawashiro et al. (2008) detected 2,4,6-TBP in Japanese umbilical cord, cord blood and maternal blood samples at mean concentrations of 33, 37 and 22 pg g⁻¹ w.w, respectively. A low frequency of detection of TBP in blood plasma samples from Hong Kong people was reported with concentrations ranging from ND to 65 pg g⁻¹ l.w (Wang et al., 2012).

Interestingly, presenting contrast to the frequent reports of their presence in external media (see earlier sections), BTBPE and DBDPE have not to date been widely reported in biological samples. Indeed, their detection frequency in human samples is commonly <10 %. Such low detection rates of BTBPE and DBDPE suggest they are either efficiently metabolised in the human body and/or have low bioaccumulation potential (Zhou et al., 2014a; Zhu et al., 2009). Karlsson et al. (2007) could not detect BTBPE or DBDPE in plasma samples of five Swedish citizens. These two NBFs were also not detected in breast milk of first time Irish mothers (Pratt et al., 2013), serum of first time Swedish mothers and their toddlers (Sahlström et al., 2014), and the serum of Swedish aircraft personnel (Strid et al., 2014). Cequier et al. (2013) occasionally detected BTBPE in 10 Norwegian serum samples at a concentration range of nd-0.99 ng g⁻¹ l.w but no DBDPE was found. Similar results were reported in serum samples from Norwegian women (Cequier et al., 2015) or maternal serum (n=102) and milk (n=105) samples from Canada (Zhou et al., 2014a). On the other hand, very high DBDPE concentrations in Chinese serum samples have been detected: 125.2 ng g⁻¹ l.w for workers in e-waste recycling facilities, 56.1 ng g⁻¹ l.w for residents nearby and 13.8 ng g⁻¹ l.w for residents in urban area (Liang et al., 2016), however detection rates were not reported. Very recently, Tao et al., 2017 reported low median concentrations of α -BDE-DBCH, β -BDE-DBCH, EH-TBB, BEH-TEBP, BTBPE and DBDPE in UK human milk collected in 2010 and 2014-2015 ranging from <LOD to 3.1 ng g⁻¹ l.w. Interestingly, their respective detection rates were relatively high in samples collected in 2010 at 20%, 76%, 44%, 28%, 36% and 4% which was even higher in 2014-2015 samples at 100%, 100%, 90%, 40%, 50% and 10%, respectively (Tao et al., 2017).

He et al. (2013) targeted BEH-TEBP in pooled serum samples of Chinese living in Laizhou Bay area. Among 10 age-gender groups (males and female between 20 to 84 years), the authors found BEH-TEBP only in the 30 to 39 year-old female group at a mean

concentration of 260 ng g⁻¹ l.w. Low PBEB concentrations were reported in New Zealand breast milk (mean 0.001 ng g⁻¹ l.w) (Mannetje et al., 2013) and it was not detected in Chinese serum (Zhu et al., 2009).

Recently, non-invasive matrices have been considered in some studies to monitor NFRs. These include: hair, nail, urine or feces which are cost effective, easy to collect and most importantly do not require invasive sampling techniques. Zheng et al. (2011) were able to find HBB, BTBPE and DBDPE in hair of residents in Pearl River Delta, South China. The levels of BTBPE and HBB shared the same pattern: workers in e-waste workshops > residents in e-waste recycling area > residents in urban area ~ residents in rural area. Dust was proposed as a major exposure pathway for DBDPE and BTBPE as their concentrations in hair samples and dust samples were significantly correlated (Zheng et al., 2011). In a similar fashion, Liang et al (2016) reported DBDPE in human hairs from an e-waste recycling area southeastern China followed the aforementioned pattern of BTBPE and HBB: the mean concentrations were 82.5 ng g⁻¹ d.w (workers), 29.4 ng g⁻¹ d.w (residents in e-waste recycling area) and 10.9 ng g⁻¹ d.w (urban residents). These concentrations were significantly correlated between hair and serum samples for both workers and resident in e-waste recycling area (Liang et al., 2016). EH-TBB and BEH-TEBP were frequently detected in hair and fingernail samples (n=10) from donors based on the Indiana University Bloomington campus ranging between <9.2-230 and <17-240 ng g⁻¹, respectively, whereas PBB was found in only 2 hair samples (0.63 and 4.24 ng g⁻¹) (Liu et al., 2015). Using faeces as a biomonitoring matrix for toddlers (n=22), Sahlström et al. (2015) found a broad range of NFRs: BTBPE, BEH-TEBP, α- and β-DBE-DBCH, BATE, PBB, PBT, PBEB, HCDBCO and OBTMPI at sub ng g⁻¹ l.w levels. The above results support the idea that NFRs display variable bio-accumulation potentials and metabolic rates and most importantly, do accumulate in humans. At this stage, it is difficult to state which NFRs are of most concern with respect to human internal exposure. Therefore full understanding of their metabolic pathways is essential to identify the most appropriate biomarkers and thereby facilitate better-targeted biomonitoring programs.

1.2.5. NFRs metabolism

Currently, knowledge of the metabolic pathways of NBFRs is limited to a small number of *in vitro* and *in vivo* animal studies, mostly for EH-TBB, BEH-TEBP and HBB.

Yamaguchi et al. (1988b, 1986) found rapid reductive debromination of HBB administered to rats, forming 1,2,4-tribromobenzene; 1,2,3,4-, 1,2,3,5-, 1,2,4,5-tetrabromobenzene and PBB. Other HBB metabolites in rat, including pentabromophenol and some thiomethoxy (CH₃S) and methoxy (CH₃O) derivatives of tetra and pentabromobenzene were reported by Koss et al. (1982). Moreover, in humans, debrominated metabolites of HBB were detected in Japanese adipose tissue (Yamaguchi et al., 1988a), Swedish toddler faeces (Sahlström et al., 2015) and in Danish and Finnish breast milk and placenta samples (Shen et al., 2008). However, it is unclear whether these compounds derive from external exposure as opposed to metabolism of HBB.

Several *in vitro* studies have tried to identify the metabolites of EH-TBB and BEH-TEBP using different models like S9 fractions, liver microsomes or liver cytosol of humans, rats common carp, turtles and fathead minnows (Barr et al., 2012; Roberts et al., 2012). In general, while EH-TBB appears to be metabolised to 2,3,4,5-tetrabromobenzoic acid (TBBA) and 2,3,4,5-tetrabromomethylbenzoate (TBMB) at species-dependent rates; no metabolites of BEH-TEBP were identified. However, by using porcine carboxylesterase, BEH-TEBP was slowly transformed to mono (2-ethylhexyl) tetrabromophthalate (TBMEHP) (Roberts et al., 2012). No phase II metabolites (sulfation and glutathione conjugates) were found for both TBBA and TBMEHP using human liver microsomes and cytosol (Roberts et al., 2012). A later *in vivo* experiment also confirmed TBBA and 2,3,4,5-tetrabromophthalic acid (TBPA) as metabolites of the flame retardant Uniplex FRP-45 (>95 % BEH-TEBP and <5 % EH-TBB) in rat urine and serum (Silva et al., 2015). Based on these findings, TBBA was recommended as a biomarker of recent human exposure to EH-TBB (Hoffman et al., 2014; Silva et al., 2015). Indeed, TBBA was measured at a geometric mean of 5.6 pg mL⁻¹ (specific gravity corrected - SGC for urine dilution) in 77 % of adult urine samples from North Carolina, U.S and was significantly correlated with EH-TBB levels in corresponding paired handwipe samples (Hoffman et al., 2014). TBBA was also found in the urine of mothers (range, <3.0-62.2 pg mL⁻¹, SGC) and their children (range, <3.0-84.9 pg mL⁻¹, SGC) in New Jersey, U.S but with different detection rates (Butt et al., 2014). The more frequent detection in children (70 %) in comparison to their mothers (27 %), implies higher exposure to EH-TBB in children.

Metabolites of NBFRs other than EH-TBB, BEH-TEBP and HBB have been studied in some preliminary studies. Hakk et al. (2004) analyzed faeces of male rats administered BTBPE and found 2 groups of metabolites: (1) those arising from debromination and hydroxylation of aromatic rings and (2) those arising from hydrolysis of the ether linkage. A total of six metabolites were identified by the authors including 2,4,6-TBP. However, 2,4,6-TBP can be also a metabolite of other BFRs such as BDE-100, BDE-154 (Qiu et al., 2009), and TBP-DBPE (Von Der Recke and Vetter, 2007). For TBP-DBPE, in addition to 2,4,6-TBP, other potential metabolites detected were: TBP-AE (main metabolite), TBP-BAE and an unidentified compound formed under anaerobic conditions by corrinoids (Von Der Recke and Vetter, 2007). F. Wang et al. (2010) reported seven metabolites of DBDPE in male rats, but unlike BDE-209 (where reductive debromination is the primary metabolic pathway), methylsulfonyl or ethylsulfonyl substitutions were more likely. Also using rat as a model, Chu et al. (2012) identified OH-DBE-DBCH, (OH)₂-DBE-DBCH and some additional unidentified compounds as metabolites of α - and β -DBE-DBCH.

1.2.6. Current knowledge gaps

To date, knowledge of human exposure to NBFRs is scant, especially with respect to aspects other than indoor dust exposure. Notwithstanding this, NBFRs appear ubiquitous in the environment. Furthermore, bio-monitoring studies, even though limited in number to date, demonstrate the presence of these compounds in humans albeit at low concentrations thus far. Moreover, as some NBFRs are potentially readily metabolised, internal exposure levels based on detection of the parent compounds alone might be underestimates. Data to date suggests dust exposure to be an important pathway of exposure to NBFRs. In contrast, unlike PBDEs, concentrations of NBFRs in foodstuffs reported to date are very low with the exception in UK food where total NBFRs were higher than total PBDEs concentration, mostly due to β -DBE-DBCH (Tao et al., 2017). More data is needed to assess fully the extent of dietary exposure however, as it is likely that there will be a time lag between the emergence of indoor contamination and dietary exposure (Harrad and Diamond, 2006). It is noteworthy that most research to date covers only a limited range of NBFRs such as: EH-TBB, BEH-TEBP, DBDPE, BTBPE, and HBB. We therefore recommend that a wider range of NBFRs are targeted in future studies.

There is also a substantial gap in knowledge of NBFR metabolism. Understanding the metabolic pathways of NBFRs will assist assessment of their toxicity and facilitate more effective human biomonitoring. For example, evidence suggests TBBA to be a more effective biomarker of human exposure to EH-TBB, than the parent compound itself. Identification of the best exposure biomarkers remains difficult for some NBFRs however, as in many cases a metabolite may not be unique to a single compound, and/or doubts exist about whether external exposure to the metabolite may explain at least some of its presence in humans.

1.3. Pharmaceutical and Personal Care Products

1.3.1. Introduction

Pharmaceuticals and personal care products (PPCPs) are an emerging contaminant group constituted of antimicrobials, antibiotics, stimulants, natural and synthetic hormones, fragrances, UV screens and many other chemicals used in daily modern life. Recently there have been increasing concern about their environmental fate and effects following confirmation of their presence in various environmental compartments (e.g. water, sediment and biota) at relatively high concentrations (Ali et al., 2018; Blair et al., 2013; Fisch et al., 2017; Mirzaei et al., 2018; Thomas and Hilton, 2004). The main sources of PPCPs in the environment are through sewage treatment plants (STPs) and waste water treatment plants (WWTPs). As the concerns about PPCPs have emerged only recently however, many STPs/WWTPs are not equipped with the ability to detect or efficiently remove these contaminants. Therefore, it is likely that large quantities of PPCPs have been released into our aquatic environment (Bu et al., 2013; Tarpani and Azapagic, 2018). Currently, there remains very limited data about PPCPs regarding their effects on human and wildlife health, bioaccumulation and biomagnification potential, and persistence, etc.

1.3.2. Physicochemical properties

PPCPs are usually well dissolved in water in ionised forms. A summary of physicochemical properties of some PPCPs is given in Table 1.3.

Table 1.3: Physicochemical properties of some common PPCPs

Chemical	M.W (g/mol)	Solubility (mg/L)	pK _a	Log K _{ow}
----------	-------------	-------------------	-----------------	---------------------

17 β -Estradiol	272.2	3.6 ^c	10.4 ^c	3.9–4.0 ^c
Acetaminophen	151.2		9.7 ^b	0.46 ^a
Caffein	194.2		6.1 ^b	<0 ^a
Carbamazepine	236.28	17.7 ^a	7.0 ^c	2.45 ^a
Diazepam	284.8	50 ^c	3.3–3.4 ^c	2.5–3.0 ^c
Diclofenac	318.1	2.4 ^c	4.0–4.5 ^c	4.5–4.8 ^c
Erythromycin	733.9	1.4 ^c	8.9 ^c	3.06 ^a
Estriol	288.4	13.25 ^a		2.45 ^a
Estrone	270.4	12.42 ^a	10.4 ^c	3.13 ^a
Ethinylestradiol	296.2	4.83 ^a	10.5–10.7 ^c	3.67 ^a
Gemfibrozil	250.2		4.7 ^b	4.77 ^a
Ibuprofen	206.1	21 ^c	4.9–5.7 ^c	3.97 ^a
Iopromide	790.9	23.8 ^c		<0 ^a
Naproxen	230.1	16 ^c	4.2 ^c	3.18 ^a
Sulfamethoxazole	253.1	610 ^c	5.6–6.0 ^c	0.5–0.9 ^c
Testosterone	288.2	5.57 ^a	17.4 ^b	3.32
Trimethoprim	290.1	400 ^c	6.6–7.2 ^c	0.91 ^a

^a: Lintelmann et al., 2003; ^b: Westerhoff et al., 2005; ^c: Suárez et al., 2008

M.W: molecular weight; Solubility: water solubility at 25°C; pK_a: acid dissociation constant

While many PPCPs are not persistent, they continuously being used and released into the environment via activities such as: dumping of unused medications, excretion of PPCPs and their metabolites, washing off UV screens, fragrances, medical waste treatment, etc. Therefore, PPCPs are not persistent *per se*, but considered to be “pseudo-persistent”. The K_{ow} values of PPCPs are generally not high, thus few studies have reported on their bioaccumulative potential (Arnnok et al., 2017; F. Chen et al., 2017; Muir et al., 2017).

1.3.3. Toxicity and health effects

Pharmaceuticals are specifically designed to target certain biological processes at low doses for maximum activity. However, it is possible that these compounds can be bioactive in non-target organisms. As the main sources of PPCPs in the environment are

through STPs and WWTPs; being exposed throughout their life cycle has made aquatic species one of the most impacted environmental targets of these chemicals and their metabolites.

It was reported that many individual PPCPs stimulated the bioluminescent activity and disrupted biological homeostasis of *Vibrio fischeri* – an aquatic bacteria (de García et al., 2015) at environmentally relevant concentrations. This effect was even stronger when a PPCPs mixture was used. Yokota et al., 2015 reported the non-steroidal anti-inflammatory drugs (NSAIDs) diclofenac sodium and mefenamic acid to express anti-ovulatory effect *in vitro* in fish ovarian follicles. Diclofenac sodium also reduced fecundity (Yokota et al., 2015), caused oxidative stress in liver, altered testosterone levels (Guiloski et al., 2015), damaged or delayed hatching and altered reproduction (Lee et al., 2011) in fish *in vivo*. Naproxen, mefenamic acid, acetylsalicylic acid, ibuprofen and diclofenac sodium reduced the testosterone concentrations in male but increased the 17 β -estradiol and testosterone levels in female zebrafish (Ji et al., 2013). Additionally, naproxen exhibited sex-specific alteration of hormone levels and related HPG axis gene transcription in fishes (Ji et al., 2013). Lysosomal damage of clam's haemolymph has been reported following exposure to caffeine, ibuprofen, carbamazepine or novobiocin for 35 days (Aguirre-Martínez et al., 2013).

A cytotoxic drug 5-fluorouracil has been shown to be extremely toxic to aquatic organisms with $EC_{50} < 0.1 \text{ mg L}^{-1}$ by *daphnia magna* reproduction and *pseudomonas putida* growth inhibition tests (Zounkova et al., 2010). Not only PPCPs but their metabolites might also express toxicity. These metabolites are formed via chemical, physical and biological processes such as human/animal metabolism or STP/WWTP treatment (e.g. chlorination or chloramination) processes. A metabolite of 5-fluorouracil: α -fluoro- β -alanine has shown low but pronounced toxicity to aquatic organisms and is classified as harmful (Zounkova et al., 2010). Both triclosan, a widely used antibacterial chemical, and its metabolite methyltriclosan negatively affected morphology and density of abalone immune cells (hemocytes) (Gaume et al., 2012).

From an ecotoxicological perspective, exposure of living organisms to PPCPs mixtures is of most concern. As PPCPs are usually hydrophilic, they are very mobile in aquatic systems. Considering the fact that there are hundreds of PPCPs available, not to mention

their metabolites, it is very plausible that aquatic organisms are being exposed to a very complex mixture of PPCPs daily. Combined drug intoxication is a very well-known phenomenon in humans and therefore should not be taken lightly in aquatic species. However, such mixtures effects is very hard to predict/understand is the presence of complex mixtures of many individual contaminants. For example, exposures to binary mixtures of four anti-cancer drugs: 5-fluorouracil, cisplatin, etoposide and imatinib mesylate to *Pseudokirchneriella subcapitata* alga and *Synechococcus leopoliensis* cyanobacteria show different toxicities than predicted (using the concepts of concentration addition and independent action of individual PPCPs) (Brezovšek et al., 2014). This difference in mixture toxicity was both compound- and species[specific (Brezovšek et al., 2014). Similar compound-specific combined effects were also reported in fish exposed to a mix of caffeine, DEET, progesterone, gemfibrozil, ibuprofen, diphenhydramine, naproxen, atenolol, triclocarban and triclosan (Zenobio et al., 2014).

1.3.4. Occurrence in major environment compartments of concern

As previously discussed in session 1.2.3, on a toxicological perspective the major concern of PPCPs is negative effects to aquatic life, especially freshwater species. Therefore current research is often focused on PPCPs occurrence in relevant environmental compartments such as wastewater, surface water, sewage sludge and sediment.

1.3.4.1. Wastewater and surface water

In 2000, the U.S Geological Survey carried out a comprehensive investigation of 95 organic wastewater contaminants (OWCs) most of which are PPCPs in 139 potentially contaminated stream sites across the U.S (Kolpin et al., 2002). Detergent metabolites, steroids, plasticisers and nonprescription drugs together accounted for more than 85 % of the total concentration of OWCs, with coprostanol and cholesterol (steroids), caffeine and 4-nonylphenol (detergent metabolite) among the most frequently detected. Individual PPCP concentrations in these sites were reported at less than 1 $\mu\text{g L}^{-1}$ in 95 % of observations (Kolpin et al., 2002).

Another comprehensive study on antibiotics was carried out in Australia in 2005-2006. It consisted of 114 sampling sites including: hospital wastewater, WWTP influent and effluent, surface water and drinking water (Watkinson et al., 2009). The presence of

antibiotics in Australian aquatic systems is very pronounced with maximum concentrations up to $64 \mu\text{g L}^{-1}$ in WWTP influents, $14.5 \mu\text{g L}^{-1}$ in hospital wastewaters, $3.4 \mu\text{g L}^{-1}$ in WWTP effluents and $2 \mu\text{g L}^{-1}$ in surface water. Predominant among detected antibiotics in Australian water were β -lactam, quinolone, sulphonamide group compounds, and macrolide (Watkinson et al., 2009).

Carbamazepine and 6 of its metabolites have been detected in both influent and effluent water samples from three French STPs in concentration ranges of $86\text{-}420 \text{ ng L}^{-1}$ for carbamazepine and $\text{nd-}1500 \text{ ng L}^{-1}$ for its metabolites (Leclercq et al., 2009). Dihydroxylated and 10-hydroxylated metabolites of carbamazepine were found at much higher concentrations than their parent compound, up to $\mu\text{g L}^{-1}$ level, especially in effluent samples (Leclercq et al., 2009). Surface water in the Ruhr, Germany contained triclosan in concentration range <3 to 10 ng L^{-1} and that of methyltriclosan was 0.3 to 10 ng L^{-1} (Bester, 2005) while triclosan in effluent of two STPs in that area was 10 to 600 ng/L (Bester, 2005).

Surface water samples in the Han River, South Korea showed high average concentrations of cimetidine, acetaminophen, caffeine and sulfamethoxazole at 281 , 268.7 , 34.8 and 26.9 ng/L (Choi et al. 2008). The authors also suggested STPs might be the major source of PPCPs in downstream regions of the river by comparison with data obtained from samples upstream and downstream of four STPs discharging into the river. Natural and synthetic estrogens: estrone, 17β -estradiol, estriol, ethynylestradiol, diethylstilbestrol and 17 -valerate were found in both surface water and sediment in rivers of the Tianjin area, China with total concentrations ranging from $0.64\text{-}174 \text{ ng L}^{-1}$ in water and $0.98\text{-}51.6 \text{ ng g}^{-1}$ (dry weight) in sediment (Lei et al., 2009). Extremely high concentrations of PPCPs were found in WWTP effluent and surface waters in Hyderabad, India up to maximum concentrations of 14 mg L^{-1} (ciprofloxacin) (Fick et al., 2009). Drinking water in the same area was also highly contaminated with PPCPs at $\mu\text{g L}^{-1}$ levels (Fick et al., 2009).

In summary, effluents from STPs and WWTPs around the world have been found to contain PPCPs, indicating the current technologies in such facilities are not efficient in completely removing PPCPs. Moreover, even though often found at relatively low concentrations ($<1 \mu\text{g/L}$), the ubiquity of these emerging contaminants in surface water and drinking water is of concern for aquatic species and humans.

1.3.4.2. Sediment and sewage sludge

Concentrations of PPCPs in sewage sludge and sediment are usually highly variable between pharmaceutical groups, possibly due to the usage/consumption pattern as well as adsorption capacity. Sewage sludge samples (n=45) have been collected from 20 cities across China and analysed for 30 pharmaceutical chemicals; of which ofloxacin, oxytetracylin, norfloxacin and ketoprofen predominated with maximum concentrations up to 24760, 5280, 5280 and 4458 $\mu\text{g kg}^{-1}$, respectively (Chen et al., 2013). Ofloxacin also showed the highest average concentration in sewage sludge collected in Fijuan, China (2270 $\mu\text{g kg}^{-1}$), followed by triclocarban (1440 $\mu\text{g kg}^{-1}$) and tetracycline, oxytetracycline, triclosan, fenoprofen and miconazole ($>100 \mu\text{g kg}^{-1}$) (Li et al., 2016).

The occurrence of six parabens (methyl-, ethyl-, propyl-, butyl-, heptyl- and benzyl-paraben) together with five paraben metabolites (4-hydroxy benzoic acid, methyl protocatechuate, ethyl protocatechuate, 3,4-dihydroxy benzoic acid and benzoic acid) was confirmed in samples collected from five Indian STPs. The maximum total paraben concentrations in influent, effluent and sewage sludge were 920 ng L^{-1} , 67 ng L^{-1} and 1090 ng g^{-1} d.w; while those of total paraben metabolites were 34,600 ng L^{-1} , 3,800 ng L^{-1} and 35,900 ng g^{-1} d.w, respectively (Karthikraj et al., 2017). Lower levels of parabens (methyl-, ethyl-, propyl-, butyl- and benzyl-paraben) were reported in fourteen WWTPs in the U.S at a concentration range of 21.1 to 213.2 ng g^{-1} d.w total parabens (J. Chen et al., 2017).

Naproxen, salicylic acid, propranolol, caffeine and 17 α -ethinylestradiol were found in surface sediment of Guadiamar River, Spain at mean concentrations of 11.2, 9.49, 3.37, 7.21 and 48.1 $\mu\text{g kg}^{-1}$ (Martín et al., 2010). Li et al. investigated water, sediments and biota samples from Baiyangdian Lake - the largest freshwater body in North China - and observed the ubiquity of antibiotics in the lake; 17 antibiotics were detected in sediment samples with norfloxacin predominant (mean concentration 267 $\mu\text{g kg}^{-1}$) followed by roxithromycin and ofloxacin (mean concentration 64.9 and 21 $\mu\text{g kg}^{-1}$, respectively) (Li et al., 2012).

The natural hormones estrone and 17 β -estradiol were found in New Zealand sediments ranging from 0.71 to 2.2 ng g^{-1} and 0.47 to 1.0 ng g^{-1} d.w, respectively while 17 α -ethinylestradiol was not detected (Stewart et al., 2014). Common natural and synthetic

estrogens (e.g. estrone, estriol, etc.) were not detected in Perdido Bay, Alabama, U.S, however glucocorticoids, androgens and progestins were all detected. Specifically, the concentration ranges of cortisone, cortisol and prednisolone were: 1.21-4.10, 4.9-9.05 and 6.42-14.61 pg g^{-1} while those of androsterone, testosterone, epitestosterone, 5 α -dihydrotestosterone, progesterone and levonorgestrel were 39.64-128.66, 3.99-9.67, 1.94-17.87, 56.8-136.86, 2.91-13.22 and 1.16 to 3.44 pg g^{-1} w.w (Mulabagal et al., 2017).

1.3.5. PPCPs in biota

Aquatic species near WWTP effluent discharge points have been shown to accumulate some select PPCPs such as fragrance components, antibiotics, antihistamines or antidepressants (Ramirez et al., 2009; Rüdél et al., 2006). Ramirez et al. detected norflouxetine, sertraline, diphenhydramine, diltiazem and carbamazepine at several ng g^{-1} level in fish fillets collected near WWTP discharges in U.S while fluoxetine, norfluoxetine, diphenhydramine, sertraline and gemfibrozil were found in liver of the same fish at mean concentrations of several tens to hundreds ng g^{-1} (Ramirez et al., 2009). Species and organ selective bioaccumulation of antidepressants (e.g. sertraline, norfluoxetine, citalopram, etc.) and diphenhydramine were also reported in various fish species from upper Niagara River and in general bioaccumulation were in the order brain > liver > muscle > gonads (Arnnok et al., 2017). Previously, antidepressant fluoxetine, norfluoxetine, sertraline and desmethylsertraline also showed elevated concentrations in brain and liver of fish samples from Pecan Creek, U.S in comparison with muscle tissues; their respective mean concentrations in fish brain were: 1.58, 8.86, 4.27 and 15.6 ng g^{-1} while those in liver were 1.34, 10.27, 3.59, 12.94 ng g^{-1} and in muscle were 0.11, 1.07, 0.34 and 0.69 ng g^{-1} (Brooks et al., 2005).

A recent national study of PPCPs in German fish fillets collected across Germany showed relatively low concentration of diphenhydramine (0.04-0.07 ng g^{-1} w.w), desmethylsertraline (1.65-3.28 ng g^{-1} w.w), tonalide (98-392 ng g^{-1} l.w) and galaxolide (268-11100 ng g^{-1} l.w) while 25 others PPCPs (e.g. caffeine, codeine, acetaminophen, triclosan, etc.) were not found (Subedi et al., 2012). Additionally, the authors found significant correlation between the concentrations of galaxolide or tonalide and the distance between sampling point and WWTP discharge (Subedi et al., 2012).

Antihypertensive, antibiotic, anti-inflammatory, stimulant, antihistamine, anti-seizure and antidepressant drugs have been detected in periphyton and snails from the North Bosque River, Texas, U.S near an effluent discharge at several to several tens $\mu\text{g kg}^{-1}$ w.w; desmethylsertraline was predominant among detected PPCPs with a maximum concentration of $42 \mu\text{g kg}^{-1}$ w.w (Du et al., 2015). Steroidal estrogen assessment in wild fish collected from Dianchi Lake, China showed maximum estrogen concentration at 11.3 ng g^{-1} and higher bioaccumulation potential in liver than in gill and muscle (Liu et al., 2011). Aquatic plants and animals in Baiyangdian Lake, China also contained some PPCPs with quinolone antibiotics predominating in aquatic plants ($8.37\text{-}6532 \mu\text{g kg}^{-1}$) while quinolone ($17.8\text{-}167 \mu\text{g kg}^{-1}$) and macrolide ($<\text{MDL-}182 \mu\text{g kg}^{-1}$) antibiotics predominated in aquatic animals (Li et al., 2012). Fish samples from supermarkets in Guangdong, China were analyzed for 54 PPCPs, of which 22 were detected at concentrations less than $10 \mu\text{g kg}^{-1}$ (Zhang et al., 2017)

One of the very few epidemiological studies conducted into the effect of PPCPs on wildlife, revealed kidney diclofenac residues were highly correlated with renal failure in vultures in Pakistan. It was later proposed that dietary exposure to treated livestock carcasses resulted in lethal diclofenac concentrations and caused renal failure in these birds (Oaks et al., 2004).

In summary, PPCPs have been detected in biota globally. Commonly found chemicals are antidepressants, antibiotics, musks and antihistamines.

1.3.6. Current knowledge gaps

PPCPs are an emerging contaminant group consisting of hundreds of chemicals with different physicochemical properties. This makes simultaneous analysis of multiple PPCPs groups challenging. Despite efforts to conduct such multi-residue analysis, most studies conducted in aquatic environment and species have only focused on common PPCP groups such as: antibiotics, antidepressants, stimulants, antihistamines, and fragrances. Evidence of bioaccumulation of some PPCPs exists but remains very limited while biomagnification is currently not addressed.

To date, studies about PPCP toxicity and ecotoxicology are still very scarce, most of which have investigated fish exposed to individual PPCPs. Considering that multiple

PPCPs are often found together, it is necessary to investigate their combined toxic effects on non-target organisms including humans. Additionally, little to nothing is known about the impact on public health of their environmental occurrence, even at sub-therapeutic levels, in drinking water and foodstuffs.

Since evidence exists of fatalities in animals exposed to contaminated food, it is important to further study and monitor PPCPs in foodstuffs, especially fish/shellfish in contaminated areas. It is also necessary to investigate not only PPCPs but their metabolites/degradation products. Such compounds are formed via many mechanisms e.g. UV light, chlorination, temperature, biological processes, etc. and might pose even higher toxicity than the parent PPCPs.

1.4. Aims of this thesis

From the above, substantial research gaps exist about the environmental fate, metabolism, degradation and human/biota exposure to NBFRs and PPCPs. In particular, there are major gaps in our understanding of the pathways, rates and products of the metabolism of NBFRs. Moreover, our capacity to study the environmental fate and behaviour of PPCPs and their metabolites is currently restricted by the limitations of conventional analytical chemistry methods for their determination. The overall premise of this thesis, is that advances in analytical chemistry, specifically high resolution high accuracy mass spectrometry can provide tools to address these gaps. By using a UPLC-Orbitrap HRMS system, the objectives of this study are to:

1. Develop an analytical method for determination of NBFRs and screen for NBFRs metabolites/degradation products as well as brominated contaminants in one chromatographic run.
2. Develop high throughput analytical methods for simultaneous determination of a wide range of environmentally-relevant PPCPs in water samples.
3. Investigate *in vitro* metabolic profiles of EH-TBB, BEH-TEBP and BTBPE by mouse liver microsomes.
4. Study the *in vitro* metabolism and metabolic rate of TBECH by human liver microsomes.

5. Assess the extra hepatic *in vitro* metabolism of EH-TBB and FireMaster 550 mixture by human skin S9 fractions.

Chapter 2

Analytical Method

2.1. Orbitrap MS tuning

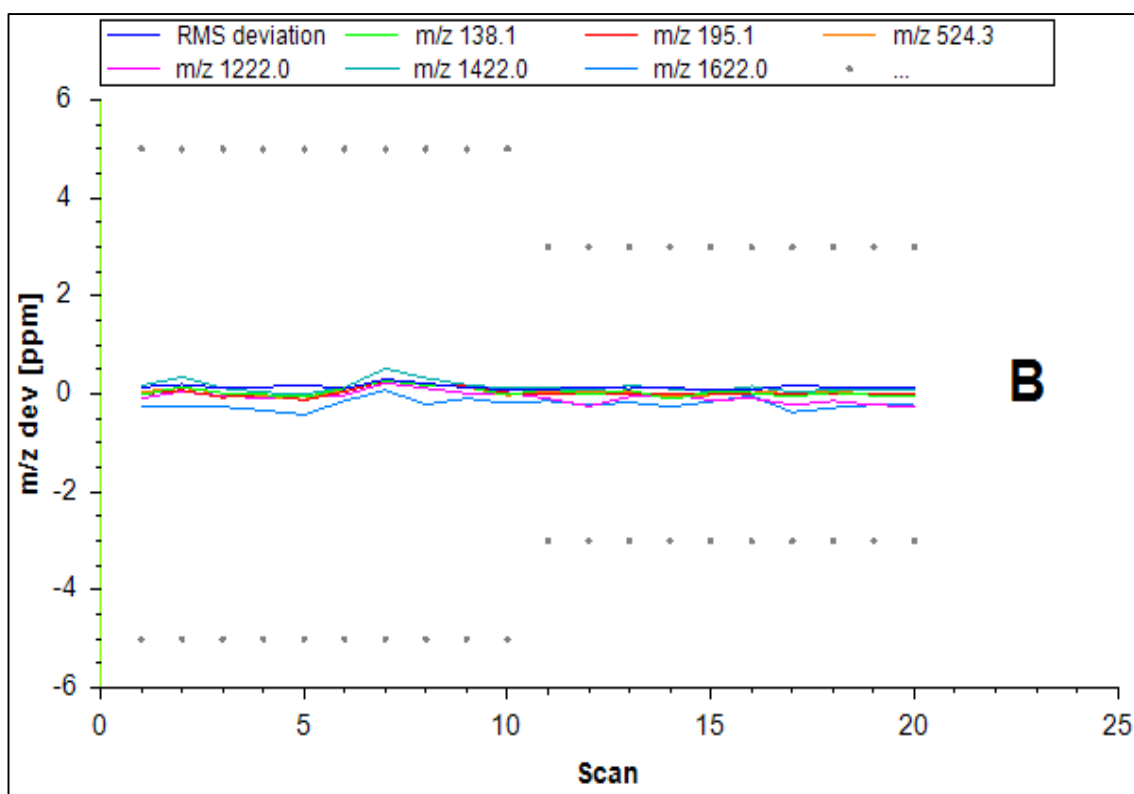
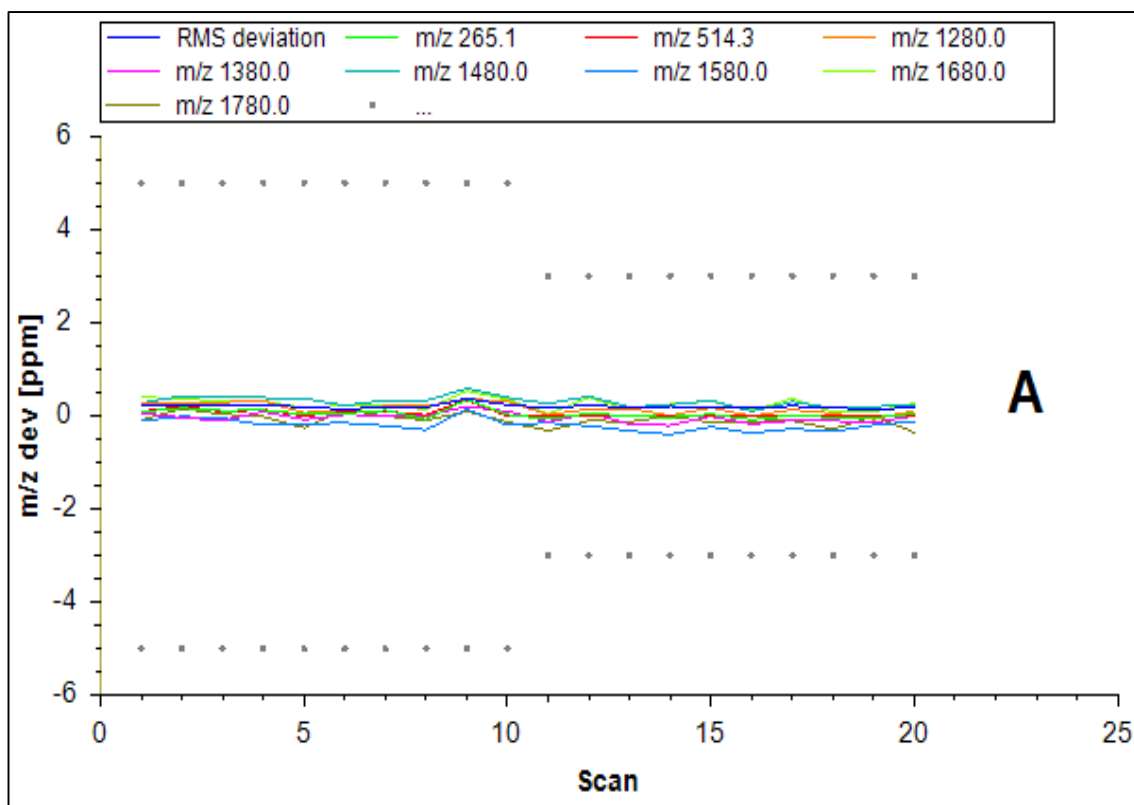
For high resolution mass spectrometry, it is extremely important to calibrate the system as this can greatly affect mass resolution of detected ions – one of the main QA/QC criteria for identifying and quantifying analytes. The instrument was externally calibrated using Pierce ESI Positive and Negative Ion calibration solutions (Table 2.1). Calibration solutions were directly infused into the system by a syringe pump at 10 μ L/min. Factory default acceptance criteria for a good calibration was used.

Table 2.1: Tuning ions for mass accuracy in positive and negative ESI mode on UPLC-Orbitrap MS instrument

Component	Positive Ion (m/z)	Negative Ion (m/z)
Caffeine	138.06619 195.08765	
MRFA	524.26496	
Ultramark 1621	1221.99064 1421.97786 1621.96509	
Ultramark 1621		1279.99721 1379.99083 1479.98444 1579.97805 1679.97166 1779.96528
Sodium Dodecyl Sulfate		265.14790
Sodium Taurocholate		514.28444

For a good mass accuracy calibration, the m/z deviation of each tuning ion (Table 2.1) has to be within ± 2.5 ppm (Figure 2.1.A and Figure 2.1.B). This tuning process is performed every other day or when needed.

Figure 2.1: Acceptable mass accuracy calibration in negative (A) and positive (B) ESI mode.



After the instrument is calibrated, the UPLC is connected to the Orbitrap MS and an isocratic UPLC method was applied in order to optimise the ionization source parameters. The flow rate was set at 400 $\mu\text{L}/\text{min}$ and the mobile phase was chosen in accordance to the studied analytes for each sample type. The parameters were chosen such that the total ion current (TIC) variation is below 10 % RSD and ion injection time (IT) less than 2 ms. Table 2.2 shows an example of optimised ionization parameters for the analysis of bisphenol A by UPLC-Orbitrap MS

Table 2.2: Optimised ionisation parameters for the analysis of Bisphenol A by UPLC-Orbitrap MS (LC flow rate 400 $\mu\text{L}/\text{min}$)

Source Parameters	Setting
Sheath gas flow rate	50
Aux gas flow rate	15
Sweep gas flow rate	0
Spray voltage (kV)	4.5
Capillary temp. ($^{\circ}\text{C}$)	275
S-lens RF level	50
Aux gas heater temp ($^{\circ}\text{C}$)	350

2.2. Data Analysis

2.2.1. Targeted Analysis

Targeted analysis of compounds of interest was performed on Quan Browser 3.0 software (Thermo Fisher Scientific, USA). Pure individual standards or standard mixtures (1 ng on column) were subjected to analysis for identification of each target compound and their corresponding retention time (t_{R}). This was achieved via different ionisation techniques and polarities including (+)/(-) APCI and (+)/(-) ESI.

After the accurate masses and retention times were established for each analyte, a 5 point calibration was conducted. Wherever possible, the isotope dilution method was used to quantify target compounds. Due to the wide range of chemicals being analyzed, only a limited number of internal standards were used. Internal standards were chosen so that

they do not naturally occur in the samples (usually deuterated or ¹³C labelled) and their retention times are close to that of the target compounds.

The concentration of target analytes were determined via relative response factor (RRF) method. The RRFs were calculated as in the following equations:

$$RRF = \frac{A_{NAT}}{A_{IS}} \times \frac{C_{IS}}{C_{NAT}} \quad (\text{Equation 1})$$

RRFs are obtained for each calibration point and an average RRF is calculated. Before and after each sample batch, a calibration standard (usually the middle concentration level within a calibration curve i.e. calibration standard level 3 in a 5 points calibration curve) is injected and the average RRFs for these two standards was calculated. This average RRF (which must be within $\pm 25\%$ of the average RRF obtained from the 5 point calibration) is used to calculate the concentration of the target analytes in real samples by the equation 2

$$C_{NAT,real\ sample} = \frac{A_{NAT}}{A_{IS}} \times \frac{1}{RRF} \times \frac{M_{IS}}{SS} \quad (\text{Equation 2})$$

Where $C_{NAT,real\ sample}$ is the concentration of target analyte in sample, A_{NAT} is the peak area of target analyte in sample, A_{IS} is the peak area of internal standard in sample, RRF is the relative response factor for the analyte, M_{IS} is the amount of internal standard added to sample (ng) and SS is the sample size (mL).

The following QA/QC criteria have to be met for confirmation of a target compound in a sample (Harrad, 2014):

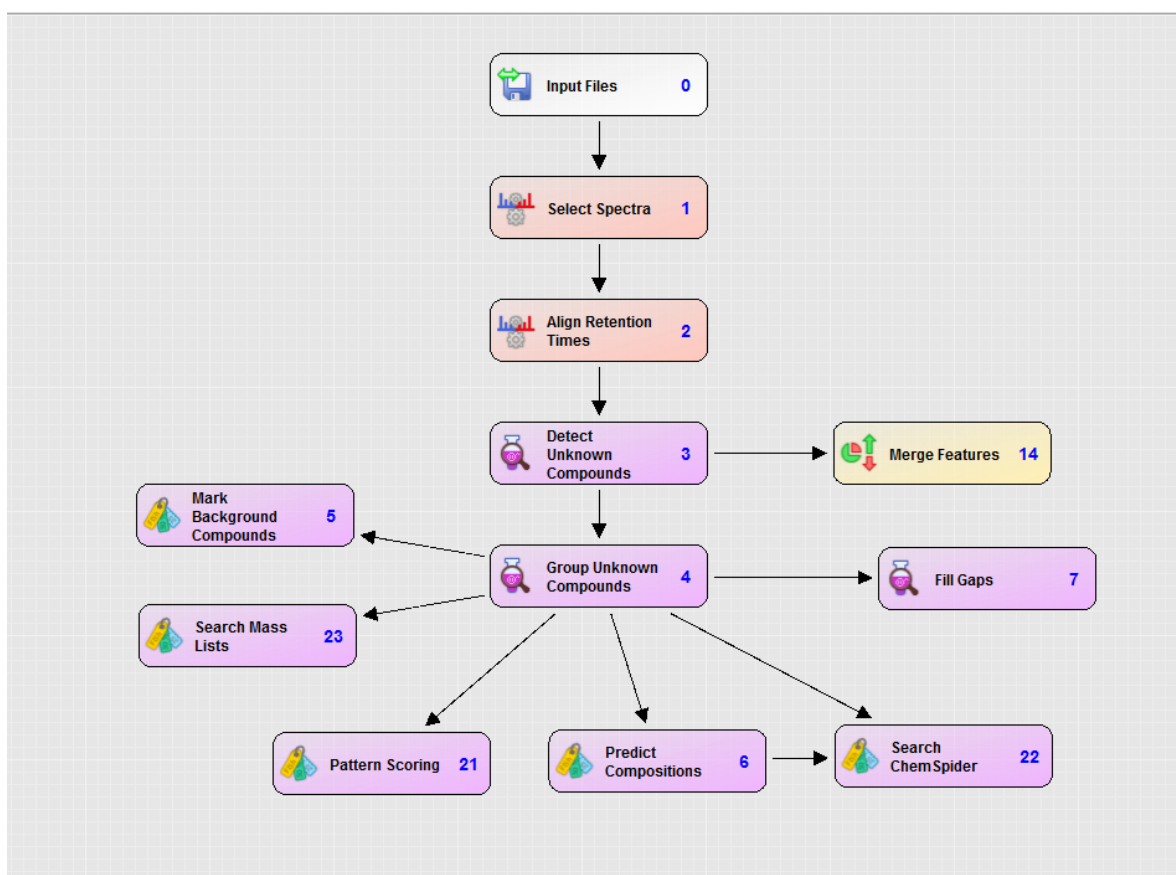
- i. Peak signal to noise ratio (S/N) must exceed 10:1.
- ii. m/z value of the molecular ion peak must be within 5 ppm of its theoretical value at resolution power of 17500 FWHM (full width at half mass).
- iii. Relative retention time of the peak in the sample must be within $\pm 0.2\%$ of the value determined for that analyte in the calibration standards ran before and after a sample batch.

For targeted screening of chemicals, a similar approach was carried out but no calibration curve was required.

2.2.2. Untargeted analysis

Compound Discoverer 2.0 software (Thermo Fisher Scientific, Bremen, Germany) was used to assist with untargeted analysis of interested emerging contaminants and/or their metabolite identification process. The software was developed for liquid chromatography - high resolution accurate mass data with different working “nodes”, each node is responsible for a specific purpose. Multiple nodes can be combined in various ways to form work flows depending on user need. A general work flow as described in Figure 2.2 was implemented in our studies.

Figure 2.2: Compound Discoverer workflow for untargeted screening of emerging contaminants and their metabolites



A detailed explanation and parameters of the workflow is provided in Table 2.3. Briefly, the software extracted spectra from input mass spectral data files and aligned the retention times of multiple LC/MS files based on mass tolerance and maximum time shift criteria. Compound Discoverer then attempted to elucidate the element compositions for each peak in every single file using predefined settings. The detected features were grouped

based on their accurate masses and retention times across all files and made ready for further analysis nodes including background compound filter, elemental composition prediction, online Chemspider library search, offline mass list search and isotope pattern scoring. Finally, a “Differential Analysis” node was used to provide some simple differential statistics such as PCA and ANOVA with Tukey HSD post-hoc testing on detected feature’s groups.

Compound identification was achieved via 4 successive filters established within the Compound Discoverer 2.0 software. Specifically, these were that the:

- iv. Peak signal to noise ratio (S/N) must exceed 10:1.
- v. m/z value of the molecular ion peak must be within 5 ppm of its theoretical value at resolution power of 17500 FWHM (full width at half mass).
- vi. Isotope pattern must match within 5 % of the theoretically predicted abundances of the predicted chemical formula (if applicable).
- vii. \log_2 fold change (calculated as \log_2 of the peak area ratio between *in vitro* samples and experiment blanks) must be > 1 (for metabolite identification), which is equivalent of fold change > 2 (Dalman et al., 2012).

Additionally, the relative retention time of the peak in the sample must be within ± 0.2 % of the value determined for that analyte in the pure standard mixture run before and after a sample batch (if the commercial standard is available).

Table 2.2: Descriptive analysis “nodes” of Compound Discoverer 2.0 Software used in untargeted screening of chemicals and metabolites.

Node	Description	Parameters
Input Files	LC/MS data file input	NA
Select Spectra	Choose spectra to process within LC/MS files	Min. Precursor Mass: 100 Da Max. Precursor Mass: 850 Da Polarity Mode: negative S/N Threshold: 1.5
Align Retention Times	Chromatographic alignment of samples with similar LC/MS method and run time	Alignment Model: Adaptive curve Mass Tolerance: 5 ppm Maximum shift: 0.5 min
Detect Unknown Compounds	Detect compounds in a file by Compound Elucidator algorithm	Mass Tolerance: 5 ppm S/N threshold: 1.5 Min. Peak Intensity: 1000 Ion: [2M-H]; [M+Cl]; [M-2H]; [M-Br+2e]; [M-Br+O]; [M-H]; [M-H-H2O] Max. Element Counts: C20 H30 Br4 O10 (for EH-TBB samples); C20 H30 Br6 O10 (for BTBPE samples); C30 H50 Br4 O10 (for BEH-TEBP samples) Min. # Scans per Peak: 5
Group Unknown Compounds	Group all detected compounds across all files by retention times and molecular weights	Mass Tolerance: 5 ppm Retention Time Tolerance: 0.1 min
Mark Background Compounds	Annotate and filter background compounds in predefined blank samples	Max. Sample/Blank: 3 Hide Background = True

Search Mass Lists	Search for compounds in offline mass list provided inside Compound Discoverer	Library: Environmental and Food Safety (EFS) HRAM Compound Database Mass tolerance: 5 ppm
Predict Compositions	Predict elemental compositions for grouped detected compounds based on user Ion definition	Mass tolerance: 5 ppm Max. Element Counts: similar with that in Detect Unknown Compounds node Max. RDBE: 20 Max. # Candidates: 10
Search ChemSpider	Search for detected compounds in ChemSpider databases	Databases: ACToR: Aggregated Computational Toxicology Resource; DrugBank; EAWAG Biocatalysis/Biodegradation Database; EPA DSSTox; FDA UNII – NLM Mass tolerance: 5 ppm
Pattern Scoring	Compare detected compounds with predefined isotope patterns and give matching scores	Isotope Pattern: C8Br, C8BR2, C8Br3, C8Br4, C8Br5, C8Br6 Mass Tolerance: 5 ppm Intensity Tolerance: 30%
Fill Gaps	Re-integrate a peak if it was found in more than one data files but not in another, trying to get the peak area even at noise level	Mass tolerance: 5 ppm S/N Threshold: 1.5 Retention Time Tolerance: 0.1 min
Differential Analysis	Perform basic statistical analysis: PCA and ANOVA	Log10 Transform Values: True

2.2.3. Biotransformation kinetic model

The metabolite formation rate and substrate concentration of the studied chemicals were fitted to different biotransformation kinetic models by nonlinear regression analysis using the SigmaPlot Enzyme Kinetics Module v.1.1 (Systat Software Inc., Richmond, CA) to determine the enzyme kinetic model that best describe the formation rates of the metabolites. The models used were the Michaelis-Menten equation (Equation 3), the Hill equation (Equation 4), and the substrate-inhibition kinetic equation (Equation 5):

$$v = \frac{V_{max} \times [S]}{K_m + [S]} \quad (\text{Equation 3})$$

$$v = \frac{V_{max} \times [S]^n}{K' + [S]^n} \quad (\text{Equation 4})$$

$$v = \frac{V_{max}}{1 + \frac{K_m + [S]}{[S]} + \frac{K_i}{[S]}} \quad (\text{Equation 5})$$

where v is initial velocity of the reaction, V_{max} is the maximum metabolic rate, $[S]$ is the substrate concentration, K_m is the Michaelis-Menten constant, K' is the Hill dissociation constant, n is the Hill coefficient and K_i is the inhibitory dissociation constant. Selection of the best fitted model was determined by statistical criteria to evaluate the goodness of the fit. The two statistical criteria used were Akaike Information Criterion corrected for small sample size (AICc) and the standard deviation of the residuals (Sy.x). The model with the lowest values for AICc and for the standard deviation of the residuals was considered to be the model that best fit the data. When the formation rate of a primary metabolite is best described by the Michaelis-Menten model (Equation 3), the part of the *in vitro* intrinsic clearance ($CL_{int,M}$) due to the formation of that metabolite can be calculated as follows:

$$CL_{int,M} = \frac{v}{[S]} = \frac{V_{max}}{K_m + [S]} (\text{Equation 6})$$

If the levels of the substrate of interest in human blood are negligible compared to the apparent K_m value associated with the formation of the metabolite, then $(K_m + [S]) \approx K_m$ therefore Equation 6 can be written as follows:

$$CL_{int} = \frac{v}{[S]} = \frac{V_{max}}{K_m} (\text{Equation 7})$$

The total CL_{int} value of the substrate of interest can then be calculated as the sum of the CL_{int} of each of its primary metabolites.

The intrinsic *in vitro* clearance of a xenobiotic by an organ on kilogram human body weight ($CL_{int-organ}$) basis can be scale up by the following equation:

$$CL_{int-organ} = CL_{int} \times p \times w \text{ (Equation 8)}$$

Where p is the amount of protein per gram of an organ and w is the average weight of that organ per kilogram body weight.

The blood flow of an organ per kilogram body weight (kg b.w) Q_h was taken into account for extrapolation of *in vitro* clearance to *in vivo* clearance (CL_h) as follows:

$$CL_{organ} = \frac{Q_h \times CL_{int-organ}}{CL_{int-organ} + Q_h} \text{ (Equation 9)}$$

2.3. Analysis of blanks, LODs and LOQs

Instrument blanks (injections of methanol into the instrument) and method blanks (samples containing a clean matrix similar to the matrix of real samples, usually deionized water in this thesis) were analysed alongside each sample batch. None of the target compounds (with the exception of 2,4,6-TBP) were detected in any of the method or instrument blanks. Limit of detection (LOD) and limit of quantification (LOQ) were estimated using the signal to noise (S:N) approach. Instrumental detection limit (IDL) was calculated as the lowest concentration that gives a S:N ratio of 3:1, while Instrumental quantification limit (IQL) was calculated as the lowest concentration that gives a S:N ratio of 10:1 (Harrad, 2014).

2.4. Statistical Analysis

Statistical analysis was conducted using IBM SPSS Statistics for Windows, version 22 (IBM Corp., Armonk, N.Y., USA), Excel (Microsoft Office 2013) and Compound Discoverer 2.0 (Thermo Fisher Scientific, Bremen, Germany). The linearity, calibration curves, standard deviation of the response and slope of calibration curve for target compounds were assessed by linear regression in Excel. Principal Component Analysis (PCA) was performed on *in vitro* samples (peak intensities were log10 transformed) by Compound Discoverer 2.0 for QA/QC purposes. The differences in means among study

factors (e.g. treated vs non-treated samples; level of chemical exposure to human liver microsomes, etc.) were statistically evaluated using ANOVA with Tukey HSD posthoc test. Kruskal Wallis test to evaluate the statistical differences between two or more groups of a variable (without normality assumption) was carried out using SPSS. The level of confidence was preset at 95 % for all statistical tests where applicable.

Chapter 3

Method development for
simultaneous analysis of multiple
pharmaceuticals and personal care
products in water by UPLC-HRMS

3.1. Synopsis

In this chapter, a high throughput analysis method for the determination of concentrations of 29 common PPCPs was developed by rapid alternate switching (+)/(-)ESI-LC-HRMS. The developed method was then applied to assess the levels of target chemicals in effluent and surface water samples collected from Egypt.

3.2. Materials and methods

3.2.1. Chemicals and standards

All solvents used in this study were purchased from Fisher Scientific (Loughborough, UK) and were of HPLC grade or higher. Individual standards of 29 PPCPs (Table 3.1, Figure 3.1), in addition to isotope-labelled Caffeine-D9, Codeine-D3, Carbamazepine-D10, Estone-D4 and 4-Chlorophenol-2,3,5,6-D4 used as internal (surrogate) standards were purchased from Sigma-Aldrich™ (Irvine, UK) at the highest possible purity (>99 %). ¹³C-tetrabromobisphenol A (¹³C-TBBPA) and Tris (2-chloroethyl) phosphate-D12 (TCEP-D12) used as recovery (syringe standards) were obtained from Wellington Laboratories (Guelph, ON, Canada). All standard stock solutions were prepared and further diluted in methanol. Oasis MCX and Oasis HLB cartridges (6 cc, 150 mg sorbent per cartridge) were obtained from Waters™ (Hertfordshire, UK). Ammonium formate (NH₄COOH), ammonium hydroxide (NH₄OH, 30 %), ammonium fluoride (NH₄F) and formic acid (HCCOH) were obtained from Sigma-Aldrich™ (Gillingham, UK). Milli-Q water was used for cleaning and sample preparation purposes.

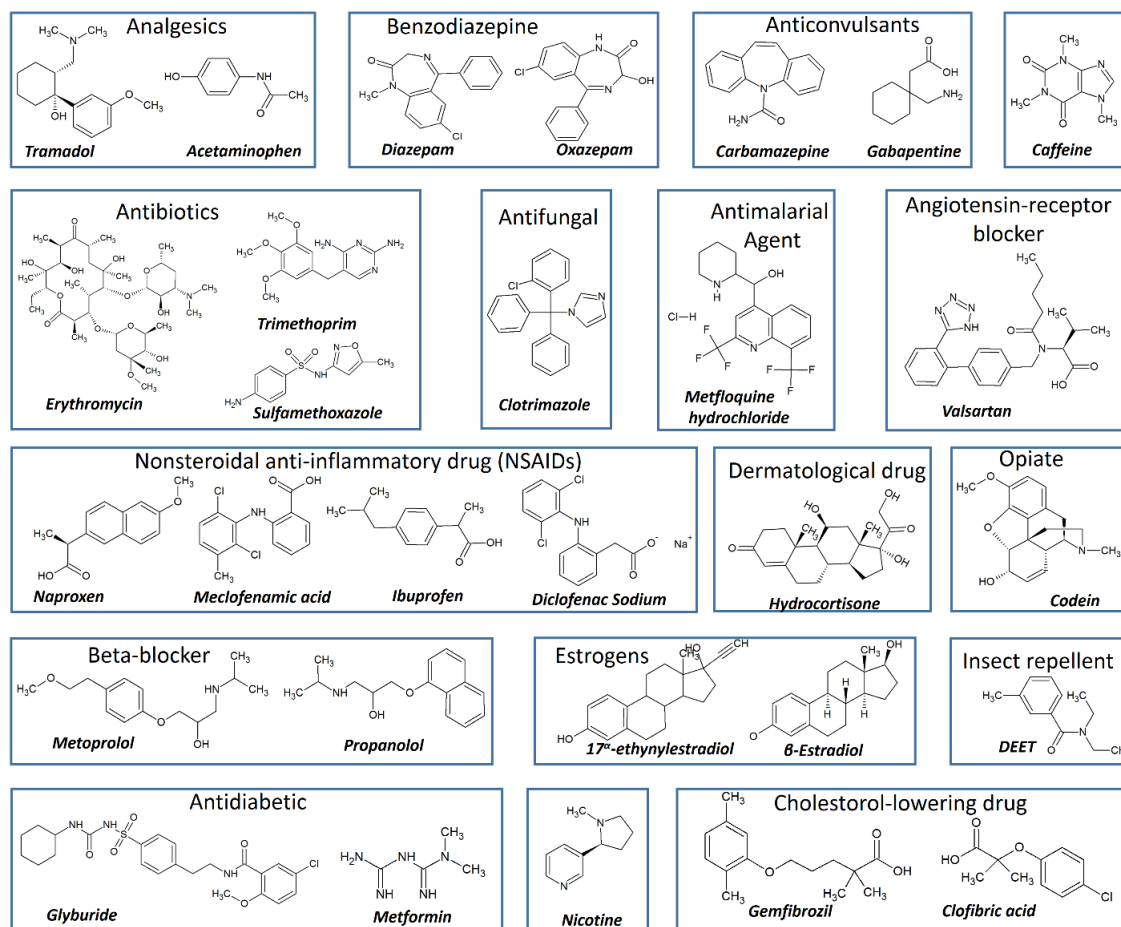
Table 3.1: List of 29 target PPCPs in this study

Compound	Pharmacological activity	Chemical Formula	CAS
Acetaminophen	Analgesics	C ₈ H ₉ NO ₂	103-90-2
Tramadol	Analgesics	C ₁₆ H ₂₅ NO ₂	36282-47-0
Valsartan	Angiotensin-receptor blocker	C ₂₄ H ₂₉ N ₅ O ₃	137862-53-4

Trimethoprim	Antibiotics	$C_{14}H_{18}N_4O_3$	738-70-5
Sulfamethoxazole	Antibiotics	$C_{10}H_{11}N_3O_3S$	723-46-6
Erythromycin	Antibiotics	$C_{37}H_{67}NO_{13}$	114-07-8
Carbamazepine	Anticonvulsants	$C_{15}H_{12}N_2O$	298-46-4
Gabapentin	Anticonvulsants	$C_9H_{17}NO_2$	60142-96-3
Metformin	Antidiabetic	$C_4H_{11}N_5$	1115-70-4
Glyburide	Antidiabetic	$C_{23}H_{28}ClN_3O_5S$	10238-21-8
Clotrimazole	Antifungal	$C_{22}H_{17}ClN_2$	23593-75-1
Mefloquine Hydrochloride	Antimalarial agent	$C_{17}H_{17}ClF_6N_2O$	51773-92-3
Oxazepam	Benzodiazepine	$C_{15}H_{11}ClN_2O_2$	6801-81-6
Diazepam	Benzodiazepine	$C_{16}H_{13}ClN_2O$	439-14-5
Metoprolol	Beta-blocker	$C_{15}H_{25}NO_3$	56392-17-7
Propranolol	Beta-blocker	$C_{16}H_{21}NO_2$	318-98-9
Clofibric acid	Cholesterol-lowering drug	$C_{10}H_{11}ClO_3$	882-09-7
Gemfibrozil	Cholesterol-lowering drug	$C_{15}H_{22}O_3$	25812-30-0
Hydrocortisone	Dermatological drug	$C_{21}H_{30}O_5$	50-23-7
17α-ethynylestradiol	Estrogen	$C_{20}H_{24}O_2$	57-63-6
DEET	Insect repellent	$C_{12}H_{17}NO$	134-62-3

Naproxen	NSAID	$C_{14}H_{14}O_3$	22204-53-1
Diclofenac Sodium	NSAID	$C_{14}H_{10}Cl_2NNaO_2$	15307-79-6
Ibuprofen	NSAID	$C_{13}H_{18}O_2$	15687-27-1
Meclofenamic Acid	NSAID	$C_{14}H_{11}Cl_2NO_2$	6385-02-0
Codeine	Opiate	$C_{18}H_{21}NO_3$	76-57-3
Nicotine	Stimulant	$C_{10}H_{14}N_2$	54-11-5
Caffeine	Stimulant	$C_8H_{10}N_4O_2$	58-08-2
17-β-estradiol (E2)	Steroid	$C_{18}H_{24}O_2$	50-28-2
Hydrocortisone (HCT)	Corticosteroid	$C_{21}H_{30}O_5$	50-23-7

Figure 3.1: Names and chemical structures of PPCPs in this study



3.2.2. Sample preparation and extraction

Surface water samples were collected by the Department of Analytical Chemistry, Assiut University, Egypt and provided to us at Birmingham. Water samples (1 L) were collected from the effluent of 5 waste water treatment plants (WWTPs) at Assiut governorate, Egypt. These include 3 major WWTPs in Assiut city (Al Helaly, Nazalat- Abdallah and El Walidiyaah), the water treatment plant of Sodfa town, in addition to the water treatment plant of Assiut University hospitals. Furthermore, surface water samples were collected from the River Nile and El-Ebrahmiya canal in Assiut city. These are grab samples collected upstream of the WWTP discharge point in deactivated glass bottles and transferred immediately to the lab, where they were kept at 4 °C until extraction.

Individual and mixture stock solutions (0.5 g/L) of the targeted PPCPs (Table 1) were prepared in methanol and stored in dark amber vials at -20 °C. Working solutions were prepared fresh daily by diluting the stock solutions to the required final concentration and

were stored at 4 °C for a maximum of 24 h. The isotope labelled internal standards were prepared and mixed separately at 1 ng/μL in methanol and kept in dark amber vials at -20 °C.

Environmental water samples were extracted by solid phase extraction (SPE) using Oasis MCX cartridges and Waters™ 20-port controlled pressure vacuum manifold equipped with 50 Hz vacuum pump (Waters, Hertfordshire, UK). The SPE cartridges were pre-conditioned with 3 mL of methanol following by 3 mL of Milli-Q water. 250 mL of the water sample were spiked with 100 ng of isotopically-labelled internal standards mixture and treated with 500 mg Na₂EDTA to release the free form of Tetracycline and Fluoroquinolone antibiotics from potential complexes with Ca⁺² and Mg⁺² in environmental waters (Kasprzyk-Hordern et al., 2007). The samples were loaded onto the pre-conditioned cartridges at a flow rate of 5 mL/min. The cartridges were washed with 3 mL of 0.5 % HCOOH in Milli-Q water (3 mL/min). After drying, PPCPs were eluted with 5 mL of methanol following by 5 mL of 5 % NH₄OH in methanol. The combined eluate was dried under a gentle stream of nitrogen using a TurboVap II® evaporator (Biotage™, Sweden) and reconstituted in 100 μL of methanol containing 25 pg/μL of ¹³C-TBBPA and TCEP-D12 used as recovery (syringe) standards for QA/QC purposes.

3.3. Instrument Analysis

Samples were analyzed on a UPLC system (Thermo Fisher Scientific, Bremen, Germany) composed of a Dionex Ultimate 3000 liquid chromatography equipped with a HPG-3400RS dual pump, a TCC-3000 column oven and a WPS-3000 auto sampler. The UPLC is coupled to a Q-Exactive Plus Orbitrap mass spectrometer equipped with a heated electrospray ionisation (HESI) ion source. 2 mM NH₄COOH/2 mM NH₄F in water (mobile phase A) and 0.5 % formic acid in methanol (mobile phase B). A gradient method at 400 μL/min flow rate was applied as follows: start at 2 % B, stay for 1 min; increase to 98 % B over 11 min, held for 1 min; then decrease to 2 % B over 0.1 min; maintained constant for a total run time of 16 min. Injection volume was 5 μL. The Orbitrap parameters were set as follows: alternate switching (-)/(+) ESI, sheath gas flow rate 50 AU (arbitrary unit), auxiliary gas flow rate 15 AU, spray voltage ± 4.5 kV, capillary temperature 275 °C, probe heater temperature 300 °C. The optimal MS parameters were: S-lens RF-level 50, resolution 17,500 FWHM (Full Width at Half Maximum) and scan

range 125 to 750 m/z. In each scan, the automated gain control (AGC) target in the C-traps was set at 1×10^6 ions and the maximum injection time (IT) was 50 ms.

3.4. Method Validation and quantification

Method linearity was investigated via triplicate injections of 6 point calibration curve for each of the studied analytes over a concentration range of 1 – 1,000 ng/mL, using a fixed concentration of 100 ng/mL of the isotope labelled IS. Linearity was evaluated through the linearity coefficients (R^2) of the obtained calibration curves.

Other method validation parameters were calculated using Milli-Q water spiked with the target PPCPs at 3 concentration levels (10, 250 and 750 ng/mL).

Accuracy was estimated as the percentage recovery of target analytes and evaluated through the percent deviation from the known spiked concentration level.

Precision was calculated as relative standard deviation (RSD %) for inter- and intra-day multiple injections). Nine injections covering the 3 concentration levels (3 injections each) were used for assessment of precision. Further validation of method precision was performed via triplicate analysis of 3 different samples (spiked tap water, surface water from the River Nile and effluent sample A).

Limit of detection (LOD) and limit of quantification (LOQ) were estimated using the signal to noise (S:N) approach. Instrumental detection limit (IDL) was calculated as the lowest concentration that gives a S:N ratio of 3:1, while instrumental quantification limit (IQL) was calculated as the lowest concentration that gives a S:N ratio of 10:1.

Method quantification limits (MQL) were determined by repeated injection of tapwater samples spiked at low concentrations of target compounds. The concentration that produces a S:N ratio of 10 (+2 standard deviation of 5 replicate injections) was estimated as the MQL.

3.5. Quality assurance/quality control (QA/QC)

None of the target compounds were detected in method blanks (one blank for every 5 samples; each blank is composed of 250 mL Milli-Q water treated like a sample). Therefore, no blank correction of the results was required.

Recoveries of the isotope-labelled internal standards were calculated against the syringe standards in all samples and blanks. QC acceptance criteria for method accuracy and precision evaluation was adapted from US EPA method 1694 for PPCPs analysis in water by HPLC/MS/MS: RSD must be smaller than 30% and recovery must be within 55-120% (USEPA, 2007). High recoveries (>80 %) of all five internal standards were obtained indicating good overall performance of the method.

A calibration standard containing all the target compounds and IS (25 pg/ μ L) was injected before and after each sample batch. For a given peak to be identified as a target analyte in a sample; the relative retention time (RRT) of the peak in the sample must be within \pm 0.2 min of the average value determined for the same analyte in the 2 calibration standards run before and after that sample batch (Harrad, 2004).

3.6. Results and discussions

3.6.1 Chromatographic separation and mass spectrometry

Individual standards of PPCPs were infused into the Orbitrap mass spectrometer by a syringe pump at 20 μ L/min in order to identify the most abundant ions and their respective ionization modes for each PPCPs and ISs. For all of the studied compounds, the most abundant ions were either positive or negative pseudo molecular ion: $[M+H]^+$ or $[M-H]^-$. Among the 29 PPCPs, 16 of them were ionized in positive mode and 6 of them were ionized in negative mode. Interestingly, 7 PPCPs were well-ionized in both positive and negative mode including sulfamethoxazole, naproxen, oxazepam, valsartan, diclofenac sodium, meclofenamic acid and glyburide. This information can be used as an additional confirmation tool for such compounds when analyzing real samples. For compounds which can be measured in both ionization modes, the mode that produced higher intensity ions (i.e. higher sensitivity) was chosen for quantification. The accurate masses of the most abundant ions were calculated using the isotope simulator function of Xcalibur software (Table 3.2).

Table 3.2: PPCPs identified by LC-Obitrap HRMS

Compound	Ionization Mode	Accurate Mass (Da)	RT (Min)	Internal Standard
Metformin	+ve	130.10884	0.64	IS1
Nicotine	+ve	163.12318	3.43	IS1
Acetaminophen	+ve	152.07143	3.46	IS1
Gabapentin	+ve	172.13417	3.65	IS1
Codeine D3 (IS1)	+ve	303.17923	4.63	
Codeine	+ve	300.16089	4.69	IS1
Caffeine D9 (IS2)	+ve	204.14500	5.03	
Caffeine	+ve	195.08862	5.07	IS2
Trimethoprim	+ve	291.14540	5.40	IS1
Sulfamethoxazole	+ve	254.05949	5.50	IS2
	-ve	252.04526		
Tramadol	+ve	264.19584	6.20	IS1
Metoprolol	+ve	268.19076	6.33	IS1
Propranolol	+ve	260.16433	7.97	IS1
4 Chlorophenol-2,3,5,6 D4 (IS3)	-ve	131.01939	8.05	
Clofibric acid	-ve	213.03217	8.13	IS3
Carbamazepine D10 (IS4)	+ve	247.16600	8.42	
Carbamazepine	+ve	237.10333	8.49	IS4
Hydrocortisone	+ve	363.21686	8.67	IS4
Naproxen	+ve	231.10198	9.05	IS4
	-ve	229.08824		
DEET	+ve	192.13931	9.07	IS4
Erythromycin	+ve	734.47192	9.14	IS4
Oxazepam	+ve	287.05860	9.17	IS4
	-ve	285.04430		
Valsartan	+ve	436.23466	9.38	
	-ve	434.22117		IS3

Mefloquine Hydrochloride	-ve	413.08759	9.78	IS3
17α-ethynylestradiol	-ve	295.17047	9.87	IS5
β-estradiol	-ve	271.16998	9.88	IS5
Diazepam	+ve	285.07928	9.89	IS4
Estrone-2,4,16,16 D4 (IS5)	-ve	273.18024	9.91	
Diclofenac Sodium	+ve	296.02432	10.06	IS4
	-ve	294.01031		
Glyburide	+ve	494.15155	10.34	
	-ve	492.13818		IS3
Ibuprofen	-ve	205.12297	10.61	IS3
Meclofenamic acid	+ve	296.02432	10.78	IS4
	-ve	294.01031		
Clotrimazole	+ve	345.11676	11.28	IS4
Gemfibrozil	-ve	249.15001	11.54	IS3

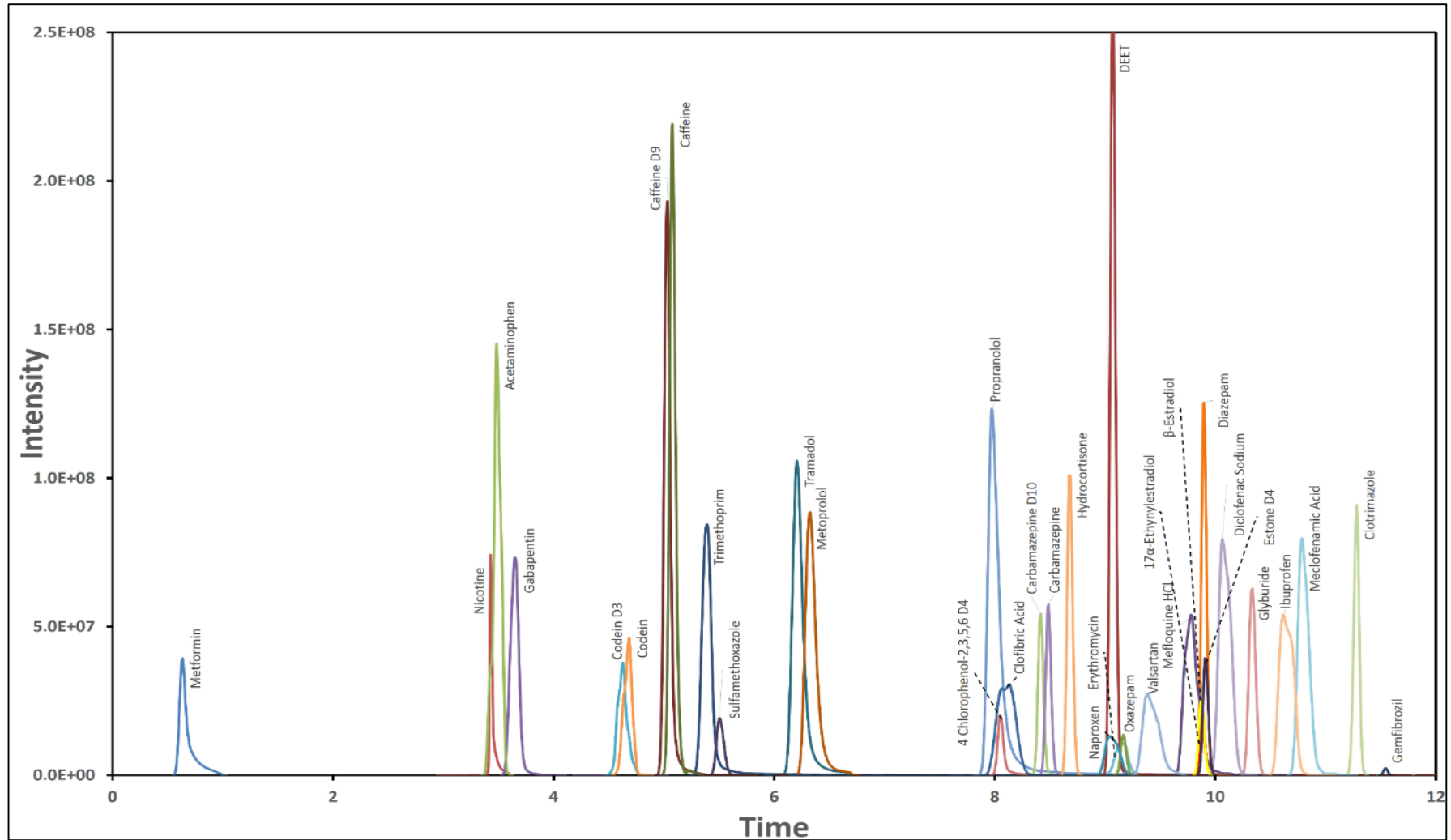
After successful identification of quantifier ions, a standard solution containing all target PPCPs and ISSs were subjected to UPLC-HRMS for optimization of UPLC separation and mass spectrometry parameters. We evaluated the effects of UPLC gradient, flow rate, mobile phase composition and modifiers, column temperature and injection volume on the peak shape and separation of 29 PPCPs. Optimal conditions for UPLC have been reported in section 3.3.

The chromatogram of calibration standard level 3 following the analysis using optimal UPLC conditions is presented in Figure 3.2. The targeted compounds were eluted within the retention time range 0.64 to 11 min indicating their broad polarity range (Table 3.2). Due to the different accurate masses of quantifier ions for each PPCP (with the exception of diclofenac sodium and meclofenamic acid), it is not essential to baseline separate every peak. Theoretically a much shorter gradient can be applied, however a gradient with a total run time of 16 min was chosen to allow enough time for column equilibration and avoid potential ion suppression due to co-elution of analytes (to allow for possible addition of other target compounds to the method in future studies). Additionally, as we

used alternate switching ionization in this study, a 16 min gradient provided sufficient data points on each peak for reproducible PPCP quantification.

The ionization and mass spectrometry parameters were optimized using spiked tap water extracts and peak intensities of the targeted PPCPs as well as the number of data points for each peak were the main evaluation criteria. The optimal ionization and mass spectrometric parameters are reported in section 3.3. Despite the fact that the Q Exactive Plus instrument can run at a resolution as high as 240,000 FWHM, a resolution of 17,500 FWHM was chosen in this study. This was a trade-off between the ion mass accuracy and scan rate (or the number of data points for a peak). When the instrument runs at higher resolving power, a much more accurate ion mass will be recorded and consequently a better selectivity of analyzing compounds against isobaric matrix interferences can be achieved. However, in order to obtain such high resolution, the orbitrap mass spectrometer requires much more time to scan. For example, the scan rate for a 200 m/z ion at 140,000 FWHM is 1.5 Hz compared to 12 Hz at 17,500 FWHM. In other words, a two second chromatographic peak will contain 3 or 36 data points at a resolution of 140,000 or 17,500 FWHM, respectively. In addition, we used alternate ionization switching in this study which would reduce the number of data points by half for a given peak in comparison with single polarity ionization mode. Therefore, a resolving power of 17,500 FWHM was selected as it offered sufficient data points (> 10) with sufficient mass accuracy for identification and quantification (mass deviation < 5 ppm).

Figure 3.2: Extracted Ion Chromatogram of our target PPCPs and Internal Standards in calibration standard level 3



3.6.2. Quantification and validation

3.6.2.1. Method linearity

The calibration curves of the 29 PPCPs were obtained by plotting concentration of targeted compounds versus the peak area ratio of each compound and its corresponding internal standard. Calibration plots and R^2 (linearity coefficient) values for each PPCP showed very good linearity over the calibration range (1 to 1000 ng/mL) where the majority of R^2 values exceeded 0.99 (Table 3.3.)

Table 3.3: Linearity coefficient and calibration equation for PPCPs analysis by UPLC-HRMS in this study

Compound	R^2	Equation
Nicotine	0.999	$Y = 0.0145 + 0.0028 * X$
Metformin	0.997	$Y = 0.0108 + 0.0019 * X$
Acetaminophen	0.994	$Y = 0.0166 + 0.0004 * X$
Gabapentin	0.995	$Y = 0.0098 + 0.0021 * X$
Codeine	0.998	$Y = 0.0343 + 0.002 * X$
Caffeine	0.995	$Y = 0.0385 + 0.0018 * X$
Trimethoprim	0.998	$Y = 0.0494 + 0.0027 * X$
Sulfamethoxazole	0.996	$Y = 0.0825 + 0.0026 * X$
Tramadol	0.996	$Y = 0.3368 + 0.0226 * X$
Metoprolol	0.999	$Y = 0.1824 + 0.0201 * X$
Propranolol	0.996	$Y = 0.5527 + 0.0284 * X$
Doxycycline	0.998	$Y = -0.0595 + 0.0092 * X$
Carbamazepine	0.975	$Y = 0.1566 + 0.0014 * X$
Hydrocortisone	0.986	$Y = 0.0149 + 0.00023 * X$

Naproxen	0.963	$Y = 0.0079 + 9E-5*X$
DEET	0.952	$Y = 0.8109 + 0.0055*X$
Erythromycin	0.992	$Y = 0.009 + 0.0009*X$
Oxazepam	0.992	$Y = 0.0157 + 0.0004*X$
Valsartan	0.995	$Y = 0.0009 + 0.0002*X$
Mefloquine hydrochloride	0.994	$Y = -0.0025 + 0.0002*X$
17α-ethynylestradiol	0.995	$Y = 0.0290 + 0.0009*X$
β-estradiol	0.995	$Y = 0.0483 + 0.0011*X$
Diazepam	0.974	$Y = 0.1909 + 0.0033*X$
Diclofenac Sodium	0.994	$Y = 0.0012 + 0.0002*X$
Glyburide	0.995	$Y = 0.00162 + 0.0002*X$
Ibuprofen	0.995	$Y = -0.0014 + 0.0004*X$
Meclofenamic acid	0.999	$Y = -0.0017 + 0.0001*X$
Clotrimazole	0.962	$Y = 0.0105 + 0.0002*X$
Gemfibrozil	0.991	$Y = -0.0007 + 3E-5*X$

3.6.2.2. Accuracy and precision

The method accuracy was estimated as the percentage recovery of target analytes and evaluated through the percent deviation from three spiked concentration levels: 10 ng/mL, 250 ng/mL and 750 ng/mL. For every concentration level, three injections of triplicate samples (total 9 injections) were made and the results are presented in Table 3.4.

Table 3.4: Method accuracy expressed as % recovery at 3 spiked concentration levels of PPCPs in Milli-Q water

Compound	10 ng/mL	250 ng/mL	750 ng/mL
Nicotine	91.2 ± 7.2	93.1 ± 8.6	95.3 ± 2.7
Metformin	91.5 ± 6.6	90.8 ± 8.0	94.2 ± 2.9
Acetaminophen	93.4 ± 7.8	98.1 ± 2.8	97.6 ± 2.8
Amoxicillin	88.1 ± 3.1	88.2 ± 3.3	89.5 ± 2.8
Gabapentin	90.7 ± 7.6	88.1 ± 3.7	92.6 ± 6.0
Codeine	92.7 ± 3.2	92.2 ± 3.8	91.2 ± 2.5
Caffeine	103.4 ± 5.9	101.1 ± 4.6	99.7 ± 4.2
Trimethoprim	95.6 ± 6.6	96.8 ± 2.6	96.4 ± 3.1
Sulfamethoxazole	93.2 ± 3.1	92.3 ± 3.1	93.0 ± 2.8
Tramadol	89.6 ± 5.8	93.8 ± 2.5	92.2 ± 3.5
Metoprolol	92.0 ± 2.9	93.6 ± 3.6	93.6 ± 3.3
Propranolol	95.2 ± 9.4	93.7 ± 5.6	97.8 ± 2.6
Doxycycline	86.3 ± 4.2	85.1 ± 4.0	85.7 ± 4.1
Carbamazepine	87.7 ± 2.8	88.0 ± 3.5	88.7 ± 3.3
Hydrocortisone	82.4 ± 5.1	84.0 ± 5.8	84.2 ± 3.7
Naproxen	89.0 ± 5.4	90.2 ± 4.2	91.4 ± 4.6
DEET	87.1 ± 8.1	95.8 ± 3.0	99.3 ± 2.1
Erythromycin	81.9 ± 4.2	85.6 ± 3.8	83.1 ± 3.2
Oxazepam	92.6 ± 6.8	96.5 ± 4.2	94.9 ± 4.8
Valsartan	86.6 ± 9.3	92.8 ± 8.0	98.2 ± 4.5

Mefloquine hydrochloride	85.7 ± 4.3	87.2 ± 5.1	87.2 ± 4.2
17α-ethynylestradiol	79.0 ± 6.2	78.4 ± 5.0	79.2 ± 3.9
β-estradiol	77.8 ± 5.1	76.6 ± 4.9	76.2 ± 5.7
Diazepam	93.4 ± 9.7	93.7 ± 7.1	97.5 ± 3.5
Diclofenac Sodium	89.9 ± 3.4	88.2 ± 4.3	89.9 ± 3.9
Glyburide	86.5 ± 4.8	87.9 ± 3.9	90.5 ± 4.7
Ibuprofen	91.7 ± 2.9	90.4 ± 3.5	90.7 ± 3.5
Meclofenamic acid	86.7 ± 5.7	85.7 ± 4.6	85.9 ± 3.9
Clotrimazole	102.4 ± 4.9	100.7 ± 3.5	102.4 ± 3.5
Gemfibrozil	89.0 ± 8.0	92.1 ± 7.6	95.8 ± 4.2

As can be seen in Table 3.4, our method showed very good accuracy ranging from 76.2 to 103.4 % recovery for all targeted compounds across three concentration levels. The relative standard deviations (RSD) of the recoveries were all below 10 %. These recoveries are similar to those previously reported for PPCPs analysis by (-)/(+)APCI-UPLC-Orbitrap HRMS (Huysman et al., 2017) and better than some LC-MS/MS methods (Al-Odaini et al., 2010; Caldas et al., 2016).

The precision was evaluated by RSD for repeatability (intra-day precision) and reproducibility (inter-day precision). The RSD for repeatability and reproducibility ranged between 0.4 to 13.5% and 2.2 to 10.8%, respectively (Table 3.5).

Table 3.5: Intra- and inter-day precision expressed as RSD% for targeted PPCPs

Compounds	Intra-day precision			Inter-day precision		
	10 ng/mL	250 ng/mL	750 ng/mL	10 ng/mL	250 ng/mL	750 ng/mL
Nicotine	3.2	9.1	1.8	7.9	9.2	2.8

Metformin	2.3	6.8	3.2	7.2	8.8	3.1
Acetaminophen	3.1	3.1	3.8	8.4	2.8	2.9
Amoxicillin	1.6	3.7	1.1	3.5	3.8	3.1
Gabapentin	8.8	6.0	8.4	8.4	4.2	6.5
Codeine	2.8	1.7	3.6	3.4	4.1	2.7
Caffeine	2.2	4.8	5.1	5.7	4.6	4.2
Trimethoprim	2.3	4.1	4.3	6.9	2.7	3.2
Sulfamethoxazole	1.4	1.5	4.2	3.3	3.3	3.1
Tramadol	2.2	2.8	5.4	6.5	2.7	3.8
Metoprolol	2.1	0.4	3.5	3.1	3.8	3.6
Propranolol	13.5	5.6	1.2	9.8	5.9	2.6
Doxycycline	4.6	4.1	5.2	4.8	4.7	4.8
Carbamazepine	2.2	5.6	3.9	3.1	4.0	3.8
Hydrocortisone	6.1	4.8	4.4	6.2	6.8	4.3
Naproxen	2.8	3.3	4.0	6.1	4.6	5.0
DEET	7.4	3.5	2.5	9.3	3.1	2.2
Erythromycin	5.4	1.8	2.4	5.1	4.4	3.9
Oxazepam	11.0	2.3	5.5	7.3	4.4	5.0
Valsartan	12.9	10.5	4.0	10.8	8.7	4.6
Mefloquine hydrochloride	5.2	8.0	5.8	5.0	5.9	4.8
17α-ethynylestradiol	8.2	2.9	4.8	7.9	6.4	4.9

β-estradiol	7.9	2.0	4.0	6.5	6.4	7.4
Diazepam	3.7	6.7	3.6	10.4	7.6	3.6
Diclofenac Sodium	2.4	6.5	5.9	3.8	4.9	4.3
Glyburide	2.6	3.4	6.6	5.5	4.4	5.2
Ibuprofen	2.6	3.8	4.0	3.2	3.9	3.9
Meclofenamic acid	1.3	6.1	4.3	6.5	5.3	4.6
Clotrimazole	6.8	3.3	1.1	4.8	3.5	3.4

As Milli-Q water is ultrapure, this might underestimate the matrix effects of real samples on the method's performance. Therefore, we further evaluated the precision for some aquatic matrices including spiked tap water (at 500 ng/L), river water and effluent from a waste water treatment plant. Among the three investigated matrices, spiked tap water showed the lowest RSDs while the effluent sample had higher RSDs than river water for most of the detected PPCPs (Table 3.6). This is reasonable as effluent samples usually contain more chemicals and organic matter than river water. The results in Table 3.6 demonstrated that similar precision values were obtained in comparison with spiked Milli-Q water experiment. Therefore, it is projected that this method can be extended to other complex aquatic matrices e.g. leachate, influent and effluent of waste water treatment plants or river water without losing the precision and accuracy.

Table 3.6: Precision for complex matrices expressed as RSD% for triplicate analysis of target PPCPs

Compounds	Spiked tap water	Effluent	Surface water
Nicotine	6.8	9.3	10.9
Metformin	5.6	11.6	6.9
Acetaminophen	2.1	5.1	5.9
Amoxicillin	3.8	12.2	7.4

Gabapentin	9.5	<MQL	9.9
Codeine	6.0	<MQL	9.7
Caffeine	8.2	5.4	8.3
Trimethoprim	1.5	11.2	7.6
Sulfamethoxazole	4.9	13.4	3.3
Tramadol	4.2	10.8	9.9
Metoprolol	4.8	<MQL	<MQL
Propranolol	8.0	15.1	11.9
Doxycycline	4.0	<MQL	<MQL
Carbamazepine	5.2	16.3	13.8
Hydrocortisone	6.2	12.6	7.5
Naproxen	5.4	<MQL	<MQL
DEET	3.6	<MQL	<MQL
Erythromycin	5.1	8.5	<MQL
Oxazepam	3.4	<MQL	<MQL
Valsartan	4.5	10.3	8.2
Mefloquine hydrochloride	6.0	<MQL	12.1
17α-ethynylestradiol	6.3	<MQL	<MQL
β-estradiol	4.9	<MQL	<MQL
Diazepam	6.3	<MQL	<MQL
Diclofenac Sodium	4.7	8.9	6.9
Glyburide	6.2	3.5	3.6

Ibuprofen	8.7	11.3	<MQL
Meclofenamic acid	8.8	6.3	6.8
Clotrimazole	6.9	13.5	8.9
Gemfibrozil	8.7	<MQL	9.6

3.6.2.3 Detection and quantification limits.

The instrument detection and quantification limits were determined by analysis of pure standards. A wide range of IDLs and IQLs was acquired (Table 3.7). The IDLs ranged from 0.02 to 1.21 ng/mL while IQLs ranged from 0.07 to 4.05 ng/mL. The big differences in IDLs and IQLs of targeted chemicals were possibly due to: 1. variable ionization efficiency for different analytes and/or polarity mode; and 2. matrix effects or co-elution at a particular retention time, which affected the sensitivity of the instrument.

Table 3.7: IDLs, IQLs and MQLs for the developed PPCP analysis method by UPLC-HRMS

Compounds	IDL (ng/mL)	IQL (ng/mL)	MQL (ng/L)
Nicotine	0.50	1.67	13.3
Metformin	0.10	0.33	9.5
Acetaminophen	0.10	0.33	2.8
Amoxicillin	1.10	3.67	22.4
Gabapentin	0.28	0.93	5.2
Codeine	0.23	0.77	5.0
Caffeine	0.80	2.80	7.2
Trimethoprim	0.04	0.12	2.4
Sulfamethoxazole	0.06	0.20	3.4
Tramadol	0.17	0.56	4.6

Metoprolol	0.02	0.07	2.7
Propranolol	0.04	0.14	4.7
Doxycycline	0.24	0.79	22.9
Carbamazepine	0.02	0.07	2.5
Hydrocortisone	0.34	1.13	37.8
Naproxen	0.09	0.30	4.7
DEET	0.11	0.37	5.7
Erythromycin	0.25	0.84	22.0
Oxazepam	0.15	0.49	6.3
Valsartan	0.32	1.05	8.6
Mefloquine hydrochloride	0.30	0.99	24.7
17α-ethynylestradiol	1.21	4.05	83.8
β-estradiol	1.16	3.87	81.0
Diazepam	0.13	0.43	4.7
Diclofenac Sodium	0.15	0.50	9.8
Glyburide	0.30	0.99	12.9
Ibuprofen	0.12	0.41	8.9
Meclofenamic acid	0.17	0.57	10.3
Clotrimazole	0.36	1.19	16.3
Gemfibrozil	0.31	1.05	14.5

MQL values were obtained by analysis of spiked tap water containing target PPCPs at concentrations that ranged from 2.4 to 83.8 ng/L (Table 3.7). Among our 29 target PPCPs, the hormones β -estradiol and 17 α -ethynylestradiol showed the highest MQLs at 81 and 83.8 ng/L, respectively. The MQLs for other chemicals were less than 37.8 ng/L.

3.6.3. Application to surface water samples

After successful validation, the method was applied to effluent and surface water samples collected in Egypt. The effluent was sampled at 5 waste water treatment plants (WWTPs) at Assiut governorate, Egypt. These include 3 major WWTPs in Assiut city (Al Helaly, Nazalat- Abdellah and El Walidiyaah), the water treatment plant of Sodfa town, in addition to the water treatment plant of Assiut University hospitals. The surface water samples were collected from the River Nile and El-Ebrahmiya canal in Assiut city upstream of the WWTP discharge point.

Among the targeted PPCPs, two of them (mefloquine hydrochloride and DEET) were not found in any samples; ten of them (nicotine, metformin, acetaminophen, caffeine, tramadol, metoprolol, hydrocortisone, valsartan, glyburide and ibuprofen) were detected in all of the samples while the rest was occasionally detected (Table 3.8). Effluent samples also showed generally higher concentrations of PPCPs than surface water samples. Similar findings have been reported previously (Ebele et al., 2017; Kolpin et al., 2002; Ternes, 1998).

Table 3.8: PPCPs concentrations in Egyptian effluent and surface water samples.

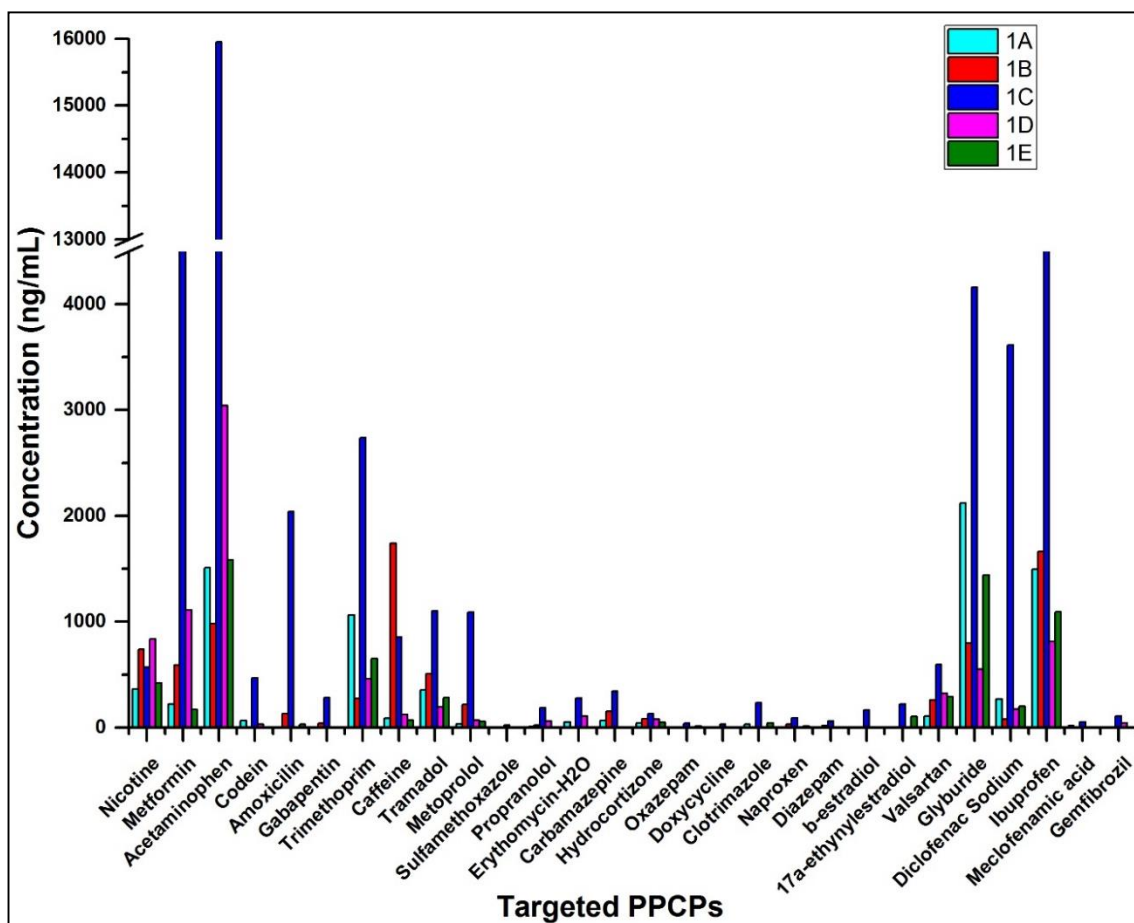
	Effluent samples (ng/L)						Surface water (ng/L)					
	1A	1B	1C	1D	1E	Median	2F	2G	2H	2I	2J	Median
Acetaminophen	1510	978	16000	3040	1580	1580	954	144	207	392	776	392
Ibuprofen	1500	1660	6700	812	1090	1500	51	26	91	62	34	51
Glyburide	2120	798	4160	550	1440	1440	333	628	393	365	253	365
Metformin	219	589	5610	1110	168	589	32	63	23	21	36	32
Trimethoprim	1060	271	2740	459	650	650	230	116	210	224	175	210
Diclofenac Sodium	269	79	3614	172	201	201	35	<9.8	77	44	<9.8	44
Nicotine	365	736	567	835	419	567	116	90	269	378	98	116
Caffeine	84	1740	855	121	70	121	12	41	15	7	54	15
Tramadol	353	508	1100	192	282	353	41	93	56	32	58	56
Amoxicillin	<22.4	129	2040	<22.4	29	129	<22.4	24	<22.4	<22.4	28	<22.4
Valsartan	107	258	594	318	290	290	63	55	104	59	36	59

Metoprolol	34	218	1100	67	57	67	17	8	5	9	12	9
Codein	63	<5	466	29	<5	63	<5	18	14	21	15	16.5
Carbamazepine	63	151	342	<2.5	<2.5	151	<2.5	6	<2.5	8	1	6
Erythromycin-H₂O	52	<22	275	106	<22	106	<22	<22	<22	33	61	<22
Hydrocortizone	43	83	128	77	46	77	36	43	64	42	40	42
17α-ethynylestradiol	<83.8	<83.8	219	<83.8	104	<83.8	<83.8	<83.8	<83.8	<83.8	<83.8	<83.8
Gabapentin	<5.2	40	279	<5.2	<5.2	<5.2	<5.2	8	<5.2	12	<5.2	<5.2
Clotrimazole	31	<16.3	231	<16.3	43	43	<16.3	23	<16.3	18	<16.3	20.5
Propranolol	8	19	187	62	<4.7	40.5	<4.7	6	<4.7	7	<4.7	<4.7
β-estradiol	<81	<81	165	<81	<81	<81	<81	<81	<81	<81	<81	<81
Gemfibrozil	<14.5	<14.5	105	44	<14.5	74.5	<14.5	17	<14.5	16	21	17
Naproxen	<4.7	29	89	<4.7	13	29	<4.7	6	<4.7	<4.7	8	7
Diazepam	<4.7	17	58	<4.7	<4.7	<4.7	<4.7	<4.7	<4.7	9	<4.7	9
Meclofenamic acid	17	<10.3	52	<10.3	<10.3	<10.3	<10.3	12	<10.3	<10.3	<10.3	<10.3

Oxazepam	<6.3	<6.3	39	<6.3	10	24.5	<6.3	<6.3	<6.3	<6.3	<6.3	<6.3
Doxycycline	22.9	22.9	29	22.9	22.9	22.9	22.9	22.9	22.9	22.9	22.9	22.9
Sulfamethoxazole	<3.4	<3.4	19	<3.4	<3.4	19	<3.4	<3.4	<3.4	<3.4	<3.4	<3.4

As can be seen in Table 3.8, acetaminophen, ibuprofen, glyburide, metformin, trimethoprim, nicotine, caffeine, tramadol, valsartan, metoprolol and hydrocortisone were detected in all of the samples, indicating their ubiquity in the Egyptian fresh-water aquatic environment. In effluent samples some analgesics, NSAIDs, antidiabetics and antibiotics were found at very high abundances (Table 3.8 and Figure 3.3). In particular, acetaminophen showed the highest concentrations ranging from 978 to 16,000 ng/L, following by ibuprofen (812-6,700 ng/L), glyburide (550-4,160 ng/L), metformin (168-5,610 ng/L), trimethoprim (271-2,740 ng/L) and diclofenac sodium (79-3,610 ng/L). Caffeine and nicotine also showed relatively high concentrations ranging from 365 to 835 ng/L and 70 to 1,740 ng/L, respectively.

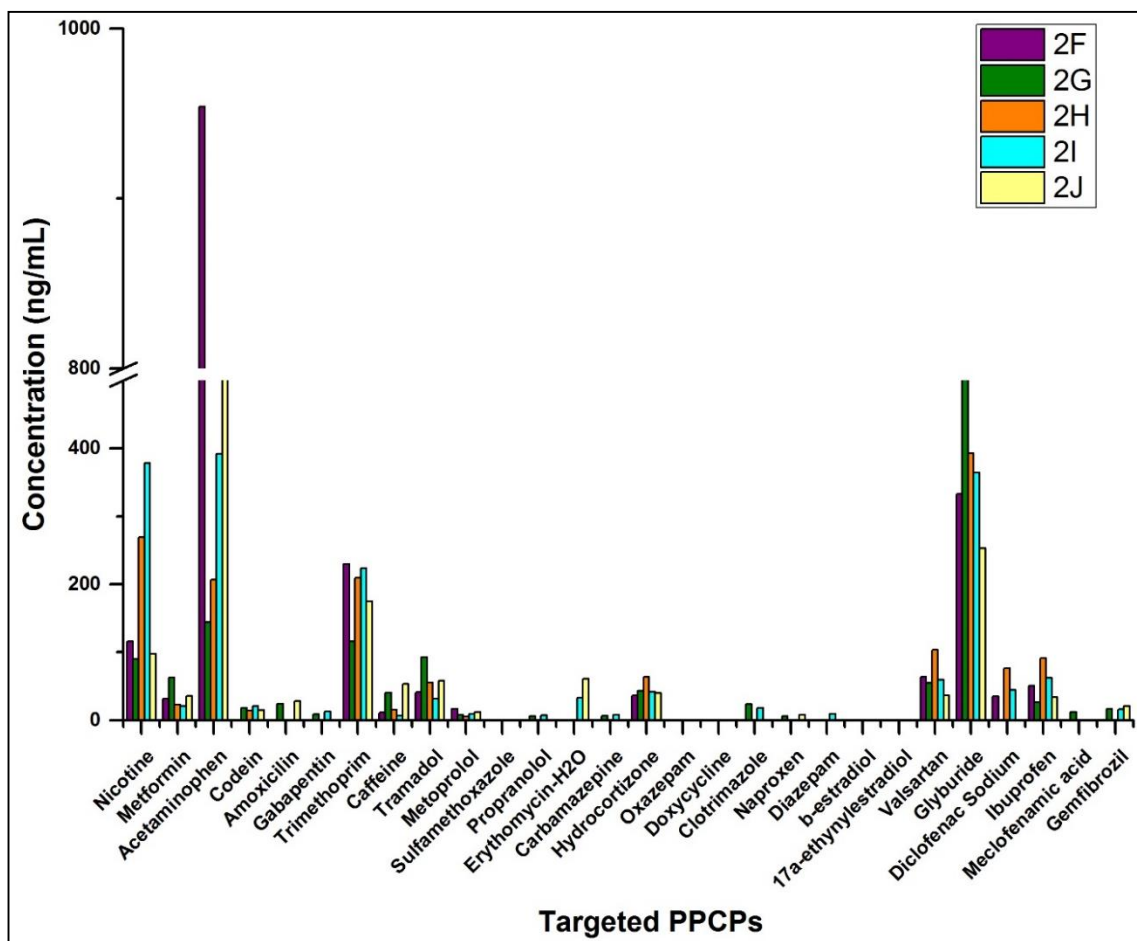
Figure 3.3: Concentrations of PPCPs (ng/L) in effluent samples from waste water treatment plants in Assiut city, Egypt



While the concentrations of PPCPs effluent samples from locations 1A, 1B and 1D-E were similar or lower than reported previously e.g. in German municipal sewage treatment plants (STPs) (Ternes, 1998), Chinese WWTPs (Zhou et al., 2009) or

Malaysian STPs (Al-Qaim et al., 2014); the detected levels of some PPCPs in location 1C were much higher. This sample was effluent from a hospital WWTP and showed the highest concentrations for most PPCPs (Figure 3.3). For example, in sample 1C, acetaminophen, ibuprofen and metformin were measured at 16,000, 6,700 and 5,610 ng/L, respectively. On the other hand, the highest nicotine and caffeine concentrations were not present in this 1C sample. This is reasonable as high consumption of pharmaceuticals is expected at hospitals while nicotine and caffeine are related to daily habits.

Figure 3.4: Concentrations (ng/mL) of PPCPs in surface water samples collected from Assiut city, Egypt



In surface water sample, analgesics, antidiabetics, antibiotics and nicotine showed higher concentrations than other detected PPCPs (Figure 3.4). Specifically, acetaminophen was detected at maximum concentration of 954 ng/L, followed by glyburide (628 ng/L), trimethoprim (230 ng/L) and nicotine (378 ng/L). High levels of acetaminophen were reported previously in effluent-dominated stream in Japan (up to 682 ng/L) (Tamura et

al., 2017) or in US streams (up to 10,000 ng/L) (Kolpin et al., 2002). Oxazepam, doxycycline, sulfamethoxazole, β -estradiol and 17 α -ethynylestradiol were not detected while other PPCPs were measured at concentrations less than 100 ng/L. In contrast to effluent samples, detected PPCPs in surface water samples did not largely differ between sampling locations with the exception of acetaminophen.

As effluent from WWTPs will be diluted after reaching fresh water streams, it is expected that PPCPs levels in effluent are higher than that in surface water. Therefore, we applied a non-parametric statistical method to test whether this hypothesis holds true for detected chemicals in this study. The results of a Kruskal-Wallis test indicated that nicotine, metformin, acetaminophen, trimethoprim, caffeine, tramadol, metoprolol, hydrocortisone, valsartan, glyburide, diclofenac sodium and ibuprofen were significantly higher in effluent samples than surface water samples at the 95 % confidence level.

3.7. Conclusions

In summary, a rapid, reproducible and accurate method for analysis of multiple PPCPs in various aquatic matrices by UPLC-Orbitrap HRMS system has been developed. The proposed method was sensitive, robust and high throughput in character, which allowed the detection of 29 compounds, with the possibility to extend the target list. The method has been successfully applied to assess the levels of 29 targeted chemicals in effluent and surface water samples collected in Egypt. Our data showed that PPCPs were ubiquitous in Egyptian aquatic samples. Among the detected compounds, analgesics, NSAIDs, antidiabetics, antibiotics, caffeine and nicotine were predominant. It is suggested that more efficient water treatment processes to remove PPCPs are needed, especially for hospital wastewater.

Chapter 4

Simultaneous targeted and
untargeted screening of BFRs and
transformation products by UPLC-
HRMS: application to samples of
waste leachate and samples
generated by *in vitro* challenge of
mouse liver microsomes with EH-TBB,
BEH-TEBP and BTBPE

4.1. Synopsis

It is reported that there are more than 75 BFRs currently available in the market (Covaci et al., 2011). This estimate might be inaccurate as chemical companies do not always publicize the exact chemicals used in their flame retardant mixture formulae. However, simultaneous monitoring of these chemicals is extremely difficult due to the large variation in physicochemical properties. Currently analysis of BFRs is often performed on GC or LC coupled with mass spectrometers (Papachlimitzou et al., 2012). Some advantages of LC over GC are that LC allows analysis of hydrophilic compounds without the need for derivatization, while thermal degradation/isomerization is minimized. In this chapter, we aimed to develop a UPLC-HRMS method for screening of BFRs, and potentially unknown BFRs and associated transformation products in environmental samples with focus on NBFRs. The method was then applied to screen for BFRs in samples generated from a leaching test (Section 2.1.1) as well as provide preliminary information about *in vitro* biotransformation of EH-TBB, BEH-TEBP and BTBPE by mouse liver microsomes (MLM) (Section 2.1.3).

4.2. Experiments

4.2.1. Chemicals

All solvents and reagents used in this study were purchased from Fisher Scientific (Loughborough, UK) and were of HPLC grade or higher. EH-TBB, BEH-TEBP and BTBPE for dosing solutions was obtained as neat solutions/powders from Accustandard, Inc. (New Haven, CT, USA). High purity standards of BFRs and internal standards (Table 4.2) were purchased from Wellington Laboratories (Guelph, ON, Canada). RapidStart NADPH regenerating system was purchased from XenoTech (Kansas, KS, USA), William's E medium was obtained and mouse liver microsomes were purchased from Thermo Fisher Scientific (Paisley, UK).

Individual EH-TBB, BEH-TEBP and BTBPE dosing solutions at 1000 μM were prepared by dissolving them in either dimethyl sulfoxide (DMSO) or Toluene.

4.2.2. Leachate sample preparation and extraction

Simulated samples generated by a series of leachate experiments carried out by Danish Waste Solutions ApS were provided to us at Birmingham. The experiments involved different types of Waste Electrical and Electronic Equipment (WEEE) undergoing leaching for 24 hours in a container using deionized water. Three different groups of WEEE items were studied, each in a separate experiment:

1. Mixed WEEE including small household items, computers, electrical tools, etc. in a 1,000 L High-density polyethylene (HDPE) container.
2. Whole liquid-crystal displays (LCDs) or cathode ray tube monitor (CRTs) in a 1,000 L HDPE container.
3. Whole fridges/freezers in a 10,000 L metal container.

Samples were provided as crude leachate without pre-filtering and stored in glass bottles in a temperature controlled room (15 °C) until analysis.

We aimed to develop an untargeted method for screening of NBFs in leachate samples. This was performed using a liquid/liquid extraction method. The samples were filtered through a 0.7 µm pore size glass fibre filter (Whatman, USA) to remove any visible particles or fibres. Because there was no information about what NBFs might be present in the sample, we selected some ¹³C-labelled BFRs as internal standards (ISs). These standards would help to quantify and semi-quantify detected NBFs, if needed. The advantages of isotope labelled internal standards are that they do not naturally occur in the environment and behave in a similar manner with the analytes during extraction, sample preparation and instrument analysis. Liquid chromatography coupled to mass spectrometry (LC-MS) is well known to be susceptible to matrix effects (e.g. ion suppression or ion enhancement) especially in Electrospray Ionization mode (ESI) but also to a lesser extent in Atmospheric Pressure Chemical Ionization mode (APCI) (Helga et al., 2011). The introduction of isotope labelled ISs can compensate for extraction and sample preparation losses as well as matrix effects in LC-MS analysis.

Six samples of each leachate test category (M, L and F) together with one field blank (BF) and transportation blank (BL) were extracted and screened for BFRs (Table 4.1). Only

one M sample needed to be filtered before extraction to remove visible particles or fibers. For extraction of semi volatile chemicals in water, there are several common organic solvents that can be used: hexane, benzene, toluene, dichloromethane (DCM) and ethyl acetate. Benzene and toluene are suitable for extraction of aromatic compounds but are more toxic than other solvents. Hexane is good for extraction of non-polar chemicals e.g. aliphatic hydrocarbons while ethyl acetate works best with semi polar compounds (e.g. ester, ether). DCM on the other hand is a polar aprotic solvent and efficient to extract both non-polar and polar compounds. Fast evaporation is also an advantage of DCM. Therefore, DCM was chosen as the solvent of choice for extraction of BFRs in our samples (Chandra, 2015).

Table 4.1: Different sample categories in stimulated leachate test

Sample types	Description
M	Mixed wasted electrical and electronic equipment
L	Whole LCDs/CRTs
F	Whole fridges/freezers
BF	Field blank (deionized water)
BL	Transportation blank (deionized water)

Twenty nanograms each of ^{13}C -BDE-28, ^{13}C -BDE-209 and ^{13}C -BTBPE were added as internal standards to 250 mL of leachate samples. Additionally, in order to decrease hydration power of water (meaning decrease the solubility of slightly soluble organic compounds), 5 mL of 2 % NaCl solution was added. However, if an undesirable emulsion in the sample was formed likely due to an excess amount of dissolved humic materials, a new portion of that sample was used for extraction without adding NaCl solution. The samples were then extracted with 50 mL of DCM by ultrasonication in 30 min following by mechanical shaking twice for 3 hours with 50 mL DCM. In each steps, the organic layers were kept and combined together. PTFE caps were used to prevent spillage and leakage of samples during the extraction process. Each sample batch consisted of 6 samples taken from at least 2 different sample categories.

The combined extracts were concentrated to 0.5 mL on a Zymark Turbovap® II (Hopkinton, MA, USA) then loaded onto a layered SPE cartridge consisted of (by order, top to bottom) 2 g Na_2SO_4 , 6 g 22 % acid silica and 2 g Na_2SO_4 pre-conditioned with 2 x

2 mL of hexane. The cartridge was eluted with 20 mL hexane followed by 20 mL DCM. The eluent was evaporated to dryness under a gentle nitrogen stream, reconstituted in 100 μ L methanol ready for analysis.

4.2.3. *In vitro* incubation experiments

The following exposure protocol was applied in triplicates for two levels of exposure to the studied NBFRs (1 and 10 μ M): 0.5 mg of mouse liver microsomes, William's E medium and 10 μ L of an NBFR dosing solution (final concentration of 1 and 10 μ M) were pre-incubated for 10 minutes at 37 °C. NADPH regenerating system (final concentration: 2.0 mM nicotinamide adenine dinucleotide phosphate, 10.0 mM glucose-6-phosphate and 2 units/mL glucose-6-phosphate dehydrogenase) was added to make a final volume of 1 mL. The samples were then incubated at 37 °C, 5 % CO₂ and 98 % relative humidity for 60 min. At the end of the incubation, 1 mL of ice-cold methanol was added to stop the reaction prior to sample extraction. Negative control samples were also carried out. These included: 1, a non-enzymatic blank in which no NADPH regenerating system was added. 2, a heat-inactivated blank featuring rat liver microsomes heated above 80 °C for 10 min and 3, a solvent blank which contained only William's E medium were performed and analyzed alongside the sample batch.

4.2.4. Extraction of *in vitro* samples

Samples were mixed with 3 mL of hexane:DCM mixture (1:1 v/v) by vortexing for 30 s, followed by ultrasonication for 5 min and centrifuged at 4000 g for 5 min. The organic layer was collected and the extraction procedure was repeated twice. The combined extracts were evaporated to dryness under a gentle stream of nitrogen then reconstituted in 100 μ L of methanol prior to instrument analysis.

4.3. Method development

4.3.1. Analysis of pure BFR standards

In order to create a mass spectrometric library for BFRs screening, available authentic standards of some BFRs and NBFRs (1 ng/ μ L) were injected into the Orbitrap MS to explore their HRMS spectra. The analysis of standards was carried out in both ESI and APCI full scan mode with positive and negative polarity (APPI was unavailable). In ESI

mode, mass spectrum of chemicals are usually easier to interpret with common pseudomolecular ions being formed: $[M-H]^-$ in negative polarity and $[M+H]^+$ in positive mode. However, a well-known issue of ESI is its liability to ion suppression due to matrix effect (Dams et al., 2003). This phenomenon can largely affect analysis results and therefore a very good sample cleanup is required. In APCI mode, ion suppression effect is much less but mass spectrum interpretation is more difficult than in ESI mode (Dams et al., 2003).

As expected for hydrophobic chemicals, almost all of the analyzed BFRs were only detected in (-)APCI mode with the exception of TBBPA and HBCDDs (ionized well in both (-)APCI and (-)ESI. A common ionization mechanism for BFRs in (-)APCI is via the formation of the pseudomolecular ion $[M-Br+O]^-$ where M is the chemical formula of the BFR; but there are exceptions (Table 4.2). The most intense ion was evaluated from obtained spectra for each compound and its accurate mass was calculated from the isotope simulation (Xcalibur 3.0, Thermo Fisher Scientific) (Figure 4.1).

Almost all of the BFRs were well ionized in (-)APCI mode with the exception of DBE-DBCH. A maximum intensity of 2E2 was observed for DBE-DBCH using the ion $[M+O_2]^-$ and the isotope pattern of this ion cluster was not clear (Figure 4.1.DBE-DBCH). Additionally, $[M+O_2]^-$ and Br^- were the only ions observed for DBE-DBCH. Br^- is not a selective ion considering the fact that there are potentially several brominated chemicals in real samples. Hence, ion $[M+O_2]^-$ was still used as qualification ion for DBE-DBCH screening purposes, with an important note that the LOD for this compound might be quite high compared to other studied BFRs.

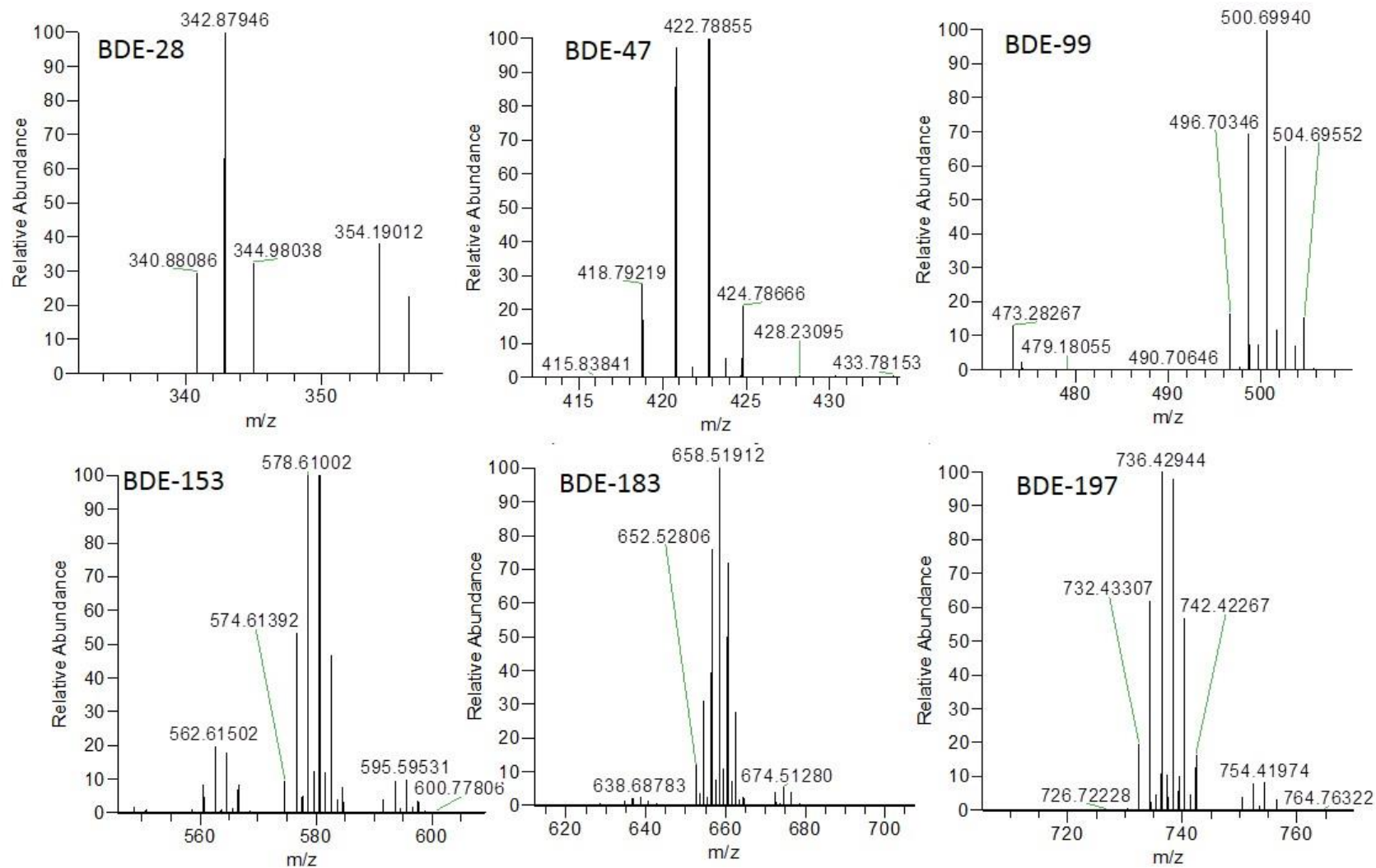
Table 4.2: BFR standards used in this chapter and their accurate ion masses analyzed by LC(-)APCI-HRMS.

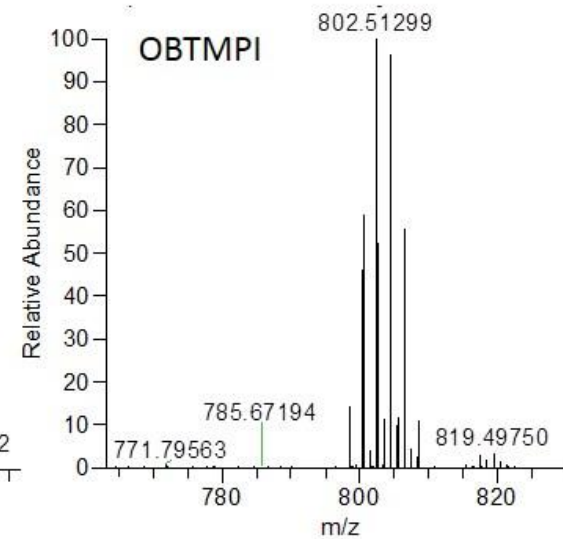
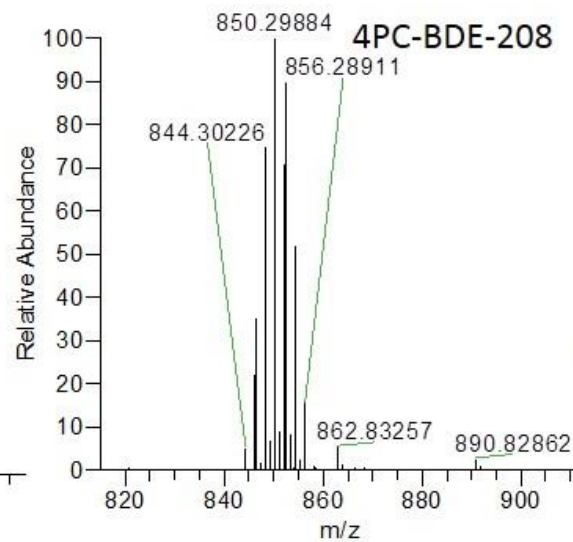
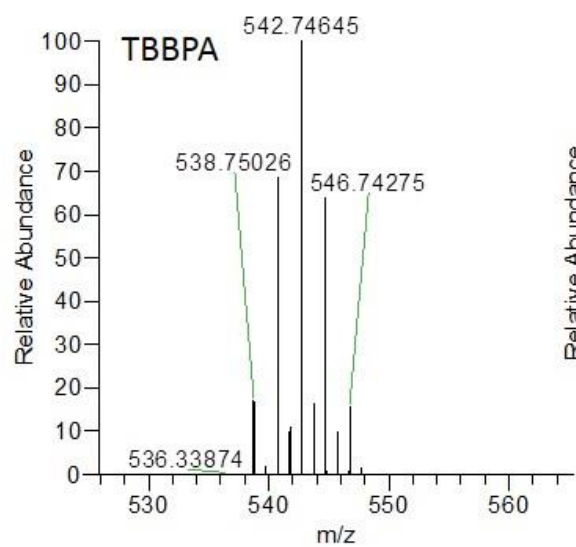
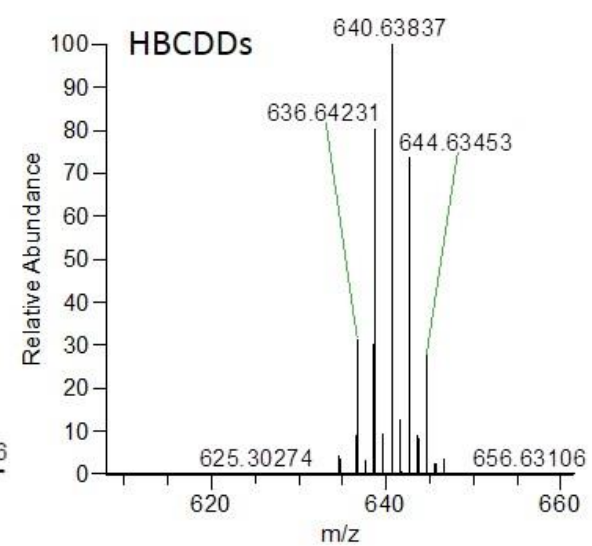
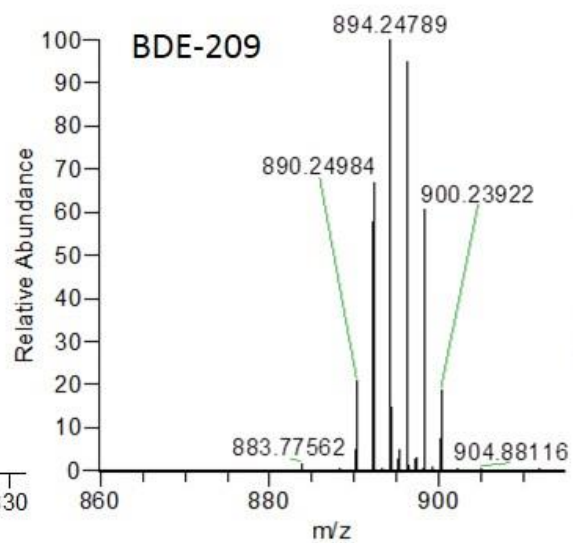
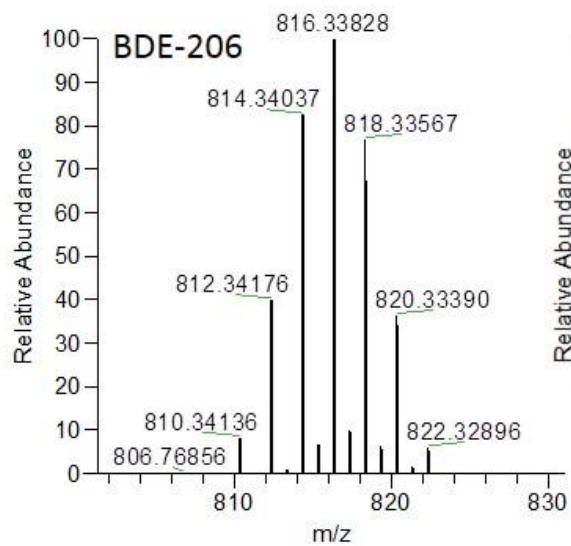
Compound	Abbreviation	Chemical Formula	Ion Type	M/Z	Intrument LOD (pg/uL)
2,4,4'-Tribromodiphenyl ether	BDE-28	C ₁₂ H ₇ Br ₃ O	[M-Br+O] ⁻	342.87923	5.8
2,2',4,4'-Tetrabromodiphenyl ether	BDE-47	C ₁₂ H ₆ Br ₄ O	[M-Br+O] ⁻	420.78975	0.7
2,2',4,4',5-Pentabromodiphenyl ether	BDE-99	C ₁₂ H ₅ Br ₅ O	[M-Br+O] ⁻	500.69821	0.9
Tetrabromobisphenol A	TBBPA	C ₁₅ H ₁₂ Br ₄ O ₂	[M-H] ⁻	542.74516	0.2
2,2',4,4',5,5'-Hexabromodiphenyl ether	BDE-153	C ₁₂ H ₄ Br ₆ O	[M-Br+O] ⁻	578.60872	0.2
Hexabromocyclododecanes	HBCDDs	C ₁₂ H ₁₈ Br ₆ O	[M-H] ⁻	640.63691	0.2
2,2',3,4,4',5',6-Heptabromodiphenyl ether	BDE-183	C ₁₂ H ₃ Br ₇ O	[M-Br+O] ⁻	658.51719	0.2
2,2',3,3',4,4',6,6'-Octabromodiphenyl ether	BDE-197	C ₁₂ H ₂ Br ₈ O	[M-Br+O] ⁻	736.42825	0.9
2,2',3,3',4,4',5,5',6-Nonabromodiphenyl ether	BDE-206	C ₁₂ HBr ₉ O	[M-Br+O] ⁻	816.33672	0.3
Nonabromo-4'-chlorodiphenyl ether	4PC-BDE-208	C ₁₂ Br ₉ ClO	[M-Br+O] ⁻	850.29720	1.0
Decabrominated diphenyl ether	BDE-209	C ₁₂ Br ₁₀ O	[M-Br+O] ⁻	894.24668	0.03
Cl10 Dechlorane Plus	aCl10DP	C ₁₈ H ₁₄ Cl ₁₀	[M-Br+O] ⁻	564.81824	1.0

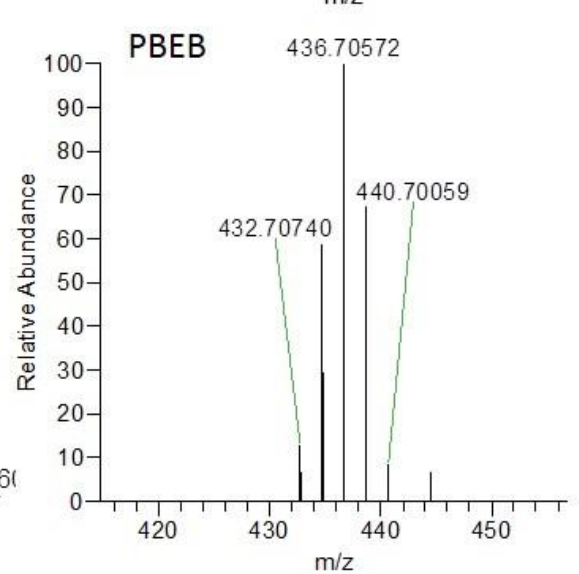
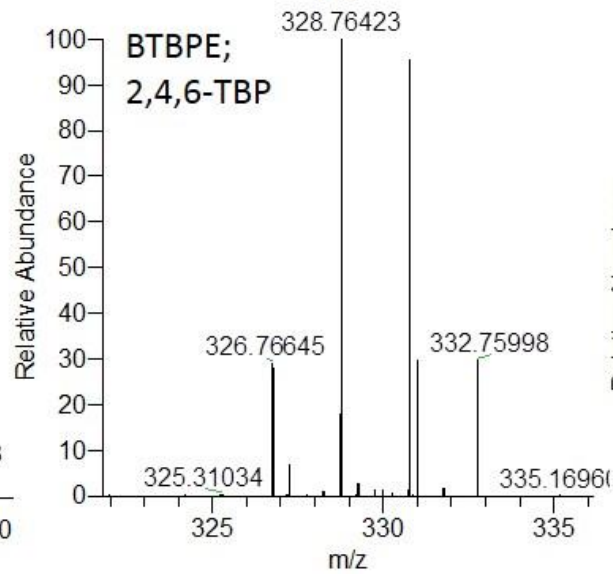
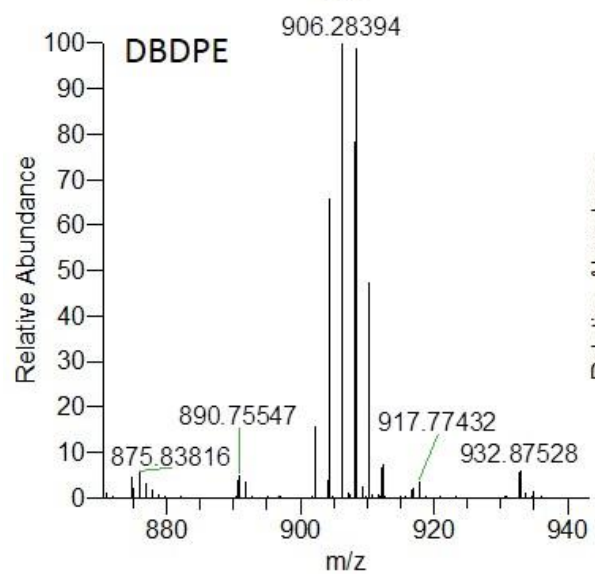
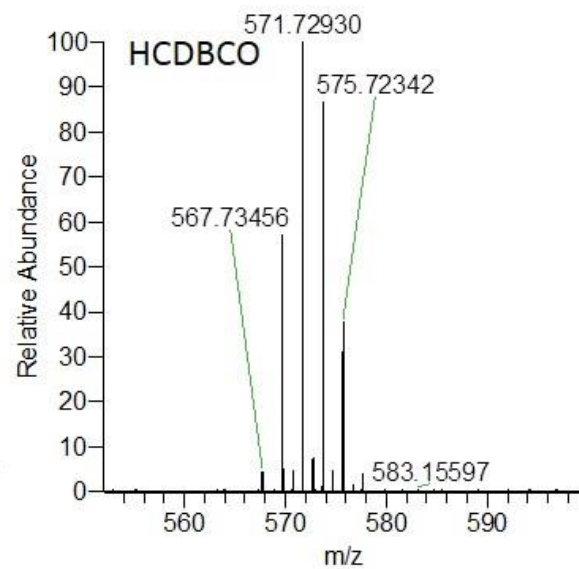
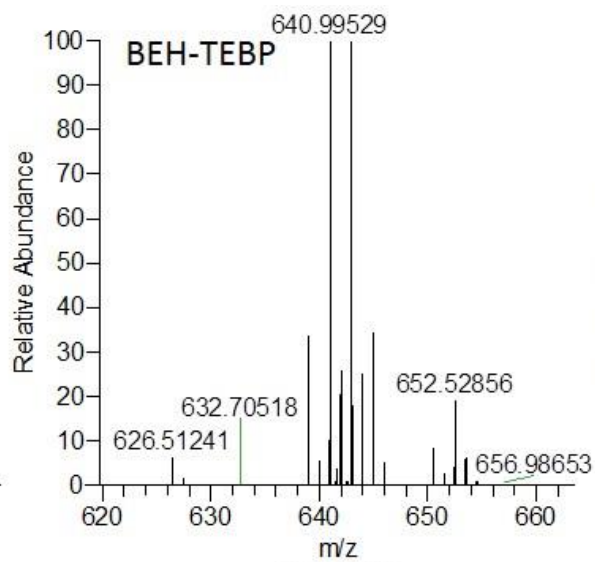
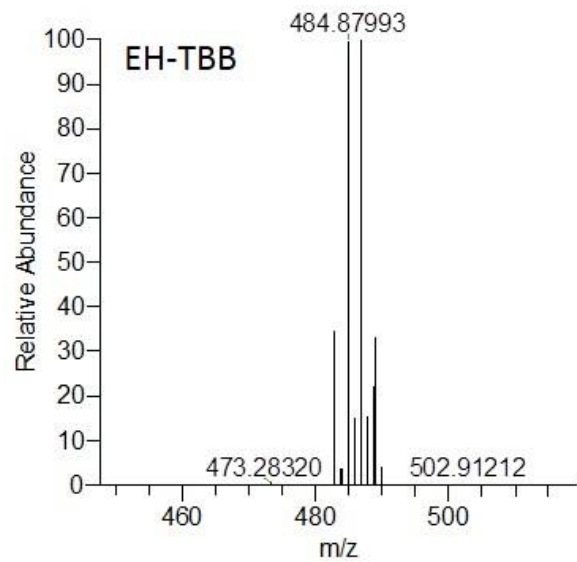
Dechlorane 602	Dec-602	C ₁₄ H ₄ Cl ₁₂ O	[M-Br+O] ⁻	592.67261	1.0
Cl11 Dechlorane Plus	aCl11DP	C ₁₈ H ₁₃ Cl ₁₁	[M-Br+O] ⁻	598.77927	1.2
Dechlorane 604	Dec-604	C ₁₃ H ₅ Br ₃ Cl ₆	[M-Br+O] ⁻	628.58836	1.0
Dechloraneplus	DDC-CO	C ₁₈ H ₁₂ Cl ₁₂	[M-Br+O] ⁻	632.74029	1.0
Dechlorane 603	Dec-603	C ₁₇ H ₈ Cl ₆	[M-Br+O] ⁻	638.68883	1.0
2,4,6-Tribromophenyl allyl ether	TBP-AE	C ₉ H ₇ Br ₃ O	[M-Br+O] ⁻	306.87923	0.5
1,2-Bis(2,4,6-tribromophenoxy)ethane	BTBPE	C ₁₄ H ₈ Br ₆ O ₂	[C ₆ Br ₃ H ₂ O] ⁻	328.76408	0.5
2,4,6-Tribromophenol	2,4,6-TBP	C ₆ H ₃ Br ₃ O	[M-H] ⁻	328.76408	0.1
2,4,6-Tribromophenyl allyl ether	TBP-BAE	C ₉ H ₆ Br ₄ O	[M-Br+O] ⁻	384.78975	0.5
Pentabromoethylbenzene	PBEB	C ₈ H ₅ Br ₅	[M-Br+O] ⁻	436.7033	1.2
1,2-dibromo-4-(1,2 dibromoethyl) cyclohexane	DBE-DBCH	C ₈ H ₁₂ Br ₄	[M+O ₂] ⁻	459.75299	27
2,3-Dibromopropyl 2,4,6-tribromophenyl ether	TBP-DBPE	C ₉ H ₇ Br ₅ O	[M-Br+O] ⁻	466.71386	1.0
2-Ethylhexyl 2,3,4,5-tetrabromobenzoate	EH-TBB	C ₁₅ H ₁₈ Br ₄ O ₂	[M-Br+O] ⁻	484.87856	0.8
Hexabromobenzene	HBB	C ₆ Br ₆	[M-Br+O] ⁻	486.58251	0.5
Brominated biphenyl 153	BB153	C ₁₂ H ₄ Br ₆	[M-Br+O] ⁻	562.61381	0.2

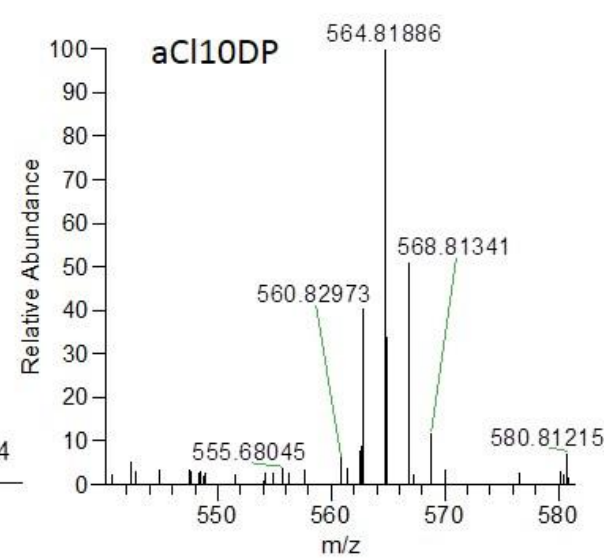
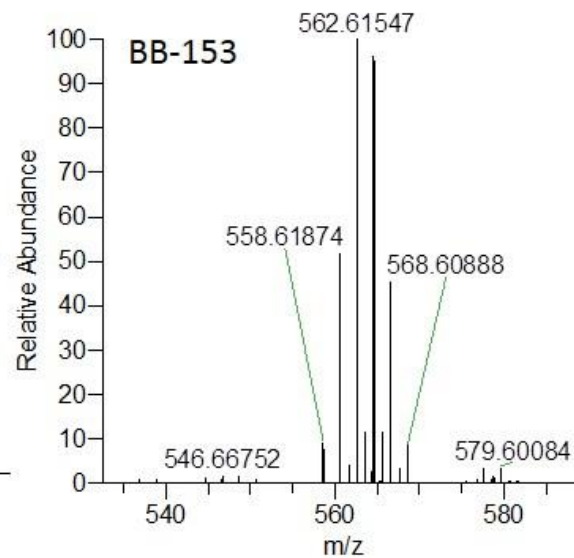
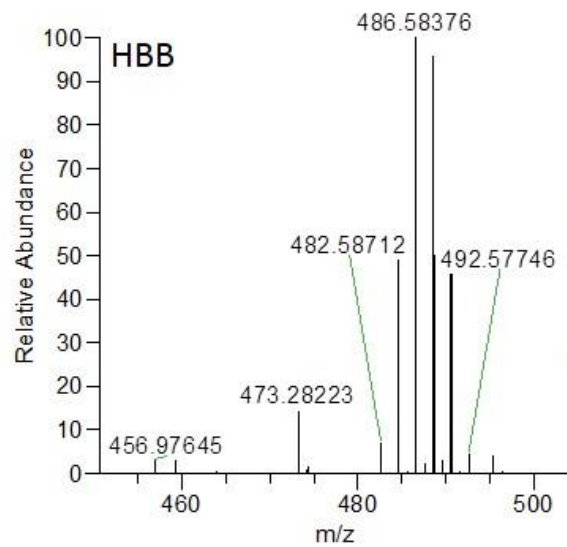
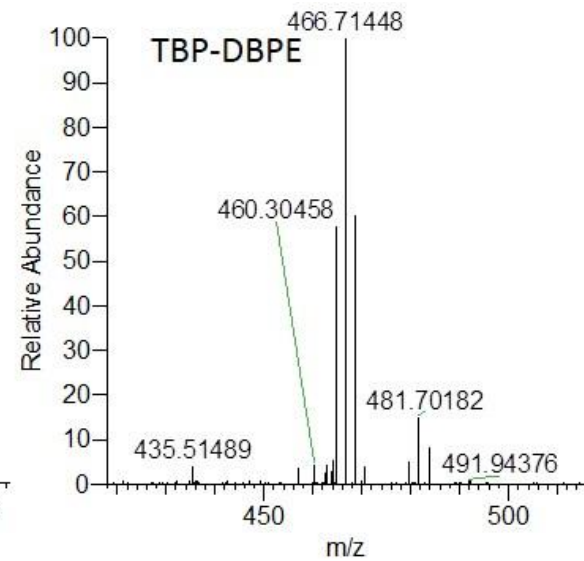
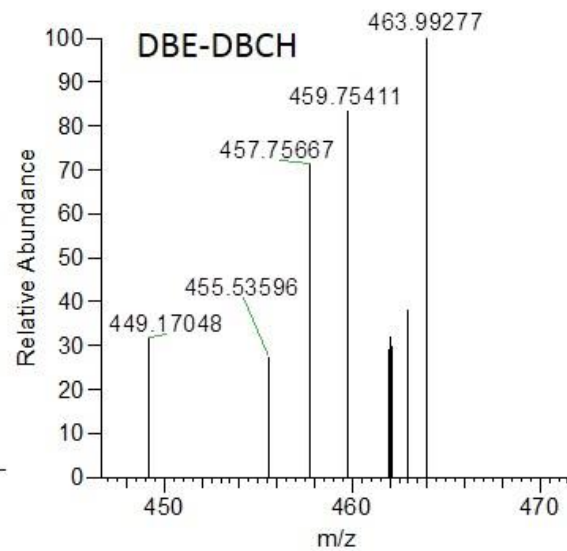
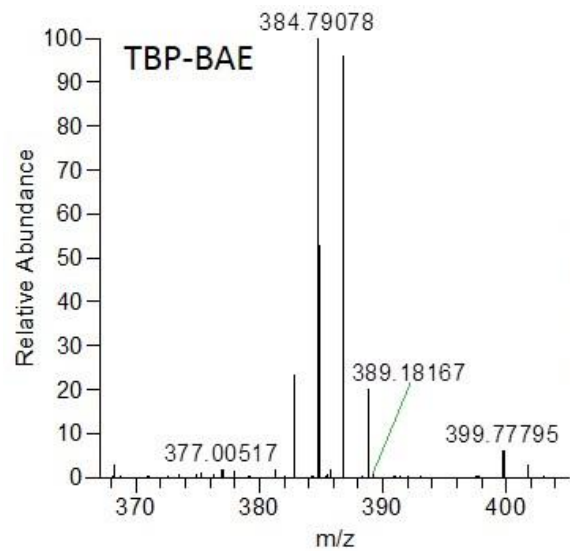
Dibromocyclooctane	HCDBCO	C ₁₈ H ₁₂ Br ₄	[M+O ₂] ⁻	571.72852	12
Bis(2-ethylhexyl) tetrabromophthalate	BEH-TEBP	C ₂₄ H ₃₄ Br ₄ O ₄	[M-Br+O] ⁻	640.99359	0.6
Octabromotrimethylphenyl indane	OBTMPI	C ₁₈ H ₁₂ Br ₈	[M-Br+O] ⁻	802.51190	2.0
Decabromodiphenyl ethane	DBDPE	C ₁₄ H ₄ Br ₁₀	[M-Br+O] ⁻	906.28307	11
Labelled ¹³ C 2,4,4'-tribromodiphenyl ether	¹³ C-BDE-28	¹³ C ₁₂ H ₇ Br ₃ O	[M-Br+O] ⁻	354.91949	5.5
Labelled ¹³ C Decabrominated diphenyl ether	¹³ C-BDE-209	¹³ C ₁₂ Br ₁₀ O	[¹³ C ₆ Br ₅ O] ⁻	492.60264	0.01
Labelled ¹³ C 1,2-Bis(2,4,6-tribromophenoxy)ethane	¹³ C-BTBPE	¹³ C ₁₄ H ₈ Br ₆ O ₂	[¹³ C ₆ Br ₃ H ₂ O] ⁻	334.78366	0.5

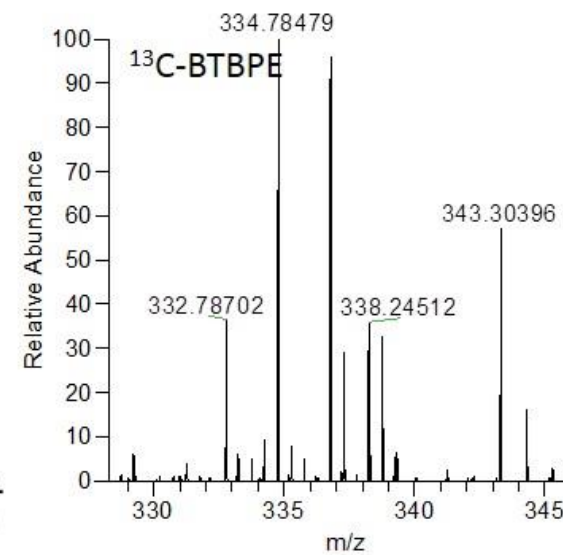
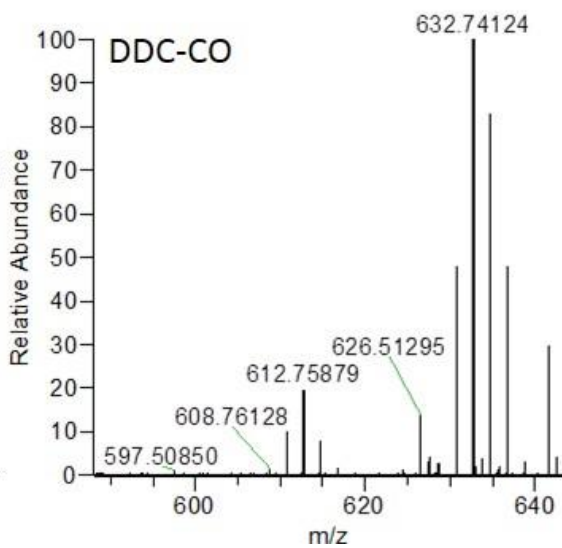
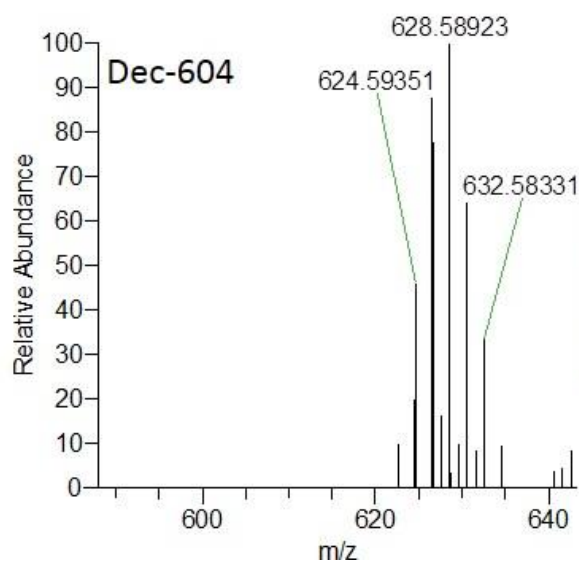
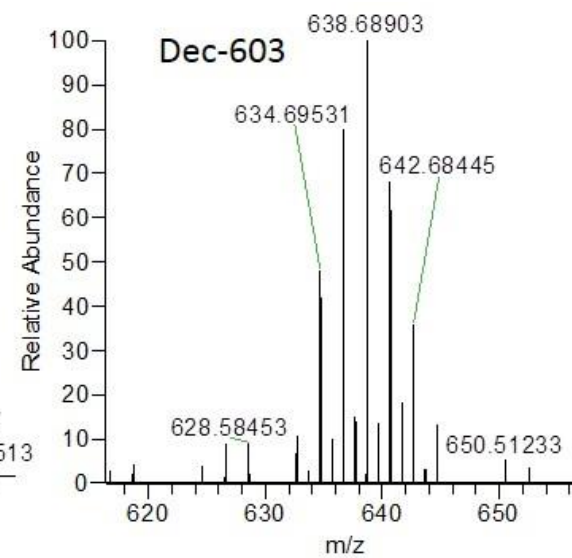
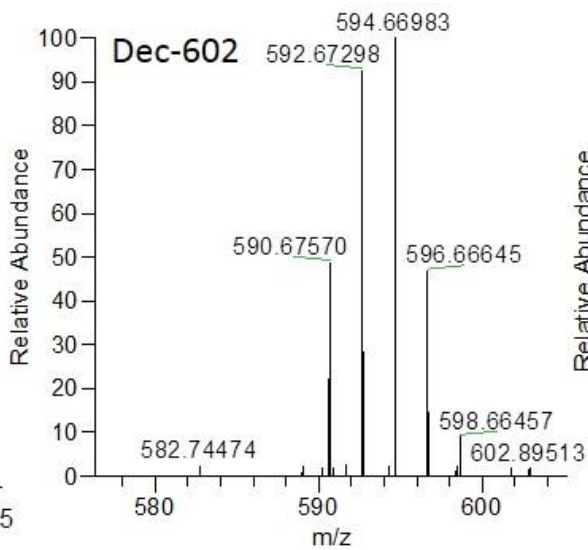
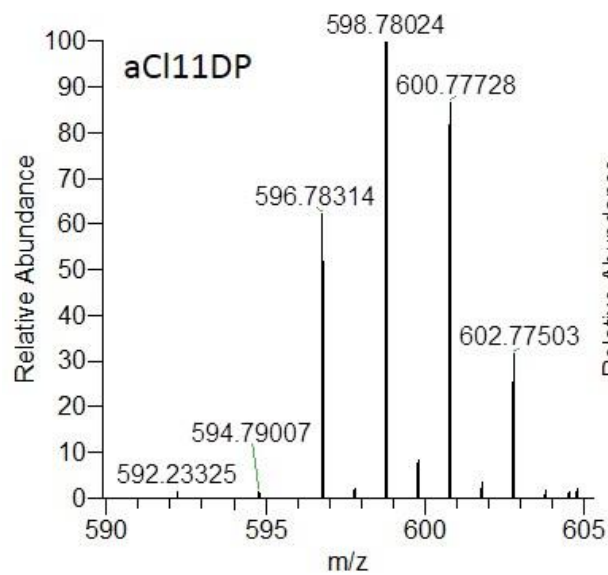
Figure 4.1: (-)APCI-HRMS Mass spectra of the identification ion cluster for each BFR standard studied in this chapter

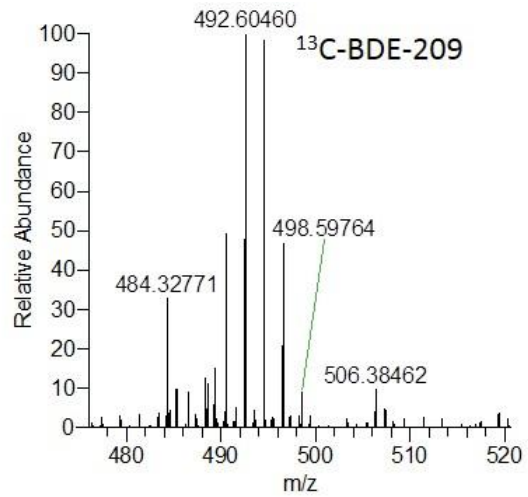
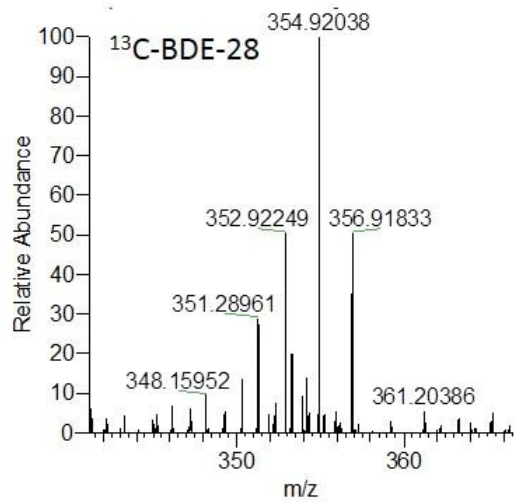












4.3.2. LC(-)APCI/(-ESI)-HRMS analysis for targeted and untargeted analysis of BFRs

Even though the Orbitrap MS can provide very accurate mass for scanned ions, due to the similarity in chemical structures of BFRs e.g. TBP-AE and TBP-BAE or EH-TBB and BEH-TEBP (Figure 1.2), it is not possible to separate and identify complex mixtures of target compounds through direct infusion analysis. Additionally, we aimed to develop a method for targeted and untargeted analysis of BFRs and other brominated compounds in one run; hence LC separation was needed to provide another layer of separation and identity confirmation via retention time. Internal standards were added for retention time reference, semi-quantify target chemicals if possible and assess the extraction efficiency. We chose ^{13}C -BDE-28, ^{13}C -BTBPE and ^{13}C -BDE-209 as internal standards to represent low, medium and high M.Wt. brominated compounds with the numbers of bromines in each standard of 3, 6 and 10, respectively.

Chromatographic separation of BFRs and internal standards was performed on an Accucore RP-MS column (100 x 2.1 mm, 2.6 μm) (Thermo Fisher Scientific Bremen, Germany). Previously, it has been reported that a water-methanol mobile phase system generate highest sensitivity for BFRs analysis by LC-APCI-MS in comparison with other common mobile phases (Zhou et al., 2010). Therefore, we chose a simple water and methanol mobile phase gradient for our analysis without any modifiers to minimize complicated mass spectra due to adduct ions formation. Details of the gradient elution programme are shown in Table 4.3. The injection volume was 5 μL and the column oven was set at 30 $^{\circ}\text{C}$.

Table 4.3: LC gradient for the analysis of BFRs standard mixture

Time (min)	% Water (A)	% Methanol (B)
0	80	20
9	0	100
12	0	100
12.1	80	20
15	80	20

The APCI source was used to ionize samples in full scan negative ion mode and the optimized Orbitrap MS parameters are shown in Table 4.4

Table 4.4: Optimized (-)APCI Orbitrap MS parameters for targeted and untargeted analysis of BFRs

Parameter	Value
MS resolution (FWHM)	17500
Sheath gas flow (a.u)	25
Auxiliary gas flow (a.u)	5
Source heater temperature (°C)	250
Capillary temperature (°C)	375
Voltage (kV)	5
S-lens frequency (Hz)	50
Maximum injection time (ms)	100
Automatic gain control (ions)	1x10 ⁶
Scan range	300-1000

Target BFRs and IS were identified in Quan Browser using accurate mass of identify ions at 5 ppm mass deviation and general knowledge of reversed phase liquid chromatography elution order: i) the more hydrophilic a compound is, the earlier it elutes and ii) higher molecular weight chemicals tend to elute later. The retention times of target compounds and internal standards were obtained as described in Table 4.5.

Table 4.5: Retention time of BFR standards analyzed by (-)APCI-LC-HRMS on Accucore RP-MS column

Compound	Retention time (min)	Compound	Retention time (min)
2,4,6-TBP	7.75	BDE-153	10.50
TBBPA	8.4	Dec-603	10.57
DBE-DBCH	8.97	BDE-183	10.63
TBP-AE	9.25	EH-TBB	10.74

HBCDDs	9.34, 9.53, 9.63	¹³ C-EH-TBB	10.74
BDE-28	9.41	aCl10DP	10.77
¹³ C-BDE-28	9.44	BTBPE	10.78
TBP-BAE	9.58	¹³ C-BTBPE	10.81
TBP-DBPE	9.75	DP	10.87
BDE-47	9.9	BDE-197	10.90
BDE-99	9.97	BDE-206	11.01
HCDBCO	10.08	OBTMPI	11.34
HBB	10.2	BDE-209	11.35
Dec-602	10.31	¹³ C-BDE-209	11.39
BB153	10.37	4PC-BDE-208	11.71
aCl11DP	10.39	BEH-TEBP	11.78
PBEB	10.46	¹³ C-BEH-TEBP	11.78
Dec-604	10.47	DBDPE	12.7

In addition to (-)APCI mode, (-)/(+) switching ESI analysis was also employed to study *in vitro* biotransformation of EH-TBB, BEH-TEBP and BTBPE with the same LC gradient but different Orbitrap MS parameters as follow:

Table 4.6: Optimized (-)ESI Orbitrap MS parameters for metabolite identification of EH-TBB, BEH-TEBP and BTBPE by MLM *in vitro*

Parameters	Value
Polarity	Pos/Neg switching
Sheath gas flow rate	25
Aux gas flow rate	5
Sweep gas flow rate	0
Spray voltage (kV)	4.5

Capillary temp. (°C)	320
S-lens RF level	50
Aux gas heater temp (°C)	350
Resolution (FWHM)	17500
AGC target (ions)	1E6
Maximum ion injection time (ms)	100
Scan mode	Full scan
Scan range	70-800

For untargeted screening of potential brominated contaminants, a Compound Discoverer approach as described in Section 2.3.2 was used with the settings in the main working nodes as following:

Table 4.7: Compound Discoverer parameters of main working nodes for screening of BFRs and brominated contaminants

Node	Parameters
Select Spectra	Min. Precursor Mass: 300 (Da) Max. Precursor Mass: 1000 (Da) Polarity Mode: negative and positive S/N Threshold: 3
Align Retention Times	Alignment Model: Adaptive curve Mass Tolerance: 5 ppm Maximum shift: 0.5 min
Detect Unknown Compounds	Mass Tolerance S/N threshold Min. Peak Intensity: 5000 Ion: [2M-H]; [M+Cl]; [M-2H]; [M-Br+2e]; [M-Br+O]; [M-H]; [M-H-H ₂ O]; [M+H] Max. Element Counts: C30 H50 Br15 Cl8 O10 Min. # Scans per Peak: 5

Mark Background Compounds	Max. Sample/Blank: 3 Hide Background = True
Predict Compositions	Max. Element Counts: C30 H50 Br15 Cl8 O10 Max. RDBE: 20 Max. # Candidates: 20
Search ChemSpider	Databases: ACToR: Aggregated Computational Toxicology Resource; DrugBank; EAWAG Biocatalysis/Biodegradation Database; EPA DSSTox; FDA UNII – NLM. Mass tolerance
Pattern Scoring	Isotope Pattern: C8Br; C8Br2; C8Br3; C8Br4; C8Br5; C8Br6; C8Br7; C8Br8; C8Br9; C8Br10; C8Br11; C8Br12; C8BrCl; C8Br2Cl; C8Br3Cl; C8BrCl6; C8Br3Cl6; C8Br3Cl Intensity Tolerance: 30%

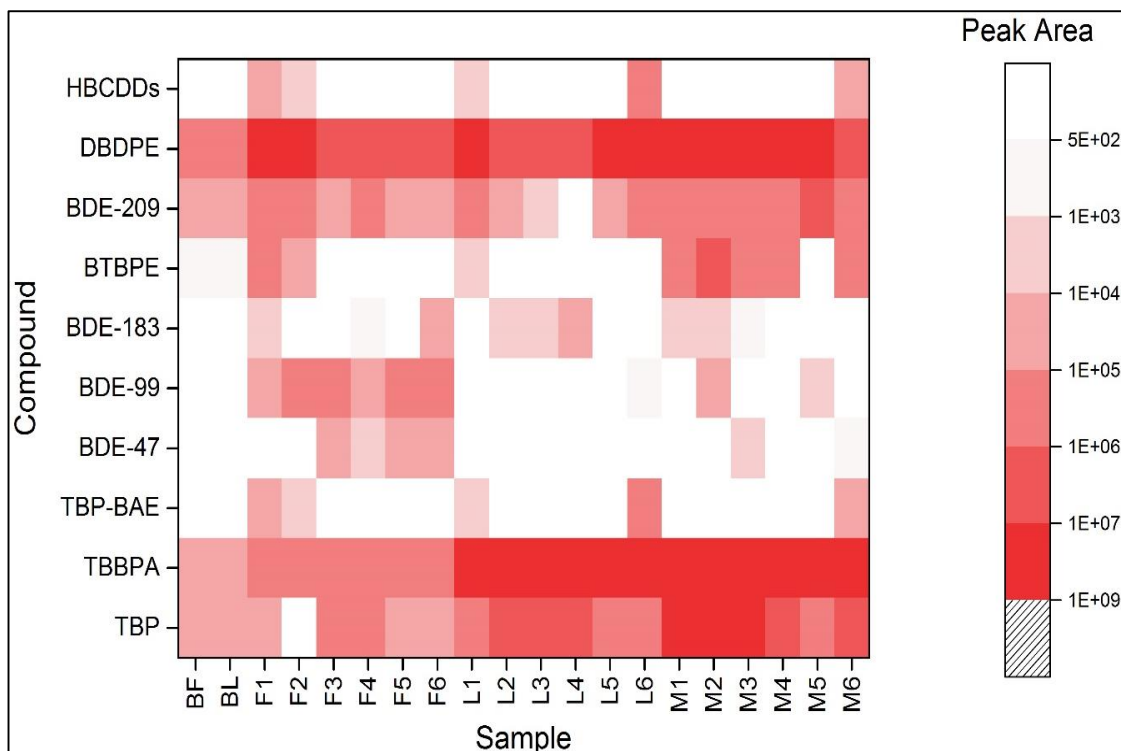
For descriptive analysis (e.g. peak area ratio), PCA and ANOVA analysis, leachate samples were divided into 4 groups based on their sample categories: M, F, L and blank while *in vitro* samples were divided into 4 groups: treated with 1 μM, treated with 10 μM, non-treated and blank. “Blank” group included (where applicable) field blank, transportation blank, solvent blank and instrument blank samples where 5 μL of methanol was injected. “Non-treated” group consisted of individual EH-TBB, BEH-TEBP and BTBPE samples as well as heated inactivated samples and non-enzymatic samples.

4.4. BFRs screening in leachate samples

4.4.1. Targeted screening of BFRs

Among 31 target BFRs, only a few were detected including BDE-47, BDE-99, BDE-183, BDE-209, DBDPE, BTBPE, TBP, TBP-AE, HBCDDs and TBBPA. Figure 4.2 shows the peak area heat map of detected BFRs in the studied leachate samples.

Figure 4.2: Peak area heat map of detected BFRs in leachate samples



As can be seen on Figure 4.2, legacy BFRs namely BDE-209, DBDPE, TBBPA were detected in almost every sample including blanks with much higher peak area than other BFRs. This indicates the ubiquitous distribution of these BFRs in the environment. Some other PBDEs were also occasionally detected, mostly in leachate from fridges/freezers (F samples) especially BDE-99. BTBPE, TBP-BAE and 2,4,6-TBP were the only NBFRs found in this leachate test. 2,4,6-TBP has the highest detection frequency, nearly 100% and also found in blanks while BTBPE mainly presented in M samples. Nearly 30% of samples contained TBP-BAE at quite low levels.

Statistical tools were applied to compare the level of each detected contaminant in three different sample types: L, M and F. Shapiro-Wilk normality test revealed non-normal distribution for all the compounds with the exception of DBDPE ($p = 0.77$). To simplify the statistical analysis process, we then applied non-parametric tests for all the compounds including DBDPE. Kruskal–Wallis test was used to determine if the levels of each contaminant are significantly different across sample categories.

Table 4.8: Nonparametric Kruskal-Wallis Test result for distribution of each detected BFR across all sample categories

Hypothesis Test Summary				
	Null Hypothesis	Test	P value	Decision
1	The distribution of TBP is the same across categories of Sample.	Independent-Samples Kruskal-Wallis Test	0.002	Reject the null hypothesis.
2	The distribution of TBBPA is the same across categories of Sample.	Independent-Samples Kruskal-Wallis Test	0.001	Reject the null hypothesis.
3	The distribution of TBPBAE is the same across categories of Sample.	Independent-Samples Kruskal-Wallis Test	0.549	Retain the null hypothesis.
4	The distribution of BDE47 is the same across categories of Sample.	Independent-Samples Kruskal-Wallis Test	0.04	Reject the null hypothesis.
5	The distribution of BDE99 is the same across categories of Sample.	Independent-Samples Kruskal-Wallis Test	0.002	Reject the null hypothesis.
6	The distribution of BDE183 is the same across categories of Sample.	Independent-Samples Kruskal-Wallis Test	0.917	Retain the null hypothesis.
7	The distribution of BTBPE is the same across categories of Sample.	Independent-Samples Kruskal-Wallis Test	0.022	Reject the null hypothesis.
8	The distribution of BDE209 is the same across categories of Sample.	Independent-Samples Kruskal-Wallis Test	0.016	Reject the null hypothesis.
9	The distribution of DBDPE is the same across categories of Sample.	Independent-Samples Kruskal-Wallis Test	0.097	Retain the null hypothesis.

10	The distribution of HBCDDs is the same across categories of Sample.	Independent-Samples Kruskal-Wallis Test	0.575	Retain the null hypothesis.
----	---	---	-------	-----------------------------

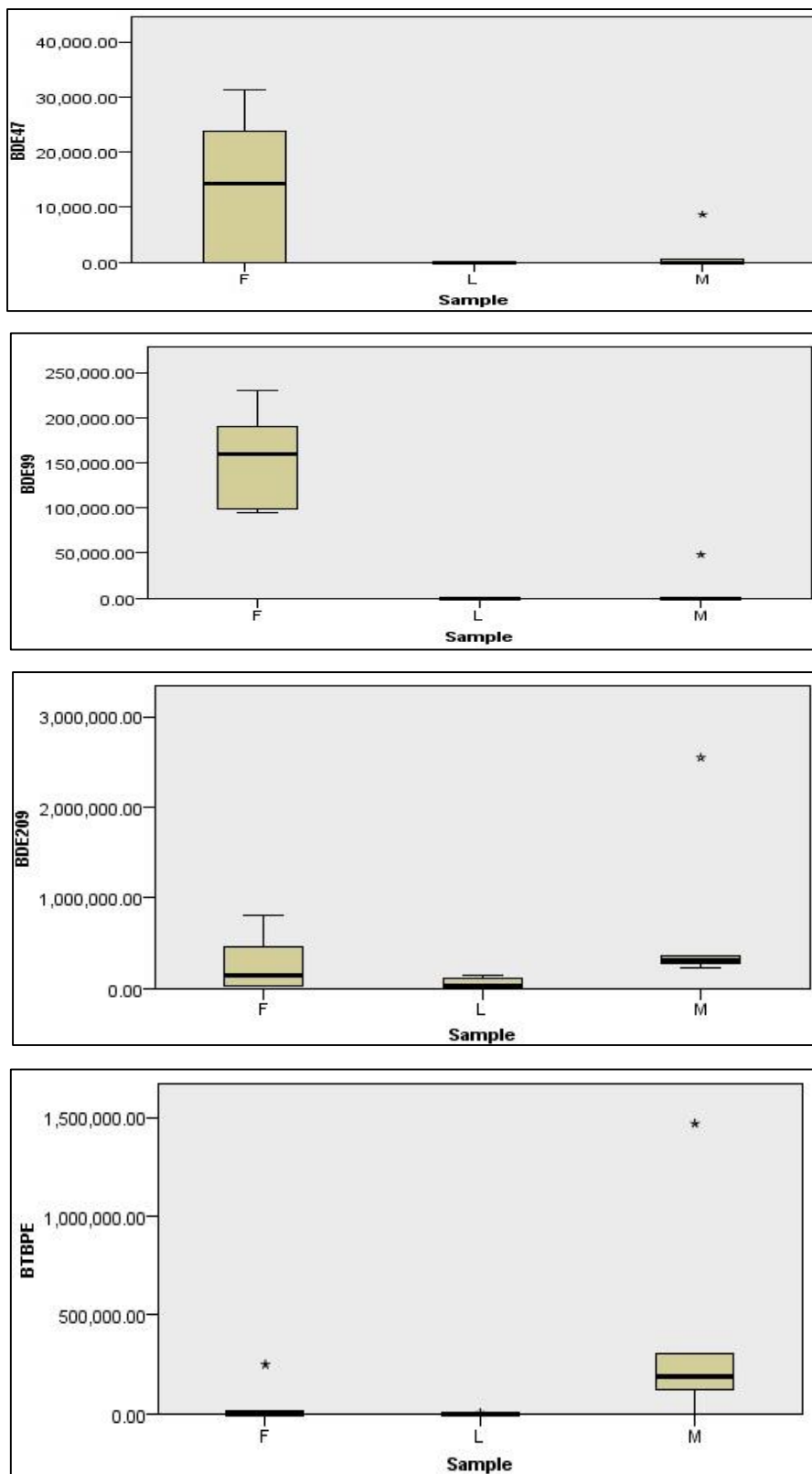
The results (Table 4.8) indicated that the abundances of TBP-BAE, BDE-183, DBDPE and HBCDDs did not differ significantly between the 3 sample groups. In contrast, the abundances of TBP, TBBPA, BDE-47, BDE-99, BTBPE and BDE-209 were significantly different between M, F and L samples. Thence Dunn post hoc analysis was carried out to assess the exact statistical relationship between contaminant levels in any two sample categories.

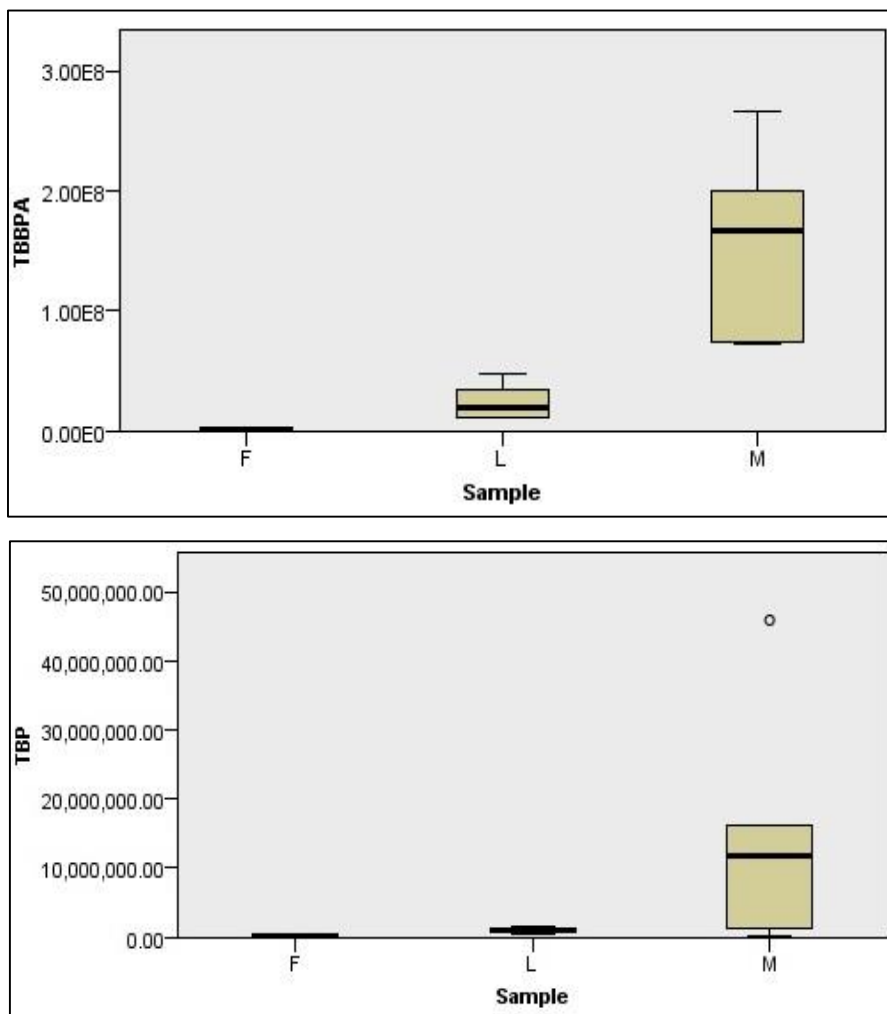
Table 4.9: P value for pairwise comparison of contaminant levels in each sample category via Dunn post hoc after significant Kruskal-Wallis Test.

Categories	TBP	TBBPA	BDE-47	BDE-99	BTBPE	BDE-209
F-L	0.017	0.052	0.012	0.002	0.355	0.004
F-M	0.001	0.000	0.122	0.003	0.073	0.094
L-M	0.279	0.052	0.334	0.821	0.007	0.234

At a 95 % confidence level, Dunn post hoc analysis results (Table 4.9 and Figure 4.3) showed that TBP and TBBPA were significantly higher in M samples than F samples while BTBPE was significantly higher in M than L samples. The amount of TBP was also significantly higher in L samples than F samples. For BDE congeners, F samples statistically contained higher levels of BDE-47 and BDE-209 than L and BDE-99 than M samples. It is clear from the Kruskal-Wallis plot (Figure 4.3) that brominated diphenyl ethers were present at higher concentrations in leachate samples stemming from fridges/freezers than other electrical waste items while leachate samples derived from mixed WEEE contained much more phenolic BFRs such as TBBPA.

Figure 4.3: Independent samples Kruskal-Wallis test results for BFRs detected in leachate samples





4.4.2. Untargeted screening of brominated contaminants

A total of 16335 potential chemicals across all our samples were flagged by Compound Discoverer. We applied some filters to narrow down the list of pur compounds of interest:

- i, Pattern matches is true in any pattern (Pattern Scoring – Table 4.7)
- ii, The maximum peak area ratio of that compound in any sample against blanks must be greater than 2
- iii, P value of per group ratio calculated by ANOVA and Tukey HSD post hoc is less than 0.1 between samples and blanks
- iv, Maximum peak area has to be greater than 1000

Using these successive filters, only 31 potential brominated compounds were left, down from 16335. After carefully examining their retention times, peak shapes and ion masses, we highlighted five unknown compounds of interest (Table 4.10).

Table 4.10: Some potential brominated contaminants list found by Compound Discoverer

Name	Ion mass (da)	Elucidated Ion formula	RT (min)	Found in samples
A	382.93953	C ₁₅ H ₁₃ Br ₂ O ₂	7.55	L2, M6
B	460.84070	C ₁₅ H ₁₂ Br ₃ O ₂	8.04	M2-5, L2-3, L6
C	380.95001	C ₁₆ H ₁₅ Br ₂ O	9.02	L1-6, F3-6
D	552.76654	C ₁₆ H ₁₃ Br ₄ O ₂	9.27	M3-4, L1-3
E	494.80075	C ₁₅ H ₁₂ Br ₃ ClO ₂	8.38	M3, M5, L1-2

The ion mass of unknown compound A was 382.93953 with a proposed ion formula of C₁₅H₁₄Br₂O₂ (Figure 4.4). ChemSpider screening found one match for A as 4,4'-(2,2-propanediyl)bis(3-bromophenol). As the exact position of bromines and hydroxyl groups were not possible to elucidate just based on accurate mass, only the chemical structure of the ChemSpider match was used as a reference for compound identification. Compound A was then tentatively identified as dibromobisphenol A (DBBPA) (C₁₅H₁₄Br₂O₂) which underwent the (-)APCI ionization M-H similar to TBBPA. It is important to note that the exact chemical configuration of A might not be the same as DBBPA. This also applies for any other compound tentatively identified in this study. Unknown compound B had an ion mass of 460.84070 and was present in many samples (Table 4.10). It showed a 3 bromine pattern in its mass spectra, with a predicted ion formula of C₁₅H₁₂Br₃O₂ (Figure 4.5). If this ion was formed via M-H mechanism, the chemical formula for A was C₁₅H₁₂Br₃O₂. There was one match from ChemSpider for this formula as 2,6-Dibromo-4-[2-(3-bromo-4-hydroxyphenyl)-2-propanyl]phenol or tribromobisphenol A (TriBBPA).

Figure 4.4: Overlay chromatogram of Unknown Compound A in leachate samples and its isotopic pattern

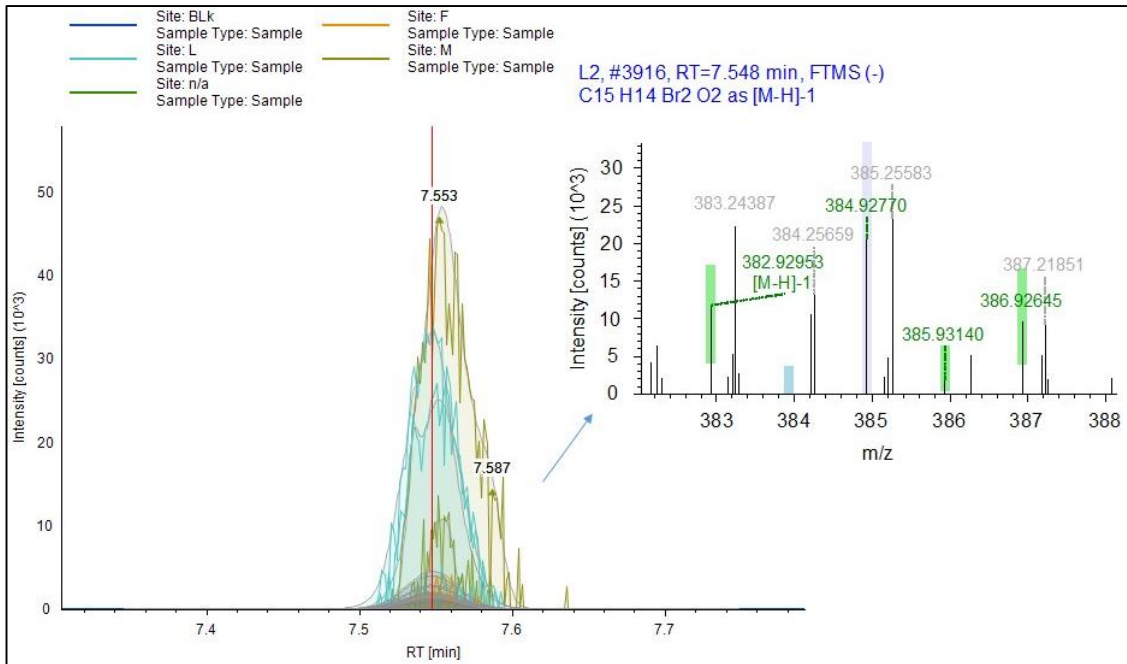


Figure 4.5: Overlay chromatogram of Unknown Compound B in leachate samples and its isotopic pattern

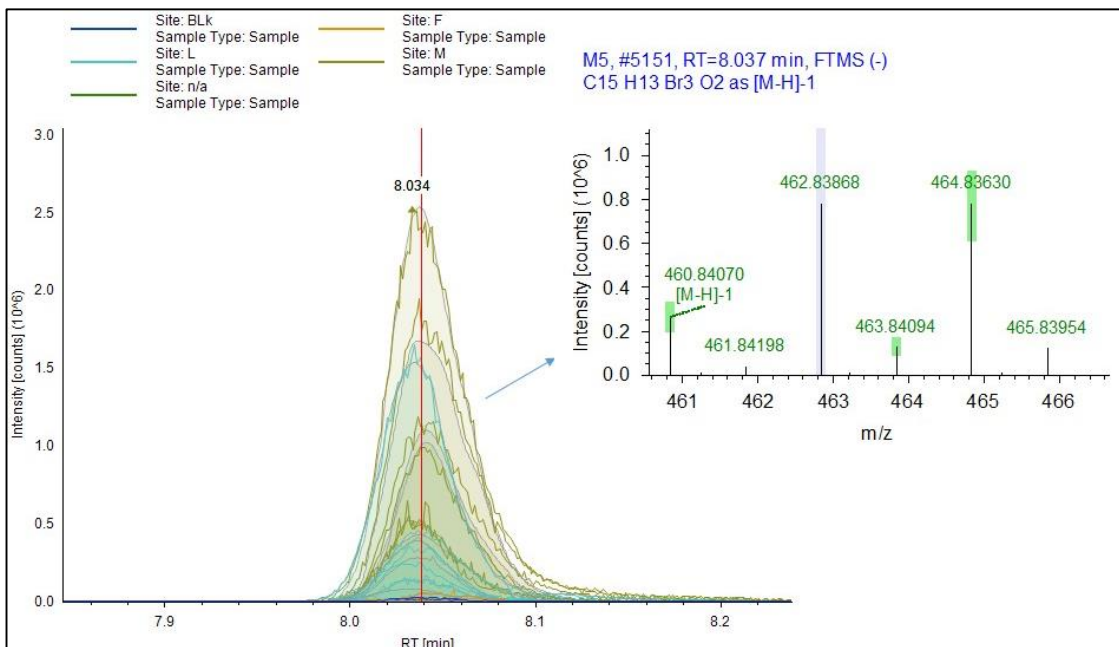
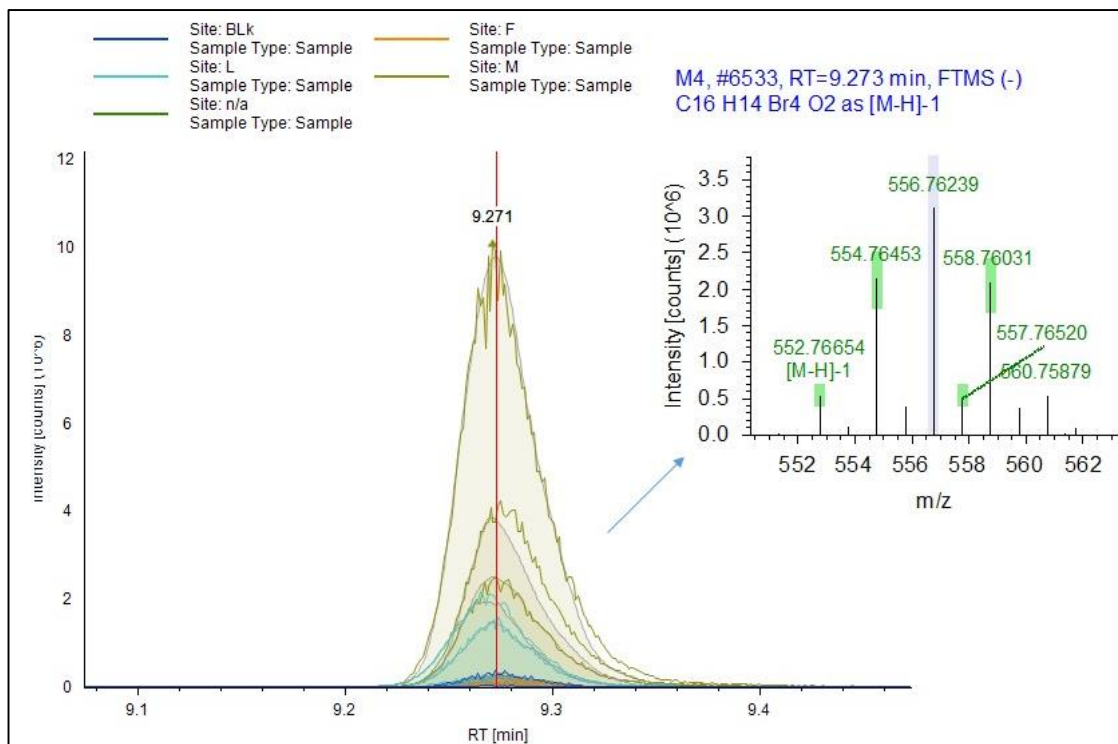


Figure 4.6: Overlay chromatogram of Unknown Compound D in leachate samples and its isotopic pattern



Similarly, D had an ion mass of 552.76654 and showed an isotopic pattern of 4 bromines in the mass spectra (Figure 4.6). It was later elucidated as C₁₆H₁₄Br₄O₂ with one match from ChemSpider being 4,4'-(2,2-butanediyl)bis2,6-dibromophenol. However, an alternative identification of a methoxylated derivative of TBBPA was noted. Indeed, methoxylated TBPPA (MeO-TBBPA) has been identified as a transformation product of TBBPA by microorganisms or in oxic soil (George and Häggblom, 2008; F. Li et al., 2015b; Sun et al., 2014). Therefore we tentatively identified compound D as MeO-TBBPA.

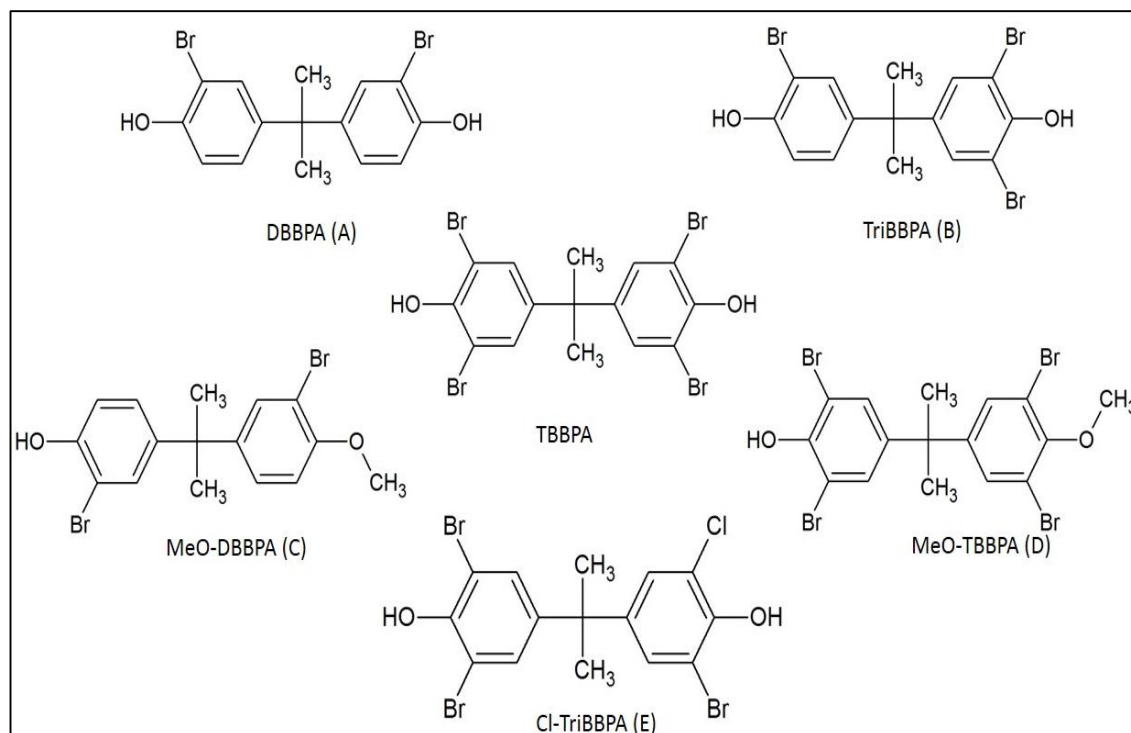
DBBPA, TriBBPA and MeO-TBBPA have been identified as the main environmental transformation products of TBBPA (Liu et al., 2017). Their detection is plausible as they were found in many M and L samples where TBBPA presented at high levels. The detection rate of TriBBPA in this study is higher than MeO-TBBPA and in good agreement with previous studies, which demonstrated that debromination on a benzene ring is the main degradation pathway of TBBPA in the environment (F. Li et al., 2015a, 2015b).

For unknown compound C, since it shares a similar chemical composition with unknown compound D, we hypothesize it is methoxylated dibromobisphenol A (MeO-DBBPA). The retention time of C also supports this hypothesis: shorter than MeO-TBBPA, which contains the same functional groups and two more bromine atoms, and longer than TBBPA which is more polar due to one more hydroxyl group in its structure.

Compound E had an ion mass of 494.80070 and showed very distinctive isotope pattern of 3 bromine atoms in the structure. Compound Discoverer elucidation node predicted the composition of E as $C_{15}H_{12}Br_3ClO_2$, which is very similar to TBBPA with the exception of one chlorine atom instead of bromine. The retention time of E was earlier but also very close to TBBPA (8.38 vs 8.46 min). Therefore, we hypothesized E to be chlorinated TriBBPA (Cl-TriBBPA).

Figure 4.7 showed the structures of tentatively identified unknown brominated contaminants in leachate testing samples. They are all structurally related to TBBPA and might be environmental degradation/transformation products of this widely used BFR.

Figure 4.7: Chemical structures of tentatively identified TBBPA-related contaminants in leachate testing samples.

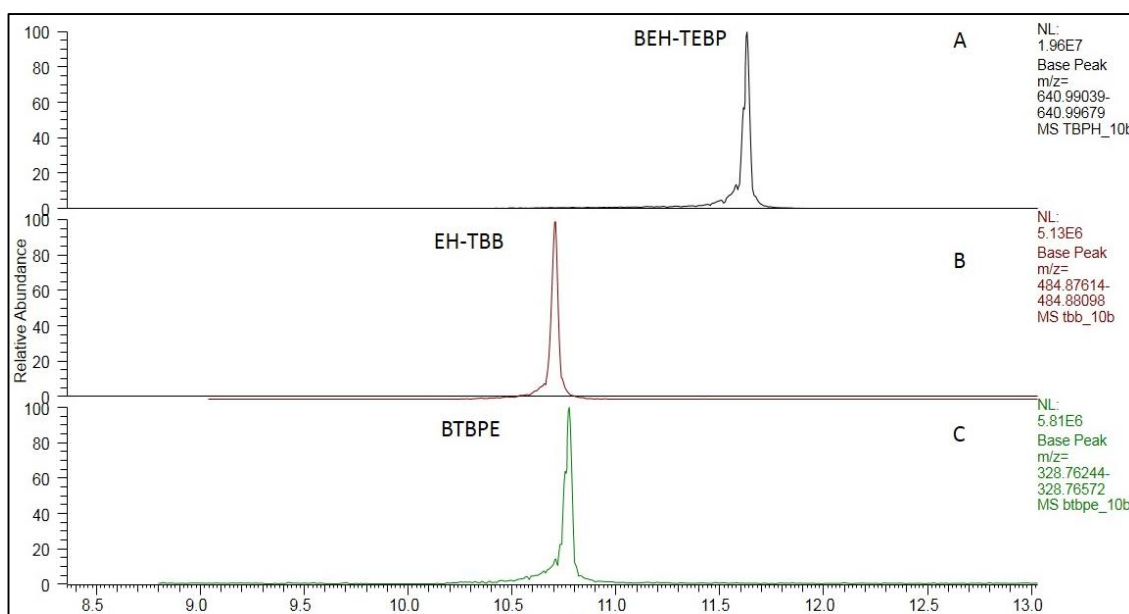


4.5. Screening of biotransformation products of EH-TBB, BEH-TEBP and BTBPE following *in vitro* incubation with mouse liver microsomes (MLM)

4.5.1. Characterisation of parent compounds

Parent NFRs were determined by the (-)APCI-LC-HRMS method described previously in this chapter. The exact ion masses of EH-TBB, BEH-TEBP and BTBPE (Table 4.2) were used for identification of each individual NFR in dosing solutions and samples generated from *in vitro* experiments. Reconstructed chromatograms of EH-TBB, BEH-TEBP and BTBPE in MLM exposed to individual NFRs are shown in Figure 4.8.

Figure 4.8: (-)APCI-LC-HRMS extracted ion chromatograms of BEH-TEBP (A), EH-TBB (B) and BTBPE (C) in *in vitro* MLM samples exposed to 10 μ M of individual NFRs for 60 min



Interestingly, some brominated impurities were detected in (-)APCI analysis of EH-TBB and BEH-TEBP dosing solutions prepared from a 95 % purity standard (Accustandard, New Haven, USA), but not in their high purity standards (>99 %, Wellington Lab, Ontario, Canada). In EH-TBB dosing solution, a small amount (~ 0.3 %) of BEH-TEBP was found together with a brominated impurity (~1 %) with the exact ion mass of 404.97057. The impurity showed the unique pattern of two bromine atoms in the chemical formula (Figure 4.9) with the proposed molecular ion formula was $[C_{15}H_{19}Br_2O_3]^-$. The common ionization mechanism for organobrominated compounds in (-)APCI mode is

[M-Br+O], therefore the impurity was tentatively identified as mono debrominated EH-TBB (EH-TriBB) with the chemical formula $C_{15}H_{19}Br_3O_2$. This was further supported by the earlier retention time of the tri-brominated compound compared to EH-TBB, as well as a good match of the Br isotope cluster with the simulated accurate mass isotope pattern for the suspect molecule (Figure 4.9).

In the BEH-TEBP dosing solution, only one brominated impurity with an exact molecular ion mass of 561.08512 was found at relative high percentage (~4 %). (-)APCI-LC-HRMS analysis of the impurity showed an isotopic pattern of two bromine atom in the impurity (Figure 4.10). Compound Discoverer proposed the ion formula to be $[C_{24}H_{35}Br_2O_5]^-$. Similar to the case of the EH-TBB dosing solution, we hypothesize this impurity to be BEH-TriBP, a debrominated product of BEH-TEBP, which was also supported by retention time and isotope cluster simulation (Figure 4.10)

The detection of such impurities in EH-TBB and BEH-TEBP dosing solutions suggested that: (i) extra attention is needed when studying biotransformation of these chemicals by biological assays. They might appear as potential metabolites despite originating from dosing solutions, and.

(ii) even though the impurities were detected at substantially lower concentrations than their parent compounds, they could still be relevant as environmental contaminants of concern.

Figure 4.9: BEH-TEBP and EH-TriBB as impurities in EH-TBB dosing solution analyzed by (-)APCI-LC-HRMS

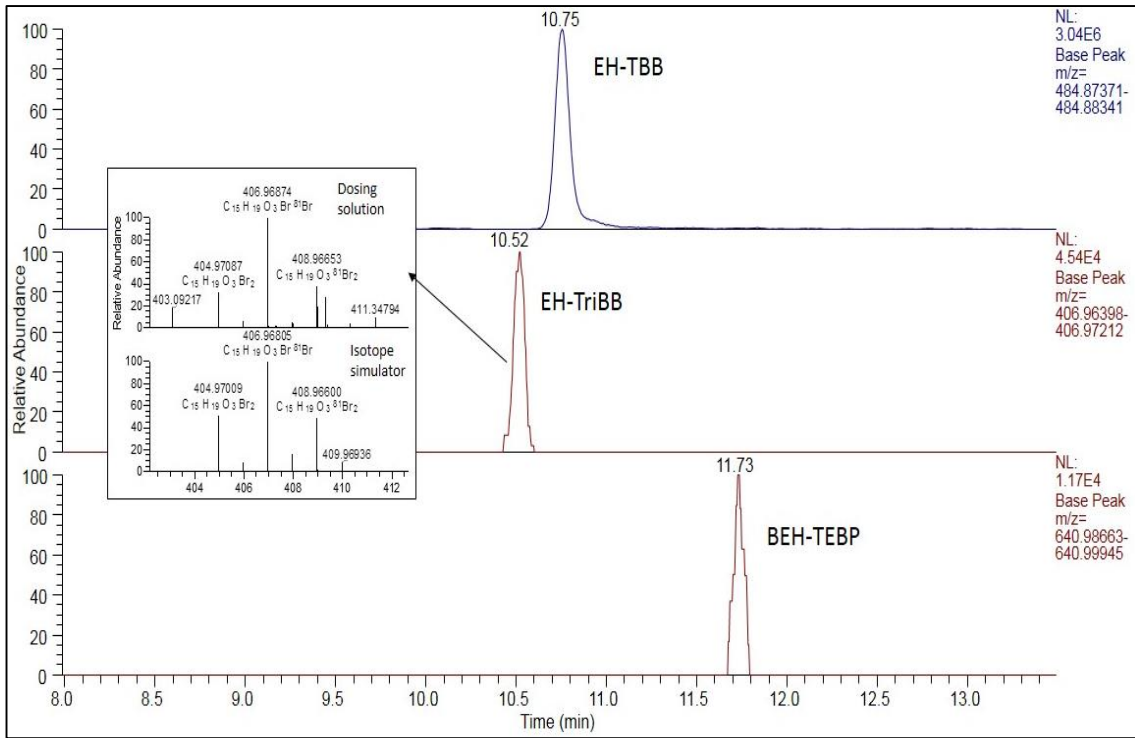
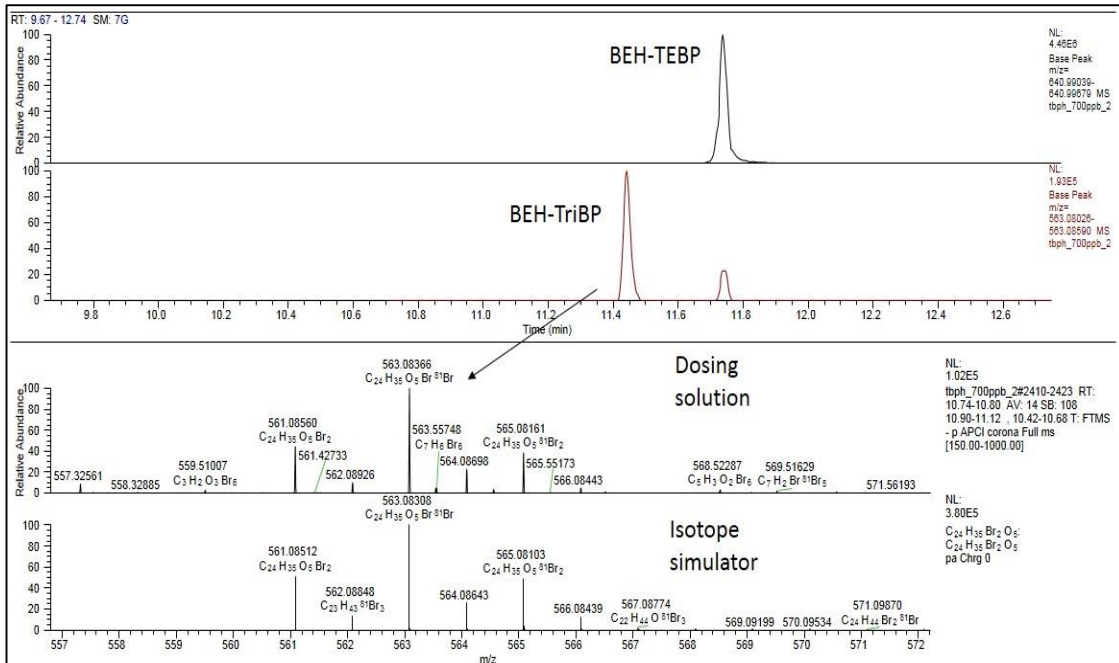


Figure 4.10: BEH-TriBP as impurity in BEH-TEBP dosing solution analyzed by (-)APCI-LC-HRMS



4.5.2. Metabolite identification

The Compound Discoverer work flow as described in Table 4.7 was employed to study the potential metabolites of individual EH-TBB ($C_{15}H_{18}Br_4O_2$), BEH-TEBP ($C_{24}H_{34}Br_4O_4$) and BTBPE ($C_{14}H_8Br_6O_2$) *in vitro* by mouse liver microsomes with some slight modification. Specifically, the Maximum Element Counts parameter in “Detect Unknown Compound” and “Predict Compositions” nodes were set as C30 H50 Br6 O10 to cover possible reactions can take place during phase I metabolism (e.g. hydroxylation). A very large number of features were detected in two groups: “treated” and “untreated” for all three compounds. In order to narrow down the metabolite candidates, we applied the following successive filters:

- i, Pattern matches is true in any pattern (Pattern Scoring – Table 4.7)
- ii, P value of per group ratio calculated by ANOVA and TukeyHSD post hoc is less than 0.1 between treated and untreated samples
- iii, Log₂ fold changes (log₂ of peak areas ratio of a feature between treated and untreated samples) is greater than 1 which is equivalent to fold change > 2 (Dalman et al., 2012).

Additionally, we also looked at the feasibility of proposed chemical formulae, the difference between log₂ fold change of 1 μ M and 10 μ M exposure level as well as visual inspection of retention time, peak shape and S/N ratio before confirming a metabolite candidate.

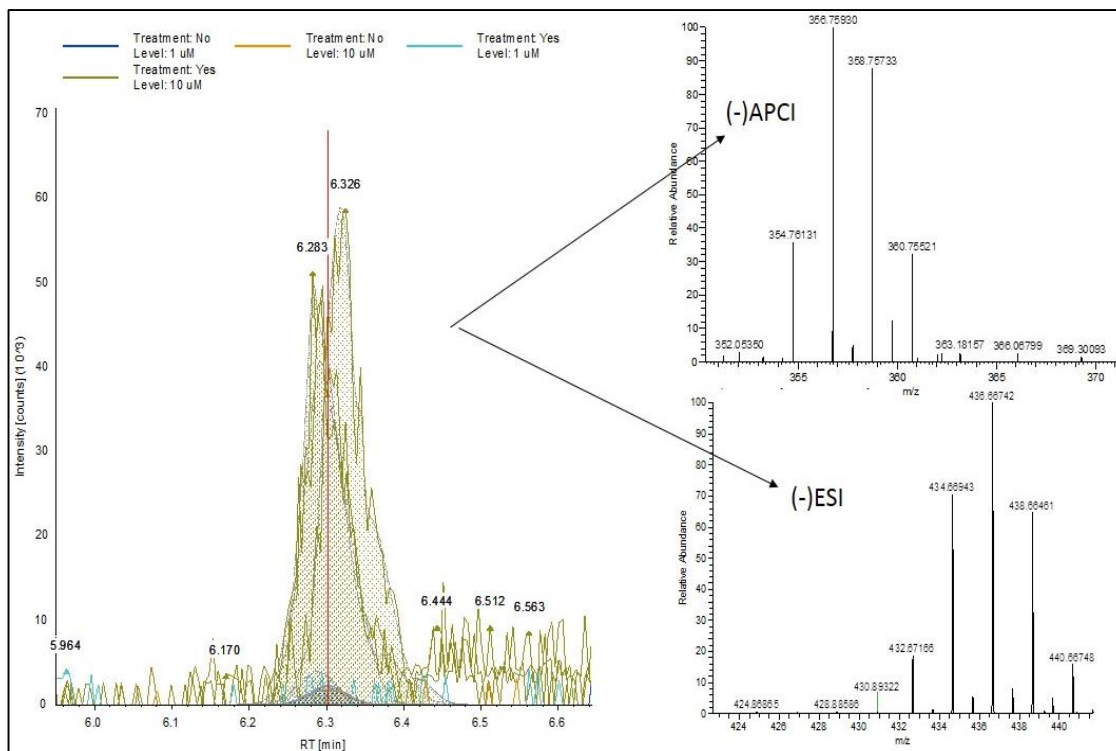
It was reported that porcine carboxylesterase can slowly metabolize BEH-TEBP into its monoester form (Roberts et al., 2012). However such a metabolite was not identified in any *in vitro* BEH-TEBP bioassays by human liver microsomes (Roberts et al., 2012) or carp, mouse and fathead minnow S9, cytosol and microsomes (Barr et al., 2012). A significant depletion of BEH-TEBP was observed in the later study in all of the bioassays, indicating potential metabolism of the substrate by the subcellular fractions into unidentified metabolites. The results from Compound Discoverer in this study also showed no monoester or identifiable oxidation metabolites of BEH-TEBP in either (-)APCI mode or (+)/(-)ESI mode.

Similarly, there were no measurable biotransformation products of BTBPE by MLM in any analysis mode. To our knowledge, there is only one *in vivo* metabolism study of BTBPE in male rats following a single oral dose at 2 mg/kg of ¹⁴C radiolabeled BTBPE (Hakk et al., 2004). BTBPE reportedly persisted against liver metabolism with less than 4 % of the dose undergoing biotransformation via oxidation, oxidative debromination and ether cleavage mechanisms (Hakk et al., 2004). Despite our extensive efforts, no similar BTBPE metabolites could be positively identified following our rigorous protocol. There was however a strong signal for 2,4,6-tribromophenol in all samples including blanks. Since the metabolic rate of BTBPE was reported to be very low *in vivo* in rat, we cannot exclude the possibility that 2,4,6-tribromophenol, a potential metabolite of BTBPE, was formed *in vitro* at low concentrations that were indistinguishable from its blank level.

Analysis of *in vitro* EH-TBB samples by Compound Discoverer revealed two potential metabolites in (-)APCI mode with accurate ion masses of 354.76151 (M1) and 384.77164 (M2). In (-)ESI mode there was one potential metabolite (M3, accurate ion mass of 434.66636) that eluted at the same retention time as M1.

M1 eluted at around 6.3 min (Figure 4.11) and had the isotopic pattern of three bromines in its proposed formula. The proposed ion composition for M1 was $[C_7H_2Br_3O_3]^-$ and \log_2 fold change in 1 and 10 μ M samples were 2.12 and 6.80, respectively. We hypothesized M1 to be tetrabromobenzoic acid (TBBA, $C_7H_2Br_4O_2$) formed via common (-)APCI ionization mechanism $[M-Br+O]^-$. This is plausible because M1 eluted quite early in the chromatogram in comparison with EH-TBB (10.75 min), implying it to be of higher polarity than the parent compound. Since M3 (identified in negative ESI mode) eluted at the same time as M1 (in negative APCI mode) and also showed a three bromines isotopic pattern, we hypothesized that M3 is the ion form of TBBA in (-)ESI. TBBA is an organic acid and expected to be ionized in (-)ESI to form a $[M-H]^-$ ion. Indeed, the proposed ion formula for M3 was $C_7HBr_4O_2$. In order to confirm our hypothesis, authentic standards of TBBA and TBBA-spiked *in vitro* samples were analyzed. An increase in intensities of both M1 and M3 was observed. The mass spectrum of TBBA in (-)APCI and (-)ESI also matched with that of M1 and M3, respectively. Therefore, M1/M3 was confirmed to be TBBA, a metabolite of EH-TBB formed by enzymatic esterification reaction (Roberts et al., 2012).

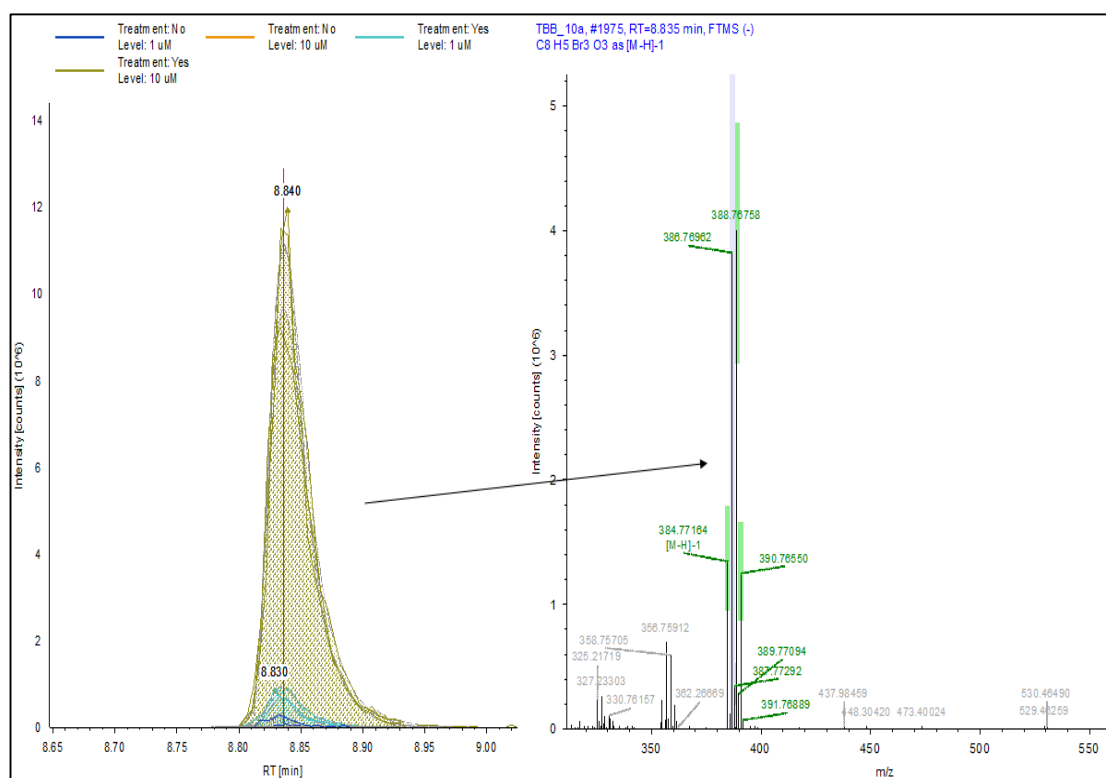
Figure 4.11: Overlay chromatogram of M1 (M3) and its chromatogram in MLM samples exposed to 10 μ M of EH-TBB *in vitro*



M2 eluted at around 8.84 min and showed an isotopic pattern of three bromines (Figure 4.12). The proposed molecular ion for M2 was $[C_8H_4O_3Br_3]^-$ which likely corresponds to 2,3,4,5-tetrabromomethylbenzoate ($C_8H_4O_2Br_4$) after common (-)APCI ionization mechanism $[M-Br+O]^-$. An increase in log₂ fold change between 1 μ M (2.59) and 10 μ M samples (9.71) was also observed. In addition to retention time and isotope cluster simulation, the identity of M2 as 2,3,4,5-tetrabromomethylbenzoate (TBMB) was confirmed via comparison of an authentic reference standard for the nominated compound. It could be formed via methylation of TBBA (M1). TBMB was reported as an *in vitro* metabolite of EH-TBB by fathead minnow S9 fractions but not mouse liver subcellular fractions (Barr et al., 2012). A potential source for TBMB could be the non-enzymatic methylation of TBBA upon addition of ice-cold methanol to stop the enzymatic reaction, which may lead to false positive identification of this compound as an *in vitro* metabolite. To test this hypothesis and confirm the authenticity of TBMB as a metabolite of EH-TBB, we carried out a series of *in vitro* exposure experiments (section 3.2), using different methods to stop the enzymatic reaction: ice-cold acetonitrile, ice-cold ethyl acetate and thermal deactivation at 70 °C. Additionally, a mixture of pure TBBA standard and

methanol were incubated at the same conditions as the *in vitro* experiments. No TBMB was observed in any of these samples. Hence, it was concluded that TBMB was not an authentic *in vitro* metabolite of EH-TBB by MLM. The exact mechanism of TBMB formation under the applied experimental condition is unknown but it is important to note that such methylation processes occurred only when there was MLM, NADPH, EH-TBB substrate and methanol added to stop the reaction. It is plausible that ice-cold methanol did not immediately stop the enzymatic activity of MLM resulting in an enzyme-mediated methylation reaction of TBBA. Since methyl transferase enzymes are active in mammalian hepatocytes, further confirmation of the metabolic fate of TBBA and its potential methylation to produce TBMB requires an *in vivo* model.

Figure 4.12: Overlay chromatogram of M2 and its spectrum in MLM samples exposed to 10 μ M of EH-TBB *in vitro*



4.6. Conclusions

In this chapter, we have successfully developed a LC(-APCI)/(-ESI)-HRMS method that allows both targeted and untargeted analysis of BFRs and their potential metabolites/degradation products. The method utilized the high mass accuracy of UPLC-Orbitrap MS instrument, an in-house mass library and a powerful bioinformatics software

package, Compound Discoverer™. This was demonstrated using simulated leachate samples derived from waste electrical and electronic equipment and samples generated from *in vitro* experiments of mouse liver microsomes exposed to EH-TBB, BEH-TEBP and BTBPE.

In simulated leachate samples, BDE-47, BDE-99, BDE-183, BDE-209, DBDPE, BTBPE, TBP, TBP-AE, HBCDDs and TBBPA were detected via our targeted approach. Among these detected BFRs: BDE-209, DBDPE, TBBPA and 2,4,6-TBP were present in almost every sample. PBDEs other than BDE-209 were occasionally found - mostly in leachate from fridges/freezers - while BTBPE was mainly detected in samples from mixed waste electrical and electronic equipment. Untargeted analysis of the same samples revealed 5 potential degradation products of TBBPA: dibromobisphenol A, tribromobisphenol A, methoxylated TBPPA, methoxylated dibromobisphenol A and chlorinated TriBBPA.

Via an untargeted analysis approach, 2,3,4,5-tetrabromobenzoic acid was identified as an *in vitro* metabolite of EH-TBB by mouse liver microsomes while no potential metabolites were identified for BEH-TEBP and BTBPE under the same experimental conditions. It is also important to note that chemical impurities and *in vitro* experiment quenching agents can introduce false positive metabolite identification.

In conclusion, our method provides a universal framework to study BFRs (including NBFRs) and their metabolites/degradation products in various environmental matrices that can be adjusted on a needed basis. The method was applied for our NBFR studies in Chapter 5 and 6.

Chapter 5

In vitro metabolism of 1,2-Dibromo-4-(1,2-dibromomethyl)cyclohexane by Human Liver Microsomes

Some material in this chapter is taken verbatim from the following publication:

Nguyen, K.-H.; Abou-Elwafa Abdallah, M.; Moehring, T.; Harrad, S. Biotransformation of the Flame Retardant 1,2-Dibromo-4-(1,2-dibromoethyl)cyclohexane (TBECH) in Vitro by Human Liver Microsomes. *Environ. Sci. Technol.* 2017, 51 (18), 10511–10518.

5.1. Synopsis

1,2-Dibromo-4-(1,2-dibromomethyl)cyclohexane (DBE-DBCH or, as used in this chapter to facilitate easier metabolite abbreviation, TBECH) is one of the NBFRs that has been widely detected recently in UK foods and indoor air and dust, which warrants human exposure to this chemical (Tao et al., 2017, 2016). However, very little is known about its toxicokinetics and fate following human exposure which is necessary to fully understand its toxic implications and assess the risk arising from this exposure. In this study, the technical mixture of TBECH and the pure β -TBECH isomer were subjected to *in vitro* biotransformation by human liver microsomes (HLM) for the first time. After 60 mins of incubation, 5 potential metabolites of TBECH were tentatively identified in microsomal assays of both the TBECH mixture and β -TBECH using UPLC- Q-Exactive Orbitrap™ mass spectrometry. The metabolic profile of TBECH indicated potential hepatic biotransformation of this chemical via Cytochrome P450-catalyzed hydroxylation, debromination and α -oxidation. Kinetic studies revealed monohydroxy-TBECH as the major metabolite of TBECH by human liver microsomes. The estimated intrinsic clearance (Cl_{int}) of TBECH mixture was slower ($P < 0.05$) than that of pure β -TBECH. While the formation of monohydroxy-TBECH may reduce the bioaccumulation potential and provide a useful biomarker for monitoring TBECH exposure, further studies are required to fully understand the levels and toxicological implications of the tentatively identified metabolites.

5.2. Introduction

1,2-Dibromo-4-(1,2-dibromomethyl)cyclohexane (TBECH or DBE-DBCH) is an additive EFR produced by Albermarle Corp., U.S.A under the trade name Saytex BCL-462. The flame retardant is used in extruded polystyrene and polyurethane foam, electrical cable coatings, adhesive in fabric and construction materials (Arsenault et al., 2008; Tomy et al., 2008). In the U.S, TBECH production volume in 2002 was 230 tons (Covaci et al.,

2011). The technical mixture of TBECH contains equimolar concentrations of two diastereoisomers, named α and β -TBECH. Although no other isomers could be detected in the technical mixture, thermal conversion into γ - and δ -TBECH was reported during incorporation into flame-retarded products at temperature of 123 °C or higher (Arsenault et al., 2008). TBECH isomers have been globally detected in environmental samples including indoor air and dust (Cequier et al., 2014; Hassan and Shoeib, 2015; Newton et al., 2015), outdoor air (Shoeib et al., 2014), herring gull eggs (Chen et al., 2012; Gauthier et al., 2009), blubber of Canadian Arctic whale (Tomy et al., 2008) and toddler's faeces (Leena M O Sahlström et al., 2015). Recently, Tao et al. reported TBECH as the predominant emerging flame retardant detected in all indoor air (n=35) and dust (n=92) samples from UK houses (mean = 173 pg/m³ and 21.4 ng/g in air and dust) and offices (mean = 320 pg/m³ and 41 ng/g in air and dust) (Tao et al., 2016). Not only in indoor air and dust, TBECH was also the predominant NBFRs in UK foods with mean concentration ranged from 1.43 to 86.1 ng g⁻¹ l.w, which was even higher than total PBDEs concentration found in many samples (Tao et al., 2017). Consequently, the compound was detected in 100% UK human milk samples collected in 2014-2015 at mean concentration of 3.37 ng g⁻¹ l.w (Tao et al., 2017). TBECH also showed the highest levels of all detected EFRs in Norwegian (mean = 209 pg/m³) and Swedish (mean = 43 pg/m³) indoor air samples (Cequier et al., 2014; Newton et al., 2015) indicating its wide application, especially in Europe.

This is of concern due to its potential toxicological effects on humans and wildlife. Several toxicological *in silico*, *in vitro* (human and chicken cell lines) and *in vivo* (birds, fishes and rats) studies show TBECH is a strong androgen receptor agonist and endocrine disruptor (Asnake et al., 2015; Curran et al., 2017; Khalaf et al., 2009; Kharlyngdoh et al., 2016; Larsson et al., 2006; Marteinson et al., 2017, 2015; Park et al., 2011; Pradhan et al., 2013). TBECH also displayed potential to disrupt thyroid and sex hormones in American kestrels (Marteinson et al., 2017), modulate thyroid axis in juvenile Brown Trout (Park et al., 2011) and alter androgen receptor regulation in human ductal breast cancer and prostate cancer cell lines (Kharlyngdoh et al., 2016). However, very little is known about the biotransformation and fate of TBECH in humans.

Previous studies have shown some BFRs can be metabolized to more toxic lower brominated congeners (Abdallah et al., 2014; Feng et al., 2015; Xie et al., 2014). Two of

the primary *in vivo* debrominated metabolites of BDE-209 in rainbow trout were identified as BDE-47 and BDE-99 (Feng et al., 2015), which are more bioaccumulative and showed much higher toxic potential than the parent compound in goldfish and zebrafish liver cell lines (Xie et al., 2014; Yang and Chan, 2015). Similarly, HBCDDS was metabolized by rat and trout liver S9 fractions into pentabromocyclododecenes (PBCDs), which showed higher affinity for binding to the thyrotropin receptor (TSH) than the parent compound (Abdallah et al., 2014). Therefore, improved understanding of the biotransformation pathways, rates and products of TBECH is essential for assessment of the risk arising from human exposure to this flame retardant.

To our knowledge, only one study has investigated the potential metabolites of TBECH and moreover used *in vitro* rat liver microsomes (Chu et al., 2012). Results revealed that after 60 min, 40 % of the exposure dose was metabolized by Cytochrome P450 enzymes into mono and dihydroxylated TBECH, together with some unidentified metabolites (Chu et al., 2012). However, this study did not provide information on the metabolic/hepatic clearance rate of TBECH. Moreover, extrapolation of results from metabolic studies in rat to human is subject to uncertainty due to inter-species variations in metabolic pathways and products. To illustrate, bioconversion from α -, β - and γ -HBCDD mixture into δ -HBCDD was observed in trout but not rat S9 fractions (Abdallah et al., 2014). Furthermore, EH-TBB was metabolized significantly faster in RLM compared to HLM (Roberts et al., 2012).

Against this background, the aims of this chapter are to: (a) investigate the phase I metabolic pathways and products of TBECH following *in vitro* exposure to human liver microsomes (HLM); (b) compare the *in vitro* HLM metabolic profile of the TBECH technical mixture to that of the pure β -isomer and (c) assess the *in vitro* metabolic rate and intrinsic clearance of TBECH by HLM.

5.3. Experiments

5.3.1. Chemicals and Standards

All solvents and reagents used in this study were purchased from Fisher Scientific (Loughborough, UK) and were of HPLC grade or higher. Technical TBECH was obtained as a neat powder from Accustandard, Inc. (New Haven, CT, USA). A dosing solution was

prepared by dissolving technical TBECH in dimethyl sulfoxide (DMSO). High purity standards of β -TBECH, α - and β -TBECH mixture (equimolar concentrations), PBDE-77, and ^{13}C -BDE-100 were purchased from Wellington Laboratories (Guelph, ON, Canada). RapidStart NADPH regenerating system was purchased from XenoTech (Kansas, KS, USA) while human liver microsomes and William's E medium were obtained from Thermo Fisher Scientific (Paisley, UK).

5.3.2. *In Vitro* Incubation Experiments

Pre-incubations were performed at different HLM concentrations and different times. After optimization of the reaction parameters, the following general exposure protocol was applied: 0.5 mg of human liver microsomes, William's E medium and 10 μL of TBECH dosing solution (final concentration 10 μM) were pre-incubated for 10 minutes at 37 $^{\circ}\text{C}$. NADPH regenerating system (final concentration: 2.0 mM nicotinamide adenine dinucleotide phosphate, 10.0 mM glucose-6-phosphate and 2 units/mL glucose-6-phosphate dehydrogenase) was added to make a final volume of 1 mL. The samples were then incubated at 37 $^{\circ}\text{C}$, 5 % CO_2 and 98 % relative humidity for 60 min. At the end of the incubation, 1 mL of ice-cold methanol was added to stop the reaction prior to sample extraction. In all incubation experiments, experiment blanks including a non-enzymatic blank in which no NADPH regenerating system was added, a heat-inactivated blank featuring liver microsomes heated above 80 $^{\circ}\text{C}$ for 10 min and a solvent blank which contained only William's E medium were performed and analyzed alongside the sample batch.

5.3.3. Sample extraction

Due to the unavailability of isotopically-labelled TBECH, incubated samples were spiked with 20 ng of ^{13}C -BDE-100 as internal standard and extracted according to a previously reported method (Abdallah et al., 2014). Briefly, samples were mixed with 3 mL of hexane:DCM mixture (1:1 v/v) by vortexing for 30 s, followed by ultrasonication for 5 min and centrifuged at 4000 g for 5 min. The organic layer was collected and the extraction procedure was repeated twice. The combined extracts were evaporated to dryness under a gentle stream of nitrogen then reconstituted in 100 μL of methanol containing 20 ng of BDE-77 as a syringe standard for QA/QC purposes.

5.3.4. Instrumental analysis

5.3.4.1. UPLC-Orbitrap MS analysis

Samples were analyzed in accordance to section 4.2.2. Briefly, chromatographic separation was performed on an Accucore RP-MS column (100 x 2.1 mm, 2.6 μ m) with water (mobile phase A) and methanol (mobile phase B). A gradient programme at 400 μ L/min flow rate was applied as follows: start at 20 % B; increase to 100 % B over 9 min, held for 3 min; then decrease to 20 % B over 0.1 min; maintained constant for a total run time of 15 min.

The parent compound was analyzed in negative APCI mode. The Orbitrap parameters were set as follows: (-) APCI full scan mode, resolution 17500, AGC target 1E6, maximum injection time 100 ms, scan range 75 to 700 m/z, sheath gas flow rate 25 AU, aux gas flow rate 5, discharge current 30 μ A, capillary temperature 250°C and S-lens RF level 50.

Accurate masses of 80.91629, 512.73847 and 420.78975 were used to monitor TBECH, ¹³C₁₂-BDE-100 (internal standard) and BDE-77 (syringe standard), respectively. The more universal, softer electrospray ionisation (ESI) mode was used for screening and identification of the produced metabolites. The optimised parameters were: (-) ESI full scan mode, resolution 17500, AGC target 1E6, maximum injection time 100 ms, scan range 75 to 750 m/z, sheath gas flow rate 20 AU, discharge voltage 2.5 kV, capillary temperature 320 °C.

5.3.4.2. GC x GC TOF-MS analysis

GCxGC-TOF MS analysis to screen for potential debrominated metabolites of TBECH. The samples were analysed by an Agilent 7890A gas chromatogram equipped with a Agilent 7693 Autosampler (Agilent Technologies, Wilmington, DE, USA) and a Zoex ZX2 GC \times GC cryogenic modulator (Houston, TX, USA), coupled with a Almsco BenchToFdx™ time of flight mass spectrometer (Almsco International, Llantrisant, UK). The first dimension column was 30 m x 250 μ m x 0.25 μ m SGC BPX 5 (SGC Analytical Science, Victoria, Australia) and the second dimension column was 4 m x 100 μ m x 0.1 μ m SGC BPX 50. Injection volume was 1 μ L using split mode (1:50) at 300 °C. Helium

was used as a carrier gas at a constant flow rate of 1 mL min⁻¹. The primary oven was programmed as 120 °C for 4 min, heated at 2.5 °C min⁻¹ to 210 °C increased to 325 °C at 2 °C min⁻¹ hold for 2 min. Modulation time was 4 sec. Ion source temperature was 320 °C and transfer line temperature 325°C. The mass spectrometer was operated in positive EI mode (70 eV) with a mass scan range of 45-800 m/z at 50 Hz scan speed. Subsequent data processing was carried out using GC Image™ v2.1 (Zoex)

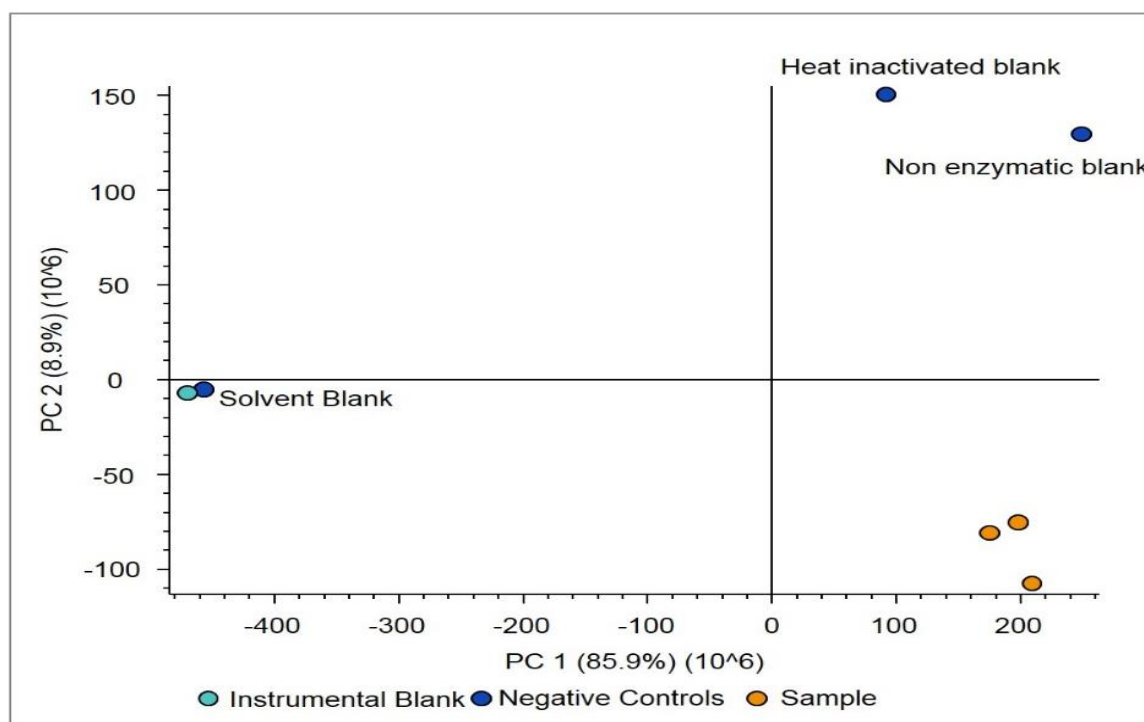
5.3.5. QA/QC

Quality control samples where the William's E medium was spiked with TBECH at all dosing concentration levels were analyzed, with recoveries of TBECH falling between 96 to 113 % of the theoretical dosing concentration. In incubation experiments, internal standard recoveries were within 60-110 %.

No parent compounds or metabolites were found in instrument and solvent blanks. Additionally, no metabolites were found in the non-enzymatic and heat-inactivated blanks.

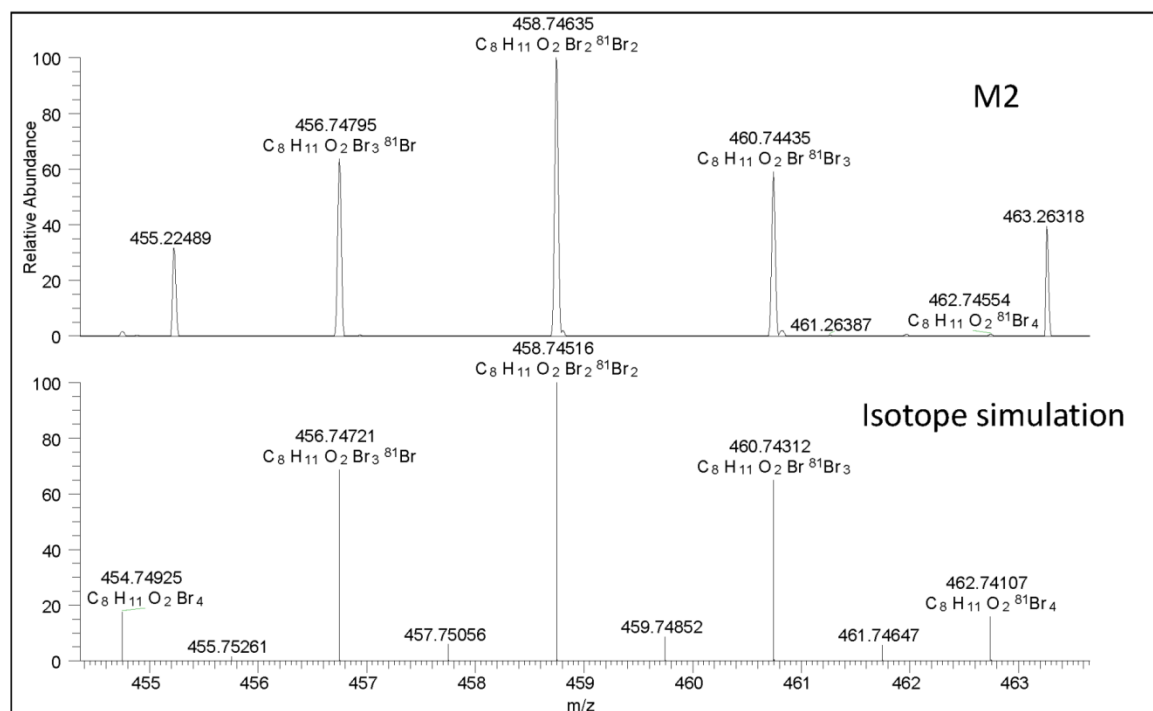
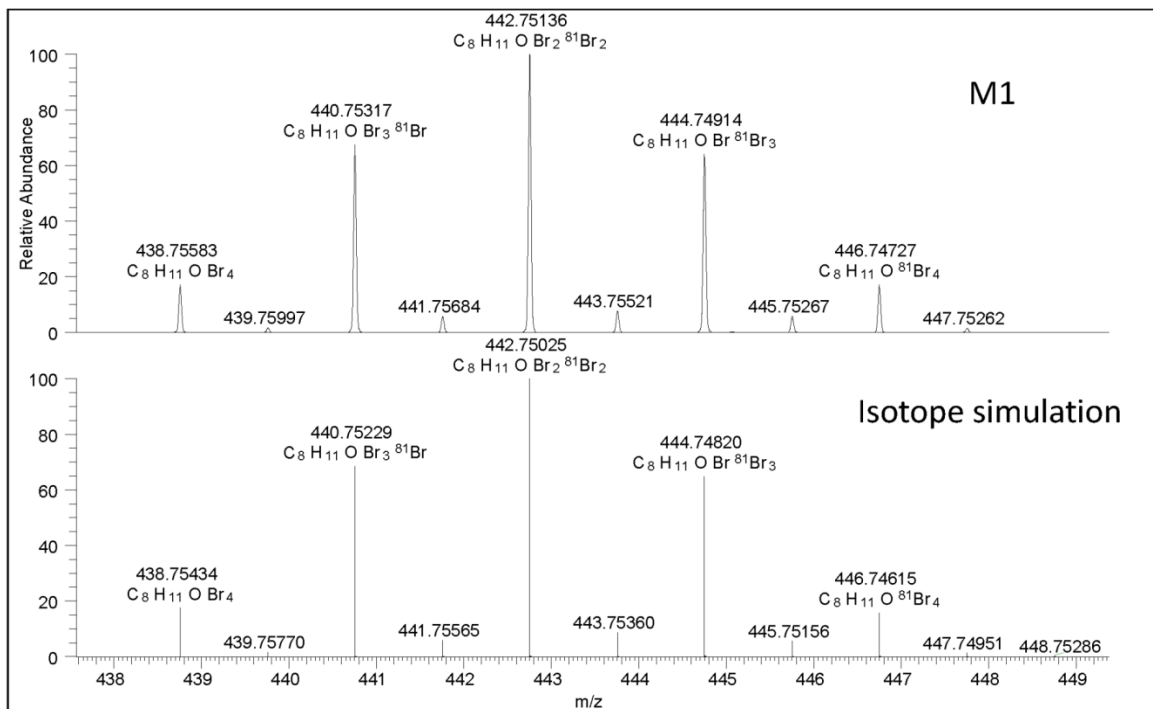
Principal component analysis results from Compound Discoverer 2.0 software also showed very distinctive separation between LC/MS chromatograms of samples generated by our *in vitro* experiments compared to those of experimental and instrument blanks (Figure 5.1). This analysis was performed using the identified peaks and their corresponding peak area in each data files. It shows the difference/similarity in chemical information contained within the samples being analyzed. As shown in Figure 6.1, the preliminary samples (HLM exposed to 10 µM of the technical TBECH) were grouped together while heat-inactivated blank (HI-blank) and non-enzymatic blank (NEB-blank) were grouped on the opposite side of PC2 to the preliminary samples. The solvent blank and instrument blank were also grouped very closely together which implied negligible difference in the detected peaks between the two samples. In other words, lab contamination during the whole *in vitro* experiment and extraction process was minimal.

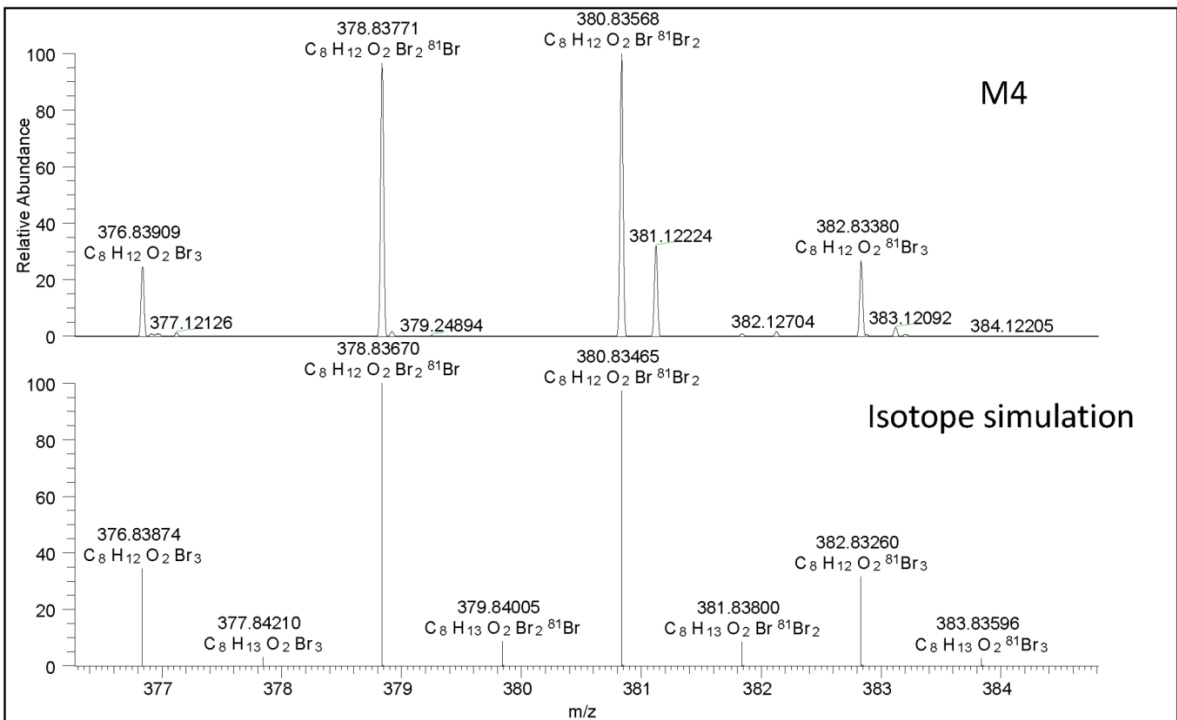
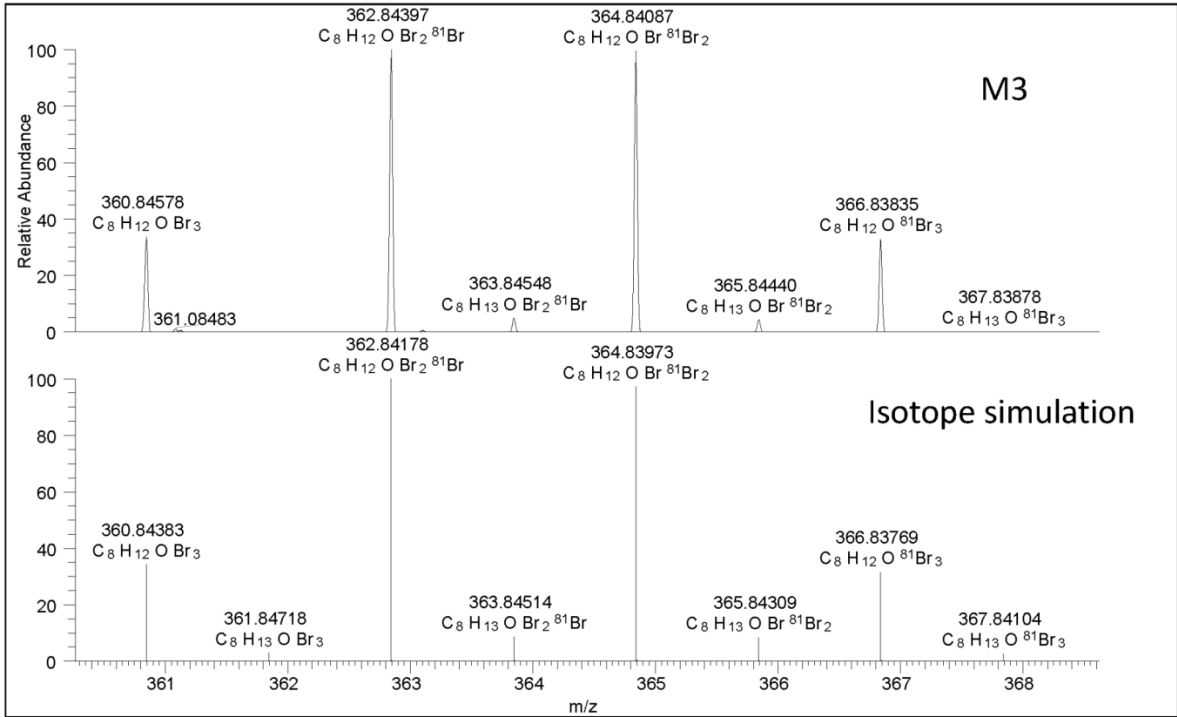
Figure 5.1: Principal component analysis score plot of negative control blanks and human liver microsomes samples exposed to 10 μ M TBECH mixture for 60 minutes

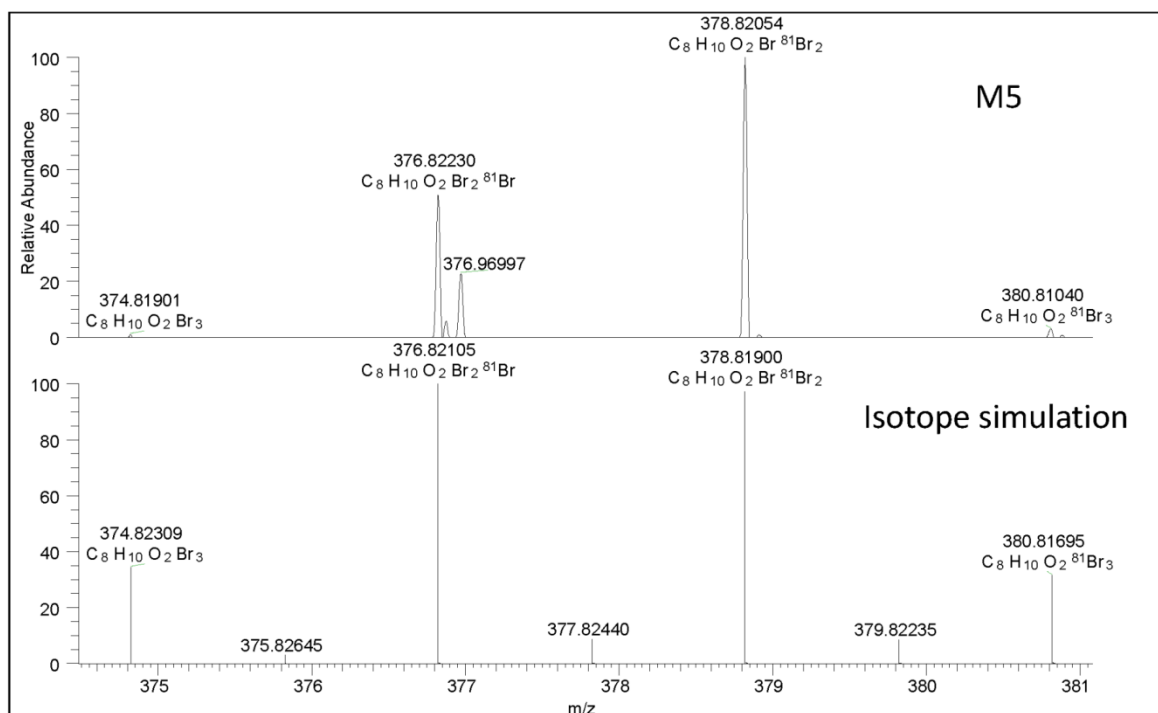


The isotopic patterns of the proposed chemical formula for detected metabolites were also matched with those of the accurate mass isotope simulations provided by Xcalibur™ software (Figure 5.2). With the assumption that the measured compounds contain naturally distributed isotopes, a match in isotopic pattern of a measured compound and simulated pattern greatly increase the confidence in elemental composition prediction of the proposed chemical formula.

Figure 5.2: Isotopic pattern of metabolites 1-5 recorded by LC-Orbitrap MS in comparison with isotope simulation







5.4. Metabolic profile of TBECH

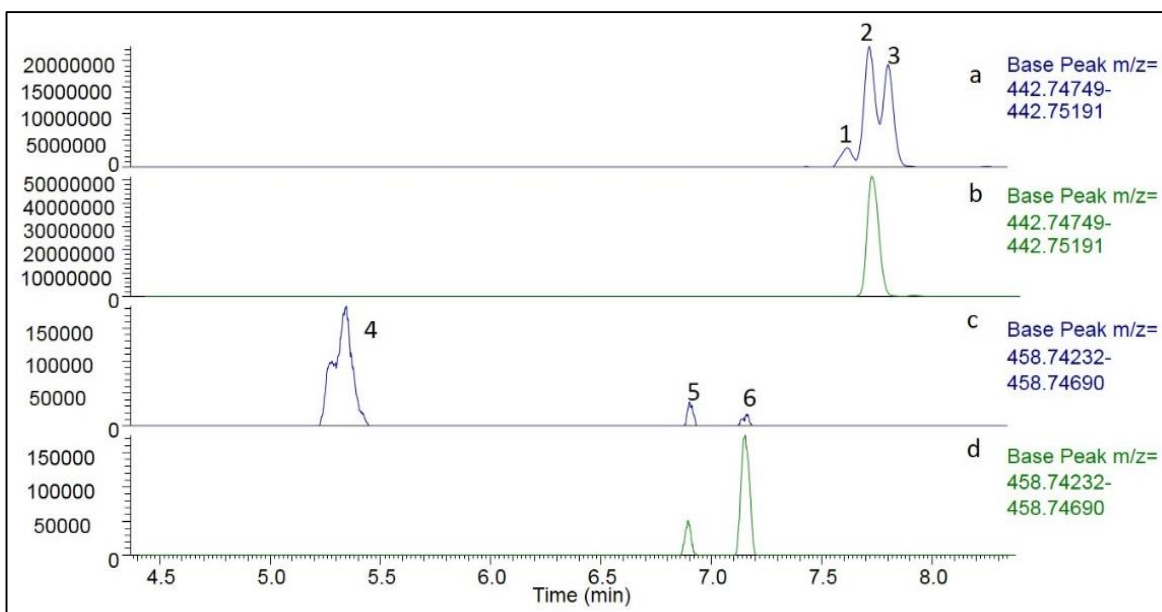
Analysis of the UPLC-Orbitrap™ MS chromatograms obtained for samples derived from the *in vitro* experiments, revealed a minimum of three monohydroxylated and three dihydroxylated metabolites of the parent TBECH following exposure of HLM to 10 μM of the technical mixture for 1 h (Figure 5.3). Bearing in mind the lack of reference standards for these metabolites, the isobaric nature of TBECH isomers in the technical mixture and the large number of theoretical isomers, co-elution of one or more metabolites in the same group (e.g. monohydroxylated TBECHs) could not be excluded. Similarly, the specific position of the hydroxyl groups could not be elucidated.

It is well known that cytochrome P450-catalyzed hydroxylation usually retains the stereochemical configuration at the substrate's reaction site (Ortiz De Montellano, 2010). Therefore, we carried a parallel strand of experiments, where HLM were exposed to pure β-TBECH (the only purified isomer available commercially) in order to gain further information on the metabolic hydroxylation process. Comparisons of LC/MS chromatograms between β-TBECH and technical TBECH exposure experiments (Figures 5.3a and 5.3b) revealed peak M1-2 as monohydroxy-β-TBECH (β-OH-TBECH). Since

the applied commercial mixture contained α - and β -TBECH isomers, it can be concluded that peaks M1-1 and M1-3 are α -OH-TBECH isomers (Figures 5.3a and 5.3b). Similarly, peak M2-4 was identified as α -(OH)₂-TBECH, while peaks M2-5 and M2-6 originated from the β -isomer (Figures 5.3c and 5.3d).

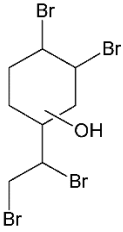
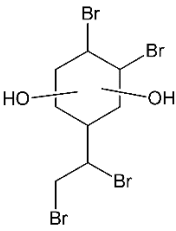
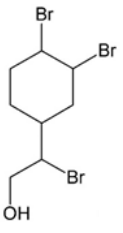
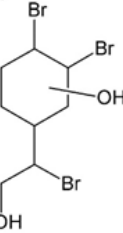
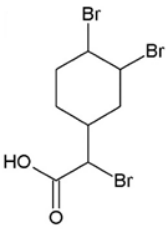
Our findings are generally in agreement with those reported using rat liver microsomes (RLM), where two monohydroxy- and two dihydroxy- isomers were identified following exposure to the TBECH technical mixture (Chu et al., 2012). While the difference in the number of isomers in each metabolite group may be attributed to inter-species variations, this hypothesis cannot be confirmed in the absence of authentic metabolite standards.

Figure 5.3: Selected UPLC-ESI-Orbitrap/MS chromatograms of monohydroxy (M1, peaks 1, 2 and 3) and dihydroxy (M2, peaks 4, 5 and 6) metabolites formed by HLM exposure to 10 μ M of technical TBECH (a and c) and β -TBECH (b and d) for 60 minutes



In addition to the hydroxylated metabolites of the parent TBECH, we also tentatively identified hydroxylated biotransformation products of debrominated TBECH with the formulae: C₈H₁₃Br₃O (M3), C₈H₁₃Br₃O₂ (M4), C₈H₁₁Br₃O₂ (M5).

Table 5.1: Potential metabolites of technical TBECH mixture produced via incubation with human liver microsomes

Code	Accurate mass [M-H] ⁻	Mass deviation (ppm)	Chemical formula	Proposed chemical structure*	Name
M1	442.75136	1.275	C ₈ H ₁₂ Br ₄ O		Monohydroxy-TBECH
M2	458.74635	1.395	C ₈ H ₁₂ Br ₄ O ₂		Dihydroxy-TBECH
M3	362.84397	4.521	C ₈ H ₁₃ Br ₃ O		Monohydroxy-TriBECH
M4	380.83568	1.267	C ₈ H ₁₃ Br ₃ O ₂		Dihydroxy-TriBECH
M5	378.82054	2.620	C ₈ H ₁₁ Br ₃ O ₂		DBCBA

* The exact position of the hydroxyl groups could not be specified via the applied standard protocol.

Metabolites M3 and M4 were assigned the chemical structures of mono- and dihydroxy-triBECH (Table 5.1). While dihydroxy-triBECH (M4; (OH)₂-triBECH) was previously reported in *in vitro* RLM experiments (Chu et al., 2012), this is the first study to identify monohydroxy-triBECH (M3; (OH)-triBECH). It is reasonable to believe that M3 can be formed by direct debromination of M1 and/or through debromination of parent TBECH followed by hydroxylation (Figure 5.6). This is similar to previously reported *in vitro* metabolic pathways for hexabromocyclododecane isomers (HBCDD) in rat (Abdallah et al., 2014) and human (Erratico et al., 2016), where both hydroxylation and debromination were observed.

Interestingly, two separate peaks were identified for M3 following HLM exposure to technical TBECH (Figure 5.3a), while one peak (M3-7) was observed upon exposure to pure β -TBECH. Therefore, peak M3-7 was assigned as β -OH-triBECH and peak M3-8 was attributed to α -OH-triBECH. We hypothesized that the observed M3 metabolites may be produced – at least partially - from hydroxylation of a tribrominated metabolite (i.e. a tribromoethyl cyclohexane derivative or triBECH) with a molecular formula of C₈H₁₃Br₃. However, such triBECH metabolites could not be detected in our samples even using the high separation and resolution power of a GC x GC-ToF/MS platform in an independent analysis dedicated specifically to identify this potential metabolite (Figure 5.4). Similar observations were reported in muscle and liver samples of juvenile brown trout exposed to β -TBECH in their diet (Gemmill et al., 2011), where no debrominated metabolites were detected.

Figure 5.4: GC x GC - TOFMS total ion current chromatogram of HLM sample exposed to 10 μ M TBECH mixture for 60 minutes. The hypothesized metabolite $C_8H_{11}Br_3$ could not be identified.

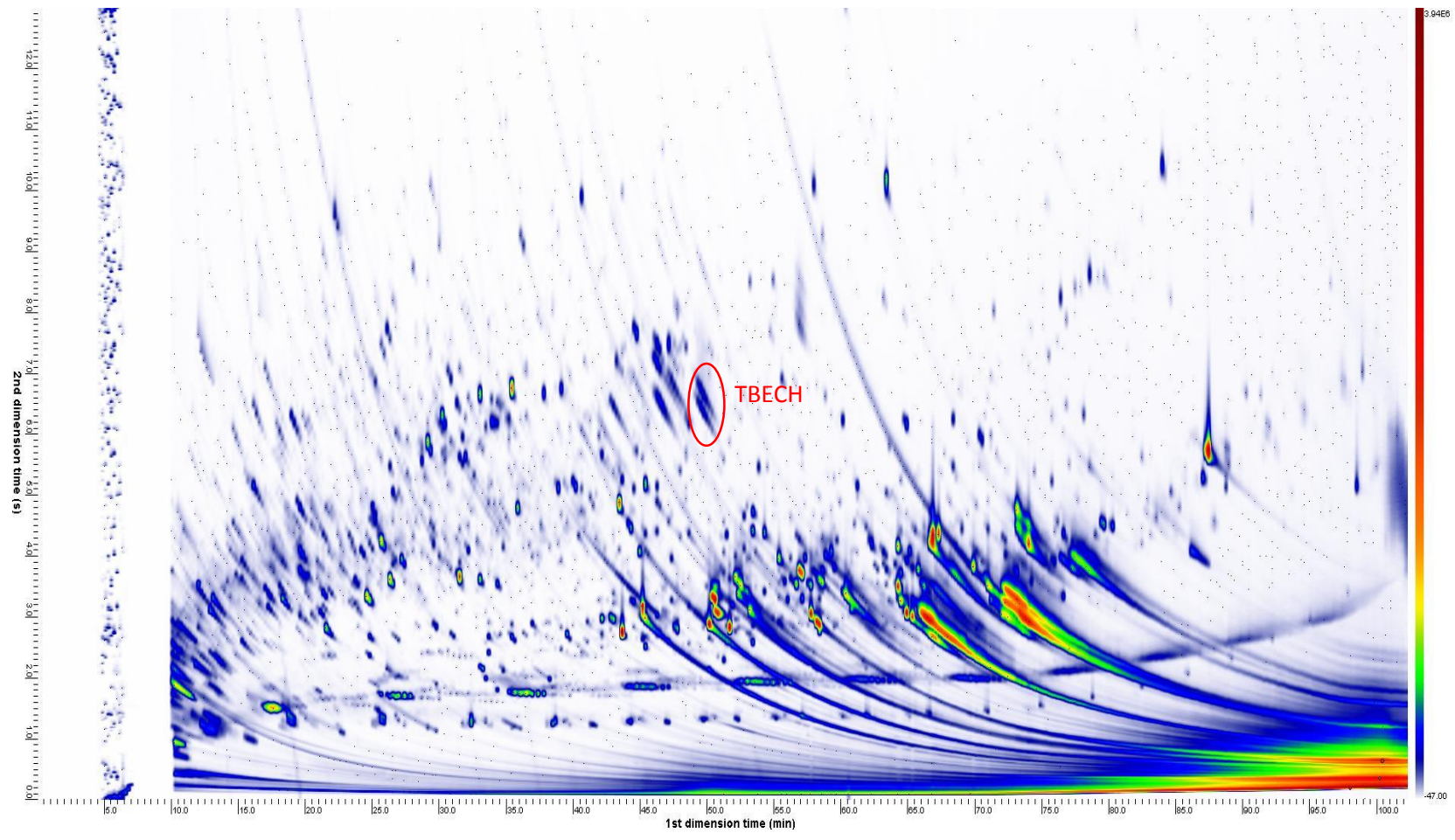
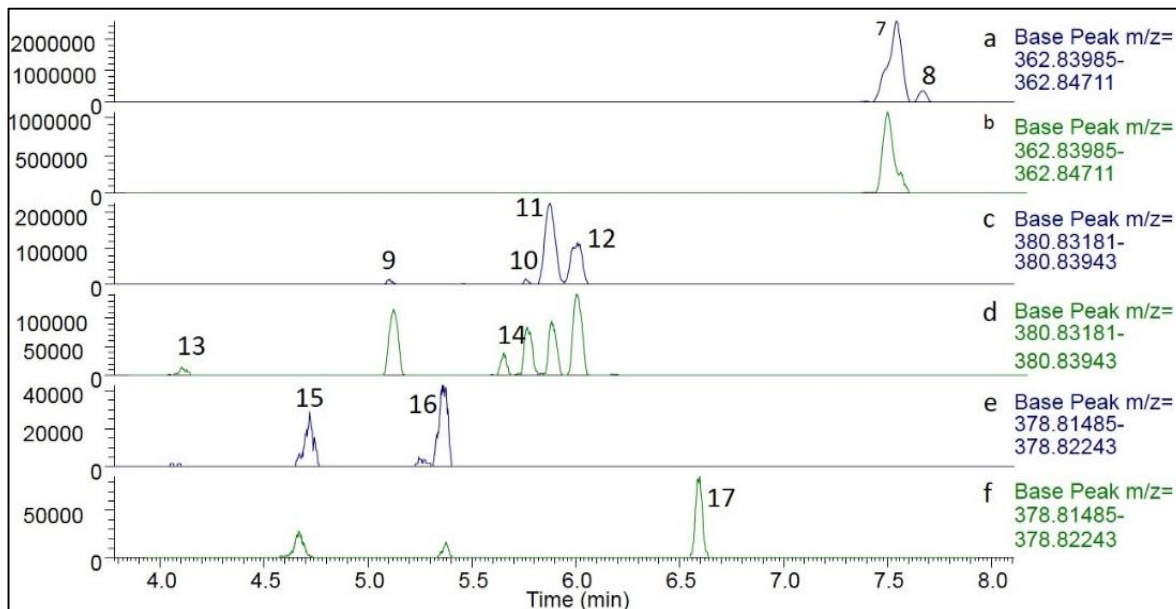


Figure 5.5: Selected UPLC-Orbitrap/MS chromatograms of metabolites M3 (peaks 7 and 8), M4 (peaks 9, 10, 11, 12 and 14) and M5 (peaks 15 and 16) formed by HLM following exposure to 10 μ M technical TBECH (a, c and e) and β -TBECH (b, d and f) for 60 minutes



While our experimental approach could not confirm the formation of triBECH, the hypothesis cannot be refuted as triBECH might be produced then transformed quickly to its hydroxylated metabolites (M3, Figure 5.5a) before the reaction is stopped after 60 min.

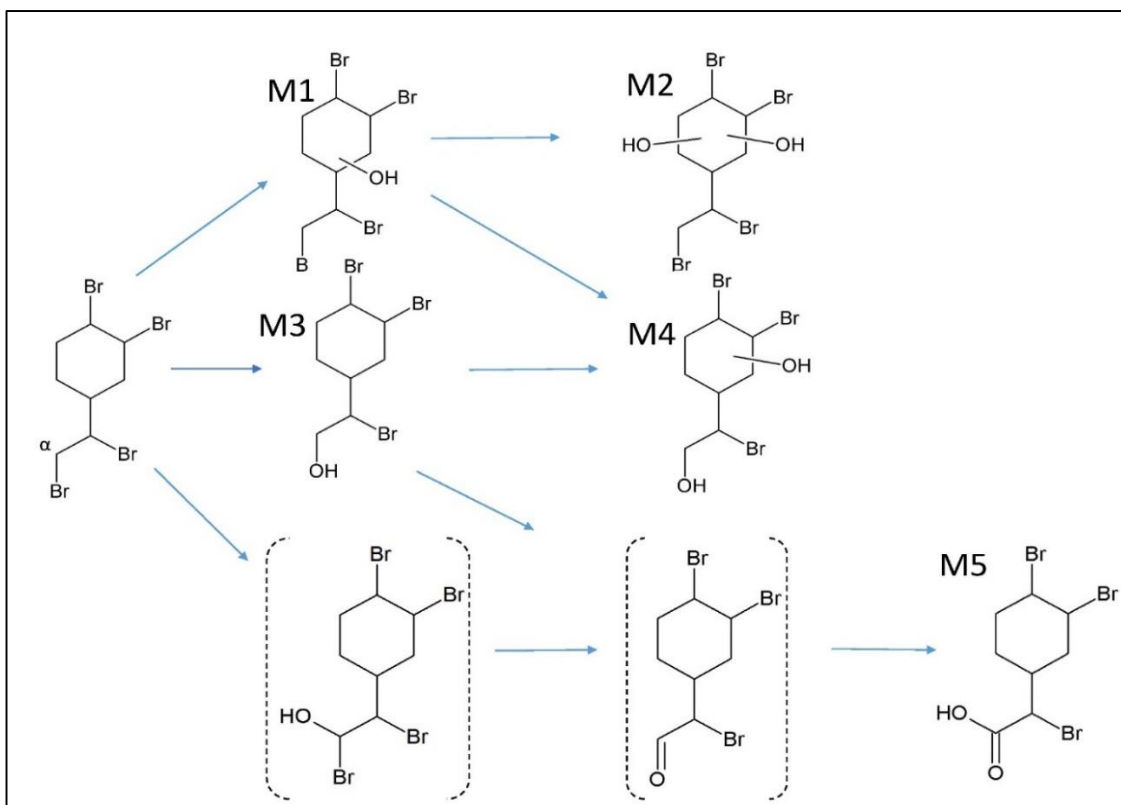
Four distinctive peaks of M4 (Figure 5.5c) were detected when HLM were exposed to either technical TBECH or pure β -TBECH. However, two additional peaks, designated as M4-13 and M4-14 were observed upon exposure to pure β -TBECH only (Figure 5.5d). Hence, M4-13 and M4-14 were tentatively identified as β -(OH)₂-triBECH. Due to the lack of a pure authentic standard for α -TBECH, it was not possible to address the stereochemistry of peaks M4-9, M4-10, M4-11 and M4-12 (Figure 5.5c).

Peaks 15 and 16 of metabolite M5 were detected in both technical TBECH and β -TBECH assays at an accurate mass of 378.81864 with predicted chemical formula of C₈H₁₁Br₃O₂ (Figures 5.5e and 5.5f). As their retention times were shorter than that of most other monohydroxylated and dihydroxylated metabolites, we hypothesized they were carboxylated TriBECH metabolites (i.e. bromo-(1,2-dibromocyclohexyl) acetic acid or DBCBA) formed via α -oxidation mechanism (Figure 5.6). The oxidative reaction starts at C α , transforming the terminal bromomethyl group initially to an aldehyde with subsequent oxidation to the carboxylic acid. This mechanism is similar to previous reports

of metabolic α -oxidative dehalogenation of structurally-similar halogenated compounds such as halothane (Kharasch et al., 1996) and tris-2-chloroethyl phosphate (TCEP) (Abdallah et al., 2015). The aldehyde intermediate (Figure 5.6) however could not be identified in our samples. This is similar to the results of a previous metabolic study on TCEP using human hepatocyte cell lines, where the inability to identify the aldehyde form was attributed to potential rapid oxidation to the corresponding carboxylic acid (Abdallah et al., 2015).

Based on the tentatively identified metabolites, we propose here the CYP450 mediated metabolic pathways of TBECH by HLM (Figure 5.6): (1) hydroxylation, (2) debromination, and (3) α -oxidation.

Figure 5.6: Proposed metabolic pathways of TBECH by Human Liver Microsomes



5.5. Kinetics of TBECH metabolism by HLM

Following metabolite identification, a series of assays with different technical TBECH and pure β -TBECH concentrations (1, 2, 5, 10 and 15 μ M) were performed. Due to the

lack of authentic standards for the metabolites, they were semi-quantified using the response factor of the parent compound. The concentrations obtained were subjected to metabolic rate modelling (including Michaelis-Menten, Hill and substrate inhibition approaches) by nonlinear regression analysis using SigmaPlot Enzyme Kinetics Module v1.1 (Systat Software Inc., Richmond, CA). We considered two statistical criteria: Akaike Information Criterion corrected for small sample size (AIC_c) and standard deviation of the residuals ($Sy.x$) to evaluate the goodness of fit. The best fit model was chosen as the one with lowest values for both AIC_c and $Sy.x$. SigmaPlot results indicated that non-linear regressions of monohydroxy-TBECH, dihydroxy-TBECH and monohydroxy-TriBECH as well as their β isomer counterparts were best fitted to a Michaelis-Menten model (Figure 5.7).

It should be noted that while monohydroxy-TBECH is a primary metabolite of the TBECH substrate, the lack of authentic metabolite standards precludes the confirmation of whether dihydroxy-TBECH and monohydroxy-TriBECH are primary and/or secondary metabolites. Therefore, the estimated kinetic parameters for dihydroxy-TBECH and monohydroxy-TriBECH should be treated with caution as they were derived assuming a primary metabolite status only.

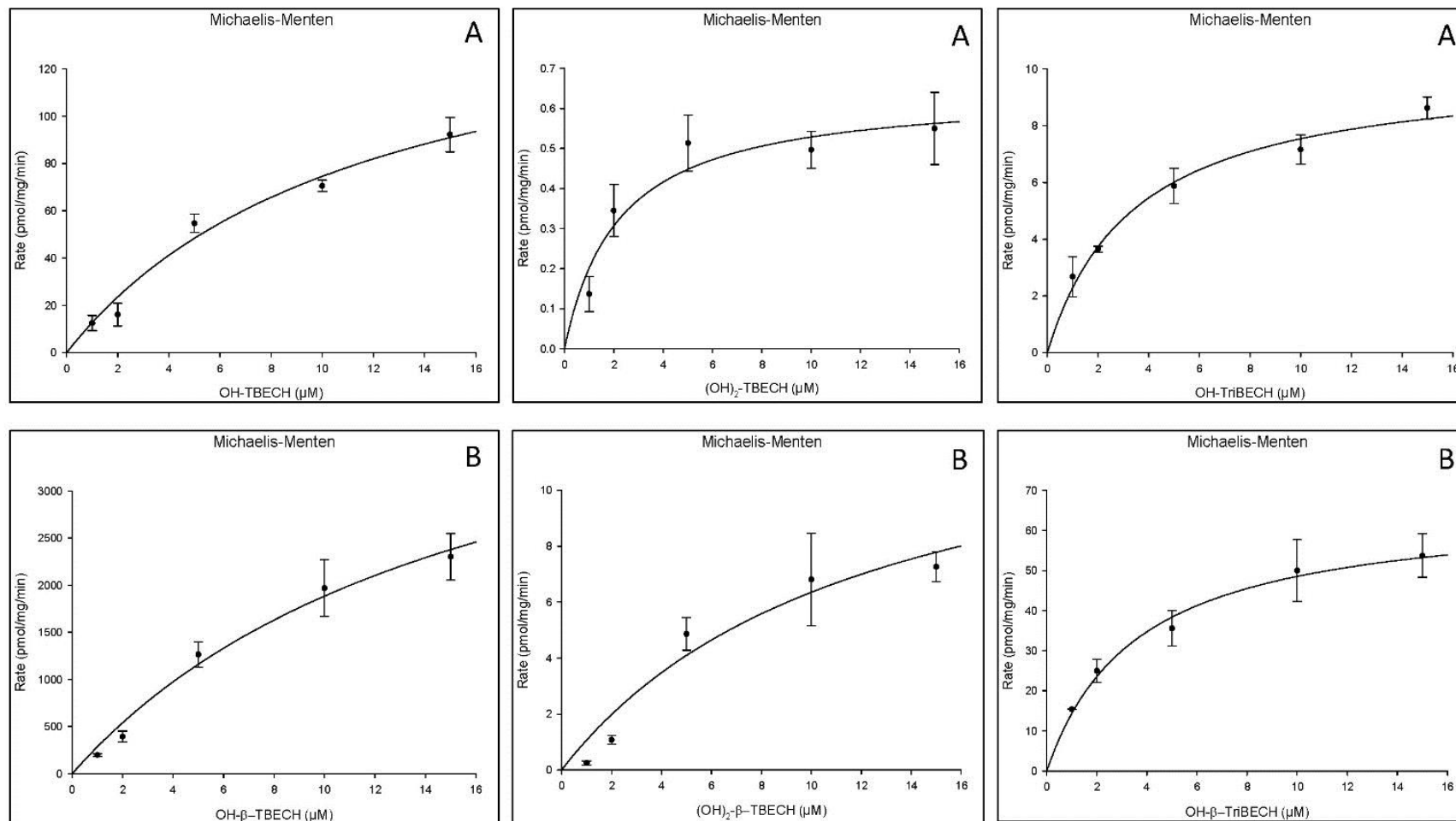
Table 5.2: Kinetic parameters derived from non-linear regression (Michaelis-Menten model) of the formation of metabolites resulting from incubation of the TBECH mixture and β -TBECH with human liver microsomes

Metabolite	K_m (μM) \pm SD	V_{max} (pmol/min/mg protein) \pm SD	CL_{int} ($\mu\text{L}/\text{min}/\text{mg}$ protein)
Technical TBECH			
OH-TBECH	11.78 \pm 4	162.5 \pm 29.6	13.8
(OH) ₂ -TBECH	2.2 \pm 1	0.64 \pm 0.08	0.3
OH-TriBECH	3.4 \pm 0.82	10.1 \pm 0.8	3
β -TBECH			
OH- β -TBECH	16.5 \pm 7.1	4991.7 \pm 1339.8	302.5
(OH) ₂ - β -TBECH	12.3 \pm 7.5	14.1 \pm 4.9	1.1
OH- β -TriBECH	3.6 \pm 1.1	66.1 \pm 7.3	18.4

The model parameters derived from non-linear regression provided useful insights into the metabolic fate of TBECH in humans (Table 5.2). Apparent V_{\max} values (maximum metabolic rate) for the formation of monohydroxy-TBECH, dihydroxy TBECH and monohydroxy-TriBECH were 162.5, 0.64 and 10.1 pmol/min/mg protein, respectively (Table 5.2). This indicates monohydroxy TBECH is the major metabolite formed *in vitro* by human liver microsomes. The only available information on toxicokinetics of this flame retardant suggested rapid *in vivo* metabolism of β -TBECH in brown trout. Depuration of the β -isomer obeyed first order kinetics with half-lives of 22.5 ± 10.4 (low dose), 13.5 ± 5.9 (medium dose) and 13.8 ± 2.2 (high dose) days (Gemmill et al., 2011). In the present study, the observed *in vitro* metabolic clearance rate for β -TBECH was significantly higher ($P < 0.05$) than that of the TBECH mixture.

Maximum metabolic formation rates of OH- β -TBECH, (OH)₂- β -TBECH and (OH)- β -TriBECH were 4991.7, 14.1 and 66.1 pmol/min/mg protein, respectively (Table 5.2); equivalent to 31, 22 and 6.5 times the corresponding metabolite formation rate resulting from exposure to the technical TBECH mixture. There are several plausible reasons for this observation including: (a) slower metabolism of the α -TBECH in the technical mixture and (b) alteration of the stereoselective enzymatic metabolism process by the presence of a larger number of stereoisomers, or even other chemicals/impurities in the TBECH mixture. Nevertheless, β -TBECH was metabolized by *in vitro* HLM at a faster rate than the TBECH mixture. Given the simultaneous exposure of hepatic cells to a large number of xenobiotics under real-life conditions, the *in vivo* metabolic and clearance rates of TBECH might be even slower than this controlled *in vitro exposure* experiment to a single compound.

Figure 5.7: Kinetic analysis of TBECH mixture (A) and β -TBECH (B) metabolite formation rate by human liver microsomes using the Michaelis-Menten model.



As the rates of OH-TBECH, (OH)₂-TBECH and OH-TriBECH formation were best described by the Michaelis Menten model, we used the corresponding equations in section 2.4.3 to estimate the intrinsic *in vitro* hepatic clearance of TBECH and β-TBECH as following:

$$CL_{int-organ} = CL_{int} \times p \times w$$

Where $CL_{int-organ}$ is the intrinsic *in vitro* clearance of a xenobiotic by an organ on kilogram human body weight, p is the amount of protein per gram of an organ and w is the average weight of that organ per kilogram body weight. For human liver microsomes, $p = 52.5$ mg protein/g liver and $w = 25.7$ g liver/kg b.w (Manevski et al., 2014).

The hepatic blood flow per kilogram body weight (kg b.w) $Q_h = 20.7$ ml/min/kg. bw (Manevski et al., 2014) was taken into account for extrapolation of *in vitro* clearance to *in vivo* clearance (CL_h) as follows:

$$CL_{organ} = \frac{Q_h \times CL_{int-organ}}{CL_{int-organ} + Q_h}$$

The intrinsic *in vitro* hepatic clearance (CL_{int}) of the TBECH mixture due to the formation of OH-TBECH, (OH)₂-TBECH and OH-TriBECH were estimated as 13.8, 0.3 and 3 μL/min/mg protein, respectively. By comparison, those of β-TBECH were 302.5, 1.1 and 18.4 μL/min/mg protein, respectively. The total $CL_{int-liver}$ from metabolic formation of all three major metabolites was then calculated: 23 mL/min/kg body weight (b.w) for the TBECH mixture and 434.45 mL/min/kg b.w for β-TBECH.

Despite the lack of authentic standards for TBECH metabolites, leading to the semi-quantitative nature of these measurements, the calculated hepatic clearance rates clearly show that β-TBECH was biotransformed at a much faster rate than the TBECH mixture. Despite reservations on the accuracy of direct extrapolation from *in vitro* to *in vivo* clearance due to simultaneous exposure to a large number of chemicals *in vivo*, we applied Equation 9 (section 2.4.3) to shed some light on the *in vivo* hepatic clearance of TBECH in humans. Our model calculations revealed an *in vivo* hepatic clearance (CL_h) of 13.5 mL/min/kg b.w for the TBECH mixture, while the rapid hepatic clearance of β-TBECH was dependent on the hepatic blood circulation (Q_h) (i.e. flow limited).

5.6. Conclusions

To our knowledge, this is the first study of TBECH metabolism by human liver microsomes. Our *results* demonstrated that TBECH was metabolized by human liver microsomes forming

a complex mixture of metabolites via cytochrome P450 enzyme-catalyzed hydroxylation and debromination. This is the first time that a monohydroxylated debrominated metabolite of TBECH has been detected *in vitro*. The other detected metabolites were OH-TBECH, (OH)₂-TBECH, (OH)₂-TriBECH and DBCBA. substrate concentration-dependent assays showed OH-TBECH to be the major primary metabolite. The differences in TBECH metabolite profiles resulting from incubation with HLM (this study) and RLM (Chu et al., 2012) underscore interspecies variation in xenobiotic metabolism. In general, higher levels of all metabolites were observed in our HLM experiments than reported previously using RLM. The metabolic rates of OH-TBECH, (OH)₂-TBECH and OH-TriBECH were found to best fit to the Michaelis-Menten model by non-linear regression analysis. Separate pure β -TBECH microsomal assays also demonstrated that β -TBECH was metabolized much faster than the technical TBECH mixture. However, authentic standards of α -TBECH and the metabolites are needed to elucidate more precise pharmacokinetic parameters, as well as better understanding of isomer-specific metabolism.

Chapter 6

EH-TBB and Firemaster 550 metabolism by Human Skin S9 Fractions

6.1. Synopsis

EH-TBB and a mixture of EH-TBB, BEH-TEBP and TPhP (prepared in a ratio similar to that in the FireMaster 550 commercial mixture – FM550) were exposed to human skin S9 fractions to evaluate their extra-hepatic *in vitro* metabolism for the first time. After 60 mins of incubation, one metabolite of EH-TBB and one metabolite of TPhP were identified. The metabolic profile of EH-TBB and TPhP indicated extra-hepatic biotransformation of these chemicals was catalyzed by esterases rather than cytochrome P450 enzymes. The metabolite formation rate of EH-TBB both as an individual standard and as a component of the FM550 mixture followed the Michaelis Menten model. *In vitro* – *in vivo* organ clearance extrapolation implied that metabolism of EH-TBB by human skin is marginal in comparison with that in human liver. However, further studies are required to understand the importance of metabolism by skin in the context of human dermal exposure to organic pollutants.

6.2. Introduction

2-ethylhexyl-2,3,4,5-tetrabromobenzoate (EH-TBB or TBB) is an additive flame retardant produced by Chemtura Chemical Corporation. It is available in 2 commercial mixtures: Firemaster 550 and Firemaster BZ-54. In Firemaster 550 (FM550) it was mixed with bis(2-ethylhexyl) tetrabromophthalate (BEH-TEBP or TBPH), triphenyl phosphate (TPhP) and assorted isopropyl triphenylphosphate (ITP) isomers in the ratio: 14 % BEH-TEBP, 36 % EH-TBB, 18 % TPhP and 32% ITPs by weight (Belcher et al., 2014). As additive FRs, EH-TBB and other components of FM550 may leach out from treated consumer goods and contaminate the environment. They have been detected globally in many environmental matrices including indoor dust (Carignan et al., 2013; Sjödin et al., 2001; Stapleton et al., 2009), indoor air (Cequier et al., 2014; Takeuchi et al., 2014; Tao et al., 2016), outdoor air (Ma et al., 2012), chicken eggs (Zheng et al., 2016), aquatic biota (Strid et al., 2013) and foodstuffs (Xu et al., 2015).

Similar to other NBFRs (as discussed in section 1.1.3), their environmental occurrence is expected to be mainly in indoor dust. Residential dust in the UK contained median concentrations of EH-TBB and BEH-TEBP at 5.8 and 320 ng/g, respectively (Al-Omran and Harrad, 2016). In the U.S, house dust samples from California collected in 2011

showed higher levels of FM550 components than those collected in 2006. Specifically, concentration ranges of EH-TBB, BEH-TEBP and TPhP in 2011 were 45-5900, <2-3800 and 790-36000 ng/g, respectively while those in 2006 were 4-740, 36-1900 and 580-14000 ng/g, respectively (Dodson et al., 2012). Extremely high concentrations of EH-TBB and BEH-TEBP were reported in dust from an American gymnasium ranging from 20.8 to 85.6 µg/g for EH-TBB and 17.3 to 44.9 µg/g for BEH-TEBP (Carignan et al., 2013).

This is of concern due to the potential toxicity of FM550 components to humans and wildlife. Both EH-TBB and BEH-TEBP expressed *in vitro* antiestrogenic and antiandrogenic effects in the yeast estrogen screen and yeast androgen screen assays (reflected in inhibition of β-galactosidase production by the assays), as well as increased oestrogen production in the human H295R steroidogenesis assays (Saunders et al., 2013). By use of primary porcine testicular cells, Mankidy et al., 2014 also observed effects of EH-TBB and BEH-TEBP on steroidogenesis, however by different mechanisms; EH-TBB induced the production of cortisol and aldosterone while BEH-TEBP promoted sex hormones synthesis. FM550-administered rats showed many negative health effects e.g. advanced female puberty, weight gain, altered exploratory behaviours, hepatic carboxylesterases activity, etc (Patisaul et al., 2013). FM550 (mainly driven by the TPhP component) was found to bind to human peroxisome proliferator-activated receptor γ (PPARγ1) and subsequently induced PPARγ1 transcription activity (Pillai et al., 2014). The same study also reported adipogenesis induction in primary mouse bone marrow cultures by FM550 and TPhP.

It is thought that dust ingestion is a major exposure pathway of humans to EH-TBB, BEH-TBP and TPhP (Christia et al., 2018; Tao et al., 2017). However, recently Abdallah et al., 2016 reported the importance of dermal absorption as a pathway of human exposure to chlorinated organophosphate flame retardants which might even exceed exposure via dust ingestion or inhalation exposure. We therefore hypothesised that dermal exposure to FM550 components is also significant. Consequently, understanding of the skin metabolism pathways, rates and products of EH-TBB and FM550 is important for risk assessment of human exposure to these chemicals. In this study, we aim to investigate the extra-hepatic biotransformation of EH-TBB and FM550 *in vitro* by human skin S9 fractions for the first time.

6.3. Experiments

6.3.1. Chemicals and Standards

All solvents and reagents used in this study were purchased from Fisher Scientific (Loughborough, UK) and were of HPLC grade or higher. 2-Ethylhexyl-2,3,4,5-tetrabromobenzoate (EH-TBB) and bis(2-ethylhexyl) tetrabromophthalate (BEH-TEBP) for dosing solutions was obtained as neat solutions from Accustandard, Inc. (New Haven, CT, USA). High purity standards of EH-TBB, BEH-TEBP, triphenyl phosphate (TPhP), 2-ethylhexyl-d₁₇-2,3,4,5-tetrabromo[¹³C₆]benzoate (¹³C-EH-TBB), bis(2-ethylhexyl-d₁₇)-tetrabromo[¹³C₆]phthalate (¹³C-BEH-TEBP), tetrabromobenzoic acid (TBBA), ¹³C-labelled tetrabromobenzoic acid (¹³C-TBBA) and α -1,2,5,6,9,10-hexabromo[¹³C₁₂-cyclododecane] (¹³C- α -HBCDD) were purchased from Wellington Laboratories (Guelph, ON, Canada). Triphenyl phosphate-d₁₅ (TPhP-d₁₅) was purchased from Sigma Aldrich (Dorset, UK). RapidStart NADPH regenerating system was purchased from XenoTech (Kansas, KS, USA), William's E medium was obtained from Thermo Fisher Scientific (Paisley, UK) and human skin S9 fractions (HS-S9) was purchased from Biopredic International (Saint Grégoire, France). The HS-S9 was prepared from the skin of a 45 years old Caucasian female (the specific skin location, area or thickness was not provided). Liquid nitrogen was used to deliver and store HS-S9.

Individual EH-TBB dosing solution was prepared by dissolving EH-TBB in dimethyl sulfoxide (DMSO). The FireMaster 550 (FM550)-equivalent mixture was prepared by dissolving EH-TBB, BEH-TEBP and TPhP in the ratio 53:20.5:26.5 by weight in DMSO, which was similar to that reported for the technical FM550 mixture (Belcher et al., 2014).

FM550 solutions were prepared such that each dosing level contained similar concentrations of EH-TBB as that in the pure EH-TBB dosing solutions.

6.3.2. *In vitro* Incubation Experiments

Pre-incubations were performed at different HS-S9 concentrations and different times. After optimisation of the reaction parameters, the following general exposure protocol was applied: 0.11 mg of HS-S9, William's E medium and 10 μ L of EH-TBB/FM550 dosing solutions (final concentration 10 μ M of EH-TBB) were pre-incubated for 5

minutes at 37 °C. NADPH regenerating system (final concentration: 2.0 mM nicotinamide adenine dinucleotide phosphate, 10.0 mM glucose-6-phosphate and 2 units/mL glucose-6-phosphate dehydrogenase) was added to make a final volume of 1 mL. The samples were then incubated at 37 °C, 5 % CO₂ and 98 % relative humidity for 60 min. At the end of the incubation, 1 mL of ice-cold ethyl acetate was added to stop the reaction prior to sample extraction. Ethyl acetate was chosen as the quenching reagent instead of methanol to minimise false positive metabolite identification for EH-TBB (see section 4.5.2). In all incubation experiments, a solvent blank which contained only William's E medium was performed and analysed alongside the sample batch.

6.3.3. Sample extraction

Incubated EH-TBB samples were spiked with 20 ng each of ¹³C-EH-TBB and ¹³C-TBBA while FM550 samples were spiked with 20 ng each of ¹³C-EH-TBB, ¹³C-TBBA, ¹³C-BEH-TEBP and TPhP-D₁₅ as internal standards. Briefly, samples were mixed with 3 mL of ethyl acetate by vortexing for 30 s, followed by ultrasonication for 5 min and centrifuged at 4000 g for 5 min. The organic layer was collected and the extraction procedure was repeated twice. Ethyl acetate is a very good solvent for esters (i.e. the chemicals studied here) as well as relatively polar organic compounds (i.e. potential metabolites of EH-TBB, BEH-TEBP and TPhP) and therefore was chosen as extraction solvent. The combined extracts were evaporated to dryness under a gentle stream of nitrogen then reconstituted in 100 µL of methanol containing 20 ng of ¹³C- α -HBCDD as a syringe standard for QA/QC purposes.

6.3.4. Instrumental analysis

The instrumental analysis method was similar to that deployed for NBFRs determination and the screening method described in section 3.2.2 with slightly modified MS parameters.

The optimised MS parameters for the analysis of EH-TBB, FM550 and their potential metabolites are shown in Table 6.1

Table 6.1: Optimized Orbitrap parameters for the analysis of EH-TBB, FM550 and their potential metabolites by UPLC-Orbitrap MS (LC flow rate 400 μ L/min)

Parameters	APCI	ESI
Polarity	Neg	Pos/Neg switching
Sheath gas flow rate	25	25
Aux gas flow rate	5	5
Sweep gas flow rate	0	0
Discharge current (μ A)	30	
Spray voltage (kV)		4.5
Capillary temp. ($^{\circ}$ C)	275	320
S-lens RF level	50	50
Aux gas heater temp ($^{\circ}$ C)	350	350
Resolution (FWHM)	17500	17500
AGC target (ions)	1E6	1E6
Maximum ion injection time (ms)	100	100
Scan mode	Full scan	Full scan
Scan range (m/z)	70-800	70-800

MS data from both ionisation modes was acquired for each sample. Negative APCI was used for determination of EH-TBB, 13 C-EH-TBB, BEH-TEBP, 13 C-BEH-TEBP and screening for potential metabolites. The more universal, softer electrospray ionisation (ESI) mode was used in positive/negative alternative switching mode for screening and identification of the produced metabolites, as well as determination of TPhP and TPhP-d₁₅. Table 6.2 shows accurate ion masses for monitoring parent compounds and internal standards.

Table 6.2: Monitoring ions for parent compounds and internal standards in different ionisation modes of the UPLC-HRAM Orbitrap/MS

Chemical	Mode	Ion Type	Accurate Mass (amu)
EH-TBB	(-)APCI	[M-Br+O] ⁻	484.87856
13 C-EH-TBB	(-)APCI	[M-Br+O] ⁻	508.00539

BEH-TEBP	(-)APCI	[M-Br+O] ⁻	640.99359
¹³ C-BEH-TEBP	(-)APCI	[M-Br+O] ⁻	681.22768
¹³ C- α -HBCDD	(-)APCI, (-)ESI	[M-H] ⁻	652.67717
TPhP	(+)ESI	[M+H] ⁺	327.07807
TPhP-d ₁₅	(+)ESI	[M+H] ⁺	364.15417

Compound Discoverer 2.0 software (Thermo Fisher Scientific, Bremen, Germany) was used to detect potential metabolites and elucidate their chemical formulae, while quantification of target compounds was performed using Quan Browser 3.0 (Thermo Fisher Scientific, Bremen, Germany).

6.4. QA/QC

Metabolic activity of phases I enzymes including NADPH-cytochrome C reductase, carboxyl esterase and FMO3 were measured by the provider prior to the HS-S9 batch release. Results provided by Biopredic International showed normal activities of all enzymes after HS-S9 thawing.

Quality assurance samples where the William's E medium was spiked with EH-TBB and FM550 at all dosing levels were analyzed, with recoveries of dosing chemicals falling between 80 to 115 % of the theoretical dosing concentrations. In incubation experiments, internal standard recoveries were within 50-115 %.

No parent compounds or metabolites were found in instrument and solvent blanks with the exception of TPhP at negligible levels (< 1.05% of the lowest dosing level). Therefore, no blank correction was needed. Additionally, no metabolites were found in the non-enzymatic and heat-inactivated blanks.

6.5. Results

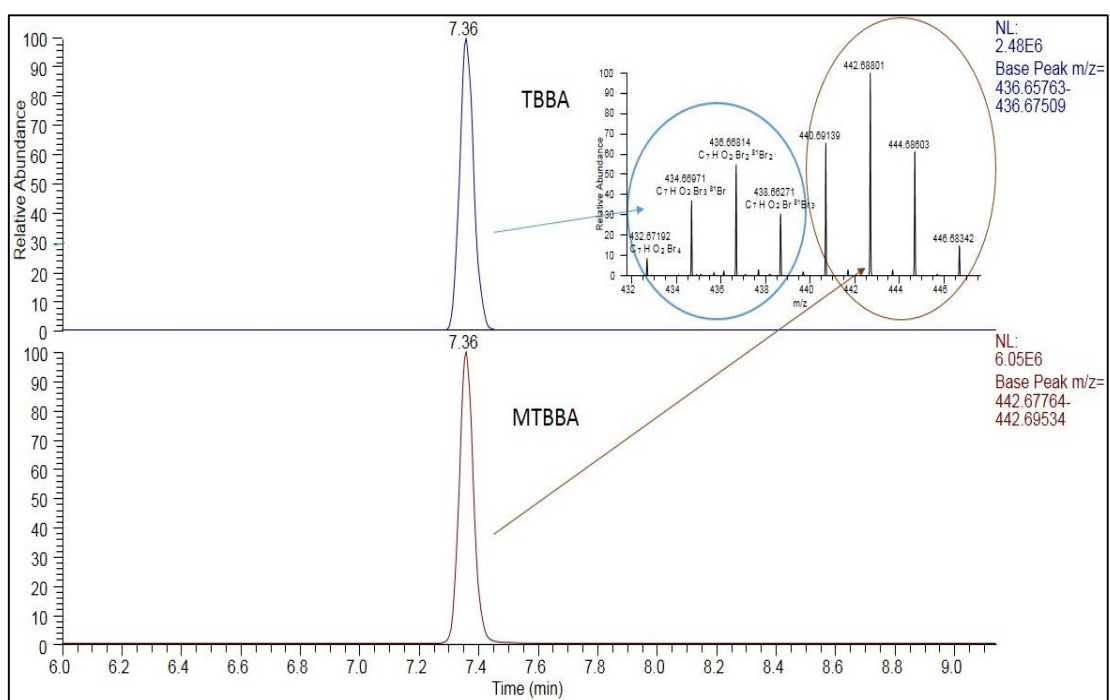
6.5.1. Metabolic profiles of EH-TBB and FM550

Due to the structure of EH-TBB, BEH-TEBP and TPhP, we hypothesised that their metabolism by HS-S9 would be catalysed by carboxyesterases and/or cytochrome P450. Full scan mode with either negative APCI or ion switching positive/negative ESI were

used to screen for EH-TBB and FM550 metabolites. No potential metabolites were found in (+)ESI or (-)APCI mode.

For EH-TBB samples, in (-)ESI mode there was one potential metabolite with the ion mass of 436.66814 and the proposed ion formula $C_7HBr_4O_2$. By comparing with the authentic standard, this was confirmed as the $[M-H]^-$ molecular ion for TBBA (Figure 6.1). This is in agreement with a previous study, which reported TBBA as the only *in vitro* metabolite of EH-TBB by human and rat liver microsomes (Roberts et al., 2012).

Figure 6.1: TBBA and MTBBA in a Human S9 Skin fraction (HS-S9) sample exposed to 10 μ M of EH-TBB



Similar to HS-S9 exposure to pure EH-TBB, TBBA was also detected as the sole metabolite of EH-TBB when HS-S9 was exposed to FM550 mixture.

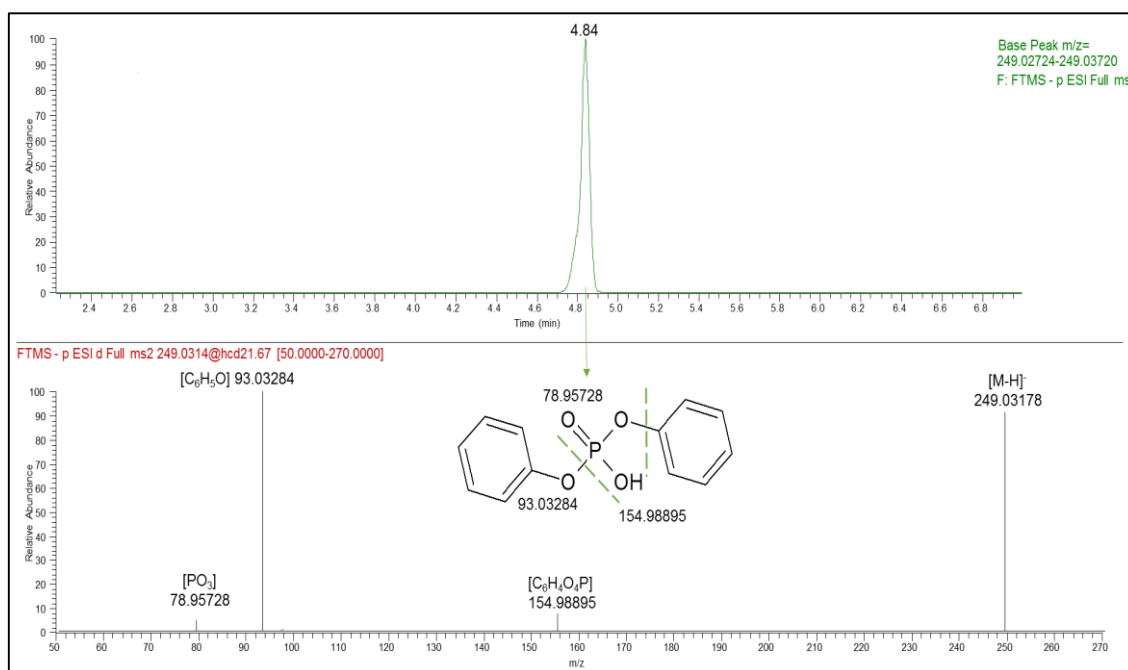
In addition, another potential metabolite with the ion mass of 249.03204 was detected in (-)ESI mode. The proposed chemical structure for this ion was $[C_{12}H_{10}O_4P]^-$. In order to elucidate the chemical structure of this compound, a MS/MS experiment was carried out in (-)ESI-SIM-MS² mode. The ion source parameters were the same as those described in section 6.4.3 for (-)ESI mode while MS parameters are described in Table 6.3.

Table 6.3: SIM-MS² parameters for ion 249.03204 by (-)ESI-UPLC-Orbitrap HRMS

MS Parameters	Value
Scan mode	SIM-MS ²
SIM	
Inclusion ion (m/z)	249.03204
Isolation window (m/z)	0.4
Resolution (FWHM)	17500
AGC target (ions)	5E4
Maximum ion injection time (ms)	100
MS ²	
Resolution (FWHM)	17500
AGC target (ions)	5E4
Maximum ion injection time (ms)	100
Stepped Normalised Collision Energy	15, 20, 30

A combination of low, medium and high collision energies were applied stepwise to achieve a diverse range of fragmentation ions. The results from this experiment are shown in Figure 6.2

Figure 6.2: (-)ESI-MS/MS spectrum of ion 249.03204 by UPLC-Orbitrap HRMS



The ion 249.03204 was fragmented mainly into three ions: 154.98895, 93.03284 and 78.95728. The proposed chemical formula for these fragments were: $[C_6H_4O_4P]^-$, $[C_6H_5O]^-$ and $[PO_3]^-$, respectively. Based on the proposed parent ion formula and the MS/MS fragment data, this metabolite is identified as diphenyl phosphate (DPhP), which is a primary metabolite of TPhP. This was further confirmed via comparison and augmentation with an authentic standard of DPhP.

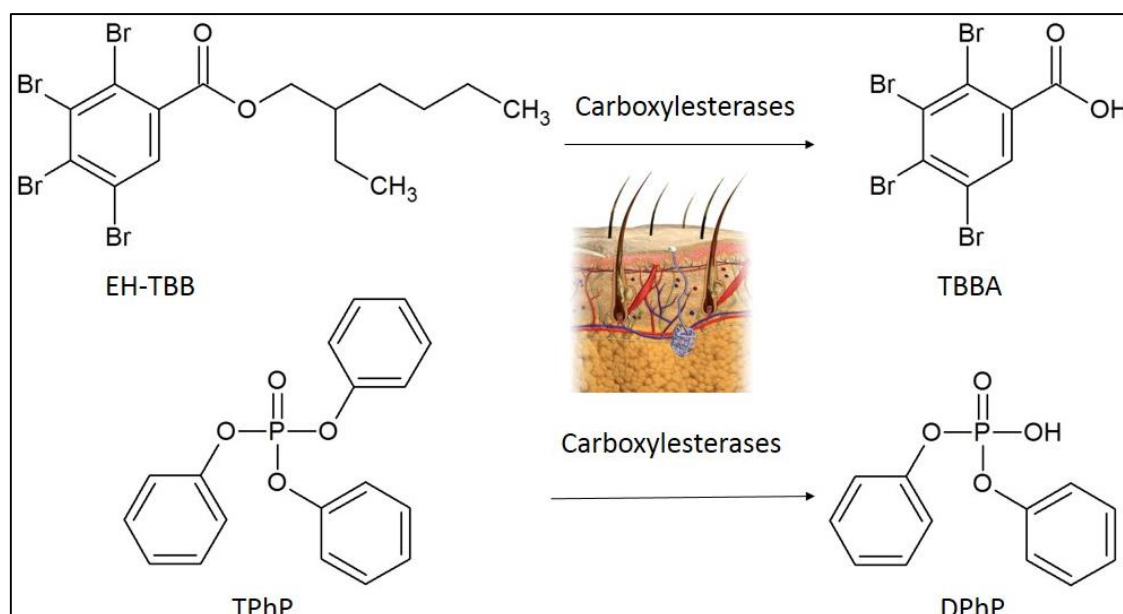
It was reported that *in vitro* metabolism of TPhP by human liver microsomes or chicken embryo hepatocytes formed DPhP, hydroxylated TPhP (OH-TPhP) and dihydroxylated TPhP ((OH)₂-TPhP) (Su et al., 2014; Van den Eede et al., 2013). *In vivo* metabolism of TPhP in fish produced DPhP, OH-TPhP, (OH)₂-TPhP and monophenyl phosphate (MPhP) among which DPhP was the major metabolite (Wang et al., 2016). However in this study, we only detected DPhP as the sole metabolite of TPhP by HS-S9. No potential metabolites of BEH-TEBP were identified in HS-S9 exposed to FM550 mixture which was in line with reported HLM and RLM *in vitro* studies (Roberts et al., 2012).

By comparison of the dermal (this study) and hepatic metabolic profiles (Roberts et al., 2012; Van den Eede et al., 2013) of EH-TBB and TPhP, it was obvious that the oxidative metabolites were not observed in the human skin S9 fractions. The metabolic profile of dermal S9 fractions show that both CYP450 and carboxylesterases are active, albeit at much lower levels than in the liver cells. This is in agreement with previous studies on the metabolic activity of human skin cells in comparison with liver cells. The functional activity of a CYP450 enzyme on the substrate benzyl-O-methyl-cyanocoumarin was reported to be twice as much in human liver than that in the skin (Smith et al., 2018). Similarly, hydrolysis rate of p-nitrophenyl acetate by carboxylesterase was 4 times slower in human skin than that in human liver (Fu et al., 2016).

In order to test our hypothesis, we performed the NADPH independent experiment. Incubations of EH-TBB and FM550 without NADPH cofactor were carried out with the same conditions as described in section 6.3.2. The absence of NADPH did not result in significant changes in the formation rates of TBBA, DPhP concentrations or depletion rates of the parent compounds ($p > 0.05$). Our results show differences from hepatic metabolism as dermal carboxylesterases seem to be more involved in the metabolism of the target FRs than CYP450. Therefore it is likely that not CYP enzymes but NADP-

independent enzymes (e.g. carboxylesterases) catalysed EH-TBB and TPhP metabolism in HS-S9 (Figure 6.3). While, this does not eliminate the possibility of oxidative metabolite formation upon dermal contact under real-life situations (i.e.e upon exposure to larger doses) but if formed, they are likely to be at lower rates and concentrations than de-esterified metabolites. Indeed, proteomic profiling of xenobiotic metabolism enzymes revealed that the levels of CYP450 enzymes in human skin were at least 300 folds lower than that in human liver (van Eijl et al., 2012). In contrast, the relative level of carboxylesterase 1 (CES1) in human skin and liver was 0.62 with no significant level difference ($p=0.21$) (van Eijl et al., 2012). Such low level of CYP450 enzymes and similar level of CES1 in the skin in comparison with liver might explain why no oxidative metabolites were observed in our study.

Figure 6.3: Proposed metabolic pathways of EH-TBB and TPhP by human skin S9 fraction



6.5.2. Metabolic kinetics of EH-TBB and FM 550 metabolism by HS-S9

As discussed in chapter 5, the metabolic rates of TBECH were largely dependent on whether the human liver microsomes were challenged with pure β -TBECH isomer or technical TBECH mixture (containing both α - and β -TBECH as well as other potential chemical residues). Therefore, following metabolite identification, a series of assays with different concentrations of EH-TBB and FM550 (Table 6.4) were performed. With this experiment, we aimed to investigate whether the metabolic rate will be different upon

challenging the HS-S9 with a multi-component mixture representing FM550 formula (i.e. mimicking real-life situation) than upon exposure to a single compound (EH-TBB) and what is the effect of the multi-components (e.g. synergistic or antagonistic) on the kinetics of dermal metabolism of these compounds. The concentrations of TBBA and DPhP were quantified using an isotope dilution series method with ^{13}C -TBBA as internal standard.

Table 6.4: Exposure levels of human skin S9 fraction to EH-TBB and FM550 mixture

Level	EH-TBB (μM)	FM550		
		EH-TBB (μM)	BEH-TEBP (μM)	TPhP(μM)
1	1	1	0.3	0.84
2	2	2	0.6	1.68
3	5	5	1.5	4.2
4	10	10	3	8.4
5	15	15	4.5	12.6

The results from enzymatic kinetic modelling in Sigmaplot indicated that the formation of TBBA in both pure EH-TBB and FM550 mixture experiments was best described by Michaelis Menten model (Figure 6.4).

Figure 6.4: Kinetic analysis of TBBA formation of EH-TBB (A) and FM550 mixture (B) by human skin S9 fraction using the Michaelis-Menten model.

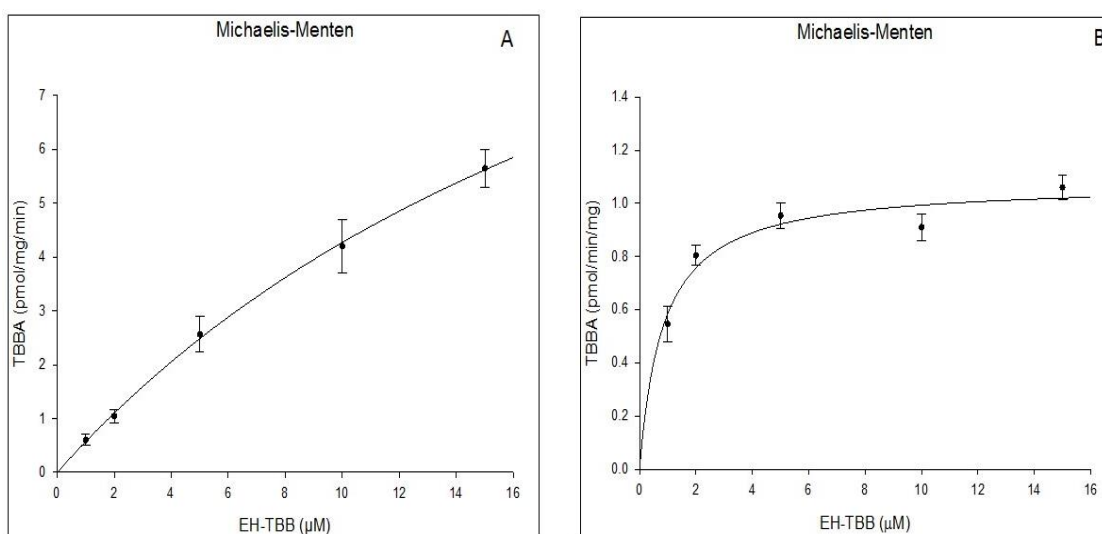


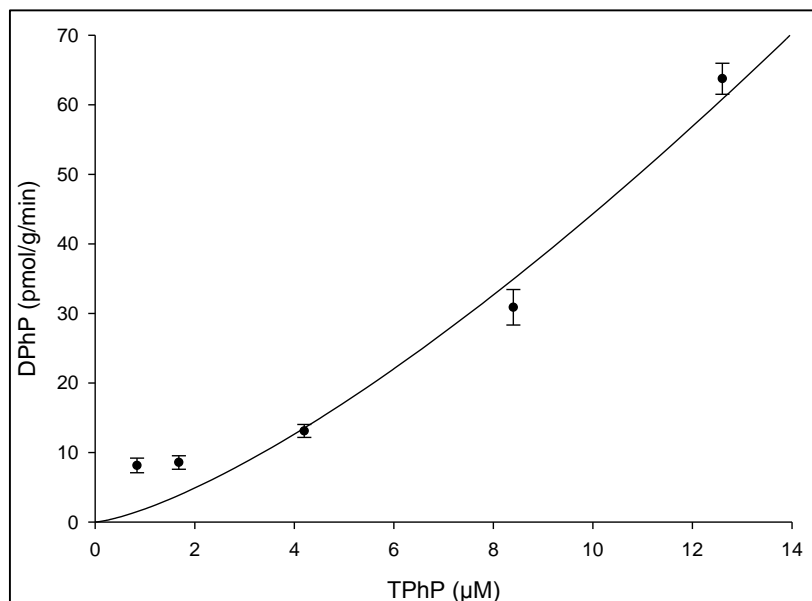
Table 6.5: Kinetic parameters derived from non-linear regression (Michaelis-Menten model) of the formation of TBBA resulting from incubation of HS-S9 with pure EH-TBB and FM550 mixture in this study and comparison with EH-TBB incubation with HLM (Roberts et al. 2012)

Substrate	Model	K_m (μM) \pm SD	V_{\max} (pmol/min/mg protein) \pm SD	Reference
EH-TBB	HS-S9	25.7 ± 12.2	15.2 ± 5	This study
FM550	HS-S9	0.84 ± 0.19	1.08 ± 0.05	This study
EH-TBB	HLM	11.1 ± 3.9	644 ± 144	Roberts et al., 2012

The metabolic parameters derived from the Michaelis-Menten model are presented in Table 6.5. Estimated maximum metabolic rate V_{\max} for the formation of TBBA by HS-S9 exposed to FM550 were significantly lower ($p < 0.05$) than to individual EH-TBB (1.08 and 15.2 pmol/min/mg protein, respectively). However in both cases, V_{\max} was still much smaller than what observed previously in HLM (644 pmol/min/mg protein) (Roberts et al., 2012). It is also important to note that the Michaelis constant K_m for FM550 is much lower than K_m for EH-TBB metabolism by HS-S9 (Table 6.5). Such significant decreases in both K_m and V_{\max} suggested that the formation of TBBA from FM550 by HS-S9 has potentially been inhibited by competitive inhibitor(s). Such inhibitors could be BEH-TEBP, TPhP or impurities in the FM550 dosing solution.

The formation rate of DPhP, on the other hand, did not fit into any assessed enzyme kinetic model (Michaelis-Menten, Hill or substrate-inhibition). Indeed, it did not show any signs of reaching a plateau to indicate a steady state was reached (Figure 6.5). Another series of bioassays with higher doses of FM550 were carried out at equivalent TPhP concentrations of 16.8, 25 and 33.6 μM . Close to linearity increment of DPhP formation rate was still observed (data not shown). Such observation is in agreement with previous study on kinetic profile of TPhP biotransformation in human serum where formation rate of DPhP did not reach a plateau even up to 100 μM of TPhP was used (Van den Eede et al., 2016). This precluded the estimation of metabolic kinetic parameters for TPhP under the applied experimental conditions.

Figure 6.5: Kinetic analysis of DPhP formation from FM550 mixture by human skin S9 fractions



6.5.3. *In vitro* – *in vivo* extrapolation for clearance of EH-TBB

As the formation rates of TBBA were best described by the Michaelis Menten model, the equations in section 2.4.3 were employed to estimate *in vivo* extra-hepatic clearance and compare with estimated *in vivo* hepatic clearance of EH-TBB (data for hepatic clearance estimation were obtained from Roberts et al., 2012). Metabolic clearance was estimated for an adult with average body weight (70 kg). The following parameters were applied: 24.84 mg protein/g skin for HS-S9 (Jewell et al., 2007, calculated as total of microsomes and cytosol), 37 g skin/kg b.w, 52.5 mg protein/g liver for HLM, 25.7 g liver/kg b.w, $Q_h = 20.7$ mL/min/kg b.w and $Q_{skin} = 4.37$ mL/min/kg b.w (Manevski et al., 2014). The results for estimated *in vitro* and *in vivo* clearance of EH-TBB are shown in Table 6.6.

Table 6.6: Estimated *in vitro* and *in vivo* clearance of EH-TBB by human skin (this study) and human liver (Roberts et al., 2012)

Chemical	Organ	$CL_{int-organ}$ (<i>in vitro</i> , mL/min/kg b.w)	CL_{organ} (<i>in vivo</i> , mL/min/kg b.w)
EH-TBB	Skin	0.54	0.48
EH-TBB in FM550	Skin	1.18	0.92
EH-TBB	Liver	78.3	16.4

Our model calculations estimated *in vivo* extra-hepatic clearance of individual EH-TBB and EH-TBB in FM-550 by human skin to be 0.48 and 0.92 mL/min/kg b.w, respectively. It was much smaller than the skin blood flow (4.37 mL/min/kg b.w), suggesting EH-TBB was not efficiently cleared by dermal metabolism. Indeed, the extraction ratios (defined as the ratio between the *in vivo* clearance of a xenobiotic to the blood flow for a specific organ) of EH-TBB by human skin were only 11 % and 21 % for individual and mixture exposures respectively. In contrast, human liver showed excellent EH-TBB extraction ratio up to 80 % with *in vivo* hepatic clearance of 16.4 mL/min/kg b.w. These results suggested that dermal metabolism contributed marginally to the clearance of internal EH-TBB body burden in comparison with liver metabolism.

6.5.4. Implications for human exposure

Even though the outermost layer of skin (stratum corneum) serves as a barrier to prevent unwanted chemicals from entering our body, recent studies have confirmed the dermal uptake of many lipophilic pollutants such as HBCDDs, TBBPA, chlorinated organophosphate flame retardants or novel brominated flame retardants via contact with skin (Abdallah et al., 2015; Abdallah et al., 2016; Frederiksen et al., 2016; Knudsen et al., 2017). Frederiksen et al. reported roughly 10 % dermal absorption and 0.1 %-0.2 % penetration of several FRs including EH-TBB following a single dose (of several hundred nanograms) onto *ex vivo* human skin for 72 h (Frederiksen et al., 2016). Higher skin absorption at 20 % with 0.2 % penetration into receptor fluid (mimicking blood flow) of administered ¹⁴C-labelled EH-TBB onto *in vitro* human skin after 24 h were observed (Knudsen et al., 2017). Nevertheless, it is proven that EH-TBB as well as other organic contaminants could pass by the skin barrier and be “trapped” in the skin without reaching the blood circulation. In such an event, skin metabolism may play an important role in the clearance of the trapped dose within the skin tissue, yet it may also help create a concentration gradient through the different layers of the skin tissue to facilitate further uptake of the parent flame retardant. Abdallah et al., 2016 highlighted the significance of the dermal pathway of human exposure to dust-bound organophosphate contaminants, which might be even more significant if dermal metabolism is considered. As EH-TBB is found mainly in indoor dust (see section 1.1.3), it is believed dermal uptake via contact with indoor dust is also an important human exposure pathway to this compound.

However, the slow *in vitro* clearance rates in the skin could translate into slow EH-TBB *in vivo* percutaneous metabolism and subsequently results in inefficient EH-TBB elimination from the skin, which explains the reported dermal penetration of 0.2 % of applied EH-TBB unchanged through human skin (Knudsen et al., 2017). Therefore, more studies about dermal exposure and metabolism of emerging contaminants and specifically EH-TBB are recommended.

6.6. Limitations of this study

It is important to note that the skin HS-S9 was prepared from a single donor. There might be a large bias in metabolic activity depending on the skin location, age, race and gender. Additionally, our calculations were based on several assumptions which may introduce uncertainties to the study. Firstly, the unbound fraction of the pollutant to blood proteins was equal to 1, meaning all EH-TBB in the blood was free and available for metabolism. This might cause overestimation of xenobiotics clearance. Secondly, the hematic concentration of a substrate was much smaller than its corresponding K_m . Finally, TBBA was the only metabolite of EH-TBB. While our findings and data in literature support this assumption, it is possible that other metabolites were formed but not detected (e.g. debrominated EH-TBB or debrominated TBBA).

6.7. Conclusions

To our knowledge, this is the first study of EH-TBB and FM550 metabolism by human skin S9 fractions. Our *in vitro* experiments demonstrated that extra-hepatic dermal metabolism occurs for EH-TBB and TPhP, mainly via NADPH-independent carboxylesterases forming TBBA and DPhP, respectively. The rate and efficiency of metabolism of EH-TBB by human skin is much smaller than reported for the human liver. This implies that *in vivo* clearance of EH-TBB is marginal via dermal metabolism in comparison with hepatic metabolism. Additionally, the dermal metabolic rate observed when exposure is to individual chemical components, is altered when exposure occurs via a multi-component mixture of chemicals. Specifically, we observed a higher rate of clearance for EH-TBB alone compared to EH-TBB when applied as a mixture reflecting FM550, which might be partially explained by the very high metabolic rate for TPhP (i.e. competitive substrate inhibition). Finally, the dermal metabolism of EH-TBB and FM550

is likely to have implications for the human dermal exposure to these FRs via contact with contaminated dust or consumer items (e.g. furniture upholstery, toys, etc.) in real-life situations, yet more studies are required to fully understand these implications.

Chapter 7

Summary and Conclusions

7.1. Summary

Novel brominated flame retardants (NBFRs), pharmaceutical and personal care products (PPCPs) are two of the emerging contaminant groups that have been brought to the attention of the public and scientific community recently. NBFRs are a group of brominated organic pollutants widely added to polyurethane foam, textiles, plastics and electronic equipment to increase their fire resistance. Their ubiquity in the environment together with their persistent, bioaccumulative and toxic potential have caused great concern (Feng et al., 2013; Harrad et al., 2008; La Guardia et al., 2012; Saunders et al., 2015a, 2015b; Tao et al., 2017). To date, there are very few data on human exposure to NBFRs and those data are limited to some common NBFRs such as EH-TBB, BEH-TEBP, DBDPE and BTBPE. Additionally, there is a substantial gap in knowledge of NBFRs metabolism in humans. PPCPs on the other hand are designed for human and/or animal use and therefore their biosafety profiles are often available. However, they have recently attracted attention due to their detection in various environmental compartments at relatively high concentrations (Ali et al., 2018; Blair et al., 2013; Fisch et al., 2017; Mirzaei et al., 2018; Thomas and Hilton, 2004). PPCPs consist of hundreds of chemicals and consequently pose a substantial analytical chemistry challenge to study their environmental fate.

Given the above, the main objective of this work was to develop analytical methods using advanced mass spectrometry (ultra performance liquid chromatography couple to Orbitrap high resolution mass spectrometry in particular) for simultaneous determination of a wide range of NBFRs or PPCPs in environmental samples in one run. NBFR metabolites/degradation products screening was also included in the NBFRs method. Secondary objectives were to apply the developed analytical methods to real environmental samples to provide novel insights into the levels, profiles and biotransformation/degradation products of the studied emerging contaminants in the environment and humans.

The main achievements and outcomes of this research are summarised below:

- A high throughput analytical method (PPCPs method) was developed for determination of 29 PPCPs by alternate switching (+)/(-)ESI-UPLC-Orbitrap

HRMS in one run, with possibility to extend the target list upon availability of authentic standards. Excellent method accuracy, precision, repeatability and reproducibility were obtained.

- The PPCPs method was applied to assess the level of these contaminants in effluent and surface water samples collected in Assiut city, Egypt. Our results revealed that multiple PPCPs are ubiquitous in Egyptian water samples. In effluent samples, analgesics, NSAIDs, antidiabetics and antibiotics were found at high concentrations: acetaminophen ranged from 978 to 16,000 ng/L, followed by ibuprofen (812-6,700 ng/L), glyburide (550-4,160 ng/L), metformin (168-5,610 ng/L), trimethoprim (271-2,740 ng/L) and diclofenac sodium (79-3,610 ng/L). The effluent sample collected from a hospital wastewater treatment plant showed extremely high level of acetaminophen, ibuprofen and metformin at 16,000, 6,700 and 5,610 ng/L, respectively which implied more efficient water treatment processes are needed to remove PPCPs at this location. In surface water sample, analgesics, antidiabetics, antibiotics and nicotine showed higher concentrations than other detected PPCPs: acetaminophen was measured at a mean concentration of 495 ng/L, followed by glyburide (394 ng/L), trimethoprim (191 ng/L) and nicotine (190 ng/L).
- An analytical method (NBFRs method), which combined both targeted and untargeted approaches to both determine NBFRs and screen for NBFRs metabolites/degradation products together with brominated contaminants in one run, was developed using (-)APCI-UPLC-Orbitrap HRMS. This method utilized the high mass accuracy of the Orbitrap platform coupled with the power of bioinformatic software (i.e. Compound Discoverer™) to screen for brominated contaminants including NBFRs metabolites/degradation products while the native manufacturer software Xcalibur was used for targeted analysis.
- The NBFRs method was applied to the study of simulated leachate samples derived from mixed waste electrical and electronic equipment, whole LCDs/CRTs and whole fridges/freezers. BDE-47, BDE-99, BDE-183, BDE-209, DBDPE, BTBPE, TBP, TBP-AE, HBCDDs and TBBPA were detected in these samples via our targeted approach. Among the detected BFRs, BDE-209, DBDPE, TBBPA and 2,4,6-TBP were present in almost every sample. PBDEs other than

BDE-209 were occasionally found - mostly in leachate from fridges/freezers - while BTBPE was mainly detected in samples from mixed waste electrical and electronic equipment. Untargeted analysis of the same samples revealed 5 potential degradation products of TBBPA: dibromobisphenol A, tribromobisphenol A, methoxylated TBPPA, methoxylated dibromobisphenol A and chlorinated TriBBPA.

- *In vitro* bioassays were successfully designed and applied to provide new insights into the metabolism of EH-TBB by mouse liver microsomes, TBECH by human liver microsomes and EH-TBB and Firemaster 550 (comprising EH-TBB, BEH-TEBP and TPhP) by human skin S9 fractions. The *in vitro* samples were extracted by a QuEChERS method then analysed by the NBFrs method.
- TBECH metabolism by human liver microsomes was studied for the first time. TBECH was metabolized *in vitro* by HLM via cytochrome P450 enzyme-catalyzed hydroxylation and debromination to produce mono- and di-hydroxylated TBECH, mono- and di-hydroxylated TriBECH as well as an α -oxidation metabolite bromo-(1,2-dibromocyclohexyl)-acetic acid with mono-hydroxylated TBECH the major metabolite. The metabolic rates of OH-TBECH, (OH)₂-TBECH and OH-TriBECH were found to best fit to the Michaelis-Menten model by non-linear regression analysis. Separate pure β -TBECH microsomal assays showed that β -TBECH was metabolized much faster than the technical TBECH mixture possibly due to slower metabolism of the α -TBECH in the technical mixture and/or alteration of the stereoselective enzymatic metabolism process by the presence of a larger number of stereoisomers, or even other chemicals/impurities in the TBECH commercial mixture. The *in vitro* and *in vivo* hepatic clearance of the TBECH mixture and the β -TBECH isomer was also estimated. Our model calculations revealed an *in vivo* hepatic clearance rate of 13.5 mL/min/kg b.w for the TBECH mixture, while the rapid hepatic clearance rate of β -TBECH (20.7 ml/min/kg. bw) was dependent on the hepatic blood circulation.
- EH-TBB was metabolized to TBBA *in vitro* by mouse liver microsomes. It is important to note that methylation of TBBA to produce TBMB can take place when ice-cold methanol is used as stopping agent in the presence of mouse liver

microsomes and NADPH. This may refer to methylation of TBBA as a phase II metabolic reaction *in vivo* via methyl transferase enzymes. However, this cannot be confirmed via our *in vitro* protocol, using only mouse liver microsomes to investigate phase I metabolic reactions.

- Human skin S9 fractions metabolized EH-TBB into TBBA and TPhP to DPhP *in vitro* via carboxylesterase not CYP450. Enzymatic kinetic modelling revealed that the metabolic rate of EH-TBB was significantly inhibited by the presence of other chemicals e.g. BEH-TEBP, TPhP or chemical impurities. The formation rate of TBBA from EH-TBB by HS-S9 was best fitted to the Michaelis-Menten model by non-linear regression analysis. On the other hand, the formation rate of DPhP showed close to linearity increment with increasing TPhP dosing concentration. *In vitro – in vivo* extrapolation suggested that extra-hepatic clearance rates of individual EH-TBB and EH-TBB in FM-550 by human skin were 0.48 and 0.92 mL/min/kg b.w, respectively and were much smaller than the skin blood flow (4.37 mL/min/kg b.w). The extraction ratios of EH-TBB by human skin were calculated as 11 % and 21 % for individual and mixture exposures respectively. The slow *in vivo* clearance rates in the skin could translate into slow EH-TBB percutaneous metabolism and subsequently results in inefficient EH-TBB elimination from the skin.

7.2. Research gap and future perspectives.

We developed analytical methods for simultaneous analysis of multiple emerging contaminants and their potential degradation/transformation products in one run by UPLC-Orbitrap HRMS which provides a great analytical tool for assessment of such contaminants in the environment. Additionally, new insights into hepatic and extra-hepatic biotransformation of TBECH, EH-TBB and TPhP were also revealed. However, there remain significant research gaps that need to be addressed as follows:

- A wider range of contaminants should be included into the target list of the developed methods.
- A HRMS library for environmental contaminants, especially in APCI ionization mode, is needed for more effective contaminant screening.

- More data on concentrations and profiles of various NBFRs and PPCPs in various environmental matrices is required to fully assess their risk to the environment and humans.
- More knowledge about human biotransformation pathways/rates of NBFRs, both hepatic and extra-hepatic, is required to fully understand their implications for human exposure to these chemicals through multiple pathways and the potential toxicity arising from the produced metabolites.
- A close to realistic approach (exposure to real-life chemical mixtures) is required to study the distribution, metabolism, clearance and toxicokinetics of emerging contaminants.
- Investigating the human bioavailability and/or bioaccessibility of NBFRs via dermal contact.
- Assessment of the environmental fate and behaviour of PPCPs post-water treatment, and their implications to the aquatic environment.

References

- Abbasi, G., Saini, A., Goosey, E., Diamond, M.L., 2016. Product screening for sources of halogenated flame retardants in Canadian house and office dust. *Sci. Total Environ.* 545–546, 299–307. doi:10.1016/j.scitotenv.2015.12.028
- Abdallah, M.A.-E., Harrad, S., 2014. Polybrominated diphenyl ethers in UK human milk: implications for infant exposure and relationship to external exposure. *Environ. Int.* 63, 130–6. doi:10.1016/j.envint.2013.11.009
- Abdallah, M.A.-E., Uchea, C., Chipman, J.K., Harrad, S., 2014. Enantioselective Biotransformation of Hexabromocyclododecane by in Vitro Rat and Trout Hepatic Sub-Cellular Fractions. *Environ. Sci. Technol.* 48, 2732–2740. doi:10.1021/es404644s
- Abdallah, M.A.-E., Zhang, J., Pawar, G., Viant, M.R., Chipman, J.K., D’Silva, K., Bromirski, M., Harrad, S., 2015. High-resolution mass spectrometry provides novel insights into products of human metabolism of organophosphate and brominated flame retardants. *Anal. Bioanal. Chem.* 1871–1883. doi:10.1007/s00216-015-8466-z
- Abdallah, M.A.E., Harrad, S., 2011. Tetrabromobisphenol-A, hexabromocyclododecane and its degradation products in UK human milk: Relationship to external exposure. *Environ. Int.* 37, 443–448. doi:10.1016/j.envint.2010.11.008
- Aguirre-Martínez, G. V., Buratti, S., Fabbri, E., DelValls, A.T., Martín-Díaz, M.L., 2013. Using lysosomal membrane stability of haemocytes in *Ruditapes philippinarum* as a biomarker of cellular stress to assess contamination by caffeine, ibuprofen, carbamazepine and novobiocin. *J. Environ. Sci. (China)* 25, 1408–1418. doi:10.1016/S1001-0742(12)60207-1
- Al-Odaini, N.A., Zakaria, M.P., Yaziz, M.I., Surif, S., 2010. Multi-residue analytical method for human pharmaceuticals and synthetic hormones in river water and sewage effluents by solid-phase extraction and liquid chromatography-tandem mass spectrometry. *J. Chromatogr. A* 1217, 6791–6806. doi:10.1016/j.chroma.2010.08.033
- Al-Omran, L.S., Harrad, S., 2015. Polybrominated diphenyl ethers and “novel” brominated flame retardants in floor and elevated surface house dust from Iraq: Implications for human exposure assessment. *Emerg. Contam.* 2, 1–7. doi:10.1016/j.emcon.2015.10.001
- Al-Qaim, F.F., Abdullah, M.P., Othman, M.R., Latip, J., Zakaria, Z., 2014. Multi-residue analytical methodology-based liquid chromatography-time-of-flight-mass spectrometry for the analysis of pharmaceutical residues in surface water and effluents from sewage treatment plants and hospitals. *J. Chromatogr. A* 1345, 139–153. doi:10.1016/j.chroma.2014.04.025
- Ali, A.M., Thorsen, H., Sydnes, L.K., Alarif, W.M., Kallenborn, R., Al-lihaibi, S.S., 2018. Detection of PPCPs in marine organisms from contaminated coastal waters of the Saudi Red Sea. *Sci. Total Environ.* 621, 654–662. doi:10.1016/j.scitotenv.2017.11.298
- Ali, N., Ali, L., Mehdi, T., Dirtu, A.C., Al-Shammari, F., Neels, H., Covaci, A., 2013. Levels and profiles of organochlorines and flame retardants in car and house dust from Kuwait and Pakistan: Implication for human exposure via dust ingestion. *Environ. Int.* 55, 62–70. doi:10.1016/j.envint.2013.02.001
- Ali, N., Dirtu, A.C., Eede, N.V.D., Goosey, E., Harrad, S., Neels, H., t Mannetje, A.,

- Coakley, J., Douwes, J., Covaci, A., 2012. Occurrence of alternative flame retardants in indoor dust from New Zealand: Indoor sources and human exposure assessment. *Chemosphere* 88, 1276–1282. doi:10.1016/j.chemosphere.2012.03.100
- Ali, N., Harrad, S., Goosey, E., Neels, H., Covaci, A., 2011. “ Novel” brominated flame retardants in Belgian and UK indoor dust: Implications for human exposure. *Chemosphere* 83, 1360–1365. doi:10.1016/j.chemosphere.2011.02.078
- Allen, J.G., Stapleton, H.M., Vallarino, J., McNeely, E., McClean, M.D., Harrad, S.J., Rauert, C.B., Spengler, J.D., 2013. Exposure to flame retardant chemicals on commercial airplanes. *Environ. Health* 12, 17. doi:10.1186/1476-069X-12-17
- Arnnok, P., Singh, R.R., Burakham, R., Pérez-Fuentetaja, A., Aga, D.S., 2017. Selective Uptake and Bioaccumulation of Antidepressants in Fish from Effluent-Impacted Niagara River. *Environ. Sci. Technol.* 51, 10652–10662. doi:10.1021/acs.est.7b02912
- Arsenault, G., Lough, A., Marvin, C., McAlees, A., McCrindle, R., MacInnis, G., Pleskach, K., Potter, D., Riddell, N., Sverko, E., Tittlemier, S., Tomy, G., 2008. Structure characterization and thermal stabilities of the isomers of the brominated flame retardant 1,2-dibromo-4-(1,2-dibromoethyl)cyclohexane. *Chemosphere* 72, 1163–1170. doi:10.1016/j.chemosphere.2008.03.044
- Asnake, S., Pradhan, A., Kharlyngdoh, J.B., Modig, C., Olsson, P.-E., 2015. The brominated flame retardants TBP-AE and TBP-DBPE antagonize the chicken androgen receptor and act as potential endocrine disrupters in chicken LMH cells. *Toxicol. Vitr.* 29, 1993–2000. doi:10.1016/j.tiv.2015.08.009
- Barr, J.S., Mitchelmore, C.L., Roberts, S.C., Stapleton, H.M., 2012. Species specific differences in the in vitro metabolism of the flame retardant mixture, Firemaster® BZ-54. *Aquat. Toxicol.* 124–125, 41–47. doi:10.1016/j.aquatox.2012.06.006
- Belcher, S.M., Cookman, C.J., Patisaul, H.B., Stapleton, H.M., 2014. In vitro assessment of human nuclear hormone receptor activity and cytotoxicity of the flame retardant mixture FM 550 and its triarylphosphate and brominated components. *Toxicol. Lett.* 228, 93–102. doi:10.1016/j.toxlet.2014.04.017
- Bendig, P., Hägele, F., Vetter, W., 2013. Widespread occurrence of polyhalogenated compounds in fat from kitchen hoods. *Anal. Bioanal. Chem.* 405, 7485–7496. doi:10.1007/s00216-013-7194-5
- Bester, K., 2005. Fate of triclosan and triclosan-methyl in sewage treatment plants and surface waters. *Arch. Environ. Contam. Toxicol.* 49, 9–17. doi:10.1007/s00244-004-0155-4
- Blair, B.D., Crago, J.P., Hedman, C.J., Klaper, R.D., 2013. Pharmaceuticals and personal care products found in the Great Lakes above concentrations of environmental concern. *Chemosphere* 93, 2116–2123. doi:10.1016/j.chemosphere.2013.07.057
- Brezovšek, P., Eleršek, T., Filipič, M., 2014. Toxicities of four anti-neoplastic drugs and their binary mixtures tested on the green alga *Pseudokirchneriella subcapitata* and the cyanobacterium *Synechococcus leopoliensis*. *Water Res.* 52, 168–177. doi:10.1016/j.watres.2014.01.007
- Brooks, B.W., Chambliss, C.K., Stanley, J.K., Ramirez, A., Banks, K.E., Johnson, R.D., Lewis, R.J., 2005. Determination of select antidepressants in fish from an effluent-dominated stream. *Environ. Toxicol. Chem.* 24, 464–469.
- Brown, F.R., Whitehead, T.P., Park, J.-S., Metayer, C., Petreas, M.X., 2014. Levels of non-polybrominated diphenyl ether brominated flame retardants in residential house dust samples and fire station dust samples in California. *Environ. Res.* 135, 9–14.

- doi:10.1016/j.envres.2014.08.022
- Bu, Q., Wang, B., Huang, J., Deng, S., Yu, G., 2013. Pharmaceuticals and personal care products in the aquatic environment in China: A review. *J. Hazard. Mater.* 262, 189–211. doi:<https://doi.org/10.1016/j.jhazmat.2013.08.040>
- Butt, C.M., Congleton, J., Hoffman, K., Fang, M., Stapleton, H.M., 2014. Metabolites of organophosphate flame retardants and 2-ethylhexyl tetrabromobenzoate in urine from paired mothers and toddlers. *Environ. Sci. Technol.* 48, 10432–8. doi:10.1021/es5025299
- Caldas, S.S., Rombaldi, C., De Oliveira Arias, J.L., Marube, L.C., Primel, E.G., 2016. Multi-residue method for determination of 58 pesticides, pharmaceuticals and personal care products in water using solvent demulsification dispersive liquid-liquid microextraction combined with liquid chromatography-tandem mass spectrometry. *Talanta* 146, 676–688. doi:10.1016/j.talanta.2015.06.047
- Carignan, C.C., Heiger-Bernays, W., McClean, M.D., Roberts, S.C., Stapleton, H.M., Sjödin, A., Webster, T.F., 2013. Flame retardant exposure among collegiate United States gymnasts. *Environ. Sci. Technol.* 47, 13848–13856. doi:10.1021/es4037868
- Cequier, E., Ionas, A.C., Covaci, A., Marcé, R.M., Becher, G., Thomsen, C., 2014. Occurrence of a broad range of legacy and emerging flame retardants in indoor environments in Norway. *Environ. Sci. Technol.* 48, 6827–6835. doi:10.1021/es500516u
- Cequier, E., Marcé, R.M., Becher, G., Thomsen, C., 2015. Comparing human exposure to emerging and legacy flame retardants from the indoor environment and diet with concentrations measured in serum. *Environ. Int.* 74, 54–59. doi:10.1016/j.envint.2014.10.003
- Cequier, E., Marcé, R.M., Becher, G., Thomsen, C., 2013. Determination of emerging halogenated flame retardants and polybrominated diphenyl ethers in serum by gas chromatography mass spectrometry. *J. Chromatogr. A* 1310, 126–132. doi:10.1016/j.chroma.2013.08.067
- Chandra, R., 2015. *Environmental Waste Management*. CRC Press.
- Chen, D., Letcher, R.J., Burgess, N.M., Champoux, L., Elliott, J.E., Hebert, C.E., Martin, P., Wayland, M., Chip Weseloh, D. V., Wilson, L., 2012. Flame retardants in eggs of four gull species (Laridae) from breeding sites spanning Atlantic to Pacific Canada. *Environ. Pollut.* 168, 1–9. doi:10.1016/j.envpol.2012.03.040
- Chen, F., Gong, Z., Kelly, B.C., 2017. Bioaccumulation Behavior of Pharmaceuticals and Personal Care Products in Adult Zebrafish (*Danio rerio*): Influence of Physical-Chemical Properties and Biotransformation. *Environ. Sci. Technol.* 51, 11085–11095. doi:10.1021/acs.est.7b02918
- Chen, J., Pycke, B.F.G., Brownawell, B.J., Kinney, C.A., Furlong, E.T., Kolpin, D.W., Halden, R.U., 2017. Occurrence, temporal variation, and estrogenic burden of five parabens in sewage sludge collected across the United States. *Sci. Total Environ.* 593–594, 368–374. doi:10.1016/j.scitotenv.2017.03.162
- Chen, Y., Yu, G., Cao, Q., Zhang, H., Lin, Q., Hong, Y., 2013. Occurrence and environmental implications of pharmaceuticals in Chinese municipal sewage sludge. *Chemosphere* 93, 1765–1772. doi:10.1016/j.chemosphere.2013.06.007
- Choi, K., Kim, Y., Park, J., Park, C.K., Kim, M.Y., Kim, H.S., Kim, P., 2008. Seasonal variations of several pharmaceutical residues in surface water and sewage treatment plants of Han River, Korea. *Sci. Total Environ.* 405, 120–128. doi:10.1016/j.scitotenv.2008.06.038

- Chu, S., Gauthier, L.T., Letcher, R.J., 2012. Alpha and Beta Isomers of Tetrabromoethylcyclohexane (TBECH) Flame Retardant: Depletion and Metabolite Formation In Vitro Using a Model Rat Microsomal Assay. *Environ. Sci. Technol.* 46, 120828073313006. doi:10.1021/es301546h
- Covaci, A., Harrad, S., Abdallah, M. a E., Ali, N., Law, R.J., Herzke, D., de Wit, C. a., 2011. Novel brominated flame retardants: A review of their analysis, environmental fate and behaviour. *Environ. Int.* 37, 532–556. doi:10.1016/j.envint.2010.11.007
- Curran, I.H.A., Liston, V., Nunnikhoven, A., Caldwell, D., Scuby, M.J.S., Pantazopoulos, P., Rawn, D.F.K., Coady, L., Armstrong, C., Lefebvre, D.E., Bondy, G.S., 2017. Toxicologic effects of 28-day dietary exposure to the flame retardant 1,2-dibromo-4-(1,2-dibromoethyl)-cyclohexane (TBECH) in F344 rats. *Toxicology* 377, 1–13. doi:10.1016/j.tox.2016.12.001
- Dallaire, R., Ayotte, P., Pereg, D., Déry, S., Dumas, P., Langlois, É., Dewailly, É., 2009. Determinants of plasma concentrations of perfluorooctanesulfonate and brominated organic compounds in Nunavik Inuit adults (Canada). *Environ. Sci. Technol.* 43, 5130–5136. doi:10.1021/es9001604
- Dalman, M.R., Deeter, A., Nimishakavi, G., Duan, Z.-H., 2012. Fold change and p-value cutoffs significantly alter microarray interpretations. *BMC Bioinformatics* 13, S11–S11. doi:10.1186/1471-2105-13-S2-S11
- Dams, R., Huestis, M.A., Lambert, W.E., Murphy, C.M., 2003. Matrix effect in bioanalysis of illicit drugs with LC-MS/MS: Influence of ionization type, sample preparation, and biofluid. *J. Am. Soc. Mass Spectrom.* 14, 1290–1294. doi:10.1016/S1044-0305(03)00574-9
- Davis, E., Stapleton, H., 2009. Photodegradation pathways of nonabrominated diphenyl ethers, 2-ethylhexyltetrabromobenzoate and di (2-ethylhexyl) tetrabromophthalate: identifying potential. *Environ. Sci. Technol.* 43, 5739–5746.
- de García, S.O., García-Encina, P. a, Irusta-Mata, R., 2015. Dose–response behavior of the bacterium *Vibrio fischeri* exposed to pharmaceuticals and personal care products. *Ecotoxicology* 141–162. doi:10.1007/s10646-015-1576-8
- Devanathan, G., Subramanian, A., Isobe, T., Kajiwara, N., Suzuki, G., Ka, A., Takahashi, S., Tanabe, S., 2011. Organohalogen Contaminants in Dust Samples From Different Indoor Environments in India : Implications on Human Exposure. *Organohalogen Compd.* 73, 1101–1104.
- Ding, N., Wang, T., Chen, S., Yu, M., Zhu, Z., Tian, M., Luo, X., Mai, B., 2016. Brominated flame retardants (BFRs) in indoor and outdoor air in a community in Guangzhou , a megacity of southern China *. *Environ. Pollut.* 212, 457–463. doi:10.1016/j.envpol.2016.02.038
- Dirtu, A.C., Ali, N., Van den Eede, N., Neels, H., Covaci, A., 2012. Country specific comparison for profile of chlorinated, brominated and phosphate organic contaminants in indoor dust. Case study for Eastern Romania, 2010. *Environ. Int.* 49, 1–8. doi:10.1016/j.envint.2012.08.002
- Dodson, R.E., Perovich, L.J., Covaci, A., Van den Eede, N., Ionas, A.C., Dirtu, A.C., Brody, J.G., Rudel, R. a., 2012. After the PBDE Phase-Out: A Broad Suite of Flame Retardants in Repeat House Dust Samples from California. *Environ. Sci. Technol.* 46, 13056–13066. doi:10.1021/es303879n
- Du, B., Haddad, S.P., Scott, W.C., Chambliss, C.K., Brooks, B.W., 2015. Pharmaceutical bioaccumulation by periphyton and snails in an effluent-dependent stream during an extreme drought. *Chemosphere* 119, 927–934.

- doi:10.1016/j.chemosphere.2014.08.044
- Dunn, W.B., Broadhurst, D., Brown, M., Baker, P.N., Redman, C.W.G., Kenny, L.C., Kell, D.B., 2008. Metabolic profiling of serum using Ultra Performance Liquid Chromatography and the LTQ-Orbitrap mass spectrometry system. *J. Chromatogr. B Anal. Technol. Biomed. Life Sci.* 871, 288–298. doi:10.1016/j.jchromb.2008.03.021
- Ebele, A.J., Abou-Elwafa Abdallah, M., Harrad, S., 2017. Pharmaceuticals and personal care products (PPCPs) in the freshwater aquatic environment. *Emerg. Contam.* 3, 1–16. doi:10.1016/j.emcon.2016.12.004
- Eichhorn, P., Pérez, S., Barceló, D., 2012. Time-of-Flight Mass Spectrometry Versus Orbitrap-Based Mass Spectrometry for the Screening and Identification of Drugs and Metabolites, in: *Comprehensive Analytical Chemistry*. pp. 217–272. doi:10.1016/B978-0-444-53810-9.00009-2
- Erratico, C., Zheng, X., van den Eede, N., Tomy, G., Covaci, A., 2016. Stereoselective Metabolism of α -, β -, and γ -Hexabromocyclododecanes (HBCDs) by Human Liver Microsomes and CYP3A4. *Environ. Sci. Technol.* 50, 8263–8273. doi:10.1021/acs.est.6b01059
- Fan, X., Kubwabo, C., Rasmussen, P.E., Wu, F., 2016. Non-PBDE halogenated flame retardants in Canadian indoor house dust: sampling, analysis, and occurrence. *Environ. Sci. Pollut. Res.* 23, 7998–8007. doi:10.1007/s11356-015-5956-7
- Feng, C., Xu, Y., Zha, J., Li, J., Wu, F., Wang, Z., 2015. Metabolic pathways of decabromodiphenyl ether (BDE209) in rainbow trout (*Oncorhynchus mykiss*) via intraperitoneal injection. *Environ. Toxicol. Pharmacol.* 39, 536–544. doi:10.1016/j.etap.2015.01.006
- Feng, M., Li, Y., Qu, R., Wang, L., Wang, Z., 2013. Oxidative stress biomarkers in freshwater fish *Carassius auratus* exposed to decabromodiphenyl ether and ethane, or their mixture. *Ecotoxicology* 22, 1101–1110. doi:10.1007/s10646-013-1097-2
- Fernandes, A., Smith, F., Petch, R., Panton, S., Carr, M., Rose, M., 2009. Occurrence of brominated contaminants in selected food, Food and Environmental Research Agency UK.
- Fick, J., Söderström, H., Lindberg, R.H., Phan, C., Tysklind, M., Larsson, D.G.J., 2009. Contamination of surface, ground, and drinking water from pharmaceutical production. *Environ. Toxicol. Chem.* 28, 2522–2527. doi:10.1897/09-073.1
- Fisch, K., Waniek, J.J., Schulz-bull, D.E., 2017. Occurrence of pharmaceuticals and UV-filters in riverine run-offs and waters of the German Baltic Sea. *Mar. Pollut. Bull.* 124, 388–399. doi:10.1016/j.marpolbul.2017.07.057
- Fromme, H., Hilger, B., Kopp, E., Miserok, M., Völkel, W., 2014. Polybrominated diphenyl ethers (PBDEs), hexabromocyclododecane (HBCD) and “novel” brominated flame retardants in house dust in Germany. *Environ. Int.* 64, 61–68. doi:10.1016/j.envint.2013.11.017
- Fu, J., Sadgrove, M., Marson, L., Jay, M., 2016. Biotransformation capacity of carboxylesterase in skin and keratinocytes for the penta-ethyl ester prodrug of DTPA. *Drug Metab. Dispos.* 44, 1313–1318. doi:10.1124/dmd.116.069377
- Gaume, B., Bourgougnon, N., Auzoux-Bordenave, S., Roig, B., Le Bot, B., Bedoux, G., 2012. In vitro effects of triclosan and methyl-triclosan on the marine gastropod *Haliotis tuberculata*. *Comp. Biochem. Physiol. - C Toxicol. Pharmacol.* 156, 87–94. doi:10.1016/j.cbpc.2012.04.006
- Gauthier, L.T., Potter, D., Hebert, C.E., Letcher, R.J., 2009. Temporal trends and spatial

- distribution of non-polybrominated diphenyl ether flame retardants in the eggs of colonial populations of Great Lakes herring gulls. *Environ. Sci. Technol.* 43, 312–317. doi:10.1021/es801687d
- Gemmill, B., Pleskach, K., Peters, L., Palace, V., Wautier, K., Park, B., Darling, C., Rosenberg, B., McCrindle, R., Tomy, G.T., 2011. Toxicokinetics of tetrabromoethylcyclohexane (TBECH) in juvenile brown trout (*Salmo trutta*) and effects on plasma sex hormones. *Aquat. Toxicol.* 101, 309–317. doi:10.1016/j.aquatox.2010.11.003
- George, K.W., Häggblom, M.M., 2008. Microbial O-methylation of the flame retardant tetrabromobisphenol-A. *Environ. Sci. Technol.* 42, 5555–5561. doi:10.1021/es800038q
- Ghaste, M., Mistrik, R., Shulaev, V., 2016. Applications of Fourier Transform Ion Cyclotron Resonance (FT-ICR) and Orbitrap Based High Resolution Mass Spectrometry in Metabolomics and Lipidomics. *Int. J. Mol. Sci.* 17, 816. doi:10.3390/ijms17060816
- Giraud, M., Douville, M., Letcher, R.J., Houde, M., 2017. Effects of food-borne exposure of juvenile rainbow trout (*Oncorhynchus mykiss*) to emerging brominated flame retardants 1,2-bis(2,4,6-tribromophenoxy)ethane and 2-ethylhexyl-2,3,4,5-tetrabromobenzoate. *Aquat. Toxicol.* 186, 40–49. doi:10.1016/j.aquatox.2017.02.023
- Guiloski, I.C., Ribas, J.L.C., Pereira, L. da S., Neves, A.P.P., Silva de Assis, H.C., 2015. Effects of trophic exposure to dexamethasone and diclofenac in freshwater fish. *Ecotoxicol. Environ. Saf.* 114, 204–211. doi:10.1016/j.ecoenv.2014.11.020
- Hakk, H., Larsen, G., Bowers, J., 2004. Metabolism, tissue disposition, and excretion of 1,2-bis(2,4,6-tribromophenoxy)ethane (BTBPE) in male Sprague-Dawley rats. *Chemosphere* 54, 1367–1374. doi:10.1016/j.chemosphere.2003.10.032
- Hardy, M.L., Krueger, H.O., Blankinship, A.S., Thomas, S., Kendall, T.Z., Desjardins, D., 2012. Studies and evaluation of the potential toxicity of decabromodiphenyl ethane to five aquatic and sediment organisms. *Ecotoxicol. Environ. Saf.* 75, 73–79. doi:10.1016/j.ecoenv.2011.08.005
- Harju, M.T., Heimstad, E.S., Herzke, D., Sandanger, T., Posner, S., Wania, F., 2008. Current state of knowledge and monitoring requirements: Emerging “new” brominated flame retardants in flame retarded products and the environment (TA-2462/2008). *Nor. Pollut. Control Auth. SFT.*
- Harrad, S., 2014. Summary of Analytical Methods and Associated Quality Assurance/Quality Control (QA/QC) Procedures for Semi-Volatile Organic Compounds, University of Birmingham internal document, revised 12/3/2014.
- Harrad, S., Diamond, M., 2006. New Directions: Exposure to polybrominated diphenyl ethers (PBDEs) and polychlorinated biphenyls (PCBs): Current and future scenarios. *Atmos. Environ.* 40, 1187–1188. doi:10.1016/j.atmosenv.2005.10.006
- Harrad, S., Ibarra, C., Abdallah, M.A.E., Boon, R., Neels, H., Covaci, A., 2008. Concentrations of brominated flame retardants in dust from United Kingdom cars, homes, and offices: Causes of variability and implications for human exposure. *Environ. Int.* 34, 1170–1175. doi:10.1016/j.envint.2008.05.001
- Hassan, Y., Shoeib, T., 2015. Levels of polybrominated diphenyl ethers and novel flame retardants in microenvironment dust from Egypt: An assessment of human exposure. *Sci. Total Environ.* 505, 47–55. doi:10.1016/j.scitotenv.2014.09.080
- He, S., Li, M., Jin, J., Wang, Y., Bu, Y., Xu, M., Yang, X., Liu, A., 2013. Concentrations

- and trends of halogenated flame retardants in the pooled serum of residents of Laizhou Bay, China. *Environ. Toxicol. Chem.* 32, 1242–1247. doi:10.1002/etc.2172
- Helga, T., Pierangela, P., Giorgio, F., Achille, C., 2011. An overview of matrix effects in liquid chromatography–mass spectrometry. *Mass Spectrom. Rev.* 30, 491–509. doi:10.1002/mas.20298
- Hoffman, K., Fang, M., Horman, B., Patisaul, H.B., Garantziotis, S., Birnbaum, L.S., Stapleton, H.M., 2014. Urinary tetrabromobenzoic acid (TBBA) as a biomarker of exposure to the flame retardant mixture Firemaster® 550. *Environ. Health Perspect.* 122, 963–9. doi:10.1289/ehp.1308028
- Huysman, S., Van Meulebroek, L., Vanryckeghem, F., Van Langenhove, H., Demeestere, K., Vanhaecke, L., 2017. Development and validation of an ultra-high performance liquid chromatographic high resolution Q-Orbitrap mass spectrometric method for the simultaneous determination of steroidal endocrine disrupting compounds in aquatic matrices. *Anal. Chim. Acta* 984, 140–150. doi:10.1016/j.aca.2017.07.001
- Ismail, N., Gewurtz, S.B., Pleskach, K., Whittle, D.M., Helm, P. a, Marvin, C.H., Tomy, G.T., 2009. Brominated and chlorinated flame retardants in Lake Ontario, Canada, lake trout (*Salvelinus namaycush*) between 1979 and 2004 and possible influences of food-web changes. *Environ. Toxicol. Chem.* 28, 910–920. doi:10.1897/08-162.1
- Isobe, T., Ogawa, S.P., Ramu, K., Sudaryanto, A., Tanabe, S., 2012. Geographical distribution of non-PBDE-brominated flame retardants in mussels from Asian coastal waters. *Environ. Sci. Pollut. Res.* 19, 3107–3117. doi:10.1007/s11356-012-0945-6
- IUPAC, 1997. Resolution in mass spectroscopy, in: *IUPAC Compendium of Chemical Terminology*. IUPAC, Research Triangle Park, NC, p. 5318. doi:10.1351/goldbook.R05318
- Jewell, C., Ackermann, C., Payne, N.A., Fate, G., Voorman, R., Williams, F.M., 2007. Specificity of Procaine and Ester Hydrolysis by Human, Minipig, and Rat Skin and Liver. *Drug Metab. Dispos.* 35, 2015–2022. doi:10.1124/dmd.107.015727
- Ji, K., Liu, X., Lee, S., Kang, S., Kho, Y., Giesy, J.P., Choi, K., 2013. Effects of non-steroidal anti-inflammatory drugs on hormones and genes of the hypothalamic-pituitary-gonad axis, and reproduction of zebrafish. *J. Hazard. Mater.* 254–255, 242–251. doi:10.1016/j.jhazmat.2013.03.036
- Johnson, P.I., Stapleton, H.M., Mukherjee, B., Hauser, R., Meeker, J.D., 2013. Associations between brominated flame retardants in house dust and hormone levels in men. *Sci. Total Environ.* 445–446, 177–184. doi:10.1016/j.scitotenv.2012.12.017
- Julander, A., Westberg, H., Engwall, M., Van Bavel, B., 2005. Distribution of brominated flame retardants in different dust fractions in air from an electronics recycling facility. *Sci. Total Environ.* 350, 151–160. doi:10.1016/j.scitotenv.2005.01.015
- Kalachova, K., Hradkova, P., Lankova, D., Hajslova, J., Pulkrabova, J., 2012. Occurrence of brominated flame retardants in household and car dust from the Czech Republic. *Sci. Total Environ.* 441, 182–193. doi:10.1016/j.scitotenv.2012.09.061
- Karlsson, M., Julander, a., van Bavel, B., Hardell, L., 2007. Levels of brominated flame retardants in blood in relation to levels in household air and dust. *Environ. Int.* 33, 62–69. doi:10.1016/j.envint.2006.06.025
- Karthikraj, R., Vasu, A.K., Balakrishna, K., Sinha, R.K., Kannan, K., 2017. Occurrence and fate of parabens and their metabolites in five sewage treatment plants in India. *Sci. Total Environ.* 593–594, 592–598. doi:10.1016/j.scitotenv.2017.03.173
- Kasprzyk-Hordern, B., Dinsdale, R.M., Guwy, A.J., 2007. Multi-residue method for the

- determination of basic/neutral pharmaceuticals and illicit drugs in surface water by solid-phase extraction and ultra performance liquid chromatography-positive electrospray ionisation tandem mass spectrometry. *J. Chromatogr. A* 1161, 132–145. doi:10.1016/j.chroma.2007.05.074
- Kawashiro, Y., Fukata, H., Omori-Inoue, M., Kubonoya, K., Jotaki, T., Takigami, H., Sakai, S., Mori, C., 2008. Perinatal exposure to brominated flame retardants and polychlorinated biphenyls in Japan. *Endocr. J.* 55, 1071–1084. doi:10.1507/endocrj.K08E-155
- Khalaf, H., Larsson, A., Berg, H., McCrindle, R., Arsenault, G., Olsson, P.E., 2009. Diastereomers of the brominated flame retardant 1,2-dibromo-4-(1,2 dibromoethyl)cyclohexane induce androgen receptor activation in the HepG2 hepatocellular carcinoma cell line and the LNCaP prostate cancer cell line. *Environ. Health Perspect.* 117, 1853–1859. doi:10.1289/ehp.0901065
- Kharasch, E.D., Hankins, D., Mautz, D., Thummel, K.E., 1996. Identification of the enzyme responsible for oxidative halothane metabolism: Implications for prevention of halothane hepatitis. *Lancet* 347, 1367–1371. doi:10.1016/S0140-6736(96)91011-9
- Kharlyngdoh, J.B., Asnake, S., Pradhan, A., Olsson, P.-E., 2016. TBECH, 1,2-dibromo-4-(1,2 dibromoethyl) cyclohexane, alters androgen receptor regulation in response to mutations associated with prostate cancer. *Toxicol. Appl. Pharmacol.* 307, 91–101. doi:10.1016/j.taap.2016.07.018
- Klosterhaus, S.L., Stapleton, H.M., La Guardia, M.J., Greig, D.J., 2012. Brominated and chlorinated flame retardants in San Francisco Bay sediments and wildlife. *Environ. Int.* 47, 56–65. doi:10.1016/j.envint.2012.06.005
- Kolpin, D.W., Furlong, E.T., Meyer, M.T., Thurman, E.M., Zaugg, S.D., Barber, L.B., Buxton, H.T., 2002. Pharmaceuticals, hormones, and other organic wastewater contaminants in U.S. streams, 1999–2000: A national reconnaissance. *Environ. Sci. Technol.* 36, 1202–1211. doi:10.1021/es011055j
- Koss, G., Döring, H., Würminghausen, B., Koransky, W., 1982. Metabolic fate of Hexabromobenzene in rats. *Toxicol. Lett.* 14, 69–77.
- Kovarich, S., Papa, E., Gramatica, P., 2011. QSAR classification models for the prediction of endocrine disrupting activity of brominated flame retardants. *J. Hazard. Mater.* 190, 106–112. doi:10.1016/j.jhazmat.2011.03.008
- Kuang, J., Abdallah, M.A.E., Harrad, S., 2018. Brominated flame retardants in black plastic kitchen utensils: Concentrations and human exposure implications. *Sci. Total Environ.* 610–611, 1138–1146. doi:10.1016/j.scitotenv.2017.08.173
- Kuang, J., Ma, Y., Harrad, S., 2016. Concentrations of “legacy” and novel brominated flame retardants in matched samples of UK kitchen and living room/bedroom dust. *Chemosphere* 149, 224–230. doi:10.1016/j.chemosphere.2016.01.092
- La Guardia, M.J., Hale, R.C., 2015. Halogenated flame-retardant concentrations in settled dust, respirable and inhalable particulates and polyurethane foam at gymnastic training facilities and residences. *Environ. Int.* 79, 106–114. doi:10.1016/j.envint.2015.02.014
- La Guardia, M.J., Hale, R.C., Harvey, E., Mainor, T.M., Ciparis, S., 2012. In situ accumulation of HBCD, PBDEs, and several alternative flame-retardants in the bivalve (*Corbicula fluminea*) and gastropod (*Elimia proxima*). *Environ. Sci. Technol.* 46, 5798–805. doi:10.1021/es3004238
- Labunska, I., Abdallah, M.A.-E., Eulaers, I., Covaci, A., Tao, F., Wang, M., Santillo, D.,

- Johnston, P., Harrad, S., 2015. Human dietary intake of organohalogen contaminants at e-waste recycling sites in Eastern China. *Environ. Int.* 74, 209–220. doi:10.1016/j.envint.2014.10.020
- Larsson, A., Eriksson, L. a, Andersson, P.L., Ivarson, P., Olsson, P.-E., 2006. Identification of the brominated flame retardant 1,2-dibromo-4-(1,2-dibromoethyl)cyclohexane as an androgen agonist. *J. Med. Chem.* 49, 7366–7372. doi:10.1021/jm060713d
- Leclercq, M., Mathieu, O., Gomez, E., Casellas, C., Fenet, H., Hillaire-Buys, D., 2009. Presence and fate of carbamazepine, oxcarbazepine, and seven of their metabolites at wastewater treatment plants. *Arch. Environ. Contam. Toxicol.* 56, 408–415. doi:10.1007/s00244-008-9202-x
- Lee, J., Ji, K., Lim Kho, Y., Kim, P., Choi, K., 2011. Chronic exposure to diclofenac on two freshwater cladocerans and Japanese medaka. *Ecotoxicol. Environ. Saf.* 74, 1216–1225. doi:10.1016/j.ecoenv.2011.03.014
- Lei, B., Huang, S., Zhou, Y., Wang, D., Wang, Z., 2009. Levels of six estrogens in water and sediment from three rivers in Tianjin area, China. *Chemosphere* 76, 36–42. doi:10.1016/j.chemosphere.2009.02.035
- Li, F., Jiang, B., Nastold, P., Kolvenbach, B.A., Chen, J., Wang, L., Guo, H., Corvini, P.F.X., Ji, R., 2015a. Enhanced transformation of tetrabromobisphenol A by nitrifiers in nitrifying activated sludge. *Environ. Sci. Technol.* 49, 4283–4292. doi:10.1021/es5059007
- Li, F., Wang, J., Jiang, B., Yang, X., Nastold, P., Kolvenbach, B., Wang, L., Ma, Y., Corvini, P.F.X., Ji, R., 2015b. Fate of Tetrabromobisphenol A (TBBPA) and Formation of Ester- and Ether-Linked Bound Residues in an Oxidic Sandy Soil. *Environ. Sci. Technol.* 49, 12758–12765. doi:10.1021/acs.est.5b01900
- Li, J., Zhang, X., Bao, J., Liu, Y., Li, J., Li, J., Liang, Y., Zhang, J., Zhang, A., 2015. Toxicity of new emerging pollutant tris-(2,3-dibromopropyl) isocyanurate on BALB/c mice. *J. Appl. Toxicol.* 35, 375–382. doi:10.1002/jat.3026
- Li, M., Sun, Q., Li, Y., Lv, M., Lin, L., Wu, Y., Ashfaq, M., Yu, C. ping, 2016. Simultaneous analysis of 45 pharmaceuticals and personal care products in sludge by matrix solid-phase dispersion and liquid chromatography tandem mass spectrometry. *Anal. Bioanal. Chem.* 408, 4953–4964. doi:10.1007/s00216-016-9590-0
- Li, W., Shi, Y., Gao, L., Liu, J., Cai, Y., 2012. Occurrence of antibiotics in water, sediments, aquatic plants, and animals from Baiyangdian Lake in North China. *Chemosphere* 89, 1307–1315. doi:10.1016/j.chemosphere.2012.05.079
- Liang, S., Xu, F., Tang, W., Zhang, Z., Zhang, W., Liu, L., Wang, J., Lin, K., 2016. Brominated flame retardants in the hair and serum samples from an e-waste recycling area in southeastern China: the possibility of using hair for biomonitoring. *Environ. Sci. Pollut. Res.* 23, 14889–14897. doi:10.1007/s11356-016-6491-x
- Lintelmann, J., Katayama, A., Kurihara, N., Shore, L., Wenzel, A., 2003. Endocrine disruptors in the environment (IUPAC Technical Report). *Pure Appl. Chem.* 75, 631–681. doi:10.1351/pac200375050631
- Liu, A., Shi, J., Qu, G., Hu, L., Ma, Q., Song, M., Jing, C., Jiang, G., 2017. Identification of Emerging Brominated Chemicals as the Transformation Products of Tetrabromobisphenol A (TBBPA) Derivatives in Soil. *Environ. Sci. Technol.* 51, 5434–5444. doi:10.1021/acs.est.7b01071
- Liu, J., Wang, R., Huang, B., Lin, C., Wang, Y., Pan, X., 2011. Distribution and

- bioaccumulation of steroidal and phenolic endocrine disrupting chemicals in wild fish species from Dianchi Lake, China. *Environ. Pollut.* 159, 2815–2822. doi:10.1016/j.envpol.2011.05.013
- Liu, L.-Y., Salamova, A., He, K., Hites, R. a., 2015. Analysis of Polybrominated Diphenyl Ethers and Emerging Halogenated and Organophosphate Flame Retardants in Human Hair and Nails. *J. Chromatogr. A* 1406, 251–257. doi:10.1016/j.chroma.2015.06.003
- Liu, L.-Y., Salamova, A., Hites, R. a., 2014. Halogenated flame retardants in baby food from the United States and from china and the estimated dietary intakes by infants. *Environ. Sci. Technol.* 48, 9812–8. doi:10.1021/es502743q
- Lorber, M., 2008. Exposure of Americans to polybrominated diphenyl ethers. *J. Expo. Sci. Environ. Epidemiol.* 18, 2–19. doi:10.1038/sj.jes.7500572
- Lu, W., Bennett, B.D., Rabinowitz, J.D., 2008. Analytical strategies for LC-MS-based targeted metabolomics. *J. Chromatogr. B Anal. Technol. Biomed. Life Sci.* 871, 236–242. doi:10.1016/j.jchromb.2008.04.031
- Makarov, A., 2000. Electrostatic Axially Harmonic Orbital Trapping: A High-Performance Technique of Mass Analysis. *Anal. Chem.* 72, 1156–1162. doi:10.1021/ac991131p
- Manevski, N., Swart, P., Balavenkatraman, K.K., Bertschi, B., Camenisch, G., Kretz, O., Schiller, H., Walles, M., Ling, B., Wettstein, R., Schaefer, D.J., Itin, P., Ashton-Chess, J., Pognan, F., Wolf, A., Litherland, K., 2014. Phase II Metabolism in Human Skin: Skin Explants Show Full Coverage for Glucuronidation, Sulfation, N-Acetylation, Catechol Methylation, and Glutathione Conjugation. *Drug Metab. Dispos.* 43, 126–139. doi:10.1124/dmd.114.060350
- Mankidy, R., Ranjan, B., Honaramooz, A., Giesy, J.P., 2014. Effects of novel brominated flame retardants on steroidogenesis in primary porcine testicular cells. *Toxicol. Lett.* 224, 141–146. doi:10.1016/j.toxlet.2013.10.018
- Mannetje, A.T., Coakley, J., Bridgen, P., Brooks, C., Harrad, S., Smith, A.H., Pearce, N., Douwes, J., 2013. Current concentrations, temporal trends and determinants of persistent organic pollutants in breast milk of New Zealand women. *Sci. Total Environ.* 458–460, 399–407. doi:10.1016/j.scitotenv.2013.04.055
- Martinson, S.C., Letcher, R.J., Fernie, K.J., 2015. Exposure to the androgenic brominated flame retardant 1,2-dibromo-4-(1,2-dibromoethyl)-cyclohexane alters reproductive and aggressive behaviors in birds. *Environ. Toxicol. Chem.* 34, 2395–2402. doi:10.1002/etc.3078
- Martinson, S.C., Palace, V., Letcher, R.J., Fernie, K.J., 2017. Disruption of thyroxine and sex hormones by 1,2-dibromo-4-(1,2-dibromoethyl)cyclohexane (DBE-DBCH) in American kestrels (*Falco sparverius*) and associations with reproductive and behavioral changes. *Environ. Res.* 154, 389–397. doi:10.1016/j.envres.2017.01.005
- Martín, J., Santos, J.L., Aparicio, I., Alonso, E., 2010. Multi-residue method for the analysis of pharmaceutical compounds in sewage sludge, compost and sediments by sonication-assisted extraction and LC determination. *J. Sep. Sci.* 33, 1760–1766. doi:10.1002/jssc.200900873
- Michalski, A., Damoc, E., Hauschild, J.-P., Lange, O., Wiegand, A., Makarov, A., Nagaraj, N., Cox, J., Mann, M., Horning, S., 2011. Mass Spectrometry-based Proteomics Using Q Exactive, a High-performance Benchtop Quadrupole Orbitrap Mass Spectrometer. *Mol. Cell. Proteomics* 10, M111.011015. doi:10.1074/mcp.M111.011015

- Michalski, A., Damoc, E., Hauschild, J.-P., Lange, O., Wieghaus, A., Makarov, A., Nagaraj, N., Cox, J., Mann, M., Horning, S., 2011. Mass spectrometry-based proteomics using Q exactive, a high-performance benchtop quadrupole orbitrap mass spectrometer. *Mol. Cell. Proteomics* 10. doi:10.1074/mcp.M111.011015
- Mirzaei, R., Yunesian, M., Nasser, S., Gholami, M., Jalilzadeh, E., 2018. Occurrence and fate of most prescribed antibiotics in different water environments of Tehran, Iran. *Sci. Total Environ.* 619–620, 446–459. doi:10.1016/j.scitotenv.2017.07.272
- Mizouchi, S., Ichiba, M., Takigami, H., Kajiwara, N., Takamuku, T., Miyajima, T., Kodama, H., Someya, T., Ueno, D., 2015. Exposure assessment of organophosphorus and organobromine flame retardants via indoor dust from elementary schools and domestic houses. *Chemosphere* 123, 17–25. doi:10.1016/j.chemosphere.2014.11.028
- Mohr, S., García-Bermejo, Á., Herrero, L., Gómara, B., Costabeber, I.H., González, M.J., 2014. Levels of brominated flame retardants (BFRs) in honey samples from different geographic regions. *Sci. Total Environ.* 472, 741–745. doi:10.1016/j.scitotenv.2013.11.035
- Muenhor, D., Harrad, S., Ali, N., Covaci, A., 2010. Brominated flame retardants (BFRs) in air and dust from electronic waste storage facilities in Thailand. *Environ. Int.* 36, 690–698. doi:10.1016/j.envint.2010.05.002
- Muir, D., Simmons, D., Wang, X., Peart, T., Villella, M., Miller, J., Sherry, J., 2017. Bioaccumulation of pharmaceuticals and personal care product chemicals in fish exposed to wastewater effluent in an urban wetland. *Sci. Rep.* 7, 16999. doi:10.1038/s41598-017-15462-x
- Mulabagal, V., Wilson, C., Hayworth, J.S., 2017. An ultrahigh-performance chromatography/tandem mass spectrometry quantitative method for trace analysis of potential endocrine disrupting steroid hormones in estuarine sediments. *Rapid Commun. Mass Spectrom.* 31, 419–429. doi:10.1002/rcm.7807
- Munsch, C., Olivier, N., Veyrand, B., Marchand, P., 2015. Occurrence of legacy and emerging halogenated organic contaminants in marine shellfish along French coasts. *Chemosphere* 118, 329–335. doi:10.1016/j.chemosphere.2014.09.106
- Newton, S., Sellström, U., de Wit, C. a., 2015. Emerging Flame Retardants, PBDEs, and HBCDDs in indoor and outdoor media in Stockholm, Sweden. *Environ. Sci. Technol.* 150210152433003. doi:10.1021/es505946e
- Oaks, J.L., Gilbert, M., Virani, M.Z., Watson, R.T., Meteyer, C.U., Rideout, B.A., Shivaprasad, H.L., Ahmed, S., Chaudhry, M.J.I., Arshad, M., Mahmood, S., Ali, A., Khan, A.A., 2004. Diclofenac residues as the cause of vulture population decline in Pakistan. *Nature* 427, 630–633.
- Ortiz De Montellano, P.R., 2010. Hydrocarbon hydroxylation by cytochrome P450 enzymes. *Chem. Rev.* 110, 932–948. doi:10.1021/cr9002193
- Papachlimitzou, A., Barber, J.L., Losada, S., Bersuder, P., Law, R.J., 2012. A review of the analysis of novel brominated flame retardants. *J. Chromatogr. A* 1219, 15–28. doi:10.1016/j.chroma.2011.11.029
- Parcher, J.F., Wang, M., Chittiboyina, A.G., Khan, I.A., 2017. In-source collision-induced dissociation (IS-CID): Applications, issues and structure elucidation with single-stage mass analyzers. *Drug Test. Anal.* 1–9. doi:10.1002/dta.2249
- Park, B.J., Palace, V., Wautier, K., Gemmill, B., Tomy, G., 2011. Thyroid Axis Disruption in Juvenile Brown Trout (*Salmo trutta*) Exposed to the Flame Retardant β -Tetrabromoethylcyclohexane (β -TBECH) via the Diet. *Environ. Sci. Technol.* 45,

- 7923–7927. doi:10.1021/es201530m
- Pettersson-Julander, A., van Bavel, B., Engwall, M., Westberg, H., 2004. Personal air sampling and analysis of polybrominated diphenyl ethers and other bromine containing compounds at an electronic recycling facility in Sweden. *J. Environ. Monit.* 6, 874–80. doi:10.1039/b408381d
- Polder, A., Müller, M.B., Brynildsrud, O.B., de Boer, J., Hamers, T., Kamstra, J.H., Lie, E., Mdegela, R.H., Moberg, H., Nonga, H.E., Sandvik, M., Skaare, J.U., Lyche, J.L., 2016. Dioxins, PCBs, chlorinated pesticides and brominated flame retardants in free-range chicken eggs from peri-urban areas in Arusha, Tanzania: Levels and implications for human health. *Sci. Total Environ.* 551–552, 656–667. doi:10.1016/j.scitotenv.2016.02.021
- Pradhan, A., Kharlyngdoh, J.B., Asnake, S., Olsson, P.E., 2013. The brominated flame retardant TBECHE activates the zebrafish (*Danio rerio*) androgen receptor, alters gene transcription and causes developmental disturbances. *Aquat. Toxicol.* 142–143, 63–72. doi:10.1016/j.aquatox.2013.07.018
- Pratt, I., Anderson, W., Crowley, D., Daly, S., Evans, R., Fernandes, A., Fitzgerald, M., Geary, M., Keane, D., Morrison, J.J., Reilly, A., Tlustos, C., 2013. Brominated and fluorinated organic pollutants in the breast milk of first-time Irish mothers: is there a relationship to levels in food? *Food Addit. Contam. A, Chem. Anal. Control. Expo. risk Assess.* 30, 1788–1798. doi:10.1080/19440049.2013.822569
- Puype, F., Samsonok, J., Knoop, J., Egelkraut-Holtus, M., Ortlieb, M., 2015. Evidence of waste electrical and electronic equipment (WEEE) relevant substances in polymeric food-contact articles sold on the European market. *Food Addit. Contam. Part A* 49, 150119061656008. doi:10.1080/19440049.2015.1009499
- Qi, H., Li, W.L., Liu, L.Y., Zhang, Z.F., Zhu, N.Z., Song, W.W., Ma, W.L., Li, Y.F., 2014. Levels, distribution and human exposure of new non-BDE brominated flame retardants in the indoor dust of China. *Environ. Pollut.* 195, 1–8. doi:10.1016/j.envpol.2014.08.008
- Qiu, X., Bigsby, R.M., Hites, R.A., 2009. Hydroxylated Metabolites of Polybrominated Diphenyl Ethers in Human Blood Samples from the United States. *Environ. Health Perspect.* 93–98. doi:10.1289/ehp.11660
- Qizhi, H., J., N.R., Hongyan, L., Alexander, M., Mark, H., R., G.C., 2005. The Orbitrap: a new mass spectrometer. *J. Mass Spectrom.* 40, 430–443. doi:10.1002/jms.856
- Ramirez, A., Brain, R., Usenko, S., Mottaleb, M., O'Donnell, J., Stahl, L., Wathen, J., Snyder, B., Pitt, J., Perez-Hurtado, P., Dobbins, L., Brooks, B., Chambliss, C., 2009. Occurrence of pharmaceuticals and personal care products in fish: results of a national pilot study in the United States. *Environ. Toxicol. Chem.* 28, 2587–2597. doi:10.1897/08-561.1
- Roberts, S.C., Macaulay, L.J., Stapleton, H.M., 2012. In Vitro Metabolism of the Brominated Flame Retardants 2-Ethylhexyl-2,3,4,5-Tetrabromobenzoate (TBB) and Bis(2-ethylhexyl) 2,3,4,5-Tetrabromophthalate (TBPH) in Human and Rat Tissues. *Chem. Res. Toxicol.* 25, 1435–1441.
- Rosenberg, C., Hämeilä, M., Tornaes, J., Säkkinen, K., Puttonen, K., Korpi, A., Kiilunen, M., Linnainmaa, M., Hesso, A., 2011. Exposure to flame retardants in electronics recycling sites. *Ann. Occup. Hyg.* 55, 658–665. doi:10.1093/annhyg/mer033
- Rüdel, H., Böhmer, W., Schröter-Kermani, C., 2006. Retrospective monitoring of synthetic musk compounds in aquatic biota from German rivers and coastal areas. *J. Environ. Monit.* 8, 812–823. doi:10.1039/B602389B

- Sahlström, L.M.O., Sellström, U., de Wit, C.A., Lignell, S., Darnerud, P.O., 2015. Feasibility study of feces for noninvasive biomonitoring of brominated flame retardants in toddlers. *Environ. Sci. Technol.* 49, 606–15. doi:10.1021/es504708c
- Sahlström, L.M.O., Sellström, U., de Wit, C.A., Lignell, S., Darnerud, P.O., 2014. Brominated flame retardants in matched serum samples from Swedish first-time mothers and their toddlers. *Environ. Sci. Technol.* 48, 7584–92. doi:10.1021/es501139d
- Sahlström, L.M.O., Sellström, U., de Wit, C. a., Lignell, S., Darnerud, P.O., 2015. Estimated intakes of brominated flame retardants via diet and dust compared to internal concentrations in a Swedish mother–toddler cohort. *Int. J. Hyg. Environ. Health* 218, 422–432. doi:10.1016/j.ijheh.2015.03.011
- Saito, I., Onuki, a., Seto, H., 2007. Indoor organophosphate and polybrominated flame retardants in Tokyo. *Indoor Air* 17, 28–36. doi:10.1111/j.1600-0668.2006.00442.x
- Samsonak, J., Puype, F., 2013. Occurrence of brominated flame retardants in black thermo cups and selected kitchen utensils purchased on the European market. *Food Addit. Contam. Part A. Chem. Anal. Control. Expo. Risk Assess.* 30, 1976–86. doi:10.1080/19440049.2013.829246
- Saunders, D.M.V., Podaima, M., Codling, G., Giesy, J.P., Wiseman, S., 2015a. A mixture of the novel brominated flame retardants TBPH and TBB affects fecundity and transcript profiles of the HPGL-axis in Japanese medaka. *Aquat. Toxicol.* 158, 14–21. doi:10.1016/j.aquatox.2014.10.019
- Saunders, D.M.V., Podaima, M., Wiseman, S., Giesy, J.P., 2015b. Effects of the brominated flame retardant TBCO on fecundity and profiles of transcripts of the HPGL-axis in Japanese medaka. *Aquat. Toxicol.* 160, 180–187. doi:10.1016/j.aquatox.2015.01.018
- Saunders, D.M. V, Higley, E.B., Hecker, M., Mankidy, R., Giesy, J.P., 2013. In vitro endocrine disruption and TCDD-like effects of three novel brominated flame retardants: TBPH, TBB, & TBCO. *Toxicol. Lett.* 223, 252–259. doi:10.1016/j.toxlet.2013.09.009
- Shen, H., Main, K.M., Andersson, A.-M., Damgaard, I.N., Virtanen, H.E., Skakkebaek, N.E., Toppari, J., Schramm, K.-W., 2008. Concentrations of persistent organochlorine compounds in human milk and placenta are higher in Denmark than in Finland. *Hum. Reprod.* 23, 201–10. doi:10.1093/humrep/dem199
- Shoeib, M., Ahrens, L., Jantunen, L., Harner, T., 2014. Concentrations in air of organobromine, organochlorine and organophosphate flame retardants in Toronto, Canada. *Atmos. Environ.* 99, 140–147. doi:http://dx.doi.org/10.1016/j.atmosenv.2014.09.040
- Shoeib, M., Harner, T., Webster, G.M., Sverko, E., Cheng, Y., 2012. Legacy and current-use flame retardants in house dust from Vancouver, Canada. *Environ. Pollut.* 169, 175–182. doi:10.1016/j.envpol.2012.01.043
- Silva, M.J., Hilton, D., Furr, J., Gray, L.E., Preau, J.L., Calafat, A.M., Ye, X., 2015. Quantification of tetrabromo benzoic acid and tetrabromo phthalic acid in rats exposed to the flame retardant Uniplex FPR-45. *Arch. Toxicol.* doi:10.1007/s00204-015-1489-6
- Sjödin, A., Carlsson, H., Thuresson, K., Sjölin, S., Bergman, Å., Östman, C., 2001. Flame retardants in indoor air at an electronics recycling plant and at other work environments. *Environ. Sci. Technol.* 35, 448–454. doi:10.1021/es000077n
- Smith, S.A., Colley, H.E., Sharma, P., Slowik, K.M., Andrew, R.S., Steven, S., Craig,

- D.W., 2018. Expression and enzyme activity of cytochrome P450 enzymes CYP3A4 and CYP3A5 in human skin and tissue- - engineered skin equivalents 5–7. doi:10.1111/exd.13483
- Smythe, T.A., Butt, C.M., Stapleton, H.M., Pleskach, K., Ratnayake, G., Song, C.Y., Riddell, N., Konstantinov, A., Tomy, G.T., 2017. Impacts of Unregulated Novel Brominated Flame Retardants on Human Liver Thyroid Deiodination and Sulfotransferation. *Environ. Sci. Technol.* 51, 7245–7253. doi:10.1021/acs.est.7b01143
- Stapleton, H.M., Allen, J.G., Kelly, S.M., Konstantinov, A., Klosterhaus, S., Watkins, D., Mcclean, M.D., Webster, T.F., 2008. Alternate and new brominated flame retardants detected in U.S. house dust. *Environ. Sci. Technol.* 42, 6910–6916. doi:10.1021/es801070p
- Stewart, M., Olsen, G., Hickey, C.W., Ferreira, B., Jelić, A., Petrović, M., Barcelo, D., 2014. A survey of emerging contaminants in the estuarine receiving environment around Auckland, New Zealand. *Sci. Total Environ.* 468–469, 202–210. doi:10.1016/j.scitotenv.2013.08.039
- Strid, A., Smedje, G., Athanassiadis, I., Lindgren, T., Lundgren, H., Jakobsson, K., Bergman, Å., 2014. Brominated flame retardant exposure of aircraft personnel. *Chemosphere* 116, 83–90. doi:10.1016/j.chemosphere.2014.03.073
- Suárez, S., Carballa, M., Omil, F., Lema, J.M., 2008. How are pharmaceutical and personal care products (PPCPs) removed from urban wastewaters? *Rev. Environ. Sci. Biotechnol.* 7, 125–138. doi:10.1007/s11157-008-9130-2
- Subedi, B., Du, B., Chambliss, C.K., Koschorreck, J., Rüdell, H., Quack, M., Brooks, B.W., Usenko, S., 2012. Occurrence of Pharmaceuticals and Personal Care Products in German Fish Tissue: A National Study. *Environ. Sci. Technol.* 46, 9047–9054. doi:10.1021/es301359t
- Sühring, R., Byer, J., Freese, M., Pohlmann, J.D., Wolschke, H., Möller, A., Hodson, P. V., Alae, M., Hanel, R., Ebinghaus, R., 2014. Brominated flame retardants and Dechloranes in European and American eels from glass to silver life stages. *Chemosphere* 116, 104–111. doi:10.1016/j.chemosphere.2013.10.096
- Sun, F., Kolvenbach, B.A., Nastold, P., Jiang, B., Ji, R., Corvini, P.F.X., 2014. Degradation and metabolism of tetrabromobisphenol A (TBBPA) in submerged soil and soil-plant systems. *Environ. Sci. Technol.* 48, 14291–14299. doi:10.1021/es503383h
- Takigami, H., Suzuki, G., Hirai, Y., Sakai, S.I., 2009. Brominated flame retardants and other polyhalogenated compounds in indoor air and dust from two houses in Japan. *Chemosphere* 76, 270–277. doi:10.1016/j.chemosphere.2009.03.006
- Tamura, I., Yasuda, Y., Kagota, K., Yoneda, S., Nakada, N., 2017. Contribution of pharmaceuticals and personal care products (PPCPs) to whole toxicity of water samples collected in effluent-dominated urban streams. *Ecotoxicol. Environ. Saf.* 144, 338–350. doi:10.1016/j.ecoenv.2017.06.032
- Tao, F., Abdallah, M.A., Harrad, S., 2016. Emerging and Legacy Flame Retardants in UK Indoor Air and Dust: Evidence for Replacement of PBDEs by Emerging Flame Retardants? *Environ. Sci. Technol.* 50, 13052–13061. doi:10.1021/acs.est.6b02816
- Tao, F., Abou-Elwafa Abdallah, M., Ashworth, D.C., Douglas, P., Toledano, M.B., Harrad, S., 2017. Emerging and legacy flame retardants in UK human milk and food suggest slow response to restrictions on use of PBDEs and HBCDD. *Environ. Int.* 105, 95–104. doi:10.1016/j.envint.2017.05.010

- Tarpani, R.R.Z., Azapagic, A., 2018. A methodology for estimating concentrations of pharmaceuticals and personal care products (PPCPs) in wastewater treatment plants and in freshwaters. *Sci. Total Environ.* 622–623, 1417–1430. doi:<https://doi.org/10.1016/j.scitotenv.2017.12.059>
- Ternes, T.A., 1998. Occurrence of drugs in German sewage treatment plants and rivers. *Water Res.* 32, 3245–3260.
- Thomas, K. V., Hilton, M.J., 2004. The occurrence of selected human pharmaceutical compounds in UK estuaries. *Mar. Pollut. Bull.* 49, 436–444. doi:10.1016/j.marpolbul.2004.02.028
- Thomsen, C., Lundanes, E., Becher, G., 2001. Brominated flame retardants in plasma samples from three different occupational groups in Norway. *J. Environ. Monit.* 3, 366–370. doi:10.1039/b104304h
- Tlustos, C., A., F., Rose, M., 2010. The emerging BFRs - Hexabromobenzene (HBB), bis(2,4,6-tribromophenoxy)ethane (BTBPE) and decabromodiphenylethane (DBDPE) - in irish foods. *Organohalogen Compd.* 72, 1577–1579.
- Tomy, G.T., Pleskach, K., Arsenault, G., Potter, D., Mccrindle, R., Marvin, C.H., Sverko, E., Tittlemier, S., 2008. Identification of the novel cycloaliphatic brominated flame retardant 1,2-dibromo4-(1,2-dibromoethyl)cyclohexane in Canadian Arctic Beluga (*Delphinapterus leucas*). *Environ. Sci. Technol.* 42, 543–549. doi:10.1021/es072043m
- Tue, N.M., Takahashi, S., Suzuki, G., Isobe, T., Viet, P.H., Kobara, Y., Seike, N., Zhang, G., Sudaryanto, A., Tanabe, S., 2013. Contamination of indoor dust and air by polychlorinated biphenyls and brominated flame retardants and relevance of non-dietary exposure in Vietnamese informal e-waste recycling sites. *Environ. Int.* 51, 160–167. doi:10.1016/j.envint.2012.11.006
- USEPA, 2010. Emerging Contaminants – Nanomaterials At a Glance.
- USEPA, 2007. Method 1694: Pharmaceuticals and Personal Care Products in Water, Soil, Sediment, and Biosolids by HPLC/MS/MS [WWW Document]. URL https://www.epa.gov/sites/production/files/2015-10/documents/method_1694_2007.pdf (accessed 7.6.18).
- USEPA, 2006. Non-confidential 2006 IUR Records by Chemical. Inventory Update Reporting (IUR).
- Venier, M., Audy, O., Vojta, Š., Bečanová, J., Romanak, K., Melymuk, L., Krátká, M., Kukučka, P., Okeme, J., Saini, A., Diamond, M.L., Klánová, J., 2016. Brominated flame retardants in the indoor environment - Comparative study of indoor contamination from three countries. *Environ. Int.* 94, 150–160. doi:10.1016/j.envint.2016.04.029
- Villaverde-de-Sáa, E., Valls-Cantenys, C., Quintana, J.B., Rodil, R., Cela, R., 2013. Matrix solid-phase dispersion combined with gas chromatography-mass spectrometry for the determination of fifteen halogenated flame retardants in mollusks. *J. Chromatogr. A* 1300, 85–94. doi:10.1016/j.chroma.2013.05.064
- Von Der Recke, R., Vetter, W., 2007. Synthesis and characterization of 2,3-dibromopropyl-2,4,6-tribromophenyl ether (DPTE) and structurally related compounds evidenced in seal blubber and brain. *Environ. Sci. Technol.* 41, 1590–1595. doi:10.1021/es062383s
- Wang, F., Wang, J., Dai, J., Hu, G., Wang, J., Luo, X., Mai, B., 2010a. Comparative tissue distribution, biotransformation and associated biological effects by decabromodiphenyl ethane and decabrominated diphenyl ether in male rats after a

- 90-day oral exposure study. *Environ. Sci. Technol.* 44, 5655–5660. doi:10.1021/es101158e
- Wang, F., Wang, J., Dai, J., Hu, G., Wang, J., Luo, X., Mai, B., 2010b. Comparative tissue distribution, biotransformation and associated biological effects by decabromodiphenyl ethane and decabrominated diphenyl ether in male rats after a 90-day oral exposure study. *Environ. Sci. Technol.* 44, 5655–5660. doi:10.1021/es101158e
- Wang, H.S., Chen, Z.J., Ho, K.L., Ge, L.C., Du, J., Lam, M.H.W., Giesy, J.P., Wong, M.H., Wong, C.K.C., 2012. Hydroxylated and methoxylated polybrominated diphenyl ethers in blood plasma of humans in Hong Kong. *Environ. Int.* 47, 66–72. doi:10.1016/j.envint.2012.06.004
- Wang, J., Ma, Y.J., Chen, S.J., Tian, M., Luo, X.J., Mai, B.X., 2010. Brominated flame retardants in house dust from e-waste recycling and urban areas in South China: Implications on human exposure. *Environ. Int.* 36, 535–541. doi:10.1016/j.envint.2010.04.005
- Watkinson, A.J., Murby, E.J., Kolpin, D.W., Costanzo, S.D., 2009. The occurrence of antibiotics in an urban watershed: From wastewater to drinking water. *Sci. Total Environ.* 407, 2711–2723. doi:10.1016/j.scitotenv.2008.11.059
- Westerhoff, P., Yoon, Y., Snyder, S., Wert, E., 2005. Fate of endocrine-disruptor, pharmaceutical, and personal care product chemicals during simulated drinking water treatment processes. *Environ. Sci. Technol.* 39, 6649–6663. doi:10.1021/es0484799
- WHO, 1997. Flame retardants: a general introduction.
- Xie, Z., Lu, G., Qi, P., 2014. Effects of BDE-209 and its mixtures with BDE-47 and BDE-99 on multiple biomarkers in *Carassius auratus*. *Environ. Toxicol. Pharmacol.* 38, 554–561. doi:10.1016/j.etap.2014.08.008
- Xu, F., García-Bermejo, Á., Malarvannan, G., Gómara, B., Neels, H., Covaci, A., 2015. Multi-contaminant analysis of organophosphate and halogenated flame retardants in food matrices using ultrasonication and vacuum assisted extraction, multi-stage cleanup and gas chromatography–mass spectrometry. *J. Chromatogr. A* 1401, 33–41. doi:10.1016/j.chroma.2015.05.001
- Yamaguchi, Y., Kawano, M., Tatsukawa, R., 1988a. Hexabromobenzene and its debrominated compounds in human adipose tissues of Japan. *Chemosphere* 17, 703–707.
- Yamaguchi, Y., Kawano, M., Tatsukawa, R., 1988b. Tissue Distribution and Excretion of Hexabromobenzene and its Debrominated Metabolites in the Rat. *Environ. Contam. Toxicol.* 17, 807–812.
- Yamaguchi, Y., Kawano, M., Tatsukawa, R., 1986. Tissue distribution and excretion of hexabromobenzene(hbb) and hexachlorobenzene(hcb) administered to rats. *Chemosphere* 15, 453–459. doi:10.1017/CBO9781107415324.004
- Yang, J., Chan, K.M., 2015. Evaluation of the toxic effects of brominated compounds (BDE-47, 99, 209, TBBPA) and bisphenol a (BPA) using a zebrafish liver cell line, ZFL. *Aquat. Toxicol.* 159, 138–147. doi:10.1016/j.aquatox.2014.12.011
- Yates, J.R., Ruse, C.I., Nakorchevsky, A., 2009. Proteomics by mass spectrometry: Approaches, advances, and applications. *Annu. Rev. Biomed. Eng.* doi:10.1146/annurev-bioeng-061008-124934
- Yokota, H., Eguchi, S., Hasegawa, S., Okada, K., Yamamoto, F., 2015. Assessment of In Vitro Antioviulatory Activities of Nonsteroidal Anti-Inflammatory Drugs and

- Comparison with In Vivo Reproductive Toxicities of Medaka (*Oryzias latipes*) 1710–1719. doi:10.1002/tox
- Zacs, D., Bartkevics, V., 2015. Analytical capabilities of high performance liquid chromatography - Atmospheric pressure photoionization - Orbitrap mass spectrometry (HPLC-APPI-Orbitrap-MS) for the trace determination of novel and emerging flame retardants in fish. *Anal. Chim. Acta* 898, 60–72. doi:10.1016/j.aca.2015.10.008
- Zenobio, J.E., Sanchez, B.C., Archuleta, L.C., Sepulveda, M.S., 2014. Effects of triclocarban, N,N-diethyl-meta-toluamide, and a mixture of pharmaceuticals and personal care products on fathead minnows (*Pimephales promelas*). *Environ. Toxicol. Chem.* 33, 910–919. doi:10.1002/etc.2511
- Zhang, Y., Guo, W., Yue, Z., Lin, L., Zhao, F., Chen, P., Wu, W., Zhu, H., Yang, B., Kuang, Y., Wang, J., 2017. Rapid determination of 54 pharmaceutical and personal care products in fish samples using microwave-assisted extraction—Hollow fiber—Liquid/solid phase microextraction. *J. Chromatogr. B Anal. Technol. Biomed. Life Sci.* 1051, 41–53. doi:10.1016/j.jchromb.2017.01.026
- Zheng, J., Luo, X.J., Yuan, J.G., Wang, J., Wang, Y.T., Chen, S.J., Mai, B.X., Yang, Z.Y., 2011. Levels and sources of brominated flame retardants in human hair from urban, e-waste, and rural areas in South China. *Environ. Pollut.* 159, 3706–3713. doi:10.1016/j.envpol.2011.07.009
- Zheng, X., Xu, F., Chen, K., Zeng, Y., Luo, X., Chen, S., Mai, B., Covaci, A., 2015. Flame retardants and organochlorines in indoor dust from several e-waste recycling sites in South China: Composition variations and implications for human exposure. *Environ. Int.* 78, 1–7. doi:10.1016/j.envint.2015.02.006
- Zhou, J.L., Zhang, Z.L., Banks, E., Grover, D., Jiang, J.Q., 2009. Pharmaceutical residues in wastewater treatment works effluents and their impact on receiving river water. *J. Hazard. Mater.* 166, 655–661. doi:10.1016/j.jhazmat.2008.11.070
- Zhou, S., Reiner, E., Marvin, C., Helm, P., Riddell, N., Dorman, F., Misselwitz, M., Shen, L., Crozier, P., MacPherson, K., Brindle, I., 2010. Development of liquid chromatography atmospheric pressure chemical ionization tandem mass spectrometry for analysis of halogenated flame retardants in wastewater. *Anal. Bioanal. Chem.* 396, 1311–1320. doi:10.1007/s00216-009-3279-6
- Zhou, S.N., Buchar, A., Siddique, S., Takser, L., Abdelouahab, N., Zhu, J., 2014. Measurements of selected brominated flame retardants in nursing women: Implications for human exposure. *Environ. Sci. Technol.* 48, 8873–8880. doi:10.1021/es5016839
- Zhu, L., Ma, B., Hites, R.A., 2009. Brominated Flame Retardants in Serum from the General Population in Northern China. *Environ. Sci. Technol.* 43, 6963–6968. doi:10.1021/es901296t
- Zounkova, R., Kovalova, L., Blaha, L., Dott, W., 2010. Ecotoxicity and genotoxicity assessment of cytotoxic antineoplastic drugs and their metabolites. *Chemosphere* 81, 253–260. doi:10.1016/j.chemosphere.2010.06.029